Vehicle Stability Control Considering the Driver-in-the-Loop

by

Saeid Khosravani

A thesis
presented to the University of Waterloo
in fulfillment of the
thesis requirement for the degree of
Doctor of Philosophy
in
Mechanical Engineering

Waterloo, Ontario, Canada, 2016

AUTHOR'S DECLARATION

I hereby declare that I am the sole author of this thesis. This is a true copy of the thesis, including any required final revisions, as accepted by my examiners.

I understand that my thesis may be made electronically available to the public.

Saeid Khosravani

Abstract

A driver-in-the-loop modeling framework is essential for a full analysis of vehicle stability systems. In theory, knowing the vehicle's desired path (driver's intention), the problem is reduced to a standard control system in which one can use different methods to produce a (sub) optimal solution. In practice, however, estimation of a driver's desired path is a challenging – if not impossible – task. In this thesis, a new formulation of the problem that integrates the driver and the vehicle model is proposed to improve vehicle performance without using additional information from the future intention of the driver.

The driver's handling technique is modeled as a general function of the road preview information as well as the dynamic states of the vehicle. In order to cover a variety of driving styles, the time-varying cumulative driver's delay and model uncertainties are included in the formulation. Given that for practical implementations, the driver's future road preview data is not accessible, this information is modeled as bounded uncertainties. Subsequently, a state feedback controller is designed to counteract the negative effects of a driver's lag while makes the system robust to modeling and process uncertainties.

The vehicle's performance is improved by redesigning the controller to consider a parameter varying model of the driver-vehicle system. An LPV controller robust to unknown time-varying delay is designed and the disturbance attenuation of the closed loop system is estimated. An approach is constructed to identify the time-varying parameters of the driver model using past driving information. The obtained gains are clustered into several modes and the transition probability of switching between different driving-styles (modes) is calculated. Based on this analysis, the driver-vehicle system is modeled as a Markovian jump dynamical system. Moreover, a complementary analysis is performed on the convergence properties of the mode-dependent controller and a tighter estimation for the maximum level of disturbance rejection of the LPV controller is obtained. In addition, the effect of a driver's skills in controlling the vehicle while the tires are saturated is analyzed. A guideline for analysis of the nonlinear system performance with consideration to the driver's skills is suggested. Nonlinear controller design techniques are employed to attenuate the undesirable effects of both model uncertainties and tire saturation.

Acknowledgements

Foremost, I would like to express my sincere gratitude to my advisors Prof. Amir Khajepour and Prof. Baris Fidan for the continuous support of my Ph.D. study and research, for their patience, motivation, enthusiasm, and immense knowledge. Especially, I would like to thank Prof. Khajepour who was the first one told me: "If you can't explain it simply, you don't understand it well enough!" and was always a role model for me both in academic and personal life.

Besides my advisors, I would like to thank the rest of my thesis committee: Prof. Henk Nijmeijer, Prof. Kirsten Morris, Prof. William Melek and Prof. Soo Jeon for their encouragement, insightful comments, and hard questions.

I am thankful to my colleagues Peyman Eskandary, Iman Fadakar and Ehsan Hashemi for the stimulating discussions, their technical assistance to my project, the sleepless nights we were working together before deadlines and for all the fun we have had in the last four years.

Last, but not least, I would like to thank my wife, Mojgan, for her understanding and love during the past few years. Her support, encouragement and of course drawing the illustrations in my thesis was in the end what made this dissertation possible. My parents, Reza and Elham, and My brother, Sina, receive my deepest gratitude and love for their dedication and the many years of support that provided the foundation for this work.

Dedication

I am dedicating this thesis to four beloved people who have meant and continue to mean so much to me. My parents, Reza and Elham, my brilliant wife, Mojgan, and my brother, Sina.

Table of Contents

List of Figures

List of Tables

"Good work is no done by 'humble' men. It is one of the first duties of a researcher, to exaggerate a little both the importance of his subject and his own importance in it." [sic]
A Mathematician's Apology, 1940, G. H. Hardly

Chapter 1
Introduction

1.1 Motivation

Undoubtedly, in the history of transportation, the automobile is one of the most revolutionary inventions since the wheel. While the automobile was born more than a century ago, today's modern cars differ vastly from their earlier ancestors. Technology is now improving general vehicle safety while reducing both emissions and fuel consumption. Although automobiles have many advantages, they can have adverse effects on human health and safety. The World Health Organization (WHO) reports that every year, the lives of almost 1.3 million people are cut short as a result of road traffic crashes, and without action, it is predicted to increase to 1.9 million by 2020. Based on a study by the National Highway Traffic Safety Administration (NHTSA), driver errors are accountable as the main contributor to these accidents (more than 90% [61]). Therefore, vehicle stability analysis has become an important topic of scientific investigation.

The ultimate goal of vehicle dynamic control can be defined as "reducing the burden placed upon driver" (i.e. to increase safety level and ride comfort). Given that this aim depends on human and machine interaction; a combination of psychology, automotive engineering, computer science, control theory, etc. is needed to reach the goal.

Similar to many other research literature, stability analysis of the error dynamics is the main focus of this thesis. Note that different situations may result in poor performance of a vehicle, however, by the time that the vehicle is on the ground, the car's states will always remain in a bounded region. Even for the worst case scenarios that usually occur on an icy road, the vehicle will eventually stop at some point if the input is zero. This emphasizes that one should always be careful about using the term "stability" in vehicle handling control research.

From a control theory standpoint, the difficulty of vehicle performance analysis is rooted in two main problems:

1. The nonlinear dynamics of a vehicle makes accurate modeling and analysis of a vehicle control problem difficult. For example, in the nonlinear handling analysis of a vehicle, one of the main issues is in modeling tires. There are several static and dynamic models to mimic actual tire behavior, however, they have many tuning parameters that mostly are functions of tire aging. The effects of the nonlinear model of a vehicle in estimation problem is another major difficulty in this field. Estimation of lateral and longitudinal velocity are two of the most important signals for vehicle controllers that can be severely affected by changes in a tire model, and these changes cannot be captured by a linear model. Even considering minor nonlinearities such as the nonlinear model of the steering gear ratio will significantly improve vehicle controller performance and the estimation process. On the other hand, although control theory offers rich mathematical tools for steering a system to a desired state, a general framework to control nonlinear systems is still lacking. Ignoring vehicle nonlinearity leads to imprecise modeling, which can result in stability issues, estimation errors, and uncertainties.

2. Human-machine integration control still encounters vital problems, many of which have resisted advances. A driving process is composed of the driver (human or robot), the vehicle, the environment, and the controllers. It is clear that behavior of a closed loop vehicle with a driver as an active (in lateral and longitudinal motion), or a passive (vertical motion) element is different than the behavior of an open loop vehicle dynamic. The driver prompts the vehicle to follow the desired path with a desired speed by manipulating the main inputs: steering wheel angle and brake/accelerator pedals. Hence, it is easy to conclude that the system's architecture represents two interconnected subsystems. As such, the closed loop vehicle system has two control loops with separate decision-making and actuation tools. The first controller (driver) defines the control goal of the vehicle while the second one (vehicle controller) helps the driver obtain the desired behavioral response. The outputs of the first controller are observable for the vehicle controller, but its structure is unknown. In the vehicle dynamics literature, usually, the vehicle controller is designed without regard to a driver in the loop. The main aim of this thesis is to include the driver in the vehicle controller design to counteract the negative effect of driver's delay and dangerous driving styles in the overall vehicle control system.

A general closed loop diagram of a driver-vehicle system is depicted in Figure 1-1. In this schematic, the driver is not considered in the control loop design. Instead, the driver's block outputs (i.e. torque and steering angle) are treated as input command signals to the vehicle controller. Note that δ is the steering wheel angle and T is the torque requested by the driver.

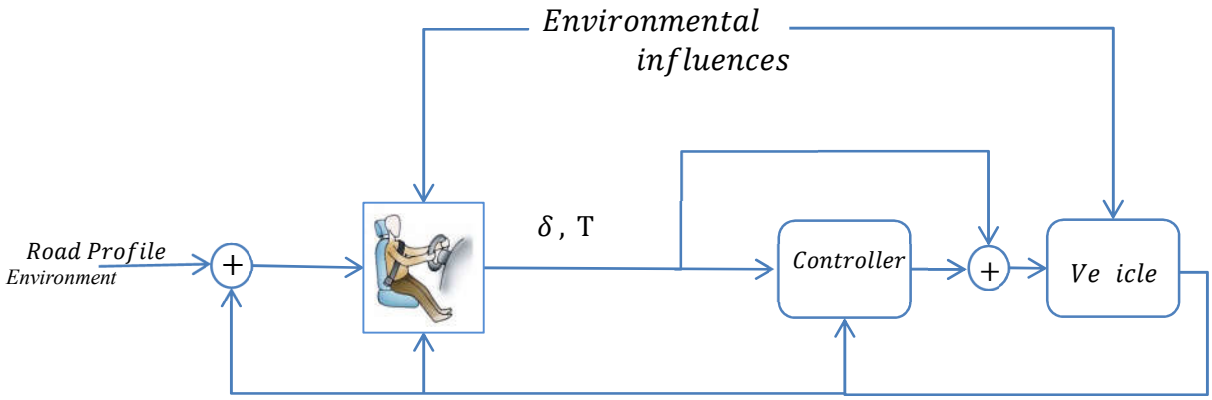

Figure 1-1 closed loop vehicle control schematic

This is the core of almost all commercial vehicle controllers, where the desired values for the conventional – (semi) autonomous - controller are always a function of the driver's request. Given the appropriate desired values, the controller can adjust the vehicle input torque and steering angle to maintain the vehicle's high-performance.

1.2 Main Objective

To the best of author's knowledge, there is no commercialized or currently developing controller that actively considers the effect of a human driver without using a desired path and environmental information. However, one can argue that advanced gearshift transmissions consider the effect of the driver and predict future requests. It should be noted that the structure of the control system in a transmission control problem is far simpler than vehicle handling, and transmission model accuracy does not have crucial effect on vehicle performance. On the other hand, there are many indicators (such as the pedal position signal acceleration and vehicle current engine torque) that a controller can use to estimate the driver's intention while there are only two options (to gear up or down) for the driver model. Basically, the results in this area lend themselves toward more classification and clustering than dynamic modeling. Even in smart transmission control structures, the author could not find any solid results that guarantee a successful driver intention prediction.

As a part of closed loop control loop, the driver has to be considered in the design procedure. A general approach is to assume a driver model and then design the controller based on this information. One approach to this problem is to assume a relatively accurate model describing driver behavior and a known driver's desired path for the vehicle controller. This way, one can assume that the reference signals are the road and environmental information rather than the driver's input. This is the main idea of all of the semi-autonomous vehicles. The schematic of this approach is presented in Figure 1-2, where the controller holds feedback information about vehicle states as well as a driver model and the intention of the driver. More precisely, in this case, there is a path planning algorithm that generated the vehicle path for the vehicle based on the driver model. Then the controller compares the path planning outputs (usually steering wheel angle and vehicle wheel torque) with the driver's request. The vehicle's lower level controller monitors vehicle states and the error from the previous block while generating the appropriate control action.

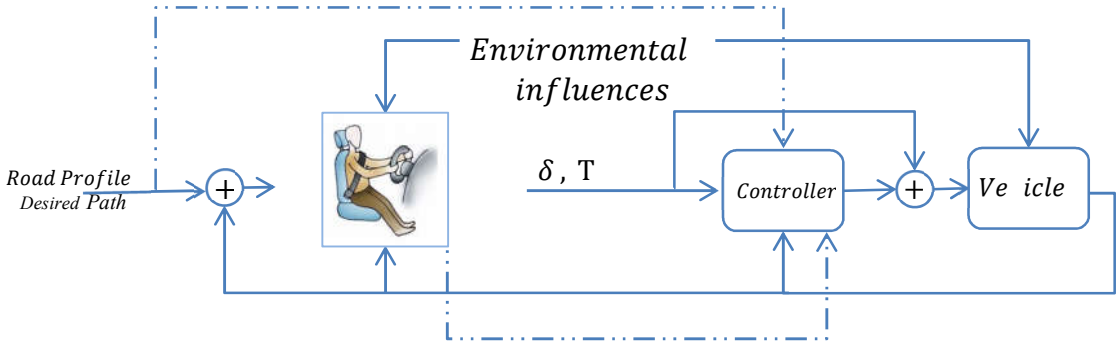

Figure 1-2 Closed loop vehicle-driver control scheme (controller has access to the desired road path)

With currently available technology, obtaining information about the driver's intended path is not possible. Although there are different proximity sensors, radars, and motion detectors available for implementation, obtaining the driver's intention requires special tools. One should also note that there is a very delicate difference between the desired road and driver's desired path. The desired road information can be estimated by the path-planning module based on the vehicle state and the environmental situation. The driver's desired path can be completely different from the one that is estimated in path-planning block. This shortfall motivates us to seek methods that can improve the overall performance of a vehicle without having predefined knowledge on desired paths.

The following control structure (Figure 1-3) is the implementable closed loop control structure that contains the driver model. As it is presented, using this method, the controller adjusts the vehicle's reaction without using information of the desired path. The idea here is to take into account the fact that the request coming from the driver is dynamic and contains useful information for improving vehicle performance. Thus, the controller design can be revised according to the extracted information from the driver's commands.

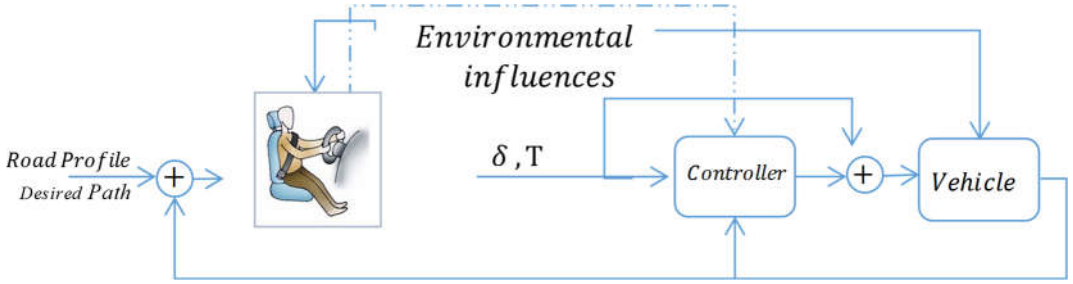

Figure 1-3 Closed loop vehicle-driver control scheme (controller has no access to desired road path)

The adaptation of new vehicle control techniques which can apply to currently in-use vehicles is also an important issue in both academia and industry. The proposed algorithm in this thesis improves the vehicle safety using only the standard IMU sensor.

Another important feature of a driver in the loop control study is in semi-autonomous vehicles. Reducing the production costs of advanced sensors – radar, Lidar, and GPS – and precise actuators –by-wire actuators and reliable electric motors – has created new horizons that expand vehicle safety boundaries and provide new perceptions of the world for intelligent vehicles. The semi-autonomous vehicle control tries to prevent vehicle skid while keeping good yaw-tracking and maintaining the vehicle on the desired path. The algorithm must be tuned to handle worst-case scenarios. Without considering the driver effect, this results in a conservative control algorithm that does not rely on the driver's expertise level and the vehicle tends greatly understeer. Assuming a short-term model for the driver to predicts the future action of the driver, the control algorithm can reduce the conservation. On the other hand, driver's style learning is another potential application of driver in the loop application in semi-autonomous vehicles where the controller gains changes on-fly based on the driving style identification. Note that because only the short term model for the driver is needed, it seems to be more realistically implementable. This way, only the current driving style would be used in the controller.

Using the driving style of a human driver, the driver-in-the-loop (DIL) controller produces more appropriate control action. The DIL-controller effect is compared with a conventional vehicle controller in Figure 1-4. The conventional controller requests a certain amount of adjustment without considering the driver expertise. As it is shown in Figure 1-4 (a) and (c), since the conventional controller does not have any information about the driver's expertise, for both of the expert and novice drivers requests the same amount of adjustment. The result will be different when a DIL-controller is taking care of the vehicle performance. Given that in this case the information about the driver's expertise is available for the controller, the controller request will be different when different drivers are steering the car. Different action of the DIL-controller for expert and novice driver is illustrated in Figure 1-4 (b) and (d) where the controller is more conservative if detects that the driver is novice. Alternatively, for the expert driver DIL-controller's interventions is less than the conventional controller.

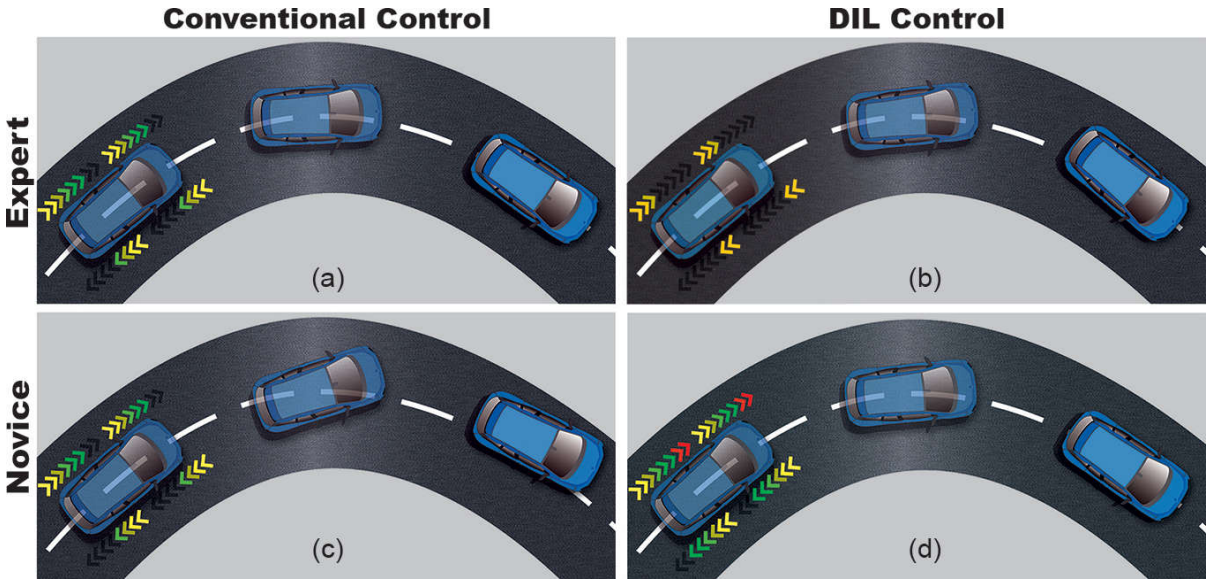

Figure 1-4: Driver in the loop controller effect

A summary of the results and research activities conducted in this thesis is as follows:

1. A new formulation for integration of driver in the vehicle control problem is proposed.
2. A new LTI H_∞ controller is designed to stabilize the vehicle dynamics while considering the effect of a human driver. The controller is robust to time-varying delay of the driver and bounded model uncertainties.
3. Considering the parameter varying nature of the driving style, an LPV model for the driver in the loop problem is proposed and the corresponding LPV controller is designed.
4. A new technique is proposed to identify the driver model's parameter using past driving information. The identification method does not require the driver's future desired path or driver's future intention.
5. Markov modeling paradigm is used to classify the driver model's parameters and calculate the probability of the corresponding transition matrix. Then, a new theorem is proposed to analyze the closed-loop LPV system and find a less conservative disturbance attenuation gain. A new theorem is proposed for the stability analysis of the Markov jump linear retarded systems that reduce the conservation of the Jensen inequality.
6. A new nonlinear analysis revealed that the driver-in-the-loop idea can be easily integrated with nonlinear structure. Nonlinear damping, sliding mode, and backstepping methods are applied to the problem and the results are compared.

1.3 Thesis Outline

Given that the stability of a closed loop vehicle system without the driver in the loop is not complete, an appropriate stability platform is needed for analyzing the driver-in-the-loop problem. In earlier works, stability was mostly considered only for the vehicle as a separate plant excluding the human driver effect, however, it turned out that this approach could not completely deal with the many nuances of closed loop vehicle stability. This issue was adequately defined after the introduction of the concept of human-machine interaction and augmented control systems. The focus of this thesis is twofold: firstly, to consider the effects of the driver on the vehicle control loop effects, and secondly, to propose a new control structure and design corresponding to possible controllers for the closed loop driver-vehicle system. This calls for assuming the availability of a driver model in the analysis that enables us to close the vehicle-driver loop.

The rest of this thesis is organized as follows: Chapter 2 presents a survey of the most important existing methods in vehicle dynamic control related to the driver-in-the-loop system as well as a summary of relevant publications. It starts with a general overview of vehicle stability techniques and proceeds to a review of the most important human modeling methods related to driver modeling. In the last portion, the publications on the driver in the loop analysis are reviewed. At the end of this chapter, the novelty of the proposed method can easily be inferred.

Chapter 3 provides details on the vehicle model, the multi-points preview path follower modeling, and driver model that are used in this thesis. Simulations in this section show the effect of closing the vehicle loop with a path follower model. The driver model is assumed to be a path follower combined with a delay block. The delay in the driver's observation and reaction is lumped into a block. This delay postpones the steering angle command of the path follower model. In the last part, a closed loop vehicle-driver model is obtained to serve as the base dynamic equations in designing a controller.

Chapter 4 details a robust controller design method where the effect of the delay is taken into consideration and handled by using a delay-dependent robust controller for the Linear Time Invariant (LTI) driver-vehicle model. The lacking information is treated as bounded-energy modeling uncertainty; thus, H_∞ method is used to design an implementable controller. The last stage is to consider driver modeling uncertainty. To address this problem, an extension to delay robust H_∞ controller is proposed. Simulations show the effectiveness of the proposed method using different vehicle speeds.

Chapter 5 is devoted to the extending the linear parameter varying case. It is known that the driver's driving style and vehicle parameters are not constant. The driver-in-the-loop robust

controller design idea is revisited accordingly and a Linear Parameter Varying(LPV) controller is proposed to stabilize the vehicle. The simulation results of vehicle performance with different road friction coefficients shows that the LPV controller outperforms the LTI controller designed in Chapter 4. By analyzing the input-output performance of the system, an estimate of the upper bound of the disturbance rejection is also calculated.

In Chapter 6, the Markov modeling method is used to improve driver style modeling. An identification method is used to first find a set of operation modes for the driver, then, using the experimental data, the Markov transition probability matrix is obtained. The main advantage of this identification method is to perform the identification task in a finite timeframe of past driving information. This way, there is no need to have the driver's desired path or intention for driver identification. Taking advantage of this extra piece of information, the robust analysis of the closed loop LPV system is revisited and a better estimation (less conservative) of the disturbance rejection level is obtained.

Chapter 7 is devoted to the nonlinear analysis of the driver-in-the-loop system. A more general nonlinear model for the vehicle is assumed, and the design is extended to handle vehicle modeling nonlinearities along with the driver's effects.

Chapter 8 concludes this thesis by listing the main contributions and outlining the steps required to extend the work. Finally, the appendix contains the mathematical background and some definitions from control theory.

"Mathematicians may find a rigorous way of solving a problem through an elegant mathematical procedure. However, this procedure may not take into account all of the relevant constraints on the problem known by the engineers. Therefore, to solve problems, it is up to the engineer to find, where applicable, the available mathematical techniques and to develop them where they do not exist."

"Frederick A. Leve" APRIL 2015 <<IEEE CONTROL SYSTEMS MAGAZINE>>

Chapter 2
Literature Review and Background

2.1 Vehicle Stability

The ultimate goal of vehicle dynamic control can be defined as "reducing the burden placed upon a driver", i.e. increase the safety level and ride comfort. Advancements in automotive safety systems such as slip controllers and electronic stability control have resulted in significant improvement in overall vehicle safety. Yet, the lack of a proper human modeling strategy to guarantee the optimal action, coerces the companies to mostly entrust a separate control structure that considers the driver as a command generator rather than a part of a closed loop system. This evinces that a key problem is a reliable integrated technique to better serve the driver's - or the autonomous path follower's - request. Given that this aim depends on human and machine interaction; an interdisciplinary framework combining psychology, automotive engineering, computer science, control theory, etc. is needed to reach the goal. To formalize the problem, some researchers assume a relatively accurate model describing driver behavior while the driver's desired path (intention) is available for the vehicle controller. This way the controller has the road and environmental information as the reference signal along with the driver model (see [23, 29, 122, 132, 133, 141]).

The increasing worldwide use of automobiles and the demand for vehicles with better performance and safety characteristics has increased the urgency of working on vehicle dynamic analyses. Both passive (e.g. shape, vehicle structure, and seats belt) and active control (e.g. ESC1,

[1] Electronically Stability Control

ABS2, and DYC3) can save many lives. In order to counteract unstable conditions, many types of controllers are devised to improve the overall performance and handling of a vehicle. The driver usually drives in normal conditions, where the tires behave linearly and are as a result, mostly predictable. However, in the case of tire saturation, a typical driver cannot guarantee the best performance of the vehicle. On the other hand, when a vehicle is on a road with low friction contact, the generated force from the motor cannot transfer to the road, so the normal thrust force is not produced. These are example situations where a controller can help the driver. Probably the most well-known controller for a vehicle is the ABS stabilizer, which tries to hold tires in a linear zone by creating a pulse-like brake pedal pushing. For a recent survey on methods of ABS and Traction Control (TC) see [69].

A number of studies have considered the effectiveness of vehicle control systems in reducing the risk of vehicle crashes. A good review is done by Ferguson ([41]), who summarized the literature, reporting that a single-vehicle crash risk was reduced by 33-35 percent for cars and 56-67 percent for SUVs. Another report given by Lie ([87]) investigates the effectiveness of ESC in reducing crashes and injuries in Sweden from 1984 to 2004. A tremendous amount of research is now available on vehicle dynamic analyses, however, it must be noted that the effects of a driver in the control loop is still an open problem. Figure 1-1 presents a general vehicle controller strategy design where the controller uses driver inputs (steering wheel and pedals as standard inputs) and vehicle states to improve vehicle stability behaviour and vehicle performance. Kasselmann et al ([74]) first introduced the idea of an active steering (AS) system based on yaw rate feedback. However, the most significant work initiated with Ackerman, who tried to formulate a mathematical model for the problem ([4, 5]). He separated driver tasks into two distinctive categories: "path following" and "disturbance attenuation". The first task involved applying a lateral acceleration to adjust the velocity vector, and the former one was to cancel the effects of disturbance torques resulting from crosswind, flat tire, or unbalanced friction on the left and right sides.

For more than 30 years, the H_∞ disturbance attenuation method has been an active branch of robust control (see [43, 156]). The approach is now well developed both in frequency and time domain and has been implemented in many applications. Given that model uncertainty is inevitable in vehicle analysis, robust control is also of growing interest in this field. In the late 90s, some work on robust steering control design have been presented based on the H_∞ method. Considering recent progress in solving the linear matrix inequality (LMI) problem, the H_∞ method is now a more effective tool in handling deterministic disturbance models with bounded energy

[2] Anti-Braking System
[3] Direct Yaw Control

L_2 signals ([54, 55, 71, 98, 147]). Using the loop shaping method, most of the works have presented digital implementable ([82]) stabilizing feedback controllers that minimize the amount of the energy transfer function between disturbances and measurements. A two degree of freedom control structure is proposed in [54], which improves the yaw dynamic of a vehicle. This method performs model reduction and disturbance rejection by using a special H_∞ loop shaping for path following. The effects of mechanical delays in steering systems is another important topic which is considered in the H_∞ active steering control ([57]). Another method, which is widely used in steering control, is the sliding mode. This is where the aim is to restrict the state space trajectory of the system to a surface titled the "sliding surface" (see [13, 18, 34, 55, 65]).

Preview control is also a recent method used in lateral motion stability analyses by a few researchers. The success of this method lies in the inherent ability to consider a finite horizon knowledge of the desired path in the control design. Using this method, the potential delay in the control loop can also be moderated. The formulation is very similar to the time domain robust H_∞ method. However, another assumption is that preview information about unpredictable disturbances in a certain future horizon is available. For more information, readers are referred to [58] and the referenced therein.

One of the most important methods for dealing with nonlinearity caused by tire saturation is linearizing the vehicle dynamics at different working points and using the Model Predictive Control (MPC) method. This method predicts future vehicle states for a finite horizon by using a plant model. Then, the MPC method offers a control input that satisfies the plant's constraints and minimizes a user-defined cost function. Falcone et al ([39]) proposed an AFS control scheme based on the MPC to stabilize the vehicle in different scenarios such as obstacle avoidance, and the double-lane-change maneuver. The main issues of using an MPC structure are rooted in two major vehicle dynamic characteristics. The first issue is the vehicle's time-varying behavior due to its varying longitudinal and lateral speed. This issue has recently been approached by some scientists working on the MPC for the LPV method (see [14], [48] and the references therein). The other important barrier in using an MPC method is the driver's input. It is known that a vehicle controller is usually active during harsh maneuvers due to the high rate of changes in driver inputs (pedal positions and steering angle). On the other hand, using predictive methods, one needs to assume that the driver's inputs do not change significantly in the prediction horizon. This is in contrast to the real situation and decreases the length of the prediction horizon significantly. Therefore, most of the time, in a real application, the MPC needs to work with a small number of preview points that usually results in a similar outcome to a gain scheduling proportional gain controller. One proper approach for tackling this problem is to combine the user modeling and control problem more tightly by adding a driver model that predicts the

driver's behavior in the prediction horizon. This way the MPC controller can use the predicted values to serve the driver better. This has been a very attractive area of research in recent years (see [23, 33, 84, 117]).

Stochastic modeling of a driver has been an important approach in closed loop vehicle behavior analyses (see [23, 85, 91, 92, 121, 122, 138]). Markov modeling is shown to be a promising approach to mimicking a driver's behavior in some situations. Similar to other modeling methods, the idea here is to see if the next action can be inferred from the current state of the driver. The main assumption is that a driver's decision can be modeled as a series of internal states which represents a memory-less random process that depends only on the current status of him/her and not on the previous decisions. In this case, the standard parameter identification process works based on temporal pattern observations and comparing the model output with the system measurement. Markov modeling is used in [33] as an online learning module to mimic the driver's behavior. Then, the model is used to predict the future decision which is then fed into a stochastic optimization technique that tries to maximize fuel efficiency.

Torque vectoring is another method, which results in the stabilization of the vehicle by adjusting the independent drive torque for all the wheels. A particular development in this method is improving the stability of the vehicle to preserve the longitudinal acceleration performance of the car [88]. This method, however, is best suited for electric vehicle designs where each torque wheel can be controlled easily.

2.2 Human and Driver Modeling

Human behavior modeling is one of the main challenging goals of many sciences. It relates to nearly every field of study: from biology, to engineering, and psychology. "Human factors, also known as human engineering or human factors engineering, consist of the application of behavioral and biological sciences to the design of machines and human-machine systems" [130]. Although it seems extremely difficult – if not completely impossible – to model a human's behavior, there are special cases where the behavior of a human can be modeled or predicted under certain conditions. In this context, modeling means something that can be calculated and consequently simulated.

The modes of a human model can be organized to describe both short-term and longer-term behaviors. Consider the automobile driving task, the longer-term behaviors of a driver can be passing, following, and turning, while shorter-term behaviors could be turning the steering wheel or changing the brake/gas pedal position. According to [115], there are four steps in human action when s/he is interacting with a machine: sensory measurements, information analysis, decision making, and action implementation (Figure 2-1). In the driver/vehicle case, although this

scheme helps us understand overall information processing, there are still difficulties in measuring some of the factors. On the other hand, the relationship between measurements and the driver's actions (which are done in brain), have not yet been fully investigated. In the rest of this section, a brief review on many researchers' findings regarding this relation is presented.

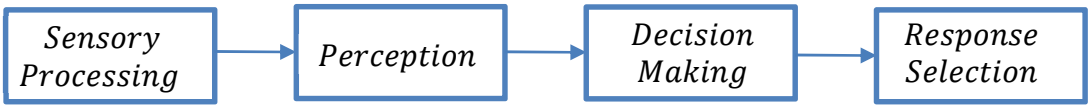

Figure 2-1. Information processing depicting human and machine interaction.

As mentioned in [126], a good driver model needs to be in harmony with science's achievement on sensorimotor and cognitive control in real drivers, accurate (predictive) enough, and simple enough to implement in real-time. Tustin is the first one to have proposed a mathematical model for describing human behavior. He published a scientific paper about approximating human behavior on a typical tracking task using a linear system [144]. Since 1960, mathematical driver modeling and corresponding parameter identification techniques have become an active field of study ([90, 104, 120]). McRuer et al, in [100] proposed the following quasi-linear dynamic model for human driver-car interaction, where a second order differential equation is combined with an output delay reaction time factor:

$$H(s) = \frac{K(T_L s + 1)}{(T_I\, s + 1)(T_N s + 1)} e^{\tau_r s} \tag{2.1}$$

here τ_r is reaction time, T_N is neuromuscular delay, and the other parameters depend on the plant interacting with the human. They also proposed a catalogue for different situations, where based on the plant that human is interacting with, the behavior of a human can be predicted. The main flaw of the quasi-linear model above is that adaptation is not considered in modeling and the model highly depends on predefined parameters. As a result, McRuer and Krendel integrated human and machine modeling in their "cross-over model", which contains only cross-over frequency information and dead time delay. Therefore, they relaxed the restrictive assumption of the quasi-linear model ([101]). In Figure 2-2, a simple driver vehicle loop is shown, where $G_d(s)$ is the driver transfer function, $G_v(s)$ is the vehicle transfer function, e is the lateral position error, and δ is the steering angle. This method is mainly proposed by experimental observation from different tests performed on a variety of drivers.

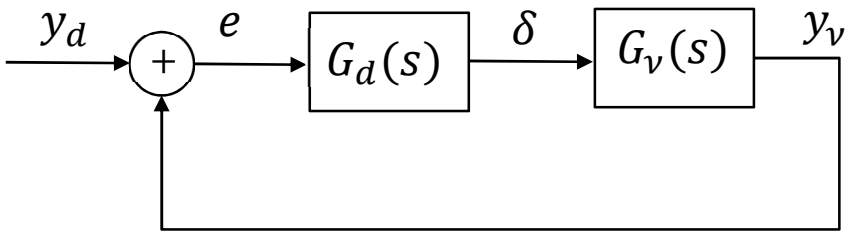

Figure 2-2 Simple driver – vehicle in a closed loop system

Recent improvements on this model are reported by Apel in [8]. From this point onward, a lot of work has been done to resolve the problem of human modeling.

Understanding how a driver steers a vehicle attracted the attention of researchers during the early 1940s ([12]). According to different applications, a variety of driver models are proposed. Driver models have already been surveyed in some papers (see [1, 97, 120] and the references therein), however due to space restriction, only a few of them are reviewed here.

There are three main tasks in the driving process: navigation (route selection), path planning (recognition, decision-making, and path selection), and control (steering, braking, and acceleration). On the other hand, there are two approaches to driver modeling; one is using (non)linear differential (algebraic) equations and subsequently obtaining transfer functions, optimal (model predictive, adaptive, fuzzy, neural-based) controllers, or online identified deterministic (stochastic, hybrid) models. The other one is using descriptive methods.

Driver models also can be categorized according to their applications. For example, the "virtual test driver" is modified for component design or closed loop vehicle behavior (especially stability) analysis. A path following vehicle with a given (or driver tunable) speed is the main goal of this model. Since many human characteristics, such as emotional status, fatigue, and learning processes are not considered; the model performs the given tasks more similarly to a path follower robot instead of a real human test driver ([68]). Even though vehicle motion may not change in the model, the input commands of the steering wheel and pedals can be different in real driving. Recently, some literature has focused on improving learning patterns, where multi-internal models are considered. Each step is based on driver identification and a certain level of capability for the driver is selected ([75]). The given model has the potential to offer an approach to modeling different driver's skills; this is achievable through considering a nonlinear vehicle model, which simulates car's behavior with tire saturation as well.

Virtual driver models generally work based on the same concept of preview point modeling. They use the fact that the driver looks a distance, L, ahead of the vehicle and tries to compensate the lateral position of the vehicle. Note that the driver's behavior on longitudinal motion control of the vehicle is another branch that mostly tries to model the driver's capability to optimize the longitudinal speed. A simple single road preview point model is presented in Figure 2-3 where the driver endeavors to minimize the lateral position error (Δy).

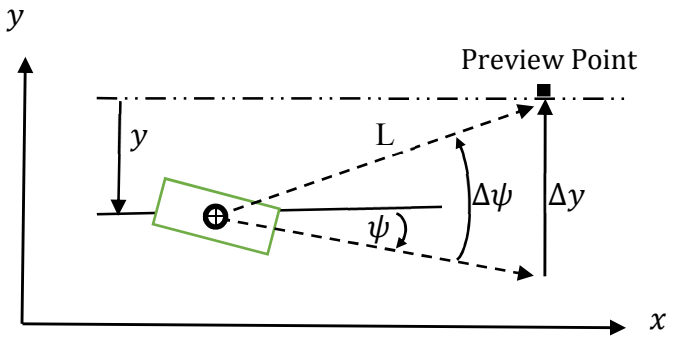

Figure 2-3 Virtual driver model based on preview point

MacAdam presented a driver model based on optimal control theory [96]. Using the state space representation of a vehicle dynamic model, the author set up an optimal controller, which tries to minimize the lateral position error with a desired path, while expending minimum effort (optimal steering angle). In order to improve the model accuracy in [146], Peng et al proposed to use an inverted vehicle model to add a learning process. They proposed the use of an ARIMAX[4] identification process for recursively identifying the model parameters.

The identification method, on the other hand, is a powerful alternative for driver modeling (see [26, 27, 90, 104, 114, 137, 138]). Chen et. al used ARMAX modeling ([26]) to find a time-varying model driver behavior. This work was extended in ([27]) where MRAC[5] is used to identify the driver and use the information in the adaptive control structure.

A complete version of the idea that a driver uses multi preview points to steer the vehicle was first reported by Sharp and Valtetsiotis in [129]. They proposed an optimal driver (an ideal path-follower) for a linear time invariant (LTI) vehicle model (constant speed), which converts the path preview sample values into steering wheel angle commands that adjust the vehicle's position to the desired path. The driver looks ahead with the length of $L = V_x T_p$ and selects N_p positions along the future trajectory of the vehicle with the current yaw angle. S/he also considers the

[4] Auto Regressive Integrated Moving Average with eXternal inputs
[5] Model Reference Adaptive Control

corresponding points on the desired path (not necessarily perpendicular to the optical lever), thus N_p lateral position errors are obtained. The first error is in an exactly lateral position to counterbalance the vehicle from the desired lateral position. The driver steering input can be written as follows:

$$\delta = K_\psi(\psi \quad \psi_d) + \sum_{i=1}^{N_p} K_i e_i \tag{2.2}$$

where K_ψ and K_i are control gains. By taking advantage of the discrete linear quadratic regulator (LQR) method, one can also define the driver's skill in path-following tasks by adjusting regulator coefficients (tightening and loosening control for different balancing in accuracy of the follower and control effort) and finding analogous control gains. Figure 2-4 illustrates a schematic of driver modeling with multiple preview points concepts; where the driver's desired yaw angle is ψ_d and e_i is the i^{th} error between the desired and current lateral position, respectively. Further explanation is provided in chapter 3. Approaching more complex and complete driver models, Frezza et al, in [45] proposed another hierarchical optimal methodology for driver modeling. This nonlinear model has three levels of decision making for task planning, strategy for trajectory planning, and motion control. The proposed model is based on a geometric nonlinear control for non-holonomic vehicles. This is the same driver that is used in the commercial software titled ADAMS.

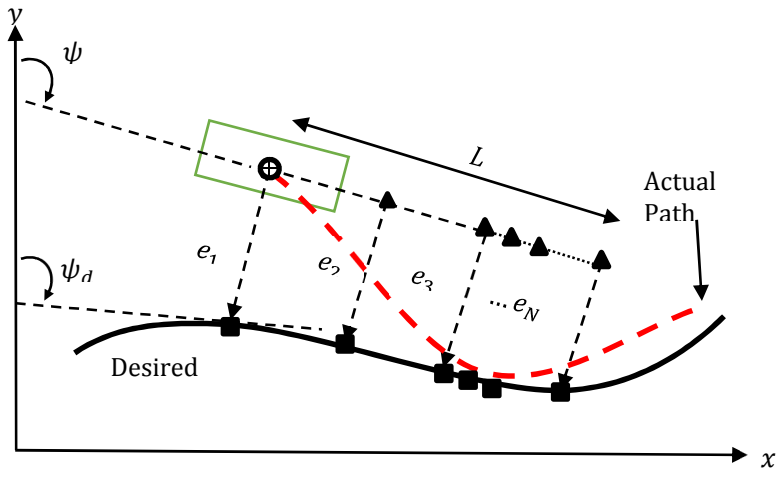

Figure 2-4 multi preview points driver model

Desired path availability is the assumption of almost all driver models. This can include road curvature, preview points, or any other vision information, any which is assumed to be available.

In general, this path needs to be optimized, however, it may be optimized with different criteria in different models. According to [120], reaching the destination as fast as possible without violating ride comfort (time-acceleration optimal), with minimum energy dissipation, with the shortest maneuver, or with a certain engine (vehicle) speed are some of the driver criteria. The optimality of the solution and the risk level of each driver is also an important uncertainty as pointed out in [72]. The main goal of all of the discussed models is to propose a model to mimic a normal driver's behavior. Although in some of these models, parameter variation may lead to some level of experience in the driving task, the problem of expert driver modeling has only recently been taken into consideration ([90, 142]).

2.3 Driver-Vehicle Interaction

Open loop vehicle stability analysis has been investigated for a long time even though the driver is an inescapable component that can destabilize the system. Novice drivers do not have much information about the nonlinear behavior region of the vehicle (tire). Hence, in certain situations, they would fail to respond in an appropriate manner to control the unstable plant and might even make the closed loop system behavior worse. In order to reach the ultimate level of safety and comfort in a driver/vehicle system, the controller needs to "know" the driver operator. Currently, there are different technologies that have reached a level of maturity ensuring the manufacturers ability to implement them safely. Intelligent cruise system, lane keeping, and lane departure avoidance systems are just a few samples of driving assist systems. Despite of all this development, the driver (human)-vehicle interaction is still at a low level of automation.

As Inagaki reports in [66], the assistant controller can be tuned better if it has information about the driver's states and intentions. Therefore, since the control system in driver assistance systems react faster and more precisely than the human drivers, they have an incredible potential to dramatically improve the vehicle's stability margin. A simple example is in applying automatic braking before the driver's action delay. This can be accomplished by having information about the road, the environment, and by predicting the driver's intentions. Using this intelligent system, not only is the overall vehicle safety improved, but the driver also feels more comfortable. Almost concurrent to Inagaki, Abe et al reported an analysis on driver effects in closed loop vehicle behavior in [2]. A simple PID[6] controller is assumed as a model for the driver, which simply uses lateral position error to provide a steering angle and handle the car. Taking advantage of the frequency domain, a nice analysis is also done to consider the effects of the driver's delay.

[6] Proportional Integral Differential

As mentioned in [86] and [67], to date, the following four main questions have not been properly answered in closed loop vehicle control theory:

1. Which part of the driver's cognition needs to be enhanced? (for example, vision enhancement)
2. What kind of action is required by the controller, and when should it be applied? (Such as visual displays for information or warning, and voice navigation systems). Note: a protocol has been approved on how and when to provide information to the driver, which answers part of the question ([105]).
3. What is the best approach to implement the control action?

The most important solutions involve using a driver-centered automation strategy ([149]) to make the driving process smoother and easier for the driver, or evaluating the driver's behavior and switching to fully autonomous vehicles when needed (especially in lane change avoidance and obstacle avoidance).

4. How much can a controller overtake handling of a vehicle?

Many scientists have considered the more general question of: to what extent can a machine take over human's life? [64]. However, from an automotive theory standpoint, the problem is mostly answered by using a weighting function, which determines the importance of the driver and the controller input.

The last problem can be categorized into two types: closed loop cooperation and closed loop conflict. For the conflict case, the problem is more visible for the active-steering controllers, when the controller and driver are counteracting each other in a certain situation. A controller can provide better decisions regarding vehicle stability and crash avoidance. In [46], Fujioka proposed a simple algorithm that weighs the steering angle of the driver and the virtual driver (steering controller) according to the following situation:

$$\delta = W\delta_{driver} + (1 \quad W)\delta_{virtual} \tag{2.3}$$

when $W = 1,$ the system becomes a manual driving system. A fully automated system occurs when $W = 0$. Using a continuous function to define $W,$ based on the current vehicle situation (Gaussian function in this paper), the problem can be addressed. However, finding the threshold for implementable conditions is still an open problem. The conflict shows up when the vehicle is commanded by two different controllers, the driver and the controller, at the same time ([24, 110,

111, 123]). The driver request may be different from what the direction of controller action. One example can be when the controller is very conservative and an expert driver is driving the vehicle. Chen et al proposed an "ideal model" for the driver that can be used to analyze human driver behavior. In cases where it is required (based on the differences between ideal model and human driver), the vehicle assist controller will be activated. For cases where there is a conflict between the controller and the vehicle driver, a weighting method is suggested to handle the conflict. Following that, Na et al designed an AFS controller assuming that the desired path information is available. Then, considering the predictive preview gain driver model, the problem of a conflict in the joint driver/controller path is presented ([111]). In [110], the driver and controller are denoted as two players of a dynamic game with the aim of maximizing stability conditions for the vehicle. In this scheme, the decision of each controller depends directly on the other controller's choice. The problem will be more apparent in an obstacle avoidance scenario: the faster controller detects the obstacle and tries to deviate the vehicle's trajectory whilst, due to the human neuromuscular delay, the driver still insists on sticking to his decision about the vehicle's direction. Using the Nash equilibrium point, the problem of strategic interaction between the controller and the driver is addressed in these works. Linear quadratic (LQ) game theory, and non-cooperative MPC are used for modeling driver-controller interaction problems.

For a cooperation scenario, the same idea is used in Tamaddoni et al, [141] to define the driver's steering angle and the direct yaw controller's (DYC) decision as two game agents. These agents use the same desired path and cooperate to improve vehicle stability. The main difference in this paper is that both the controller and the driver have the same aim while the DYC controller can effectively cooperate with the driver, especially for disturbance rejection. Another good example of the controller and driver cooperation is ABS. This actuator works well for vehicle skid prevention, which improves both the longitudinal and the lateral motion of a vehicle. However, by providing a pedal vibration feedback for the driver, the vehicle control system asks the driver to apply the brakes continuously rather than pumping.

Active trajectory planning is an effective method to relax the restrictive assumption of knowing the desired road path. This branch is also called "path planning" and has emerged as a hot topic since using an online approach. As a result, realistic control implementation can be addressed ([52, 89]). As Anderson et al reported in [7], there are researchers who have tried to propose a planning algorithm using different methods. The unique aim of all of these methods is to plan a safe vehicle path especially in obstacle avoidance conditions. The main importance of these approaches is that they do not rely on presumed desired path information, which make these methods implementable in a real situation. The authors continued with proposing an active safety framework that activates in hazardous situations and performs path planning, risk

assessment, and applies appropriate control actions to modify vehicle behavior. The only important external information available for the controller is the location of the edges of the drivable road (which are assumed to have been extracted from a forward-looking sensor).

2.4 Driver-in-the-Loop Control

Based on the amount of measurable information on the driver's desired path, the driver-in-the-loop control problem can be categorized into two main types. Most of the work in this field assumed that full information about the target path is available to the controller. However, there is another case in the closed driver/vehicle loop that has no information on the desired road available for the controller. To the best of the author's knowledge, nobody has addressed the control design problem for the driver/vehicle loop while path information is unknown. A schematic of the full-information control process is shown in Figure 1-2. In the case of full information, besides present and past information, finite future previews can also be used to determine the control action. For example, assuming knowledge on the desired path for the controller AFS is used in [148]. Preview control, as an alternative method in this category, is also proposed in [125] and [58]. Some research goes even further to propose electronic stability controllers that can guarantee lane keeping of race cars at the limit of their tire adhesion ([63, 80, 81, 140]). As an example, Talvala et al ([140]) presented a Lyapunov based stability condition and corresponding active steering controller for the vehicle's lane keeping with highly saturated tire behavior. The desired path for this controller is assumed to be available from a GPS integrated with an inertia navigation system (INS). One step ahead of this concept is designing fully automated vehicles by studying different projects, such as: Google, DARPA[7], and Audi TTS[8]. Unfortunately, the reliability of these projects is not still high enough to allow driving without human supervision and/or intervention.

Alternatively, one can consider road information as an unknown uncertainty in the system. Considering recent progress in solving LMIs, the H_∞ methods are now more effective in handling deterministic disturbance models with bounded energy ℓ_2 signals (see [82], [98]) . Regarding the robust control of a vehicle, recently some approaches have reported promising results in vehicle dynamic analysis (see [6, 49, 113, 151, 159] and the references therein).

In [113], a robust control method is proposed for the linear parameter varying (LPV) vehicle model that provides differential brake moments and front steering angles to improve vehicle stability. In the problem formulation, a driver model also is considered, where for certain bounded uncertainties (using a proposed controller), vehicle stability is guaranteed. The proposed method

[7] Defense Advanced Research Projects Agency

[8] http://news.stanford.edu/news/2010/february1/shelley-pikes-peak-020310.html

addresses a wide range of uncertainties in vehicle and driver modeling. However, the controller design availability of a predefined trajectory is assumed. Gaspar et al, in [49], modeled vehicle stability as an H_∞ problem, and addressed the problem using the corresponding robust control approach. Following these works, recently, Wu et al, proposed an integrated chassis control method which considers the driver-in-the-loop effects [151]. The authors took advantage of the H_∞ framework and considered the driver and the vehicle uncertainties, as well as proposed a method for robustly integrating active steering, longitudinal force compensation, and active yaw moment control. Also, an approach to designing the LPV controller for the integrated AFS and TV control is proposed and results are discussed in [159], however, the effect of the driver-in-the-closed-loop behavior is ignored.

On the other hand, in order to relax the assumptions about the availability of the desired road preview for the control block, online identification of the driver's behavior can be used to generate a time-varying model of the driver and apply it on the overall control scheme ([123], [42]). In [123], an online method is proposed for driver model identification in the control loop and then, a direct yaw control (DYC) algorithm is adapted based on the identified model. This approach, demonstrated in Figure 1-3, has rarely been considered by researchers. For a driver-in-the-loop analysis, the controller only has access to the driver model, driver inputs, and vehicle states.

2.5 Time Delay in Vehicle Analysis

Time-delay systems come from inherent time-delays in the components of the systems, or from the deliberate introduction of time-delays into the systems for control purposes. This phenomenon can be recognized in engineering, biology, physics, and ecology. It is well-known that time delay systems can be easily presented in a certain class of functional differential equations. A simple discrete delay element can be presented as follows in (Figure 2-5):

$$\overline{y}(k) = D_h\overline{u}(k) = \overline{u}(k \quad) \tag{2.4}$$

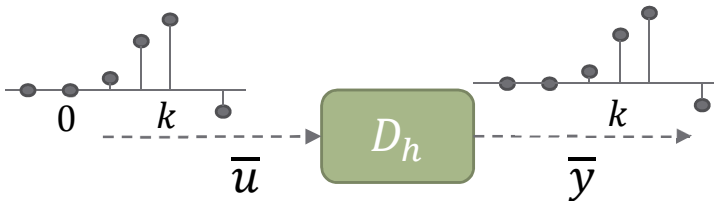

Figure 2-5: A simple delay operator

The existence of delay in a system usually causes performance degradation in the overall control loop, and in some cases, it even makes the overall system unstable. Consider the following continuous time state space representation of a system:

$$\begin{cases} x(t) = Ax(t) + Bu(t) \\ y(k) = x(t \quad d) \end{cases}, \; x(\tau) = \phi(\tau), \; \tau \in [\quad d, 0] \tag{2.5}$$

where $d > 0$ is a constant delay, x is the system state, and $\phi(.) \in C([\quad d, 0], R^n)$ is the functional initial condition. It is known that the time-delay systems are infinite -dimensional systems and the minimal information to define them properly in a function defined over the interval $[\quad d, 0]$. By applying two simple controllers of $u_1(t) = Ky(t)$, $u_2(t) = Ky(t)$, two main categories of delayed systems are obtained: retarded delayed systems:

$$x(t) = Ax(t) + BKx(t \quad d) \left(in\ gerenral\ form: x(t) = \sum_{i=0}^{r} A_i x(t \quad d_i) \right) \tag{2.6}$$

and neutral delayed systems:

$$x(t) \quad BKx(t \quad d) = Ax(t) \left(in\ general\ form: \sum_{i=0}^{r} E_i x(t \quad d_i) = \sum_{i=0}^{r} A_i x(t \quad d_i) \right) \tag{2.7}$$

In this proposal, the main focus is on are mostly dealing with retarded delayed systems. A thorough literature review of delay analysis and controller design is reported in [12, 21, 103].

There is a certain time period (time varying) required for a human driver to react properly in response to an observation. Although there are some publications reporting driver-in-the-loop control results, little consideration has been given to the delayed driver-in-the-loop control. Additionally, it is well-known that the existence of delay in a closed loop might be a contributing source of poor performance or even instability (See [102, 124, 135, 153]). Due to neuromuscular limitations, delays exist in the driver's observation, analysis, computation, and action. The significant effect of the neuromuscular system on vehicle control have been recently recognized as a very vital field of study, see [119]. There are also many other papers reporting the effects of delay on a dynamic system.

Treat et al, in [143], have listed some sources of a driver's delay, such as: careless driving, internal distractions (conversations, etc.), external distractions (accidents outside the vehicle), improper lookout (passing a vehicle), misjudgment (distance or speed of another vehicle), false assumption about another driver's decisions, and a driver's neuromuscular delay. In [25], Chen et al, published a closed loop driver/vehicle analysis, focusing on driver delays and their effects. They also proposed the control scheme (shown in Figure 2-6), which is designed as an adaptive smith predictor robust controller that is robust enough to model driver uncertainties and known constant delays of the driver.

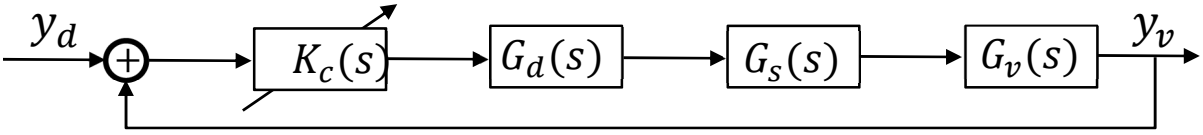

Figure 2-6 Robust adaptive smith predictor control design

In Figure 2-9, $K_c(s)$ is the adaptive controller, $G_s(s)$ is the smith predictor controller, $G_d(s)$ is the driver model transfer function and $G_v(s)$ is the linear bicycle vehicle model transfer function. A complete closed loop analysis in the frequency domain is presented in this paper, and effects of delay in driver is presented properly. However, as it is apparent from the control scheme, to provide error signal for adaptive controller of K_c , one still needs to know the desired path of the driver. A nice delay analysis for closed loop driver/vehicle has been reported by Liu et al, in [93]. These authors start with considering a bicycle vehicle model integrated with the nonlinear Pacejka tire model. The driver model is a simple model, which involves a loop gain (K), pilot visibility (L), and a cumulative driver delay of T_r. Hence, the steering input command is described as follows:

$$\delta(t) = K\left[y_N(t \quad T_r) + \frac{L}{v_x} y_N(t \quad T_r)\right] + Qcos(\omega_d(t)) \tag{2.8}$$

where v_x is the forward speed, $Qcos(\omega_d(t))$ represents the disturbance due to road surface irregularities with a frequency of ω_d, and y_N is the vehicle's lateral displacement with respect to the road's center line. Then, this driver model is combined with a state space form of the vehicle and after applying a linearization method, a retarded differential equation of the form $x(t) = A_0x(t) + A_1x(t \quad T_r)$, is obtained. The eigenvalues are computed using Fadeev algorithm [38],

and based on their values, an instability margin for different cases are calculated. For example, stability analysis in this paper shows the driver's delay and longitudinal speed as critical for certain car specifications and certain driver characteristics (K , L).

Stability results for delayed systems can generally be categorized into two main groups. The first one is to select a positive definite function and take the time derivative along the system solution; then, some negativity condition needs to be used for the calculated derivative. Usually, this method results in some LMI conditions. There is also another method of tackling the problem where the designer chooses a desired derivative function. Then, a function is calculated and computed based on the given derivative along the system's solution, and finally, the positive definiteness of the function is investigated. The former method is more complex, however, as the derivatives are adjusted based on the given derivative, the solution provides much more information about the system behavior. Regarding solving H_∞ control problems for uncertain discrete time retarded delay systems, recent results on networked control systems are useful. Miscellaneous techniques have been reported to stabilize the system with the lowest conservation. In [157], a complete survey on either delay-dependent or independent methods is presented.

2.6 Summary

Vehicle stability with a driver-in-the-control-loop has been the main subject of this chapter. Human and driver modeling methods have been reviewed and the most important approaches were presented. Several papers in the literature discussing driver-in-the-control-loop problem were reviewed. It was also mentioned that an important difficulty in solving this problem is the assumption of having access to information about the desired path of the driver. Presuming the availability of the desired path and considering different driver models, all of the previous research has tried to address the problem by minimizing the error between the driver decision and the driver model outputs. However, using current technology, this assumption is not easily implementable in the real situations. To the best of author's knowledge, nobody has addressed this problem without assuming knowledge of the desired path information. The main goal of this thesis is to propose a general design method for considering a human in the vehicle control loop system without using the desired road information.

"What we do may be small, but it has a certain character of permanence; and to have produced anything of the slightest permanent interest, is to have done something utterly beyond the powers of the vast majority of men."

A Mathematician's Apology, 1940, G. H. Hardly

Chapter 3
Vehicle and Human Driving Models

The first step analyzing vehicle behavior is understanding vehicle dynamics using appropriate mathematical modeling approaches. In normal driving conditions, cars respond to two different input sets based on its dynamic: inputs from the driver, which are communicated via the steering wheel and pedals (either acceleration, or brake), and environmental inputs such as the wind and road excitations. Generally, a vehicle can be described as an interconnected dynamic system composed of the vehicle body, the propulsion, the steering angle, and the suspension system. On the other hand, a vehicle's behavior can be judged based on different indices, such as ride, handling, performance, and safety. By considering each of these indices, a customized simplified/complex model can be adopted ([60, 99, 139]). In the rest of this thesis, the vehicle's handling is studied. As such, this chapter starts with a simplified bicycle model that describes the vehicle's handling behavior through stability analysis.

3.1 Bicycle Model

Nearly all natural and technological systems are driven by nonlinear processes. However, in some cases, corresponding linearized models describe the behavior of system around a specific operating point. This makes the analysis much easier. Considering the generalized form of Newton's second law for a group of small lumped masses, one can have the following equations of motions in the x, y, z directions to describe vehicle handling behavior:

$$\begin{aligned} \sum F_x &= m(\, v_x \quad r v_y) \\ \sum F_y &= m(\, v_x + r v_y) \\ \sum M_z &= I_z\, r \end{aligned} \tag{3.1}$$

where F_x and F_y are the external forces, M_z is the external moment, m is the vehicle's mass, I_z is the inertia, v_y is the lateral velocity, v_x is the longitudinal velocity, and r is the yaw rate. The above dynamic equations only describe the relationship between external forces and moments. A vehicle's mass, inertia and motions describe that vehicle's behavior only if the vehicle is considered to be a rigid body moving on a plane.

If the characteristics of the left and right tire are assumed to be the same — the vehicle body is symmetric about the longitudinal plane — then the lateral forces can also be considered equal. Consequently, the lateral dynamics of the vehicle can be simplified as follows ([76]):

$$\begin{gathered} m(v_x \quad rv_y) = F_{xf}cos\delta_f + F_{xr} \quad F_{yf}sin\delta_f \\ m(v_y + rv_x) = F_{yr} + F_{yf}\cos\delta_f + F_{xf}\sin\delta_f \\ I_z r = aF_{yf}\cos\delta_f \quad bF_{yr} + aF_{xf}\sin\delta_f \end{gathered} \tag{3.2}$$

where δ_f is the front steering angle. We also have the following relationship between the front/rear slip angles:

$$\alpha_f = \delta_f \quad \frac{ar + v_y}{v_x}, \alpha_r = \frac{br \quad v_y}{v_x} \tag{3.3}$$

where a is the distance from the center of mass to the front axle, b is the distance from the center of mass to the rear axis. Then, assuming that side-slip is small, the front/rear forces can be defined as follows:

$$F_{yf} = C_f\alpha_f, F_{yr} = C_r\alpha_r \tag{3.4}$$

where C_f, C_r are the front and rear tire cornering stiffness values, respectively. Hence, this prompts us to use the canonical linear, time-invariant dynamics of the following that describes the behavior in a constant longitudinal speed:

$$x(t) = A_v x(t) + B_v\delta(t) \tag{3.5}$$

$$\begin{matrix} v_y(t) \\ r(t) \\ y(t) \\ \psi(t) \end{matrix} = \begin{matrix} \frac{(C_f + C_r)}{v_x m} & \frac{(aC_f \quad bC_r)}{v_x m} \\ \frac{(aC_f \quad bC_r)}{v_x I} & \frac{(a^2 C_f + b^2 C_r)}{v_x I} \\ 1 & 0 \\ 0 & 1 \end{matrix} U + \begin{matrix} 0 & 0 \\ 0 & 0 \\ 0 & v_x \\ 0 & 0 \end{matrix} \begin{matrix} v_y(t) \\ r(t) \\ y(t) \\ \psi(t) \end{matrix} + \begin{matrix} \frac{C_f}{mG} \\ \frac{aC_f}{IG} \\ 0 \\ 0 \end{matrix} \delta(t)$$

where $x = [v_y \, r \, y \, \psi]^T$ is the state vector, and y is the lateral position of the vehicle corresponding to a fixed coordination system, G is the steering ratio between the hand wheel angle and the road wheel angle, and ψ is the yaw angle ($\delta_f = \delta$). All of the vehicle states are functions of time but their time arguments is suppressed. Figure 3-1 illustrates the schematic of a simple bicycle model.

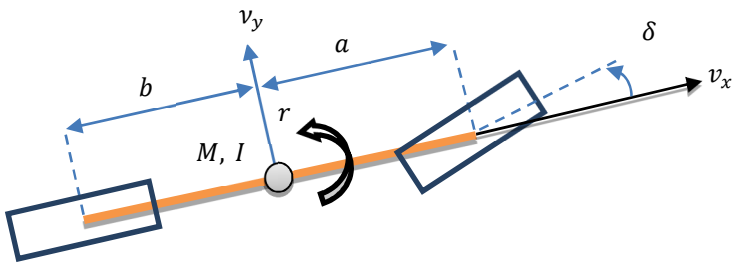

Figure 3-1 Simple bicycle model

The lateral and longitudinal velocities are:

$$\begin{cases} x(t) = U\cos\psi \quad v\sin\psi \\ y(t) = U\sin\psi + v\cos\psi \end{cases} \tag{3.6}$$

Note that for small yaw angles (ψ), the lateral velocity can be simplified as follows:

$$y(t) = v_x\psi + v_y \tag{3.7}$$

3.2 Path Follower Algorithm

Steering a car mainly involves adjusting various inputs to the vehicle such as the acceleration/brake pedal and the steering angle to make the car follow a desired path. Using the steering wheel, a driver matches a road's curvature while having the ability to maintain adequate distance from the edge of the lane. In this report, only the steering behavior of the driver is considered. Other control actions of the driver, such as adjusting the required torque by pushing the acceleration pedal and brake pedal, will be treated as system inputs. From this point of view,

a driver is a simple path follower who tries to minimize the difference of the vehicle's position and the predefined desired path. Among several methods in control theory for a path-follower controller, using an optimal controller for this task is further investigated. The model which is used here is based on Sharp's driver model presented in [129]. Sharp's model is an optimal path-follower (virtual driver) that uses multi-point future preview concepts as well as the LQR method to determine preview gains. Preview gains define the importance of both vehicle states with respect to feedback signals and errors between the vehicle's current and desired lateral positions. Figure 3-2 shows the driver's optical lever and desired path corresponding to each preview point. At each sampling time, T, a lateral position error in a fixed reference system – and transformed relative system of driver/vehicle – can be defined. Each lateral position error matches a lateral yaw angle error as well. Then, the optimal control problem can be formulated. Note that in this model, responding to external disturbances, such as cross-winds, crashes, or animal incursions is not considered.

A shift register updates the lateral position sample inputs for the path follower controller. In other words, the controller uses current lateral positioning of the vehicle and N_p samples of the future positions to produce up-to-date steering commands. Subsequently, the current lateral position value leaves the problem and a new value for y_{N_p} enters the system. The following model describes the shift register dynamic system:

$$y_r\,(k+1) = D y_r\,(k) + E y_{ri}\,(k)$$

$$D = \begin{matrix} 0 & 1 & 0 & 0 & 0 \\ 0 & 0 & 1 & 0 & 0 \\ & & & & \\ 0 & 0 & 0 & 1 & 0 \\ 0 & 0 & 0 & 0 & 1 \end{matrix}, E = \begin{matrix} 0 \\ 0 \\ \\ 0 \\ 1 \end{matrix} \tag{3.8}$$

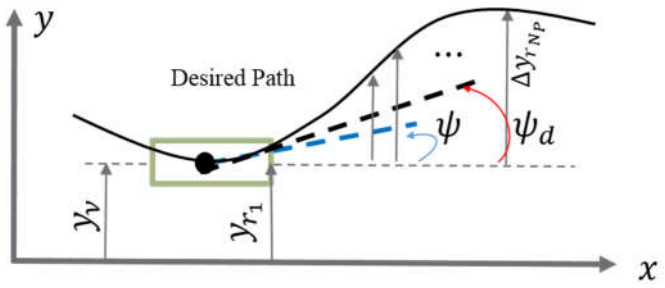

Figure 3-2 : preview points at each sampling time (Fixed and local reference system)

where $y_r(k) \in R^{N_P+1}$ is the road preview state, and y_{ri} is the new value which can be treated as white noise. Considering (3.8), the updated system is a discrete-time single input system. After augmenting it with discretized bicycle model (discretized using backward Euler at 200hz) of (3.5) one obtains:

$$v_y$$

$$\begin{gathered} w(k+1) = Fw(k) + E_1 y_i(k) + G\delta(k) \\ E_1 = \begin{bmatrix} 0 \\ E \end{bmatrix}, G_1 = \begin{bmatrix} B_v \\ 0 \end{bmatrix}, F = \begin{bmatrix} A_v & 0 \\ 0 & D \end{bmatrix} \\ w(k+1) = \begin{bmatrix} A_v & 0 \\ 0 & D \end{bmatrix} \begin{bmatrix} x_v \\ y_r \end{bmatrix} (k) + \begin{bmatrix} 0 \\ E \end{bmatrix} y_{ri}(k) + \begin{bmatrix} B_v \\ 0 \end{bmatrix} \delta(k), \end{gathered} \tag{3.9}$$

where

$$w = \begin{bmatrix} x_v \\ y_r \end{bmatrix} = \left[\overbrace{v_y \quad r \quad y_v \quad \psi}^{Vehicle} \qquad \overbrace{y_{r0} \quad y_{r1} \quad y_{r2} \quad y_{r3} \quad y_{rN_p}}^{Road\ preview} \right]^T \tag{3.10}$$

This is assuming the driver is akin to a controller with the aim of minimizing path tracking error and attitude angle error, as well as concurrently minimizing his/her effort. Now, defining the error term of the lateral velocity: $e_y = (y_v \quad y_0)$, and the error term between the yaw angle of the vehicle and the desired yaw angle: $e_\psi = (\psi \quad \psi_d) = (\psi \quad \frac{y_{r1}-y_{r0}}{v_x T})$, the following cost function establishes the corresponding optimal control problem:

$$J(N_p,k)=\sum_{j=0}^{N_p}\{e_l^T(k+j)Q_1e_l(k+j)+\delta^T(k+j)R_2\delta(k+j)\}$$
$$=\sum_{j=0}^{N_p}\{w^T(k+j)R_1w(k+j)+\delta^T(k+j)R_2\delta(k+j)\} \quad (3.11)$$

where N_P is the number of preview points that the driver uses for the steering task, $e_l=[e_y \quad e_\psi]^T$, R_1 is a positive semi-definite matrix to describe the system objectives, and R_2 is a positive scalar showing constraints on the command signal.

It shows that this cost function corresponds to error term and must be penalizes to zero. Using the fact that $y_{ri}(k)$ can be considered white noise, thus adding new road preview values to the system, the optimal problem is minimizing the expected value of (3.11) with the constraints of (3.9) under Gaussian noise excitation. When allowing N_p to approach infinity, the problem is converted to an algebraic Riccati equation (ARE). This takes advantage of the rich mathematical theory of the infinite horizon optimal control for LTI systems. An analytic closed form solution can be found below:

$$\delta(k)=(G_1^TP_\infty G_1+R)^{-1}G_1^TP_\infty Fw(k)=K_\infty w(k) \quad (3.12)$$

$$F^TP_\infty F \quad P_\infty \quad (F^TP_\infty G_1)(G_1^TP_\infty G_1+R_2)^{-1}(G_1^TP_\infty F)+R_1=0 \quad (3.13)$$

where:

$$K_\infty=[K_V \qquad K_p], \quad (3.14)$$

$$R_1=H^TQ_1H, Q_1=\begin{bmatrix}q_1 & 0\\ 0 & q_2\end{bmatrix}, H=\begin{bmatrix}0 & 0 & 1 & 0 & 1 & 0 & 0 & 0 & 0\\ 0 & 0 & 0 & 1 & \frac{1}{v_xT} & \frac{1}{v_xT} & 0 & 0 & 0\end{bmatrix}, R=1,$$

and q_1 ,q_2 are the weighting values for the lateral and yaw path errors, respectively. $K_V \in R^{1\times4}$ and $K_p \in R^{1\times N_p+1}$ are the state feedback and preview gains, respectively. T is the time step interval, R is the weighting on control effort which is the steering wheel angle, and P_∞ is the terminal weighting condition.

Thus:

$$R_1 = \begin{matrix} 0 & 0 & 0 & 0 & 0 & 0 & 0 & 0 \\ 0 & 0 & 0 & 0 & 0 & 0 & 0 & 0 \\ 0 & 0 & q_1 & 0 & q_1 & 0 & 0 & 0 \\ 0 & 0 & 0 & q_2 & \frac{q_2}{v_x T} & \frac{q_2}{v_x T} & 0 & 0 \\ 0 & 0 & q_1 & \frac{q_2}{v_x T} & \frac{q_2}{(v_x T)^2} + q_1 & \frac{q_2}{(v_x T)^2} & 0 & 0 \\ 0 & 0 & 0 & \frac{q_2}{v_x T} & \frac{q_2}{(v_x T)^2} & \frac{q_2}{(v_x T)^2} & 0 & 0 \\ 0 & 0 & 0 & 0 & 0 & 0 & 0 & 0 \\ 0 & 0 & 0 & 0 & 0 & 0 & 0 & 0 \end{matrix}$$

hence:

$$w^T R_1 w = q_1(y_v \quad y_{r0})y_v + q_2\left(\psi \quad \frac{y_{r0} \quad y_{r1}}{v_x T}\right)\psi \quad q_1(y_v \quad y_{r0})y_{r_0}$$
$$+ \frac{q_2}{v_x T}\left(\psi \quad \frac{y_{r0} \quad y_{r1}}{v_x T}\right)y_{r1} \quad \frac{q_2}{v_x T}\left(\psi \quad \frac{y_{r0} \quad y_{r1}}{v_x T}\right)y_{r0} = q_1 e_y^2 + q_2 e_\psi^2$$

Figure 3-2 presents a general schematic of the path follower and the vehicle-in-the-loop system.

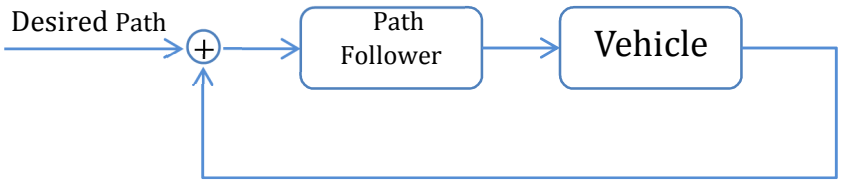

Figure 3-3: Path follower – vehicle closed loop schematic

Note that the calculation here is with respect to a fixed coordinate system; in real driving situations, the driver is steering the car based on his/her local moving position. In the fixed coordinate system, there is a fixed $x \quad axis$ and a driver who has knowledge on the positional relationship from the $x \quad axis$ in an absolute sense. However, in reality, the driver does not need any fixed coordinate reference and steers based on the relative position of the vehicle and anew the $x \quad axis$ at each step. The steering angle command, however, must be the same in both cases. An assumption is made that the $x \quad axis$, in its original position in fixed coordination, translates such that it passes through the vehicle's C.G. (See Figure 3-2). In this case, the global value of y reduces to zero. Thus, the value of $K_V(3)y$ will be zero in the feedback control of the local system.

Now, in order to have an invariant steering angle, the following condition needs to be upheld:

$$\delta_{fixed-coordination} = K_V(1)v_y + K_V(2)r + K_V(3)y + K_V(4)\psi + \sum_{i=1}^{N_p} K_p(i)\, y_i$$

$$\delta_{relative-coordination} = K_V(1)v_y + K_V(2)r + K_V(4)\psi + \sum_{i=1}^{N_p} K_p(i)\,(y_i \quad y)$$

$$\delta_{fixed-coordination} = \delta_{relative-coordination} \rightarrow K_V(3) = \sum_{i=1}^{N_p} K_p(i) \tag{3.15}$$

Similarly, the formulation must be invariant under the rotational shift. Thus, the term $K_V(4)\psi$ is lost and the i^{th} preview sample value is reduced by $(i \quad 1)v_x T\psi$. Consequently, the following relationship needs to be upheld:

$$v_x K_V(1) + K_V(4) = \sum_{i=1}^{N_p} (i \quad 1)v_x T K_p(i) \tag{3.16}$$

It is also worth mentioning that the preview points sufficiently far away from the vehicle have no effect on the current driver's decision. This results in the decaying of preview gains to zero for far enough points. As mentioned in [128], there are two main limitations in modeling drivers within this framework. The first limitation is the time invariance control structure, and the other is the assumption that future preview points can be assumed to be white noise disturbance, which is too rich in high frequency to represent a real road profile.

In order to show the effectiveness of the driver model, the 2 degrees of freedom (DOF) bicycle model vehicle described in (3.5), with the vehicle characteristics presented in Table 3-1, is considered. Simulation results show the steering behavior and the lateral position of vehicle through an ISO double lane change maneuver [136]. In the simulation procedure, one needs to calculate the state feedback (K_V) and the preview (K_P) gains. Hence, the first step is to convert the continuous vehicle model of (3.5) to discrete time. Weighting matrices of Q, corresponding to the lateral error, the yaw angle error of the path following task, and R are assumed:

$$Q = \begin{bmatrix} 0.25 & 0 \\ 0 & 100 \end{bmatrix}, R = 1$$

These values are chosen such that the model and the real driver agree [118]. The following figures show that the model has followed the desired path with high accuracy when the preview time is $N_p T$. According to [83], the preview distance is approximately 1.5 seconds into the future.

Table 3-1: Vehicle parameters

Variable	Value	Units	Description
C_f	88310	$\frac{N}{rad}$	Front-axle cornering stiffness
C_r	64076	$\frac{N}{rad}$	Rear-axle cornering stiffness
a	0.913	m	Front axle to center of mass distance
b	1.73	m	Rear axle to center of mass distance
m	1673	kg	Vehicle mass
I	2250	$kg.m^2$	Vehicle yaw moment of inertia
G	16		Hand wheel to road wheel angle ratio

The following figures present effects of a pure path follower in the vehicle loop. As depicted, the lateral position of a closed loop vehicle, shown by the dotted red line, is compared to the exact desired path of the driver. An open loop bicycle vehicle model produces the desired path data. The steering angle feeds to the open loop system to produce the desired path. Using this method, vehicle limitations are also considered. The path follower produces the steering angle for the vehicle based on the desired road preview points. This steering angle feeds into the vehicle dynamics. Then, using the vehicle response and upcoming future preview points, a new steering signal will be generated by the path follower block. Figure 3-4 shows the standard double lane change scenario and how the path follower steers the vehicle. The lateral position error small and for the given speed, with a preview time of $t = N_p T = 1.5s$, the path follower performs well.

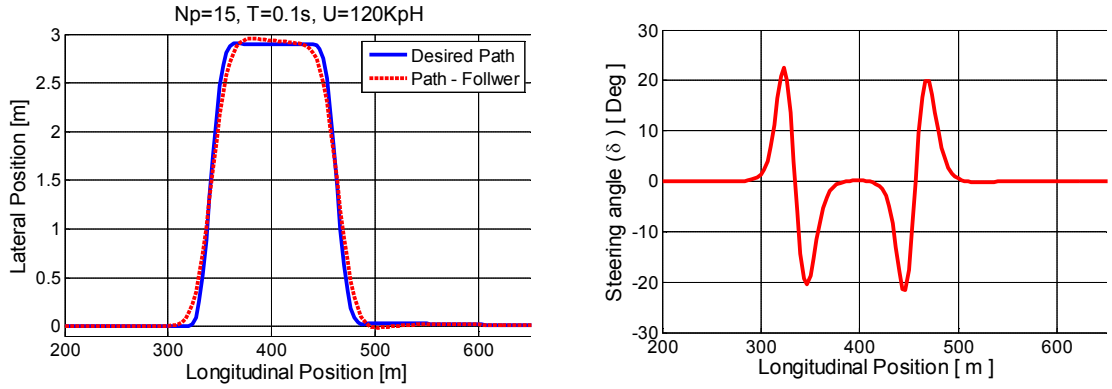

Figure 3-4 Lateral position and steering angle of a path follower driven vehicle @T=0.1, v_x=120, $N_p = 15$

Note that the number of preview points (N_p) are highly dependent on the vehicle's longitudinal speed and the desired path curvature. Figure 3-5 shows the path follower route alongside the desired path route during tracking tasks. In the first case on the left side, the future preview time is reduced. As a result, the closed loop system did not track the desired path accurately. This lateral position error is caused by the decreased preview time. Conversely, the right side figure demonstrates that increased preview time improves the closed loop vehicle behavior. In the former case, the future preview time is increased to $t = 1.5$ seconds.

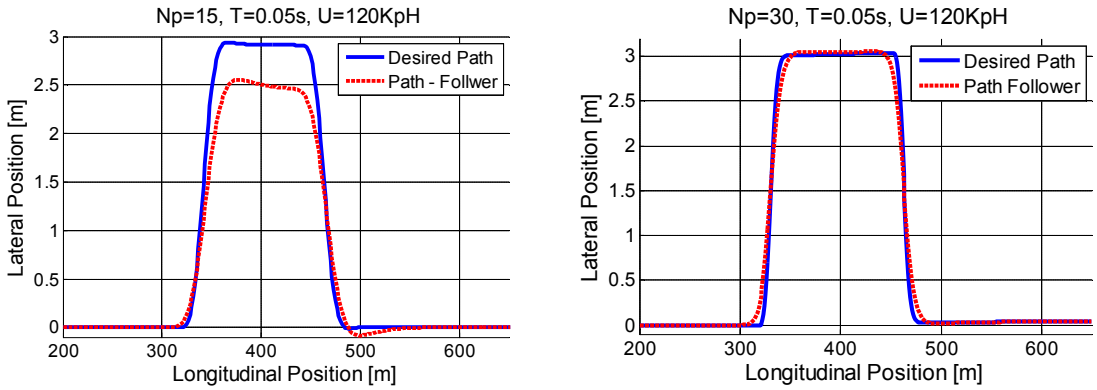

Figure 3-5 Lateral position of a path follower driven vehicle

@ $N_p = 15$ T=0.05, U=120 and @ $N_p = 30$, T=0.05, U=120

3.3 Human Modeling

There are some fundamental properties for nearly all drivers when studying humans in a vehicle control loop or during human-machine interaction. The most important part is that driver is not a linear element. In other words, the reaction time of a driver is a function of human brain processes and the neuromuscular action. From the moment an observation is made, analyzed, computed by the brain, and an action is made accordingly; a certain time has elapsed (see Figure 3-6). Based on this assumption of the linear path-follower described modeling in the previous section, one can assume that the driver has a total time delay of τ_d, which contains all of the delay sources. Considering N_d as the number of delayed samples, it is assumed that the action of a driver at time t is based on observations made at time: $t \quad \tau_1 \quad \tau_2$. The reaction the driver makes accordingly occurs at time: $t \quad \tau_2$. Thus, regarding the linear model of path-follower, it is assumed that the driver has a total delay of $\tau_d = \tau_1 + \tau_2$, then $\tau_d = N_d\, T$ (T is sampling time).

Augmenting steering (3.12) and the vehicle dynamics of (3.9) describe the closed loop behavior of vehicle as follows:

$$w(k+1) = (F + G_1 K_\infty) w(k) + E_1 y_i(k) \tag{3.17}$$

where,

$$w(k+1) = [x_{1v} \quad x_{nv} \quad y_{1i} \quad y_{Ni}]^T(k+1) =$$

$$\begin{matrix} a_{11} & a_{12} & a_{1n} & 0 & a_{1y_{r2}} & a_{1y_{rN}} \\ a_{n1} & a_{n2} & a_{nn} & 0 & a_{ny_{r2}} & a_{ny_{rN}} \\ 0 & 0 & 0 & 0 & 1 & 0 \\ 0 & 0 & 0 & 0 & 0 & 1 \\ 0 & 0 & 0 & 0 & 0 & 0 \end{matrix} \begin{matrix} x_{1v} \\ x_{nv} \\ y_{1i} \\ y_{Ni} \\ 0 \end{matrix} (k) + \begin{matrix} 0 \\ 0 \\ 0 \\ 1 \\ 0 \end{matrix} y_{new}$$

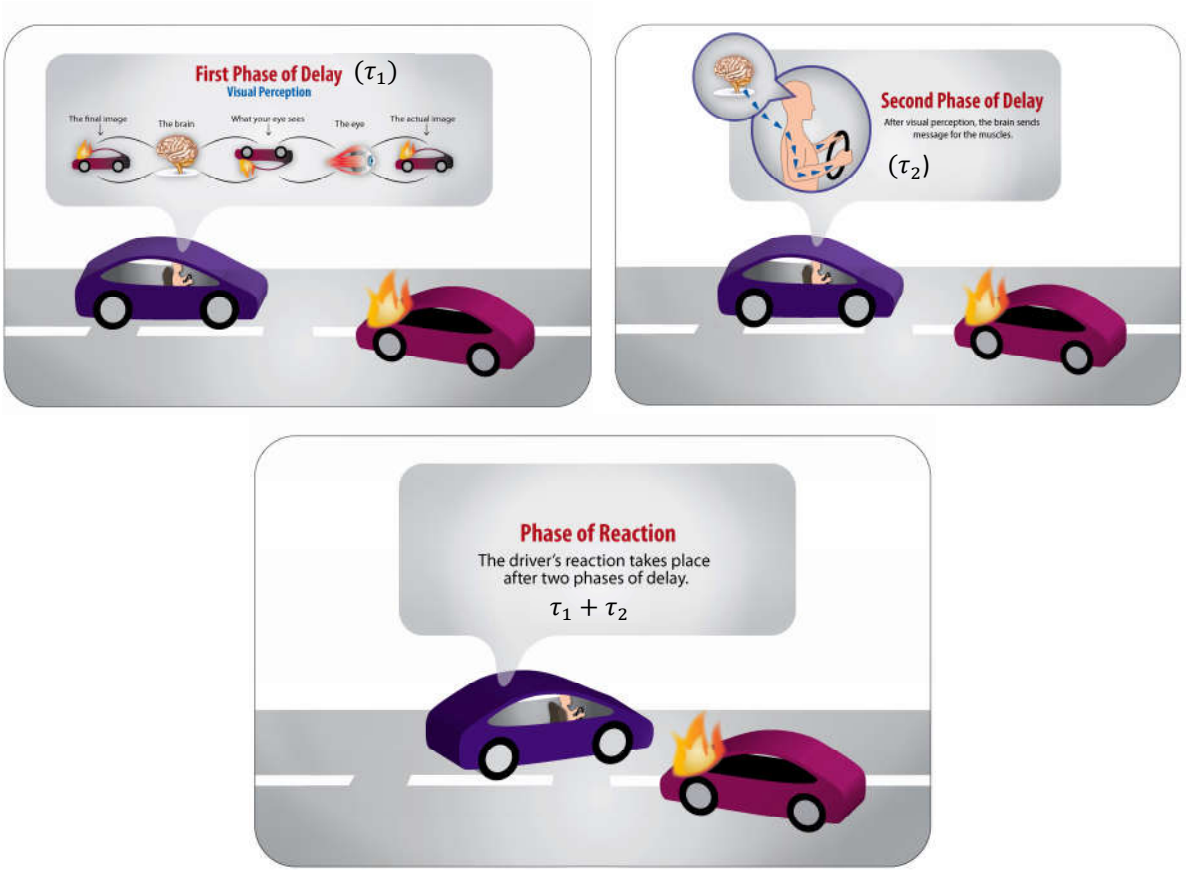

Figure 3-6: Total Driver's delay

In order to show the effects of time-delay on the closed loop system behavior, a delay block is added to the path follower (Figure 3-6). In order to introduce a steering angle input delay to the overall dynamic, one only needs to change the state space description of (3.17) as follows:

$$w(k+1) = Fw(k) + G_1 K_\infty w(k \quad N_d) + E_1 y_i(k) \tag{3.18}$$

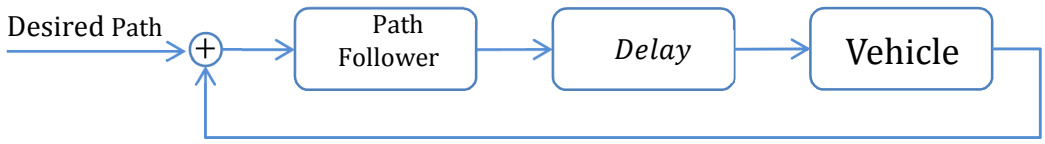

Figure 3-7: Closed loop driver (path follower + delay) in the loop vehicle modeling

To show the effects of a driver's delay on the overall system, the behavior of the vehicle in the standard double lane change maneuver is simulated. Different driver delays are shown when tracking the same desired path with the same longitudinal velocity of $120\ km/\ r$. Figure 3-8 and Figure 3-9 show that as the delay increases from $50\ ms$ to $200\ ms$, the performance of the vehicle degrades. For a maneuver scenario with this longitudinal speed, increasing the delay to 250 ms makes the overall system unstable. For the simulations, vehicle specifications given in Table 3-1 have been used.

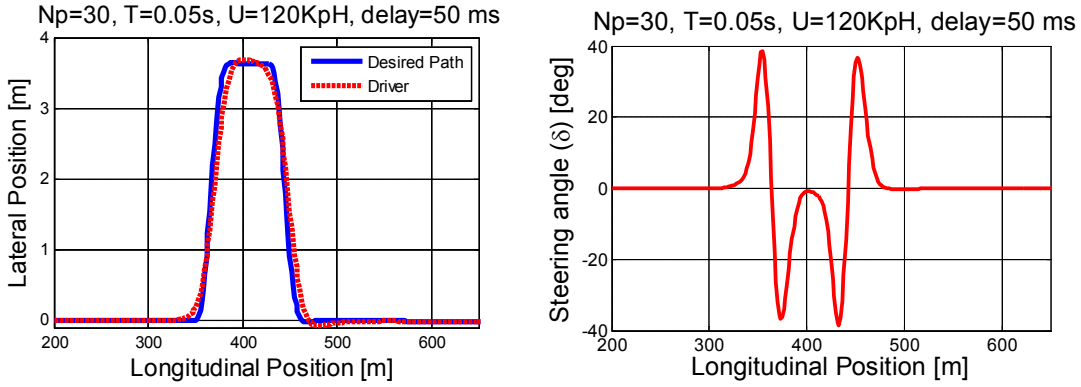

Figure 3-8 Effect of delay in driver in the loop vehicle system (Lateral position and steering angle)

@ $N_p = 30$ T=0.05, U=120, delay=50ms

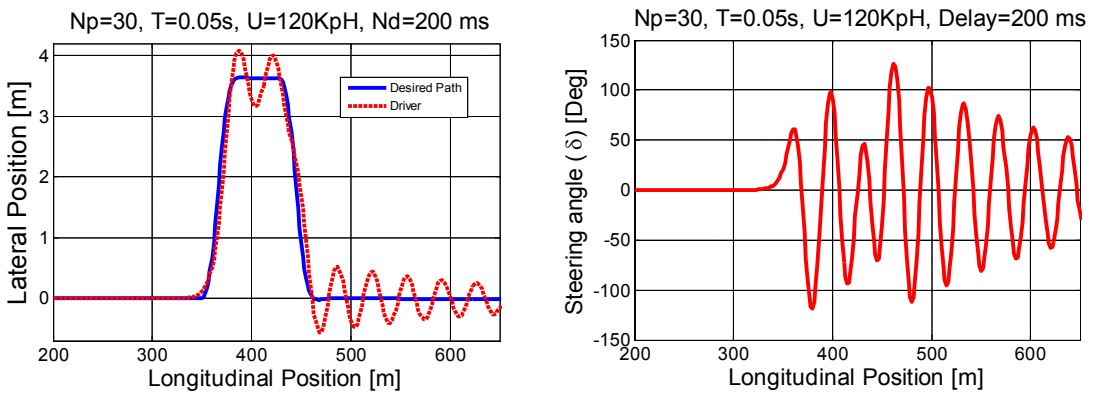

Figure 3-9 Effect of delay in driver in the loop vehicle system (Lateral position and steering angle)

@ $N_p = 30$ T=0.05, U=120, delay=200ms

In order to further investigate the effects of longitudinal velocity and time delay, the norm of summation of the lateral error is plotted versus the time delay and velocity. Figure 3-10 shows that as the delay and velocity increases, the lateral error also increases. This makes sense in a real-world driving situation.

$$v_x = 50 \rightarrow 70\ kp \quad , N_p = 200, T = 0.01s, \qquad N_d = 15 \rightarrow 20$$

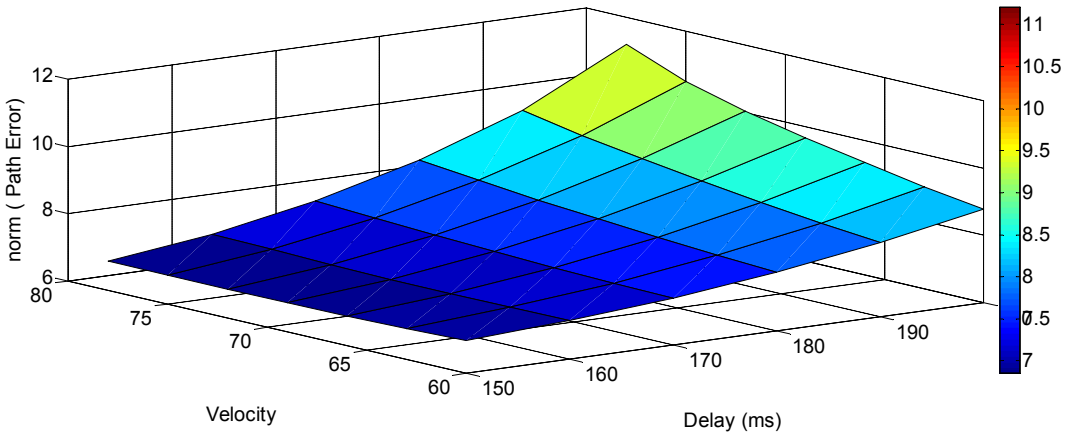

Figure 3-10 Norm of lateral position error versus variation in driver's delay and velocity

The following section presents driver delay effects using a more accurate car model. The CarSim software is employed for vehicle dynamics and driver simulation. The driver model that is used in this software has an optimal preview driver, which works on the same strategy that has been presented here. The model parameters are adopted based on the vehicle specifications presented in Table 3-1. The time preview is assumed to be $1.1\ seconds$ into the future, and the desired path is based on real driving data extracted from driving tests. Figure 3-12 shows the

lateral position of the vehicle that tracks the predefined desired path, and the driver is modeled as a pure path follower robot without any delay in sensing and acting. The simulation shows the effect of the path follower. Increasing the delay to $200\,ms$ in the tracking task leads to poor vehicle behavior. This is illustrated in Figure 3-11.

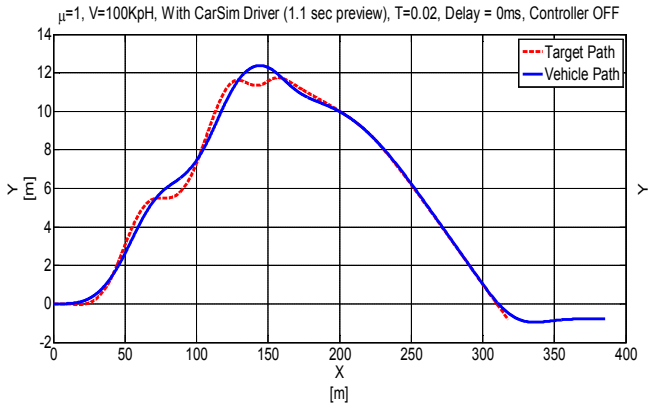

Figure 3-12 Driver's delay effect simulation in CARSIM

@ v_x =100 kph, delay=0

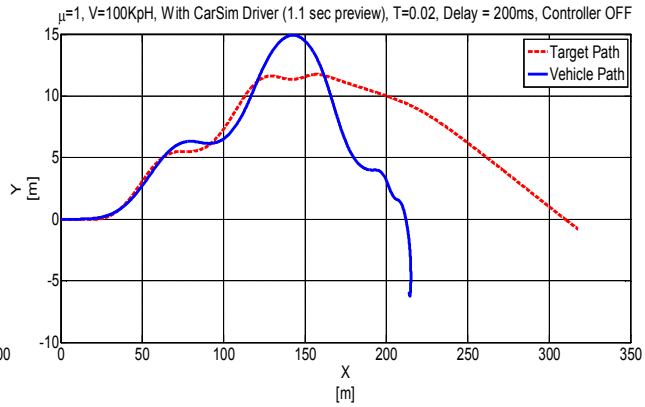

Figure 3-11 Driver's delay effect simulation in CARSIM

@ v_x =100 kph, delay=200 ms

3.4 Summary

The general vehicle dynamic equations were presented in this chapter. For the sake of simplicity, a linearized model of the vehicle for constant speed was used in the analysis and a state space form of the equation was presented. Next, using a path follower algorithm, the driver was modeled. It was assumed that the driver's goal is to minimize both the lateral position and the yaw angle error between the vehicle state and the desired path. The observation and reaction delay of the driver also are lumped into a block and considered in the model. The simulations show the deteriorative effect of the driver's delay in vehicle stability and performance. It can be inferred from the simulations that as the driver's delay and the vehicle's speed increase, the vehicle's performance decreases. This demonstrates that considering the driver model is very important in a vehicle dynamic analysis.

"A man who is always asking 'Is what I do worth while?' and 'Am I the right person to do it?' will always be ineffective himself and a discouragement to others."

A Mathematician's Apology, 1940, G. H. Hardly

Chapter 4
Controller Design with Driver-in-the-Loop

Now that a closed loop driver-vehicle model is developed, the next step is controller design for the system. The main aim of this design is to improve the overall vehicle control considering the driver dynamics and delay. Most of the publications in this field are limited to stability control at vehicle levels without taking into consideration that the driver also affects the overall system's performance. A few other researchers have tried to solve the closed loop problem by assuming accessibility of the future road information for the controller. Here, a new method is proposed that guarantees closed loop stability without requiring knowledge of future road geometry. Time varying bounded driver's delay and other bounded uncertainties of driver modeling is also considered in the controller design. Using this control method, an active front steering controller is designed.

4.1 Basic Vehicle Control Problem

As the safety system in a vehicle detects a large side slip angle or discrepancy between the vehicle's yaw-rate and the desired value, it generates the appropriate amount of yaw moment to correct the vehicle path and keep the vehicle operating point in the linear regime.

The fundamental aspect of an advanced vehicle stability system is to augment vehicle directional stability by inducing the correcting yaw moment on the vehicle. A driver's steering wheel angle, yaw-rate (measurement), longitudinal and lateral velocity (estimation), and slip-ratio (estimation) are the main signals that a conventional vehicle stability module uses directly in the control process. Besides that, the slip controllers are responsible for maintaining the wheel longitudinal slip ratio in a small neighborhood of a certain desired value based on road condition and vehicle state. A vehicle without traction control suffers from low acceleration and loss of drivability at low friction surfaces caused by high tire slip-ratios. Also, slip-ratio may degrade the performance of the stability controller dramatically. When a driver or autonomous system attempts a harsh maneuver, the vehicle might show nonlinear behavior since the vehicle may near the limit of road

traction. Since the driver or autonomous system expects a linear response, their action can result in a rear spin out or a front plow out. It is very hard for an average driver to regain control in this situation. A vehicle controller can adjust the individual wheel torques to change the vehicle's heading in an appropriate fashion. Recent developments in the realm of convex optimization open the way toward a reliable yet computationally traceable approach to merge path-planning and driver-in-the-loop problems with vehicle safety analysis.

4.2 Active Front Steering Controller

The active front steering controller (AFS) adjusts the driver's steering angle command based on the state of the vehicle. A general schematic overview of the AFS system is depicted in Figure 4-1.

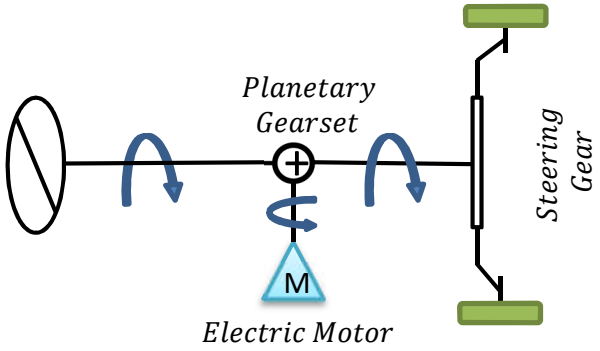

Figure 4-1 AFS Schematic view

Recalling the closed loop driver-vehicle dynamic model described in Section 0, a simple active steering controller can be modeled as follows:

$$w(k+1) = Fw(k) + G_1 K_\infty w(k) + E_1 y_i(k) + B_{AFS}\delta_{AFS} \tag{4.1}$$

where the parameters are as previously defined in Section 0; B_{AFS} is the control actuator, and δ_{AFS} is the steering angle adjustment that needs to be added to the driver's steering angle. To design the controller for a closed loop system, two main approaches may be used. These are detailed in the rest of this chapter.

4.3 Controller Design Considering Effects of Driver

4.3.1 Desired Road Information is Available

Assuming that the future road preview is a measurable signal for a controller, one can use many different control methods to stabilize the vehicle. Note that for cases where this information is available most of the time, there is no need for a driver model. The controller only needs to track the signals coming from the path following block. In the path following module, the algorithm finds the best possible way of performing a maneuver. It is obvious that with the utilization of upcoming road characteristics, a controller can guarantee lateral stability and good performance of the vehicle's linear model. Assuming this case, a desired set of values are considered for each of the vehicle states. Then the controller adjusts the input commands of the vehicle based on comparing the target states with the actual measurements or estimations. It is generally accepted that the following algebraic equation presents the state's desired values corresponding to the steering angle input and the longitudinal velocity:

$$r_d = \min\left(\delta\left(\frac{v_x}{l + K_{us}v_x^2}\right), \frac{a_{y-max}(\mu g) \quad a_y}{v_x} \quad r\right), \qquad v_{yd} = \begin{cases} v_y & |v_y| \le V_{ytrsh} \\ 0 & ot \ \ erwise \end{cases} \quad (4.2)$$

where v_{ytrsh} is a tunable threshold for lateral velocity, r_d is the desired yaw rate, $K_{us} = \frac{mb}{lC_{\alpha f}}$ $\frac{ma}{lC_{\alpha r}}$ is the under/over/natural steer stability coefficient, and $l = a + b$ is the wheelbase. r_d in (4.2) ensures that in a normal driving condition on dry or wet road, the vehicle should follow the command of the driver as much as possible. The other desired state is the lateral velocity v_{yd}, which mostly is considered to be zero. Although it is known that this state cannot be zero when there is a non-zero steering wheel angle, the desired value for the lateral velocity still can be approximated as zero.

In order to design a tracking controller, one also needs to have the desired values for other vehicle states in modeling, specifically the lateral position and the yaw angle. For cases where the controller has access to future road information, it is trivial to define a lateral position error and a yaw angle error, and then design the controller to reduce these errors. Whenever the driver tries to steer such that the vehicle deviates from the target, the controller applies appropriate adjustments to bring the vehicle back on the right track while maintaining the vehicle in its stable behavior region. Figure 4-2 shows a typical scheme of this type of controller, which uses future

information. It is clear that in this case, the linear bicycle model and the driver-in-the-loop system can always be controlled without considering the characteristics of the driver.

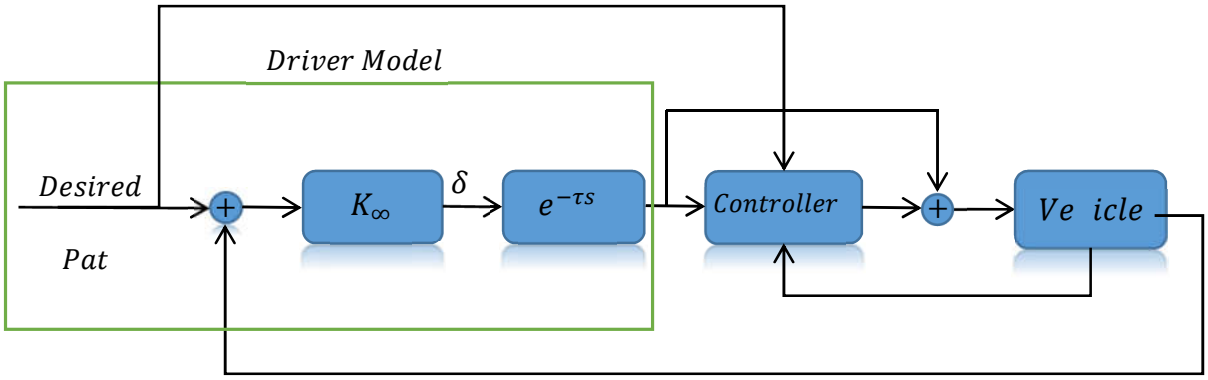

Figure 4-2 Controller design with road profile information

4.3.2 Desired Road Information is not Available

When devising an applicable design, one of the greatest restrictions for the controller is the absence of future road preview points. In spite of the existence of GPS, proximity sensors, haptics, and vision sensors that help provide useful information, all of which can be used to estimate the desired path, the driver's intention still remains difficult for the controller to determine. Note that, the desired path in this case may only be predicted for certain situations. Therefore, the are main interest is in developing a method to improve the overall performance of the vehicle for a range of different driving styles by only using the current vehicle states. Figure 4-3 shows the proposed AFS control scheme that adjusts the steering wheel angle input of the driver to make the system stable. Considering Equation (3.17) again and applying the AFS controller, the dynamic behavior can be rewritten as ([78]):

$$w(k+1) = Fw(k) + \overbrace{G_1 K_V x_v(k)}^{Driver-vehicle} + \overbrace{G_1 K_p y_{ri}(k)}^{Driver-vehicle} + E_1 y_i(k) + \underbrace{G_1 u(k)}_{Controller} \qquad (4.3)$$

The discrete dynamic state Equation (4.3) demonstrates that the driver/vehicle closed loop dynamics is composed of the vehicle states, the controller adjustment signal, and the driver's steering input. We assume that the desired lateral position is unknown information and a

bounded uncertainty for the system. Given this dynamic system, the vehicle states of the lateral velocity and the yaw rate are the only parameters that can be controlled directly (where corresponding desired values are available). We can reduce the model to a discrete vehicle model as:

$$x(k+1) = Ax(k) + B[\delta(k) + u(k)] \tag{4.4}$$

$$x(k+1) = Ax\,(k) + Bk_v x\,(k) + B\omega(k) + \ Bu(k) \tag{4.5}$$

where $x = [v_y \quad r]^T$, $A \in R^{2\times2}, B \in R^{2\times1}$ are matrices with entries defines by $A(i,j) = F(i,j), B(i,j) = G_1(i,j), k_v(i) = K_V(i)$ for $i,j \in \{1,2\}$, where F and G_1 were defined in (3.9). $\omega\,(k) = \ K_p y_{ri}\,(k) + K_V(3)x_v(3) + K_V(4)x_v(4)$. In (4.5), the value of the steering angle of $\delta(k)$ is substituted by its definition, which contains the preview point effects and the current vehicle state effects. The term $Bk_v x\,(k)$ in (4.5) represents the effect of the vehicle state in the steering angle command. Now, one can add a delay to complete the closed loop vehicle/driver formulation. When considering the driver's delay, Equation (4.5) can be rewritten to:

$$x(k+1) = Ax(k) + Bk_v x(k \quad d(k)) + B\omega(k) + \ Bu(k) \tag{4.6}$$

Taking into consideration that for the controller design, $\omega(k)$ is assumed to be unknown bounded information. For the design procedure, there is no difference between $\omega(k)$ and $\omega(k \quad d(k))$.

The problem is now formulated as a standard regulation problem of a retarded-time-delay system with an unknown bounded uncertainty. The H_∞ method can solve this problem appropriately. In the following section, a method for H_∞ regulation is proposed.

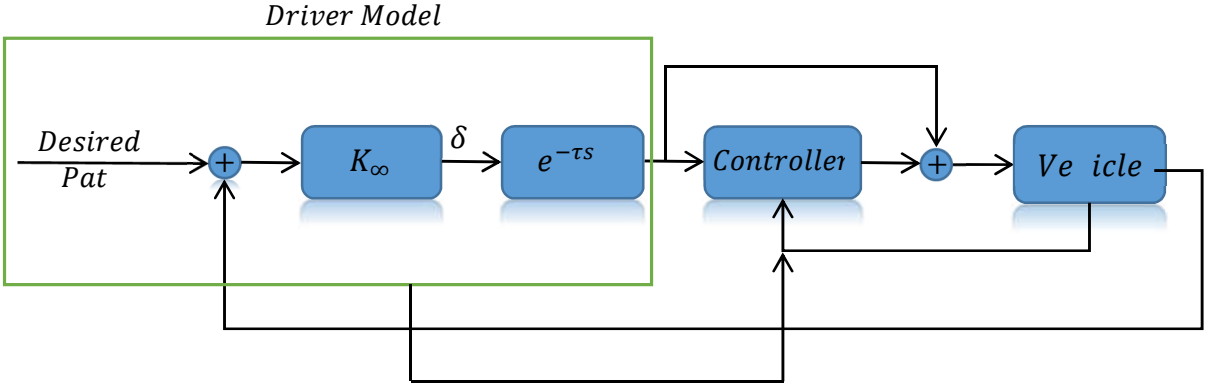

Figure 4-3 Closed loop controller design scheme without relying on future desired road profile

4.4 H_∞ Controller Design for Discrete Delayed Linear Time Invariant system

In this section, a static feedback controller $u(k) = Kx(k)$ is designed to stabilize the overall system and concurrently minimize attenuations from the parameter of γ in $\|z\|_2 \leq \gamma\|\omega\|_2$. Based on the available information about delay for H_∞ controller, there are two classes of delay-dependent and delay-independent controllers. When the time-delay is small, using a delay-dependent strategy for the controller design process provides better results in the sense of conservation. Since a delay in the driver-in-the-loop system is not very significant, a delay-dependent approach is chosen for the design. In order to make the overall design procedure more applicable, an unknown delay with known upper and lower bounds is considered.

Consider the following uncertain discrete-time retarded delay system with a time-varying delay:

$$\sum_0 : \begin{array}{c} x(k+1) = Ax(k) + A_d x\big(k \quad d(k)\big) + B_1\omega(k) + B_2 u(k), \\ z(k) = Cx(k), \\ y(k) = Cx(k) \\ x(k) = 0, \quad d_M \leq k \leq 0, \end{array} \tag{4.7}$$

where $x(k)$ is the state, $u(k) \in \quad ^m$ is the control input vector, $\omega(k) \in R^q$ is the exogenous disturbance signal assumed to belong to $\ell_2[0,\infty)$, and $z(k) \in R^p$ is the control output to be attenuated. Matrices $A, A_d, B_1, B_2,$ and C are assumed to be constant and with appropriate dimensions; $d(k)$ is a time-varying delay satisfying: $0 < d_m \leq d(k) \leq d_M$.

The control objective is to synthesize an admissible controller K that internally stabilizes the plant while also minimizing (attenuating) the H_∞ norm of the resulting closed-loop transfer function matrix from ω to z. The goal is designing a static controller to make the system stable while considering the effects of a bounded time varying delay and an exogenous input caused by the driver's steering angle, according to future road profile.

The first step is the stability analysis of the open loop delayed system ($u(k) = 0$). The following theorem, which is a modified version of theorem 1 in [59], gives a condition on the stability of the overall system (4.7). Note that throughout the rest of paper, I is the identity matrix and $P > 0$ (respectively, $P \geq 0$) means that matrix P is positive (respectively, positive semi) definite, and "*" denotes the symmetric term of a symmetric matrix.

4.4.1 Stability Analysis of Discrete System with Delay

Theorem 4.1: For the given lower and upper delay bound (d_{m} and d_M), and the attenuation coefficient of $\gamma > 0$, the system (4.7) is stable for $\omega(k) \in \ell_{2\epsilon}$ and $u(t) = 0$, if there exist matrices $T_1, T_2, N = [N_1^T \quad N_2^T \quad N_3^T \quad N_4^T \quad N_5^T]^T, M = [M_1^T \quad M_2^T \quad M_3^T \quad M_4^T \quad M_5^T]^T$ and symmetric matrices $P > 0,\ Q_1 > 0, Q_2 > 0$, and $Z \geq 0$ such that the following LMI is feasible:

$$\phi = \phi^T = \begin{bmatrix} \Phi & d_M N & d_{12} M & C_1^T \\ & d_M Z & 0 & 0 \\ & & d_{12} Z & 0 \\ & & & I \end{bmatrix} < 0 \tag{4.8}$$

where

$$\Phi = \Phi^{\mathrm{T}} = \begin{matrix} \phi_{11} & \phi_{12} & \phi_{13} & \phi_{14} & \phi_{15} \\ & \phi_{22} & \phi_{23} & M_2 & \phi_{25} \\ & & \phi_{33} & \phi_{34} & \phi_{35} \\ & & & \phi_{44} & \phi_{45} \\ & & & & \phi_{55} \end{matrix} \in R^{(4n+m)\times(4n+m)},$$

$$\phi_{11} = (d_M \quad d_m + 1)Q_1 + Q_2 \quad T_1(A \quad I) \quad (A \quad I)^T T_1^T + N_1 + N_1^T \in R^{n\times n},$$
$$\phi_{12} = P + T_1 \quad (A \quad I)^T T_2^T + N_2^T \in R^{n\times n},$$
$$\phi_{13} = \quad T_1 A_d + N_3^T \quad N_1 + M_1 \in R^{n\times n},$$
$$\phi_{14} = N_4^T \quad M_1 \in R^{n\times n}, \phi_{15} = \quad T_1 B_1 + N_5^T \in R^{m\times n},\ \phi_{22} = P + d_M Z + T_2 + T_2^T \in R^{n\times n},$$
$$\phi_{23} = \quad T_2 A_d \quad N_2 + M_2 \in R^{n\times n}, \phi_{24} = \quad M_2 \in R^{n\times n},\ \phi_{25} = \quad T_2 B_1 \in R^{m\times n},$$
$$\phi_{33} = \quad Q_1 \quad N_3 \quad N_3^T + M_3 + M_3^T \in R^{n\times n},\ \phi_{34} = \quad N_4^T + M_4^T \quad M_3 \in R^{n\times n},$$
$$\phi_{35} = \quad N_5^T + M_5^T \in R^{m\times n}, \quad \phi_{44} = \quad Q_2 \quad M_4 \quad M_4^T \in R^{n\times n}, \quad \phi_{45} = M_5^T \in R^{m\times n},$$
$$\phi_{55} = \quad \gamma^2 I \in R^{m\times m}, \quad d_{12} = d_M \quad d_m, C_1 = [C \quad 0]$$

PROOF:

This theorem is a special case of Theorem 1 of [59]. The proof is provided here to have a self-contented presentation. Let

$$y(k) = x(k+1) \quad x(k) = (A \quad I)x(k) + A_d x\big(k \quad d(k)\big) + B_1 \omega(k), \tag{4.9}$$

Then,

$$x(k) = \sum_{l=k-d(k)}^{k-1} y(l) + x\big(k \quad d(k)\big),$$
$$x\big(k \quad d(k)\big) = \sum_{l=k-d_M}^{k-d(k)} y(l) + x(k \quad d_M), \tag{4.10}$$

Consider the following Lyapunov-Krasowski function:

$$V(k) = \sum_{i=1}^{4} V_i(k)$$
$$V_1(k) = x^T(k)Px(k), \qquad V_2(k) = \sum_{\theta=-d_M+1}^{0} \sum_{l=k-1+\theta}^{k-1} y^T(l)Zy(l)$$
$$V_3(k) = \sum_{\theta=-d_M+2}^{-d_m+1} \sum_{l=k-1+\theta}^{k-1} x^T(l)Q_1x(l) + \sum_{l=k-d(k)}^{k-1} x^T(l)Q_1x(l), \tag{4.11}$$
$$V_4(k) = \sum_{l=k-d_M}^{k-1} x^T(l)Q_2x(l)$$

where $P = P^T > 0$, $Q_i = Q_i^T > 0$, $i = 1,2$ and $Z = Z^T > 0$ are to be determined. Taking the derivative ($\Delta V(k) = V(k+1) \quad V(k)$) of the Lyapunov function along the solution path yields:

$$\Delta V_1(k) = x^T(k+1)Px(k+1) \quad x^T(k)Px(k) = 2x^T(k)Py(k) + y^T(k)Py(k),$$
$$\Delta V_2(k) = d_M y^T(k)Zy(k) \quad \sum_{l=k-d_M}^{k-1} y^T(l)Zy(l)$$
$$= d_M y^T(k)Zy(k) \quad \sum_{l=k-d(k)}^{k-1} y^T(l)Zy(l) \quad \sum_{l=k-d_M}^{k-d(k)-1} y^T(l)Zy(l)$$
$$\Delta V_3(k) = (d_{12}+1)x^T(k)Q_1x(k) \quad x^T\big(k \quad d(k)\big)Q_1x\big(k \quad d(k)\big) \quad \sum_{l=k-d_m}^{k-d_M+1} y^T(l)Zy(l)$$
$$\leq (d_{12}+1)x^T(k)Q_1x(k) \quad x^T\big(k \quad d(k)\big)Q_1x\big(k \quad d(k)\big),$$
$$\Delta V_4(k) = x^T(k)Q_2x(k) \quad x^T(k \quad d_M)Q_2x(k \quad d_M),$$

Hence,

$$\Delta V(k) \le 2x^T(k)Py(k) + y^T(k)Py(k) + d_M y^T(k)Zy(k) \sum_{l=k-d(k)}^{k-1} y^T(l)Zy(l)$$
$$\sum_{l=k-d_M}^{k-d(k)-1} y^T(l)Zy(l) + (d_{12}+1)x^T(k)Q_1x(k)$$
$$x^T\big(k \quad d(k)\big)Q_1x\big(k \quad d(k)\big) + x^T(k)Q_2x(k)$$
$$x^T(k \quad d_M)Q_2x(k \quad d_M).$$

Defining $\zeta(k) = \big[x^T(k) \quad y^T(k) \quad x^T\big(k \quad d(k)\big) \quad x^T(k \quad d_{\mathrm{M}}) \quad \omega^T(k)\big]^T$, the following equations hold:

$$2\zeta^T(k)N\left(x(k) \quad x\big(k \quad d(k)\big) \quad \sum_{l=k-d(k)}^{k-1} y(l)\right) = 0 \tag{4.12}$$

$$2\zeta^T(k)M\left(x\big(k \quad d(k)\big) \quad x(k \quad d_M) \quad \sum_{l=k-d_M}^{k-d(k)-1} y(l)\right) = 0 \tag{4.13}$$

$$2[x^T(k)T_1 + y^T(k)T_2]\big[y(k) \quad (A \quad I)x(k) \quad A_d x\big(k \quad d(k)\big) \quad B_1\omega(k)\big] = 0 \tag{4.14}$$

Note that:

$$\begin{aligned}\sum_{l=k-d(k)}^{k-1} [\zeta^T(k)N + y^T(l)Z]Z^{-1}[N^T\zeta(k) + Zy(l)] \\ = d(k)\zeta^T(k)NZ^{-1}N^T\zeta(k) + 2\zeta^T(k)N \sum_{l=k-d(k)}^{k-1} y(l) \\ + \sum_{l=k-d(k)}^{k-1} y^T(l)Zy(l) \\ \le d_2\zeta^T(k)NZ^{-1}N^T\zeta(k) + 2\zeta^T(k)N \sum_{l=k-d(k)}^{k-1} y(l) + \sum_{l=k-d(k)}^{k-1} y^T(l)Zy(l)\end{aligned} \tag{4.15}$$

and,

$$\sum_{l=k-d_M}^{k-d(k)-1}[\zeta^T(k)M + y^T(l)Z]Z^{-1}[M^T\zeta(k) + Zy(l)]$$

$$= (d_M \quad d(k))\zeta^T(k)MZ^{-1}M^T\zeta(k) + 2\zeta^T(k)M\sum_{l=k-d_M}^{k-d(k)-1} y(l) + \sum_{l=k-d_M}^{k-d(k)-1} y^T(l)Zy(l) \tag{4.16}$$

$$\leq (d_M \quad d_m)\zeta^T(k)MZ^{-1}M^T\zeta(k) + 2\zeta^T(k)M\sum_{l=k-d_M}^{k-d(k)-1} y(l) + \sum_{l=k-d_M}^{k-d(k)-1} y^T(l)Zy(l)$$

Substituting (4.16) into the derivative of the Lyapunov function and using Schur complement, the following inequality obtained:

$$\Delta V(k) \leq \zeta^T(k)\left[\tilde{\phi} + d_M NZ^{-1}N^T + d_{12}MZ^{-1}M^T\right]\zeta(k)$$
$$\sum_{l=k-d(k)}^{k-1}[\zeta^T(k)N + y^T(l)Z]Z^{-1}[N^T\zeta(k) + Zy(l)]$$
$$\sum_{l=k-d_M}^{k-d(k)-1}[\zeta^T(k)M + y^T(l)Z]Z^{-1}[M^T\zeta(k) + Zy(l)]$$

$$\tilde{\phi} = \begin{matrix} \phi_{11} & \phi_{12} & \phi_{13} & \phi_{14} & \phi_{15} \\ & \phi_{22} & \phi_{23} & \phi_{24} & \phi_{25} \\ & & \phi_{33} & \phi_{34} & \phi_{35} \\ & & & \phi_{44} & \phi_{45} \\ & & & & 0 \end{matrix},$$

$$\Delta V(k) + z^T(k)z(k) \quad \gamma^2\omega^T(k)\omega(k)$$
$$\leq \zeta^T(k)\left[\hat{\phi} + d_2 NZ^{-1}N^T + d_{12}MZ^{-1}M^T\right]\zeta(k)$$
$$\sum_{l=k-d(k)}^{k-1}[N^T\zeta(k) + Zy(l)]^T Z^{-1}[N^T\zeta(k) + Zy(l)]$$
$$\sum_{l=k-d_M}^{k-d(k)-1}[M^T\zeta(k) + Zy(l)]^T Z^{-1}[M^T\zeta(k) + Zy(l)],$$

$$\hat{\phi} = \begin{matrix} \phi_{11} + C^T C & \phi_{12} & \phi_{13} & \phi_{14} & \phi_{15} \\ & \phi_{22} & \phi_{23} & \phi_{24} & \phi_{25} \\ & & \phi_{33} & \phi_{34} & \phi_{35} \\ & & & \phi_{44} & \phi_{45} \\ & & & & \phi_{55} \end{matrix}$$

Now, if $\hat{\phi} + d_M N Z^{-1} N^T + d_{12} M Z^{-1} M^T < 0$, it is easy to show that:

$$\Delta V(k) + z^T(k) z(k) \quad \gamma^2 \omega^T(k) \omega(k) < 0$$

Note: if $M \geq N > 0$ then $N^{-1} \geq M^{-1} > 0$.

It is also assumed that the initial condition is zero. As a result, one can directly conclude that $V(0) = 0, \forall k \in [\ \ d_M, 0]$.

$$\rightarrow \sum_{l=0}^{N} z^T(l) z(l) \quad \gamma^2 \sum_{l=0}^{N} \omega^T(l) \omega(l) < \quad V(N+1) \leq 0, \forall N > 0.$$

which guarantees that $\Delta V(k) < 0$ when $\omega(k) = 0$. This means that the given system is asymptotically stable with $u(k) = 0$.

Using the S-procedure in the LMI transformation, the above inequality can be described in the form of (4.8), thus completing the proof.■

Using Theorem 1, an upper bound for the delay of system (4.7) without a controller is obtained. The next step is designing a controller for the same system to stabilize it for a given upper and lower bound of delay.

4.4.2 State Feedback Stabilization of Discrete Delayed System

THEOREM 4.2: For the given lower and upper delay bound (d_m and d_M), and an attenuation coefficient of $\gamma > 0$, the system (4.7) is asymptotically stable, using $u(t) = VL^{-1}x(k)$, and $\omega(k) \in \ell_2[0, \infty)$. If the matrices $V, G = [G_1^T \quad G_2^T \quad G_3^T \quad G_4^T \quad G_5^T]^T$, $H = [H_1^T \quad H_2^T \quad H_3^T \quad H_4^T \quad H_5^T]^T$ exist, and for the symmetric matrices $R > 0$, $W_1 > 0, W_2 > 0$, and $L \geq 0$, the following matrix inequality holds:

$$\zeta = \begin{matrix} \Lambda & d_M G & d_{12} H & \widehat{\Lambda} & d_M S & S \\ & d_M L R^{-1} L & 0 & 0 & 0 & 0 \\ & & d_{12} L R^{-1} L & 0 & 0 & 0 \\ & & & I & 0 & 0 \\ & & & & d_M R & 0 \\ & & & & & L \end{matrix} < 0 \qquad (4.17)$$

where:

$$\Lambda = \begin{matrix} \Lambda_{11} & \Lambda_{12} & \Lambda_{13} & \Lambda_{14} & \Lambda_{15} \\ & \Lambda_{22} & \Lambda_{23} & H_2 & B_1 \\ & & \Lambda_{33} & \Lambda_{34} & G_5^T + H_5^T \\ & & & \Lambda_{44} & H_5^T \\ & & & & \gamma^2 I \end{matrix}$$

$$S = [S_1 \quad S_2 \quad 0 \quad 0 \quad 0]^T, \Lambda_{11} = (d_{12}+1)W_1 + W_2 + S_1 + S_1^T + G_1 + G_1^T,$$
$$\Lambda_{12} = S_2 \quad S_1^T + L(A \quad I)^T + V^T B_2^T + G_2, \Lambda_{13} = G_3^T \quad G_1 + H_1, \Lambda_{14} = G_4^T \quad H_1,$$
$$\Lambda_{15} = G_5^T, \Lambda_{22} = \quad S_2 \quad S_2^T, \Lambda_{23} = A_d\, L \quad G_2 + H_2,$$
$$\Lambda_{33} = \quad W_1 \quad G_3 \quad G_3^T + H_3 + H_3^T, \Lambda_{34} = \quad G_4^T + H_4^T \quad H_3,$$
$$\Lambda_{44} = \quad W_2 \quad H_4 \quad H_4^T, \widehat{\Lambda} = [CL^T \; 0]^T$$

PROOF:

Based on theorem 1, it is clear that $\phi_{22} < 0$. As such, $T_2 + T_2^T < 0$. Then, $T_2 + T_2^T$ is symmetric and negative definite, and as such, nonsingular. Then let:

$$U = \begin{bmatrix} P & 0 \\ T_1^T & T_2^T \end{bmatrix}, U^{-1} = \begin{bmatrix} L & 0 \\ S_1 & S_2 \end{bmatrix} = \widetilde{U}.$$

In view of the closed loop system with constant feedback, first replace A with $A + BK$. The main goal is finding matrix K, which stabilizes the overall system. However, adding this variable to the formulation, the matrix inequality that resulted in theorem 4.1 is not linear anymore. Thus, after replacing matrix A, pre and post multiply Ξ by $diag\{\widetilde{U}^T \quad L \quad L \quad I \quad L \quad L \quad I\}$ and $diag\{\widetilde{U} \quad L \quad L \quad I \quad L \quad L \quad I\}$. Subsequently, new variables must be defined as below and after carrying out some manipulations, $G = diag\{\widetilde{U}^T \quad L \quad L \quad I\}.N.L, W_i = LQ_iL, i = 1,2, V = KL, H = diag\{\widetilde{U}^T \quad L \quad L \quad I\}.M.L, R = Z^{-1}$, and $V = KL$.

After some calculations, the results are as follows:

$$\Lambda_{11} = \Big(L.\Big((d_{12}+1).Q_1 + Q_2 \quad T_1(A+BK \quad I0) \quad (A+BK \quad I0)^T.T_1^T + N_1 + N_1^T\Big)$$
$$+ S_1^T.(P + T_1^T \quad T_2(A+BK \quad I0) + N_2)\Big).L$$
$$+ \Big(L.(P + T_1 \quad (A+BK \quad I0)^T.T_2^T + N_2^T)$$
$$+ S_1^T.(P + d_2.Z + T_2 + T_2^T)\Big).S_1$$
$$\Lambda_{12} = \Big(L.(P + T_1 \quad (A+BK \quad I0)^T.T_2^T + N_2^T) + S_1^T.(P + d_2.Z + T_2 + T_2^T)\Big).S_2.$$

The other terms can also be calculated simply by pre-post multiplication. Now by considering that $UU^{-1} = I$, one can write:

$$PL = I, \quad T_1^T L = T_2^T S_1, T_2^T S_2 = I,$$

which, using the relation and the Schur complement, completes the proof.

4.4.3 State Feedback of Discrete Delay System Using LMI

Using Theorem 4.2, a solution can be obtained. However, due to calculation difficulties, the solution is not practical. In regards to the inverse variable terms in an inequality condition, it cannot be treated as an LMI. As a result, the well-known approaches for solving an LMI are not applicable. Using the algorithm proposed by Ghaoui in the late 1990s ([37]), the given matrix inequality condition can be transformed to a general nonlinear minimization problem with LMI constraints (see Appendix). This can be solved iteratively, as follows:

Finding a Feasible Solution

Require:

1 : Define the new matrix variable $\hat{R} \leq LR^{-1} L$

2 : Convert the matrix inequality of $\hat{\zeta} < 0$ to a nonlinear minimization problem based on LMI, as follows:

$$Minimize\ Tr\left(\hat{R}\bar{Q} + L\bar{S} + R\bar{F}\right)$$

Subject to:

$$L = L^T > 0, \hat{R} = \hat{R}^T > 0, W_1 > 0, W_2 > 0, R = R^T > 0$$

$$\begin{bmatrix} \bar{Q} & \bar{S} \\ \bar{S} & \bar{F} \end{bmatrix} \geq 0, \begin{bmatrix} \hat{R} & I \\ I & \bar{Q} \end{bmatrix} \geq 0, \begin{bmatrix} L & I \\ I & \bar{S} \end{bmatrix} \geq 0, \begin{bmatrix} R & I \\ I & \bar{F} \end{bmatrix} \geq 0 \tag{4.18}$$

and $\zeta < 0$ in (4.17), where $L\hat{R}^{-1}L$ is replaced by $\hat{R}$.

3 : $\gamma \leftarrow$ sufficiently small > 0

4 : $\gamma_{min} = \gamma$.

Ensure: Requirement is satisfied

5 : **while** $i < i_{max}$ **do**

6 : Find a feasible set $(L_0, \bar{S}_0, W_{10}, W_{20}, R_0, \bar{F}_0, \hat{R}_0, \hat{Q}_0, V_0, G_0, H_0, S_{10}, S_{20})$ that:

$\zeta < 0$, where $LR^{-1}\,L \leftarrow \hat{R}$

7 : $k \leftarrow 0$

8 : **for** $i = 0$ **to** i_{max} **do**

9 : Find a feasible set $\{L, \bar{S}, W_1, W_2, R, \bar{F}, \hat{R}, \bar{Q}, V, G, H, S_1, S_2\}$

$$T_k = Min\ Trace\left(L_k\bar{S} + L\bar{S}_K + R_k\bar{F} + R\bar{F}_k + \hat{R}_k\bar{Q} + \hat{R}\bar{Q}_k\right)$$

Subject to:

$\zeta < 0$ while $LR^{-1}\,L \leftarrow \hat{R}$

10 : $\bar{S}_{k+1} \leftarrow \bar{S}, L_{k+1} \leftarrow L, \bar{Q}_{k+1} \leftarrow \bar{Q}, \hat{R}_{k+1} \leftarrow \hat{R}, \bar{F}_{k+1} \leftarrow \bar{F}, R_{k+1} \leftarrow R.$

11 : **if** condition (4.17) is satisfied **and** $\|T \quad 6n\| \leq tol$

then

12 : $K \leftarrow VL^{-1}$

13 : $\gamma_{min} \leftarrow \gamma$

14 : Reduce γ

15 : break the **for** loop

16 : **end if**

17 : **end for**

18 : **end while**

4.5 Solving the LMIs

It is well known that the LMIs solving is not strictly convex problem and different solvers may result in different gains, however the corresponding attenuation levels will be quite close. Given that the minimization is to seek an infimum for γ, some solvers can lead to extremely large values for the design matrices. For this reason, the size of matrix V can be restricted to constrain the gains of the controller. One approach to limit the size of matrix V is as follow:

$$\begin{bmatrix} \lambda \begin{bmatrix} \alpha_1 & 0 \\ 0 & \alpha_2 \end{bmatrix} & V^T \\ & \lambda I \end{bmatrix} > \epsilon I \tag{4.19}$$

where the scalars of α_1 and α_2 are free variables to shape the controller gains properly and ϵ is a small number defines the numerical error tolerance. Adding this extra inequality is found to be effective in practice, however it adds another constraint in the admissible set for V which makes the analysis more conservative. Another method to avoid the numerical difficulty is to minimize $\gamma + \epsilon_0\ \mathrm{Tr}(VV^T)$ instead of γ where ε_0 is a positive scalar.

4.6 Driver-in-the-Loop Output Regulation

Theorem 4.2 guarantees the asymptotic stability of the system, which forces both of the states – the yaw rate or the lateral velocity – to approach zero as the control input applies to the system. Hence, the controller is highly conservative. Even in cases where there is no delay, the control signal is still conservative and degrades the system's overall performance. The controller performance, however, can be improved using the benefit of the output tracking methodology. To provide a good ride and good vehicle handling, the first state, which is lateral velocity, needs to be zero at all times. This is satisfied by the stabilization method. However, the other state's behavior, the yaw rate, can be presented by a linear function of the steering angle to achieve the best performance, as mentioned in (4.2). The desired value for the lateral velocity can be calculated based on zero dynamics of the system, however, since it is a small value, it is usually assumed to be zero.

4.6.1 Output Regulation for the Full-Rank Matrix $\boldsymbol{B}$ with a Known Delay of $\boldsymbol{d}$

Consider again the discrete LTI system of (4.7). An error term can be defined based on the current vehicle states and the desired state values of Equation (4.2):

$$e(k) = x(k) \quad x_d(k) \tag{4.20}$$

Then, the error dynamic can be written as follows:

$$\begin{aligned} e(k+1) &= x(k+1) \quad x_d(k+1) \\ &= Ax(k) + A_d x(k \quad d) + B_1\,\omega(k) + B_2 u(k) \quad x_d(k+1) \end{aligned} \tag{4.21}$$

The goal is to stabilize the error dynamics. Considering the fact that an upper bound for the delay is known, one can easily assume a nominal delay of $\bar{d}$ that satisfies $0 \leq \bar{d} \leq d_M$. Now, the desired value dynamics can be defined as:

$$B_2 u(k) = B_2 \tau(k) + x_d(k+1) \quad Ax_d(k) \quad A_d x_d(k \quad d) \tag{4.22}$$

Hence, one can rewrite the error dynamic of (4.21) as the following:

$$\begin{aligned} e(k+1) &= Ax(k) \quad A_d x_d(k) + B_2\tau(k) + A_d x(k \quad d) \quad A_d x_d(k \quad d) + B_1\,\omega(k) \\ &= Ae(k) + A_d e(k \quad d) + B_2\tau(k) + B_1\,\omega(k) \end{aligned} \tag{4.23}$$

Using (4.23), the problem is now in using error stabilization. This is accomplished using the aforementioned theorems. After solving the new problem based on the error dynamic term, the following equation regarding the input signal for regulation can be obtained:

$$u(k) = \tau(k) + B_2^{-1}\big(x_d(k+1) \quad Ax_d(k) \quad A_d x_d(k \quad d)\big) \tag{4.24}$$

However, usually matrix B, which is related to the actuator, is not full-rank. Rather, it is a full-column rank. Therefore, the control signal of $u(k)$ cannot be extracted from the relation of (4.24). This relation provides n different input command signals, instead of m, where $m \leq n$. The method used here is taking the benefit of a singular value decomposition (SVD) transformation, and changing the system coordination such that matrix B can be written as in (4.25):

$$B_{n\times m} = \begin{bmatrix} B_{0_{m\times m}} \\ 0_{(n-m)\times m} \end{bmatrix} \tag{4.25}$$

Then, using (4.25), the previous equation of (4.22) is now transformed to:

$$\begin{aligned} \begin{bmatrix} B_0 \\ 0 \end{bmatrix} u(k) = \begin{bmatrix} B_0 \\ 0 \end{bmatrix} \tau(k) \\ + \begin{bmatrix} x_d(k+1)_{(n-m)} & A_{(n-m)\times n} x_d(k) & A_{d(n-m\times n)} x_d(k \quad d) \\ x_d(k+1)_m & A_{m\times n} x_d(k) & A_{d(m\times n)} x_d(k \quad d) \end{bmatrix} \end{aligned} \tag{4.26}$$

Now, it can be simplified by making the assumption that the $y_{desire} = x_{id}$ output tracking can be addressed.

For the vehicle case study that is considered in this report (4.5), since$B \in \quad ^{2\times 1}$ is not of the form of $\begin{bmatrix} B_0 \\ 0 \end{bmatrix}$, using transformation based on the SVD, one can always find a transformation matrix T which change the coordinates to an appropriate space of $T \times B = \hat{B} = \begin{bmatrix} \hat{B}_0 \\ 0 \end{bmatrix}$.

Then, assuming

$$\hat{x}(k) = Tx(k), x(k) = T^{-1}\hat{x}(k), \qquad \hat{A} = TAT^{-1}, \hat{A}_d = TA_d\,T^{-1}, \qquad \hat{B} = TB,$$
$$\hat{C} = CT^{-1}$$

the system of (4.7) can be transformed to the following representation:

$$\tilde{\Sigma}_0: \begin{cases} \hat{x}_v(k+1) = \hat{A}\hat{x}(k) + \hat{A}_d\hat{x}(k \quad d) + \hat{B}\omega(k) + \hat{B}u(k) \\ z(k) = \hat{C}\hat{x}(k) \\ \hat{x}(k) = 0, \quad d_2 \le k \le 0 \end{cases} \tag{4.27}$$

This control input only guarantees that $\hat{x}(k) \to x_d(k) \qquad Tx(k) \to x_d(k)$. So, before applying this approach, one should be careful about transforming the desired values, as well by defining:

$$\hat{x}_d(k) = Tx_d(k),$$

Now,

$$\hat{x}(k) \to \hat{x}_d(k) \qquad x(k) \to x_d(k) \tag{4.28}$$

Hence, defining the new transformed error of $e(k) = T \times e(k)$: easy

$$e(k) = \hat{x}(k) \quad Tx_d(k) = Te(k)$$
$$e(k+1) = \hat{A}e(k) + \hat{A}_d e(k \quad d) + \hat{B}\tau(k) + \hat{B}\omega(k) \tag{4.29}$$

We have to find $\tau(k)$ that stabilizes the transformed equation, again with the aforementioned theorems. Based on the fact that the theorem gives a memory-less state feedback, the transformed controller is:

$$\tau(k) = \hat{K}e(k) \tag{4.30}$$

Applying this controller, the transformed error dynamic is:

$$e(k+1) = \left(\hat{A} + \hat{B}\hat{K}\right)e(k) + \hat{A}_d e(k \quad d) + \hat{B}\omega(k)$$

That can be rewritten as:

$$Te(k+1) = \left(TAT^{-1} + TB\hat{K}\right)Te(k) + TA_d T^{-1}Te(k \quad d) + TB\omega(k)$$

Considering that:

$$\hat{K} = KT^{-1}$$

One has:

$$Te(k+1) = (TAT^{-1} + TBKT^{-1})Te(k) + TA_dT^{-1}Te\big(k \quad d(k)\big) + TB\omega(k)$$
$$e(k+1) = (A+BK)e(k) + A_de(k \quad d) + B\omega(k)$$
$$\tau(k) = \hat{K}e(k) = Ke(k) = \tau(k) \tag{4.31}$$

Thus, one can easily design $\tau(k)$ for the system (4.7) and use $x_d = [x_{1d} \quad \phi_d]$ to stabilize the error dynamics.

Remark: Based on the above calculations, one can use the same control input, which was designed for transformed system, in the main system. ■

Remark: Note that in this scheme, one cannot guarantee $x_{1d} \to 0$. The reason is that when using matrix $\hat{B}$, only one of the states can be assigned, and the other states must follow specific dynamics based on system dynamics. It means that the controllable space is a subspace, which is constrained by the system dynamics, (the controllable space is $_c \in \ ^n(n=2)$). ■

4.6.2 Extension to Robust Regulation with Time Varying Delay

In order to relax the assumption of the output regulation with a known time delay, the method is modified such that a more realistic situation can be addressed. This part is the same as the robust stabilization theorem, only that the knowledge on the upper bound driver delay is presumed. Recall again, the system of (4.7) and the desired state dynamics of (4.2), where the error term is:

$$e(k) = x(k) \quad x_d(k) \tag{4.32}$$

Then, for the time varying delay case, the error dynamic can be written as follows:

$$\begin{aligned} e(k+1) &= x(k+1) \quad x_d(k+1) \\ &= Ax(k) + A_dx\big(k \quad d(k)\big) + B_1\,\omega(k) + B_2u(k) \quad x_d(k+1) \end{aligned} \tag{4.33}$$

The goal is to stabilize the error dynamics. Considering the fact that an upper bound for the delay is known, one can easily assume a nominal delay of $\bar{d}$ which satisfies $0 < \bar{d} \le d_M$. Now, one can define the desired value dynamics as:

$$B_2u(k) = B_2\tau(k) + x_d(k+1) \quad A_dx_d(k) \quad A_dx_d\big(k \quad \bar{d}\big) \tag{4.34}$$

Hence one can rewrite the error dynamic of (4.23) as follows:

$$
\begin{aligned}
e(k+1) = Ax(k) \quad & A_d x_d(k) + B_2\tau(k) + A_d x\big(k \quad d(k)\big) \quad A_d x_d\big(k \quad \bar{d}\big) \\
& + B_1\,\omega(k) \\
& = Ae(k) + A_d e\big(k \quad \bar{d}\big) + B_2\tau(k) + B_1\,\omega(k) \\
& + A_d\big[x\big(k \quad d(k)\big) \quad x\big(k \quad \bar{d}\big)\big]
\end{aligned}
\tag{4.35}
$$

Now, one should consider $B_1\,\omega(k) + A_d\big[x\big(k \quad d(k)\big) \quad x\big(k \quad \bar{d}\big)\big] = \bar{\omega}(k)$ as unknown disturbances. The new system dynamic that needs to be stabilized is as follows:

$$
e(k+1) = Ae(k) + A_d e\big(k \quad \bar{d}\big) + B_2\tau(k) + \bar{\omega}(k) \tag{4.36}
$$

Following the method proposed in the previous section, the solution can be easily obtained.

4.7 Uncertainty Analysis

In this section, the problem is reconsidered in a more revealing way, where the driver uncertainties are also included in the controller design procedure. It is worth emphasizing that usually, a drivers' behavior changes very slowly (see [109]). The driver model that is used is limited to constant preview points (N_p), sampling time (T), and longitudinal speed. Based on the formulation, one may consider a bound for different values of each parameter and study their effects on the preview gains. Among $N_p + 4$ preview gains, the focus is in the first two gains, because they have direct effects on the delayed part of the modelling. The other gains have some effects in unknown information, part (ω). These need to be considered similarly to some of the bounded uncertainties. Different values of the miscellaneous parameters for the first two gains are shown below.

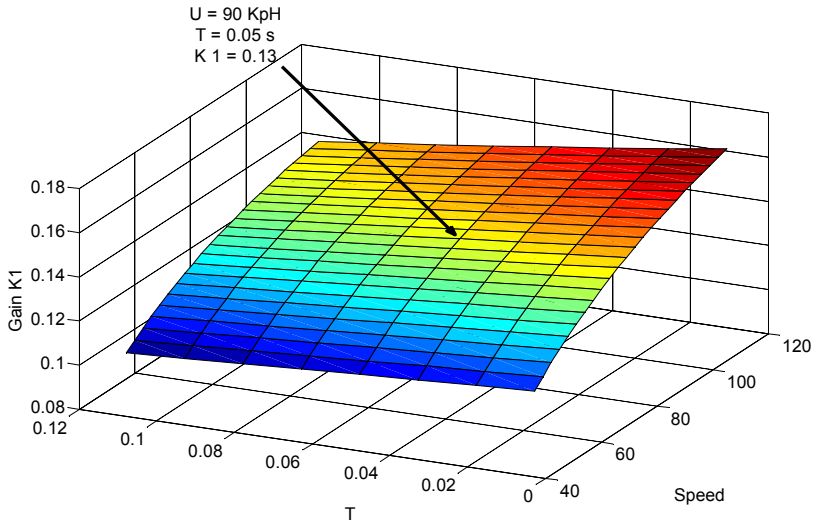

Figure 4-4 Variation of K_1 regarding to the variations in longitudinal speed and sampling time

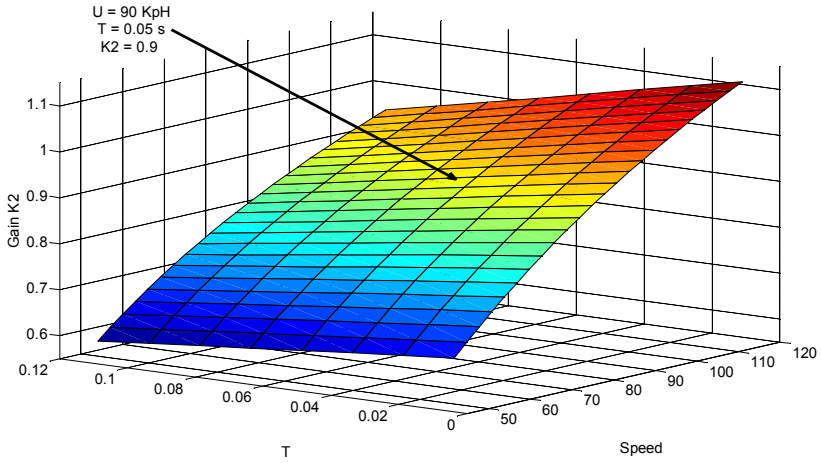

Figure 4-5 Variation of K_2 regarding to the variations in longitudinal speed and sampling time

The above figures show preview gains of K_1 and K_2 for the different ranges of speed and sampling time. In normal driving conditions, $\Delta K_1 = 0.03$ and $\Delta K_2 = 0.2$. These values are the gain's variations from a standard design at a nominal operating point of the vehicle at the longitudinal speed of $v_x = 90\ kp$ with a sampling time of $T = 50ms$. Note that the number of road preview points does not affect the steering gains of k_1 and k_2. According to this information, one can use the following modified system equation from (4.7):

$$\sum_0 : \begin{cases} x(k+1) = Ax(k) + (A_d + \Delta A_d)x\big(k \quad d(k)\big) + B_1\omega(k) + B_2u(k) \\ z(k) = Cx(k) \\ x(k) = 0, \quad d_2 \le k \le 0 \end{cases} \tag{4.37}$$

Handling this uncertainty, an assumption is added to the problem and then use the same method for the delayed system without uncertainty. Assuming that the term of $\Delta A_d (= B_2 \Delta K_v)$ denotes the parameter uncertainties satisfying the condition $\Delta A_d = MF(k)E$, where M, and E are constant matrices, and $F(t)$ is an unknown time-varying matrix, this satisfies $F^T(k)F(k) \le I$. Once again, the aim is to design a practically implementable robust controller in order to make the system stable and reliable to the effects of bounded time varying delay and the exogenous input caused by future preview points.

Lemma1 [154] For all $F \in \quad ^{q_2 \times q_3}$ satisfying $F^T F \leq R \in R^{q_3 \times q_3}, Q = Q^T \in R^{q_1 \times q_1}, H \in R^{q_1 \times q_2}, E \in R^{q_3 \times q_1}$ and $R = R^T > 0$

$$Q + HFE + E^T F^T H^T < 0$$

if and only if there exists some $\rho > 0$, such that:

$$Q + \rho HH^T + \rho^{-1} E^T RE < 0$$

Theorem 4.3: For the given lower and upper delay bound (d_m and d_M) and attenuation coefficient of $\gamma > 0$, the system (4.7) is asymptotically stable using $u(k) = VL^{-1}x(k)$, and $\omega(k) \in l_2\,[0, \infty)$. If the matrices $V, G = [G_1^T \quad G_2^T \quad G_3^T \quad G_4^T \quad G_5^T]^T$ exist, and the symmetric matrices $R > 0$, $W_1 > 0$, $W_2 > 0$, $\rho > 0$, $H = [H_1^T \quad H_2^T \quad H_3^T \quad H_4^T \quad H_5^T]^T$, and $L \geq 0$, then the following LMI is feasible:

$$\hat{\zeta} = \hat{\zeta}^T = \begin{bmatrix} \zeta & \rho\bar{M} & \bar{E}^T \\ & \rho I & 0 \\ & & \rho I \end{bmatrix} < 0 \tag{4.38}$$

where ζ is defined in Theorem 4.2, $\bar{M} = [0 \quad M^T \quad 0]^T$, and $\bar{E} = [0 \quad EL \quad 0]$.

Proof:

Using LMI (4.17) in Theorem 4.2, the robust asymptotic stability of the system (4.7) without uncertainty is addressed. Now replace A_d with $A_d + \Delta A_d$ in inequality (4.17), and use $\Delta A_d = MF(k)E$. This creates:

$$\begin{matrix} \Lambda & d_M G & d_{12} H & \widehat{\Lambda} & d_M S & S \\ & d_M L R^{-1} L & 0 & 0 & 0 & 0 \\ & & d_{12} L R^{-1} L & 0 & 0 & 0 \\ & & & I & 0 & 0 \\ & & & & d_M R & 0 \\ & & & & & L \end{matrix}$$

$$+ \begin{matrix} 0 \\ M \\ 0 \\ 0 \end{matrix} F [0 \quad 0 \quad EL \quad 0 \quad 0] + \begin{matrix} 0 \\ 0 \\ L^T E^T \\ 0 \\ 0 \end{matrix} F^T [0 \quad M^T \quad 0 \quad 0] < 0 \tag{4.39}$$

By Lemma 1, there exists some $\rho > 0$ for the inequality (4.39), such that:

$$\begin{matrix}\Lambda & d_M G & d_{12} H & \widehat{\Lambda} & d_M S & S & & & & & \\ & d_M L R^{-1} L & 0 & 0 & 0 & 0 & 0 & & & & \\ & & d_{12} L R^{-1} L & 0 & 0 & 0 & M & & & & \\ & & & I & 0 & 0 & 0 & & & & \\ & & & & d_M R & 0 & 0 & & & & \\ & & & & & L & & & & & \end{matrix} + \rho \begin{matrix} 0 \\ M \\ 0 \\ 0 \\ 0 \\ 0 \end{matrix} \begin{matrix}[0 & M^T & 0 & 0]\end{matrix}$$

$$+ \rho^{-1} \begin{matrix} 0 \\ 0 \\ L^T E^T \\ 0 \\ \\ 0 \end{matrix} \begin{matrix}[0 & 0 & EL & 0 & 0]\end{matrix} < 0$$

Using the Schur complement (Appendix), the inequality (4.38) is obtained.

4.8 Active Front Steering Simulation

The degradation effects, such as increasing the driver's delay, cause poor vehicle performance, and the instability of the delay in the driver/vehicle closed loop system were shown in Chapter 3. In order to show the effectiveness of the designed controller and the proposed method, some simulations are done in the following. An ISO harsh double lane change scenario [136] is considered as a reference (desired) path (see Figure 4-6) When considering the assumed scenario for the open loop vehicle, the steering angle that makes the simulated vehicle remain on the track, the yaw angle, and lateral velocity are all recorded for comparison. During the simulation, it is assumed that the vehicle performs the maneuver with a constant speed.

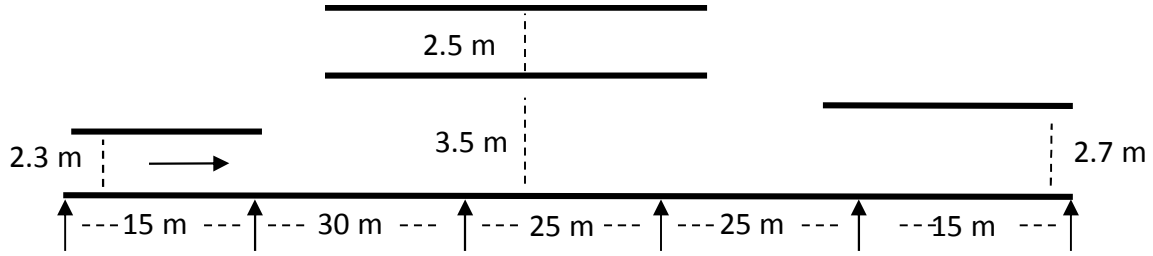

Figure 4-6: ISO harsh double lane change

The proposed controller is compared to a standard linear quadratic tracking (LQT) AFS state feedback controller. In the previous works on open loop vehicles, good performance of the LQT for a linear 2DOF bicycle model vehicle control is reported (see [28]). From a control theory standpoint, using the LQT method for a linear plant results in both stabilization and good tracking performance. The LQT controller design is presented in appendix. Note that the controller does not contain any information about the driver.

Matlab Simulink is used for the simulations of the proposed controller, where the YALMIP ([94]) package with SDPT3 ([145]) solver is added to solve the LMIs efficiently. Using theorem 4.3, a robust controller that stabilizes vehicle states to unknown driver delay (only the upper/lower bound delay is known) with an attenuation factor of γ is obtained. In order to convert it to a tracking controller to enhance performance, the proposed method in Section 4.6.2 is used, where the nominal delay is assumed to be $\bar{d} = 300\ ms$ and the robust controller is designed for time varying delay intervals of $d(k) \leq 350\ ms$.

The simulations start with a small driver delay and proceed by gradually increasing the time-delay. The simulation runs with a number of preview points of $N_p = 30$ and a sampling time of $T = 50\ ms$ for the driver simulation and $T = 5\ ms$ for vehicle model update. Given that the model is in continuous-time, the C2D command in MATLAB is used to discretize the model by sampling time, T. In order to define the desired path, the open loop behavior of the bicycle mode on the ISO double lane change scenario is simulated, and the lateral position output is assumed to be the desired path for the closed loop system. For the path follower, it is assumed that $q_1 = 0.25, q_2 = 100$, and $R = 1$. Recalling (3.12), the vehicle and preview gains are computed. Then, the recorded lateral position path data is fed into the system with a delay of the N_d sample. This leads the current (t) steering angle (δ_d) of the driver to be dependent on the vehicle state and preview points of $t \quad t_d$ (i.e: $\delta_d = \delta_{t-t_d(=N_p \times T)}$). It is also assumed that this steering angle is available for the controllers to adjust the vehicle's behavior.

Applying theorem 4.3 and adjusting the control signal by the proposed method in Section 4.5, the H_∞ robust AFS gain controller with an unknown time delay system is obtained. It has a gain of $K = [\ 0.5816 \quad 2.9205] I_z$ for a longitudinal speed of $v_x = 90\ kp$. This controller guarantees the output regulation with an attenuation factor of $\gamma = 0.5$. The driver's delay is also assumed to be bounded between $3 \leq N_d \leq 7\ (= 150ms \leq delay \leq 350\ ms)$. The state feedback for the H_∞ robust AFS gain controller with unknown time delay system for uncertain system ($\Delta k = [0.03 \quad 0.2]$) is found to be $K = [\ 1.2237 \quad 7.6781] I_z$ with a guaranteeing attenuation of $\gamma = 0.66$. Note that, referring to Figure 4-4 and Figure 4-5, when designing a controller for the longitudinal speed of $v_x = 90\ kp$ with this uncertainty bound, a good robust bound can be obtained.

The lateral position of the vehicle and the driver's steering angle are shown in different cases: Figure 4-7 presents a closed loop vehicle response while the driver has a small delay of $50\ ms$ and runs the vehicle at a speed of $90\ kp$. As shown, the performance of the LQR controller is slightly better than the other two robust controllers. The main reason lies in the conservation inherent to any robust controller. The former two designs make the system stable for a wide range of driver delays; however, they also slightly degrade the overall system's performance. It

is obvious that the larger the level of attenuation, the more conservation and consequently, the more performance reduction occurs.

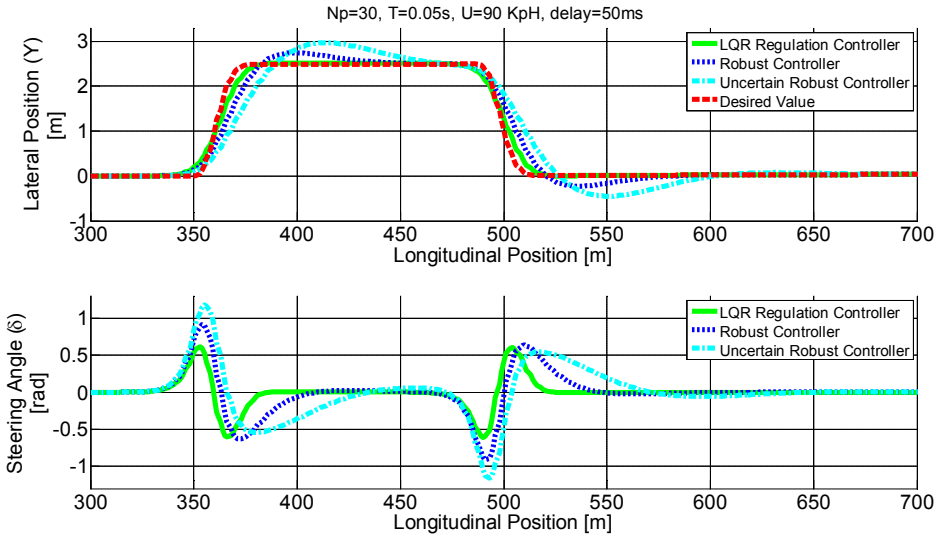

Figure 4-7 Lateral position of the vehicle and the driver's steering angle command ($v_x = 90\ kph, \tau = 50\ ms$)

While the LQR controller shows good results for small delays, it cannot stabilize the closed loop system for larger time-delays. The trend depicts a loss of stability in the vehicle-LQR controller in Figure 4-8 and Figure 4-9. It can be inferred from these figures that for a time-delay of more than $250\ ms$, the LQR controller cannot stabilize the closed loop vehicle. It is also worth mentioning again that without a controller, the closed loop system loses its stability for delays larger than $200\ ms$.

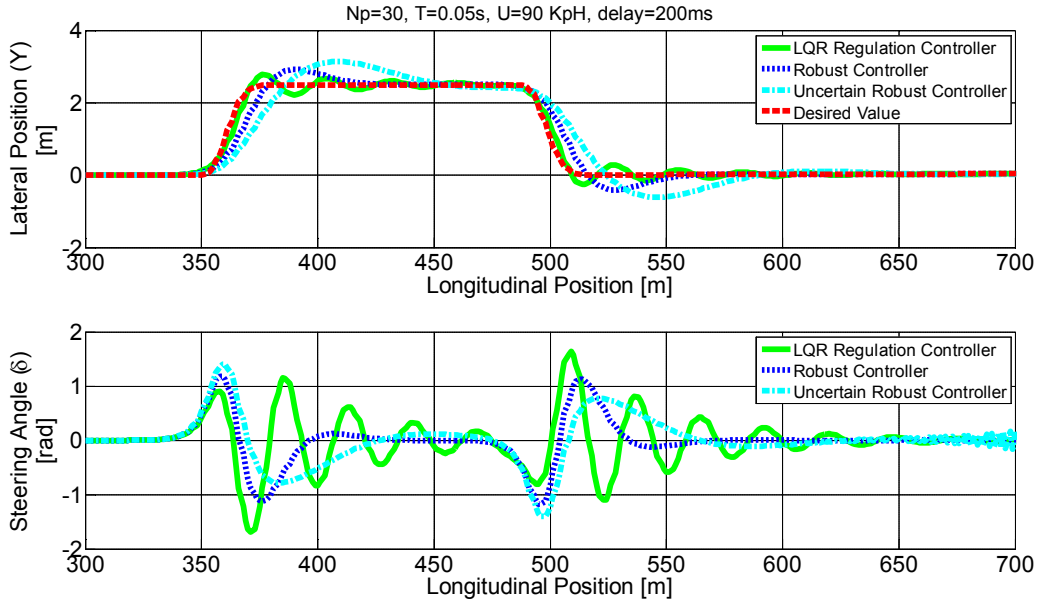

Figure 4-8 Lateral position of the vehicle and the driver's steering angle command

$(v_x = 90\ kph, \tau = 200\ ms)$

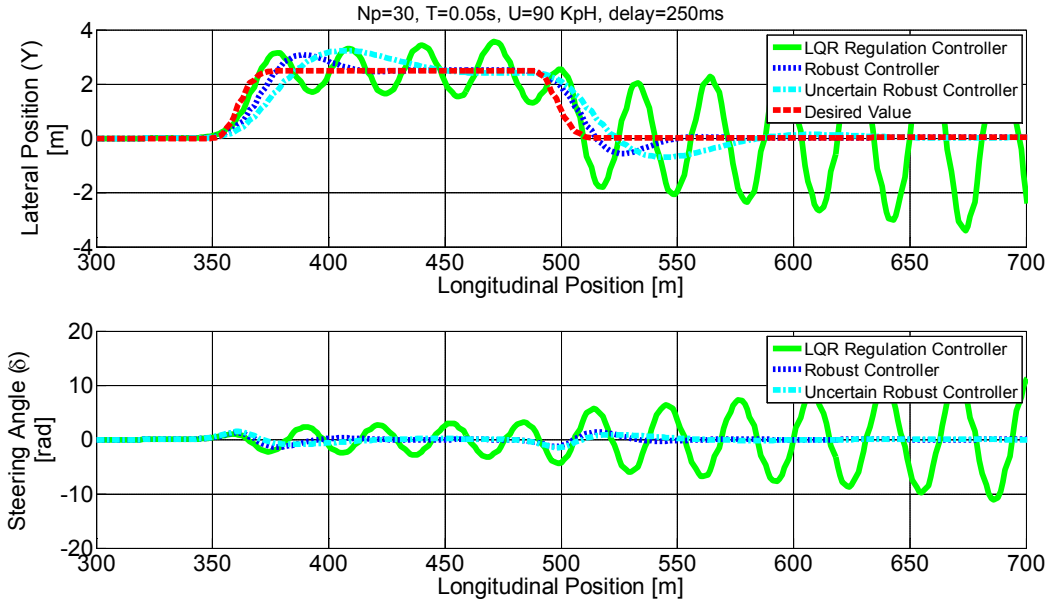

Figure 4-9 Lateral position of the vehicle and the driver's steering angle command

$(v_x = 90\ kph, \tau = 250\ ms)$

As the delay increases, the effectiveness of the robust controllers is revealed. Figure 4-10 and Figure 4-11 show that the proposed controllers prevent closed loop system instability even in the existence of a large driver time-delay (up to $350\ ms$). More robust controllers can also be designed using the proposed method; however, they would be very conservative and performance degradation would no longer be acceptable. Given that the method is proposed for harsh maneuver scenarios, considering delays larger than $400\ ms$ is not realistic in a real driving condition and are omitted here for brevity.

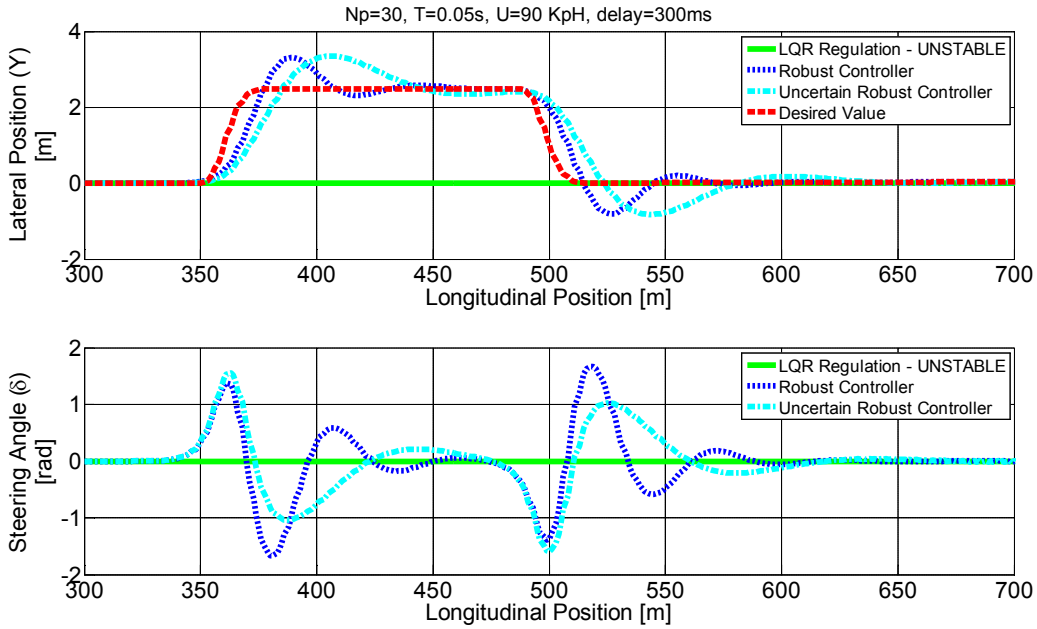

Figure 4-10 Lateral position of the vehicle and the driver's steering angle command

$(v_x = 90\ kph, \tau = 300\ ms)$

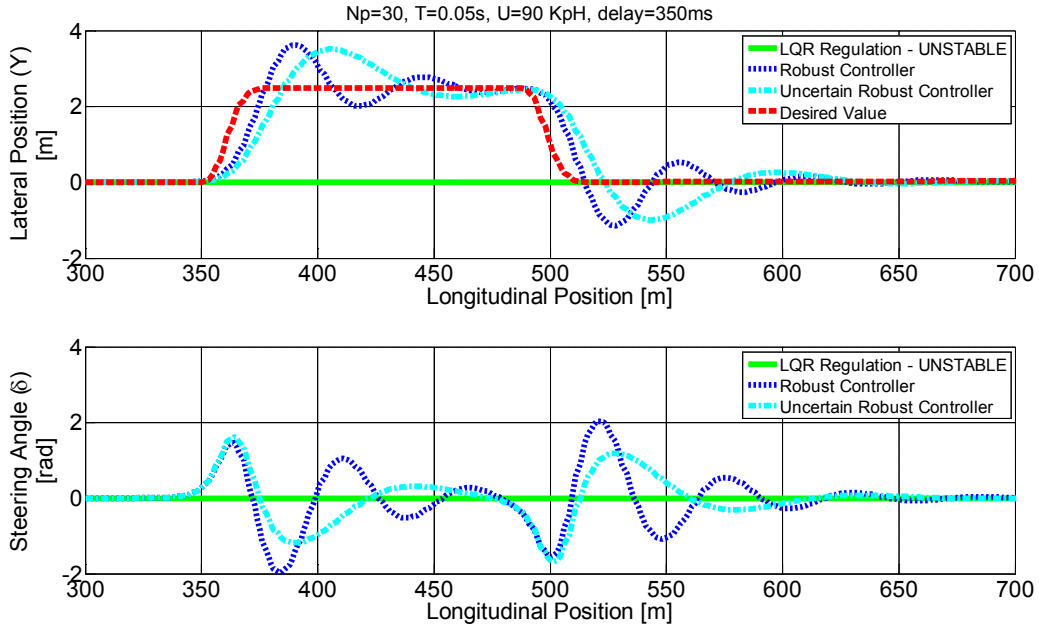

Figure 4-11 Lateral position of the vehicle and the driver's steering angle command

$$(v_x = 90\ kph, \tau = 350\ ms)$$

The simulations also show that the delay robust controller leads to better results than the delay robust uncertain controller. This can be easily explained by the fact that the former controller is more conservative than the first one. The uncertain robust controller does not perform control tasks as well as the robust controller. However, by changing the speed, the usefulness of this controller emerges. Changing the speed or the sampling time alters the vehicle's dynamic behavior subsequently changing the driver model parameters. The uncertain controller is robust to both bounded delay variation and bounded driver gain variation. In the following figure, Figure 4-12, the vehicle's longitudinal speed has been increased to $120kp$ and the controllers are kept unchanged.

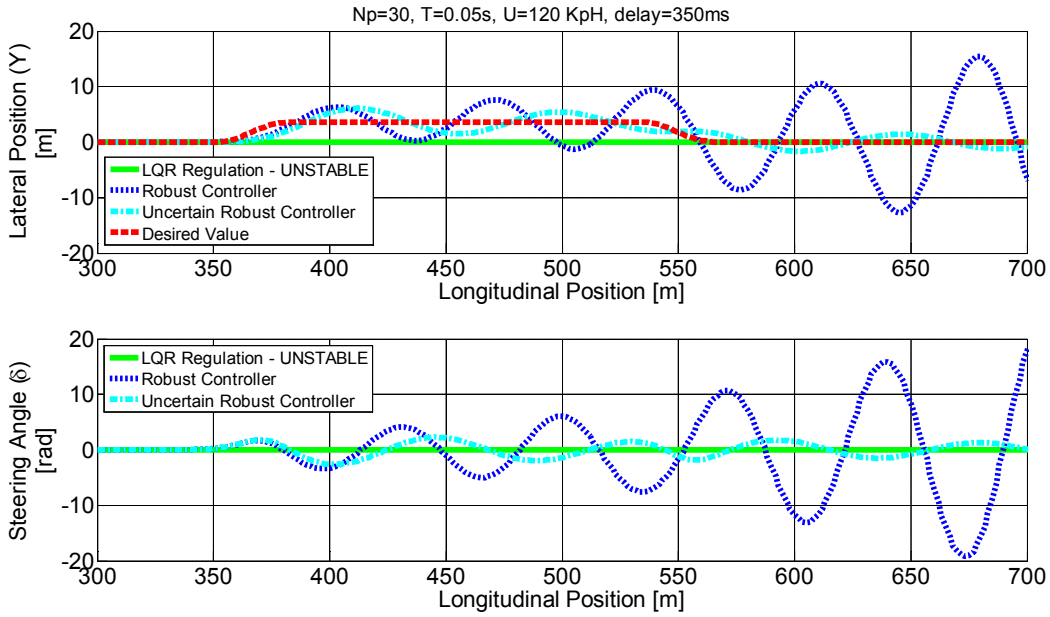

Figure 4-12 Lateral position of the vehicle and the driver's steering angle command

$$(v_x = 120\ kph, \tau = 350\ ms)$$

Figure 4-12 shows that although the robust controller is robust to delay variation, it is not robust enough to driver gain variation.

Redesigning the robust controller, a new control gain of $K = [\ \ 0.0005 \quad 4.1911] I_z$ is obtained with an attenuation factor of $\gamma = 0.8$. Now, using the new robust controller and the same robust uncertain controller, the following simulations present the vehicle behavior at a speed of $v_x = 120\ kp$. Note that the LQR controller has also been redesigned for this speed. Figure 4-13 and Figure 4-14 show the effectiveness of the proposed controller in the stabilizing closed loop vehicle, even with a large delay at high speeds.

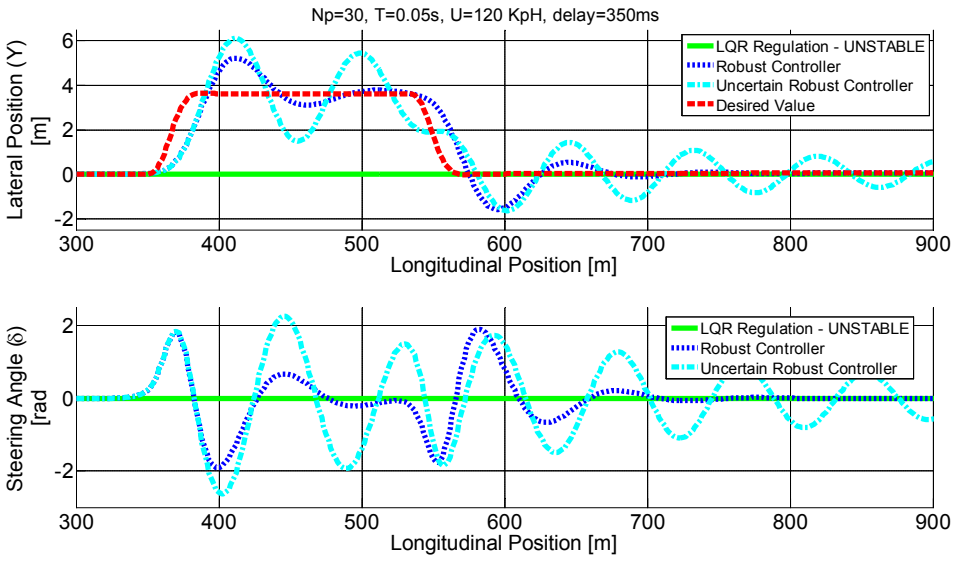

Figure 4-13 Lateral position of the vehicle and the driver's steering angle command

$(v_x = 120\ kph, \tau = 350\ ms)$

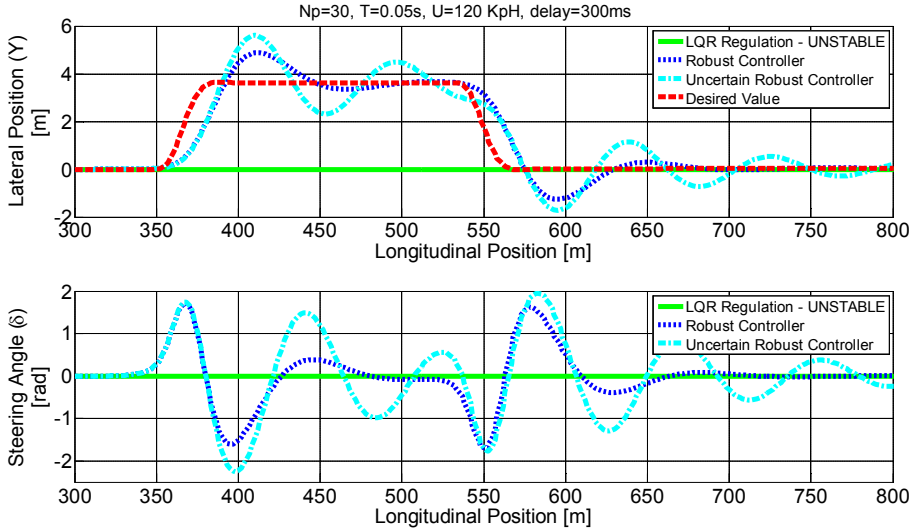

Figure 4-14 Lateral position of the vehicle and the driver's steering angle command

$(v_x = 120\ kph, \tau = 300\ ms)$

Similar to the previous simulation for lower speeds of $v_x = 90\ kp$, the redesigned delay robust controller shows slightly better performance compared to the uncertain robust controller. (See Figure 4-15)

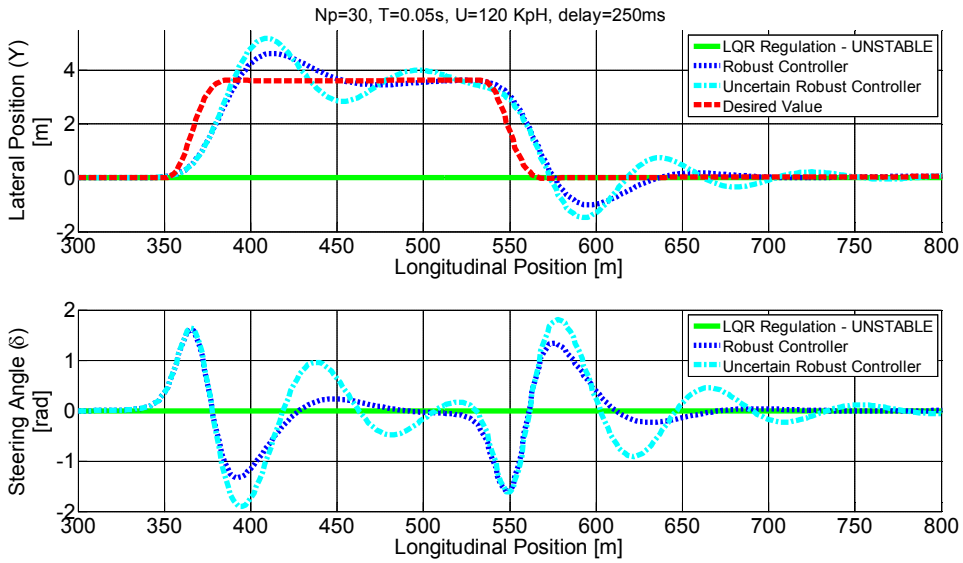

Figure 4-15 Lateral position of the vehicle and the driver's steering angle command

$$(v_x = 120\ kph, \tau = 250\ ms)$$

Figure 4-16 demonstrates that decreasing the driver's delay amount to $\tau = 150\ ms$ means that all three controllers guarantee closed loop vehicle stability.

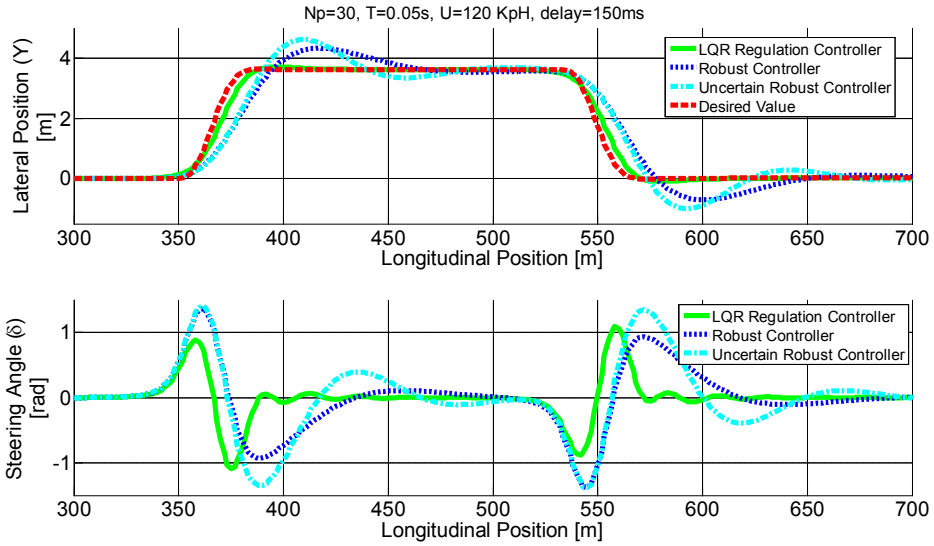

Figure 4-16 Lateral position of the vehicle and the driver's steering angle command

$$(v_x = 120\ kph, \tau = 150\ ms)$$

Finally, in order to show the effectiveness of the proposed controllers at low speeds, the following simulations have been performed at $v_x = 60\ kp$, where the LQR controller and the robust controller have been redesigned. The robust uncertain controller, however, has been left unchanged. Solving this given the LMI in (4.17), the robust regulator of the robust controller with a gain of $K = [\ \ 1.3300 \quad 0.8333] I_z$ is obtained with an attenuation coefficient of $\gamma = 0.4$. Applying the new robust controller, the LQR controller, and the previous uncertain robust controller, Figure 4-17 and Figure 4-18 present the closed loop driver-vehicle behavior for small and large driver time delays.

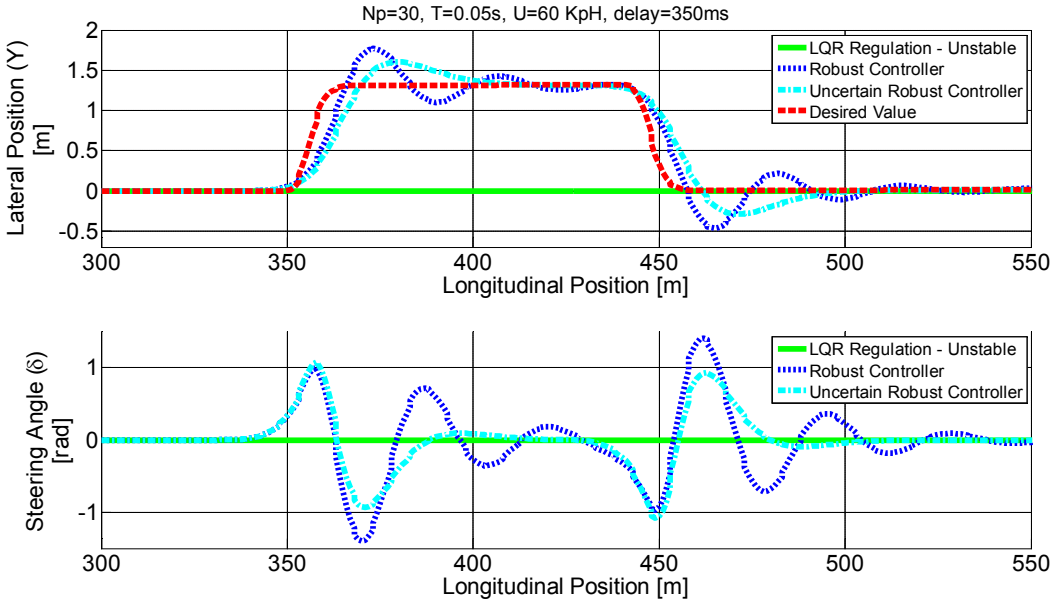

Figure 4-17 Lateral position of the vehicle and the driver's steering angle command

$(v_x = 60\ kph, \tau = 350\ ms)$

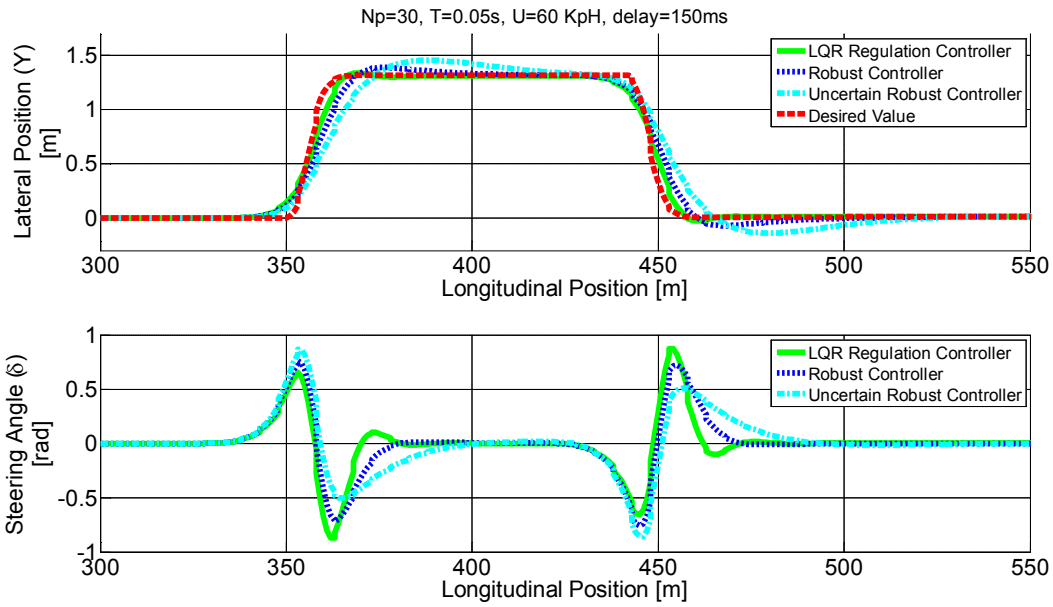

Figure 4-18 Lateral position of the vehicle and the driver's steering angle command

$(v_x = 60\ kph, \tau = 150\ ms)$

4.9 Extension to the Torque Vectoring Technique

The main advantage of using an active steering technique is that the actuator can directly control the lateral vehicle force F_y , which is very important in handling. Referring back to (4.7), there is versatility in directly controlling both lateral velocity and vehicle yaw rate. On the other hand, it is known that implementation of a controller using active steering is expensive, and at the same time, there are still some safety issues in relying on a fully electric steering system without mechanical redundancy.

The other alternative for controlling a vehicle is the method that works based on the vehicle's changing longitudinal forces. The idea here is to calculate the required moment at C.G. to improve vehicle performance. Then, changing the longitudinal forces of each wheel produces the requested moment. The most important techniques of this branch are Torque Vectoring (TV) and Differential Braking (DB). DB tries to produce the required moment only by braking, and its main advantage is that it is easy to implement. In a conventional vehicle, separate control of the torque transferred by the engine to each of the wheels is very difficult and expensive to implement. Hence, DB is an efficient method to reduce each wheel's torque without knowing each exact engine-torque. Although, in this method, one cannot use all of the capacity of the

control system since the actuators cannot add positive torque at each wheel. The TV technique, on the other hand, can produce both negative and positive torque at each wheel and potentially enable the control system to take advantage of all of the capacity in the system. The cost of having full control on the system is the additional time on wheel motors at each corner. This limits the method to hybrid and electric vehicles. Although there are very limited conventional vehicles that have actually implemented TV on a conventional platform, an improvement in conventional vehicles will not recoup the cost of implementation. Therefore, for the rest of this thesis, it is assumed that there are four individually controllable motors at each corner of the vehicle and one can implement the TV method on the car. A schematic of the structure of the control system is depicted in Figure 4-19.

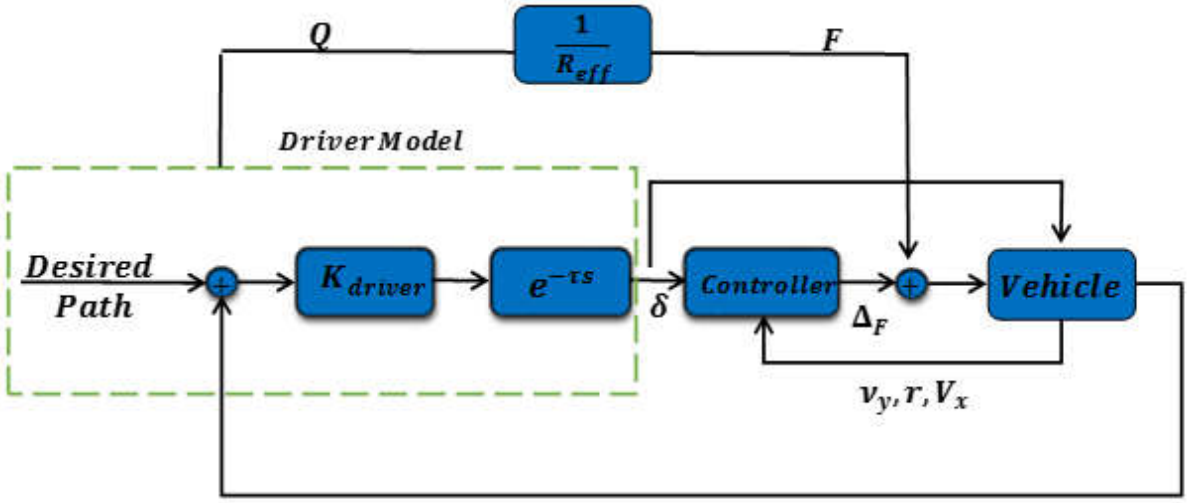

Figure 4-19: Torque vectoring control strategy

One of the main advantages of using the proposed method for integrating driver effect into the controller design is the independency of the method from the actuator type and implementation technique. The requested torque from the controller can be used by both AS and TV techniques. The detail of an optimal method for torque distribution is discussed in the next chapter.

Using the same algorithm, one can re-tune the controller for the case where TV method is targeted for the control purpose. In order to improve the simulation process, the CarSim high-fidelity software is used to model the driver in the simulation. The structure is depicted in Figure 4-20. An important note is that the driver model ([95]) in CarSim is a different from the driver model in controller design. In CarSim, the driver is a path follower model that includes many

different parameters of a driver such as the maximum steering torque, preview time, reaction delay, and many others. The important point here is that the proposed method still works robustly to the differences between the driver modeling in CarSim and the controller.

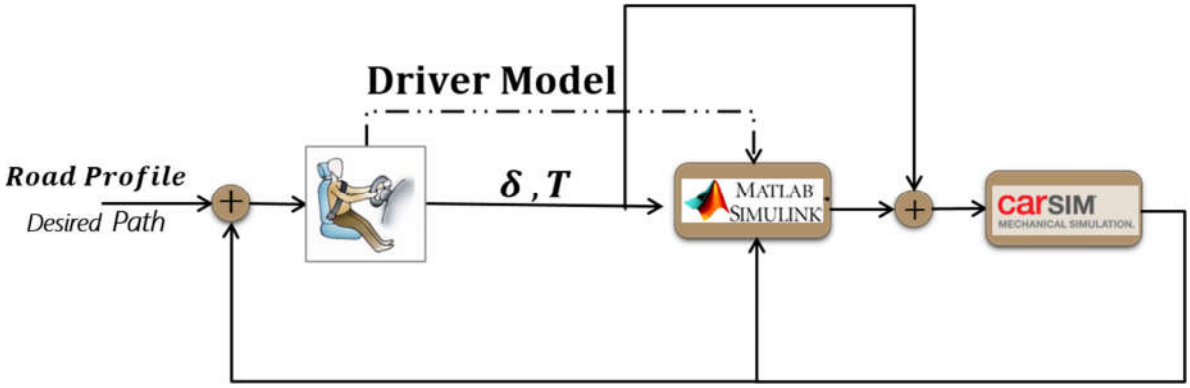

Figure 4-20: Simulation structure using CarSim

4.10 Torque Vectoring Simulation

To discretize the continuous model, a zero-order hold method with a sampling frequency of 200 Hz is used. Vehicle parameters remain the same as the AFS simulation part. The simulations are performed for different cases of longitudinal velocity and drive delay. Applying theorem 4.3, the H_∞ robust controller with an unknown time-delay system and certain driver model uncertainty bounds is obtained. The following section begins with the simulation for the case where the driver model is simulated in Matlab, which is exactly what is considered in the proposed controllers, and then, the CarSim driver model is used to make the simulation more realistic.

4.10.1 Linear Bicycle Model with Driver-in-the-Loop

To model the driver, the preview distance ahead is taken as 1.5 s. For the path follower, it is assumed that $q1 = 0.25, q2 = 100$, and $R = 1$. As shown in Figure 4-21, the vehicle with the proposed controller can track the desired path with a relatively large driver delay of ($380ms \leq d(k) \leq 450\,ms$) and on a dry road condition; however, the vehicle solely relying on the driver with a large amount of delay will not be able to follow a path, and the LQR controller cannot track the path properly. Note that similar to the previous section, the proposed controller is compared to an LQR-based designed controller (see AFS simulation for details). To show the performance of the controller for different speeds, the controller is retuned for 70 km/h longitudinal speed and the TV technique is applied for a wider range of delay ($250\,ms \leq d(k) \leq 450\,ms$) (see Figure 4-22).

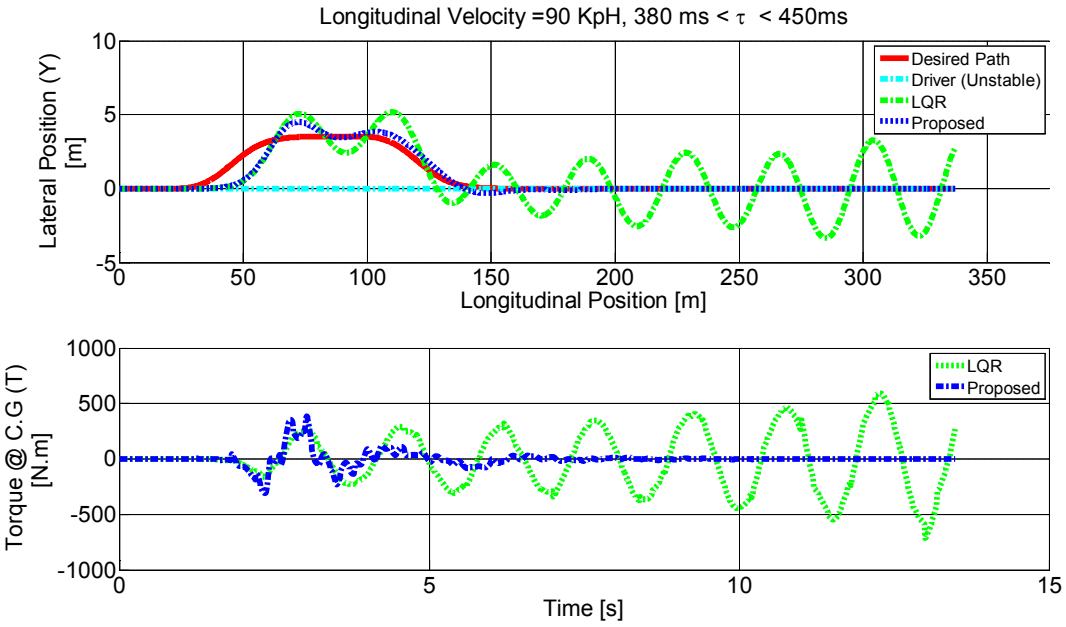

Figure 4-21 Controller performance comparison

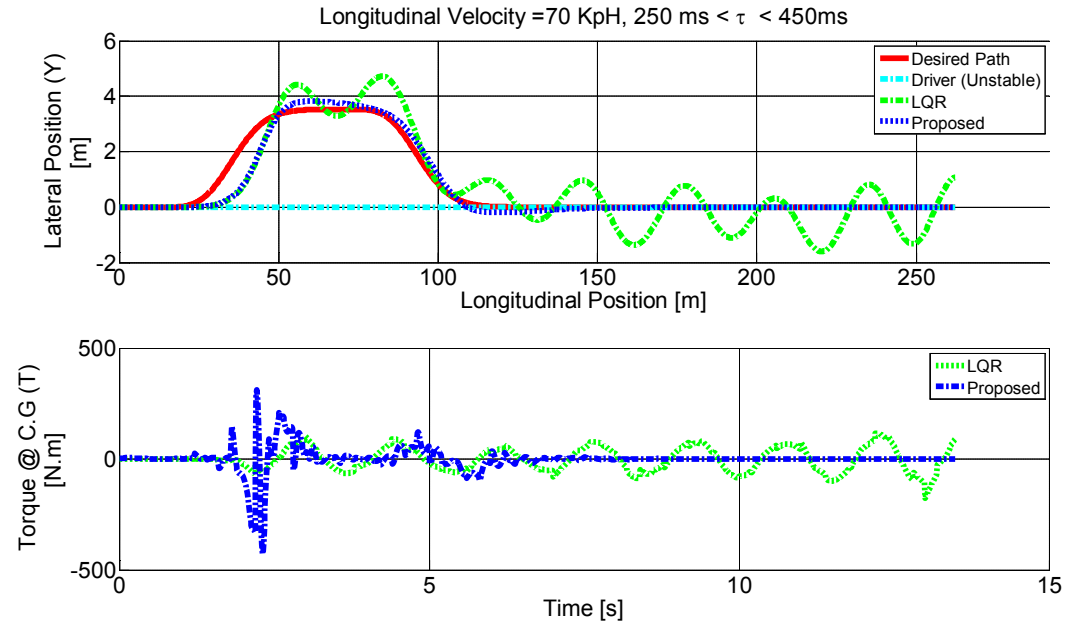

Figure 4-22 Controller performance comparison

4.10.2 CarSim Simulation Results

The first case in Figure 4-23 shows that for normal conditions and a specific given path, the CarSim driver can track the path perfectly.

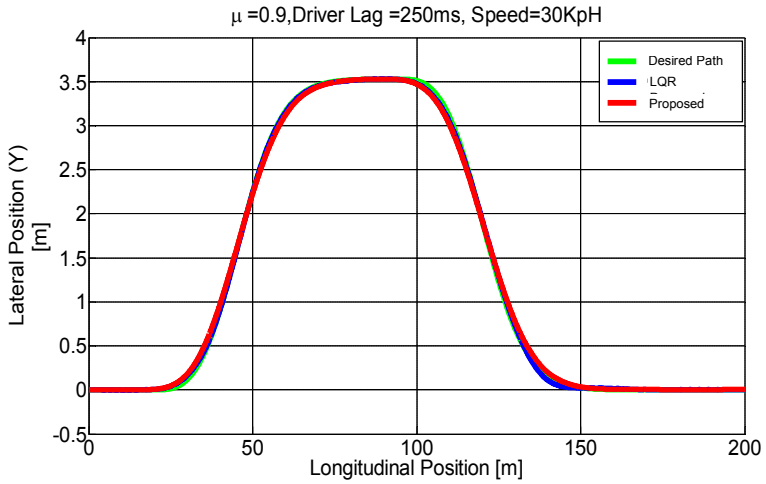

Figure 4-23 Carsim Driver test

However, as the road friction coefficient decreases to $\mu = 0.6$ (wet surface), the LQR controller shows small performance degradation even in low speed cases (Figure 4-24). The simulation shows that decreasing the road friction coefficient to a lower value of $\mu = 0.25$ increases the driver's delay to $350\ ms$ and $v_x = 50$ km/h, making the vehicle harder to control by the driver. Furthermore, the LQR controller cannot prevent vehicle skid and the system becomes unstable, while the proposed controller still keeps the vehicle in the acceptable range of performance.

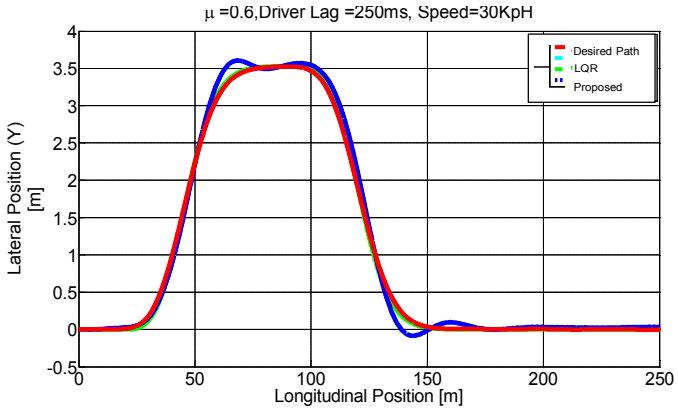

Figure 4-24 Carsim Driver - Low Speed

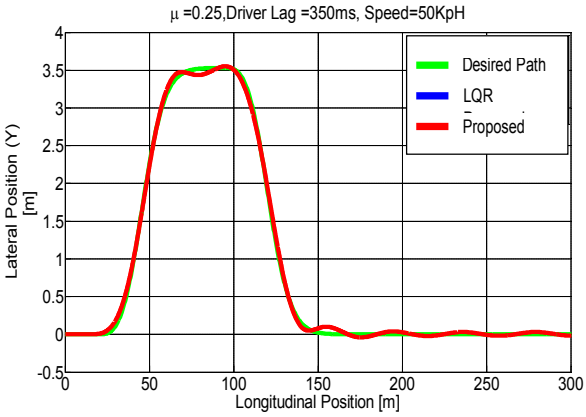

Figure 4-25 Carsim Driver - Low Friction

Another case with less, but still in the high range, friction and higher longitudinal velocity is simulated in Figure 4-27 and Figure 4-26, where the poor performance of standard controller is presented in contrast to the acceptable performance of driver in the loop.

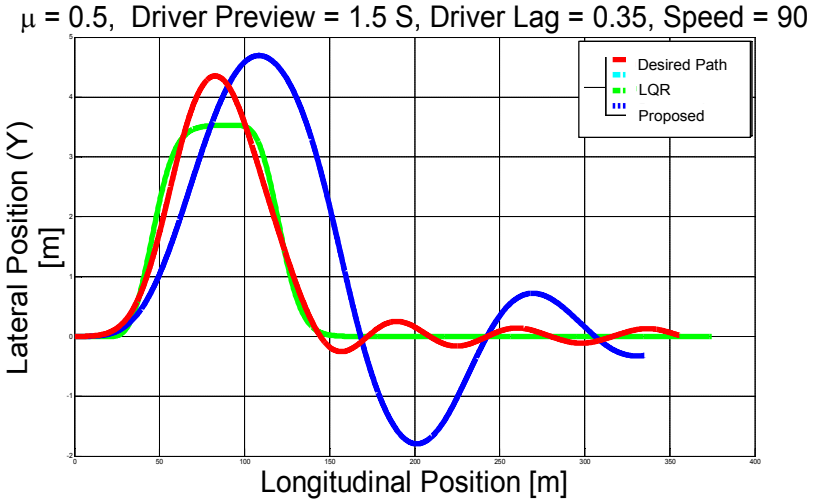

Figure 4-26 CarSim driver - high speed, wet

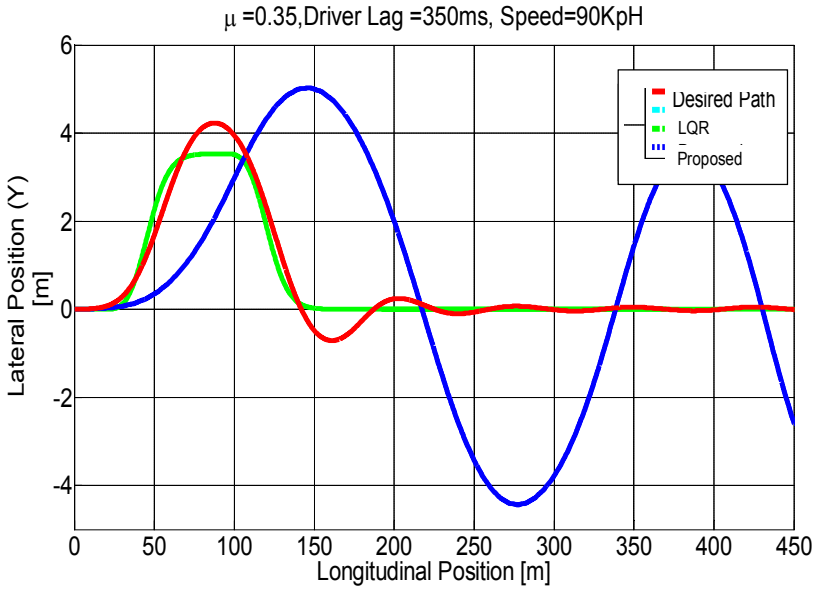

Figure 4-27 CarSim driver - high speed, slippery

As the delay and the vehicle's longitudinal speed increase while the road surface coefficient decreases, the driver cannot control the vehicle, and the effectiveness of the robust controllers is revealed.

The last simulation shows one case where an expert driver tries to steer the vehicle. The expertise can be defined by the minimum reaction delay time and the length of preview time. Here, a super human is driving the vehicle as the minimum delay for a driver is more than at least $200\ ms$. However, in order to show the idea, it is assumed that a humanoid robot driver is in the vehicle. In CarSim, the driver lag is set to be $100\ ms$ and the preview time to $1.5\ s$. The result supports the idea that an expert driver can steer the vehicle even in very harsh maneuverers. Although the proposed controller still makes the task easier for the driver compared to the ease of the task with the LQR. The comparison will be more apparent when one compares Figure 4-28 with Figure 4-27, where the effect of driver in the loop can be seen perfectly.

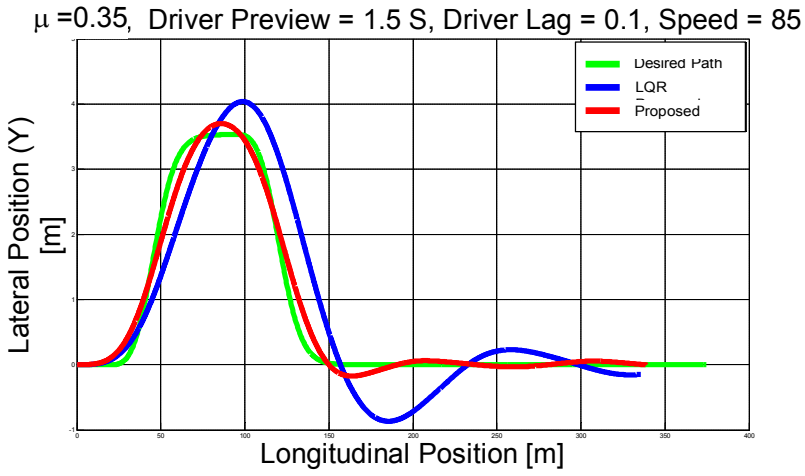

Figure 4-28 CarSim Expert Driver

4.11 Summary

The closed loop driver-vehicle dynamic stability problem was investigated in this chapter. The driver was modeled with a multi-point preview point path follower integrated with a transient delay block. The delay block represents the cumulative driver's observation and the action delay. A combination of the delayed steering angle, the path follower, and a linear vehicle bicycle model was assumed as the final closed loop system. Given that in real situations, the future road preview information (driver's intention) and the driver's delay are not accessible to the vehicle controller, the robust H_∞ control method was employed to handle unknown bounded exogenous inputs and the driver's time-varying delay. The controller in this scheme only uses the current states of the vehicle, steering wheel, and the uncertain driver model. To make the LTI controller less conservative, the robust stabilization problem was transformed into a robust output regulation. Considering the fact that the controller design is dependent on the driver's model parameters, the uncertainty in the modeling was added to the problem and a new delay robust $H\infty$ output regulator controller was proposed. The uncertain modeling can also be used as a reference for a range of drivers with varying expertise levels. The simulation results demonstrated that using a standard LQR controller, the vehicle's performance will be degraded as the driver's delay increases. However, applying the proposed controllers, the overall performance of the closed loop system remains satisfactory with even large time delays. As uncertainty is added to the system, the performance of the uncertain robust controller is not as good as the robust controller in fixed conditions. However, it preserves the system's stability, while the other controller fails. The driver-in-the-loop idea was implemented with both active steering and torque vectoring techniques.

"There are hardly any other branches of the mathematical sciences in which abstract mathematical speculation and concrete physical evidences go so beautifully together and complement each other so perfectly."

Cornelius Lanczons –The Variational Principles of Mechanics
Toronto University Press, 1962

Chapter 5
Redesign Based on Linear Parameter Varying Modeling

5.1 Introduction

Switching phenomena is a very important part of all of vehicle dynamic studies. Changes in driving style, longitudinal speed, tire slip-ratio, the lateral velocity, and rollover index are of the most important indices in vehicle dynamic studies that can drastically change the control strategy. In all implemented vehicle control modules, there are many conditions for selecting the right controller gain based on system status. The whole estimation process is mostly a function of vehicle states and there is usually a bank of observers to estimate important signals required by the stability module.

An important varying element in a vehicle is the driver. Obviously, the performance of a driver – or the driving style – is not a constant characteristic. Besides that, driving skill is another variable qualitative performance. In the previous chapter, it is shown (see Figure 4-27, Figure 4-28) that different driving characteristics result in very different vehicle performances. An expert driver can control the vehicle at its limits while a novice drive would likely not be able to control the car at its limits. Therefore, the controller must be redesigned based on each driving style if one wants to consider the driver effect in the closed loop.

Furthermore, the vehicle dynamics will be completely different when the longitudinal slip-ratio increases and passes certain thresholds (function of tire characteristics and road friction coefficient). The nonlinear behavior may cause a huge reduction in the tire force generation capacity both in the lateral and longitudinal direction, and a completely different gains for stability control will be needed to stabilize the vehicle. Basically, without maintaining slip-ratio in an acceptable region, there would not be much room for the stability controller to affect vehicle performance. The main reason is that there is no capacity in tires that the controller can use to

revise vehicle direction. Figure 5-1 shows how the longitudinal slip (λ) can decrease the tire force capacity on various road frictions.

On the other hand, it is also known that when the vehicle side slip angle or lateral velocity is large, the main task of the vehicle controller is to prevent vehicle skidding by reducing the lateral velocity. Regardless of the type of actuation structure, this task is directly related to vehicle stability (see [17, 63]). Note that having a set of gains for pure yaw tracking in this case will be extremely dangerous for vehicle safety as it can drastically increase the lateral velocity. Usually, lateral velocity control will be extremely important on low friction roads, and the main remedy to the increase in lateral velocity is to first make the vehicle understeer and in extreme cases, to drop the engine torque. In contrast, as the lateral velocity decreases and the vehicle is more controllable, yaw tracking becomes more important while the controller affects vehicle performance directly. In this case, the driver wants a vehicle which is more responsive and tracks the requested yaw rate of the driver more accurately. In normal driving, this is the case that occurs mostly on dry road and the vehicle performance can be drastically improved through better yaw tracking while the side slip maintains in certain bounded regions.

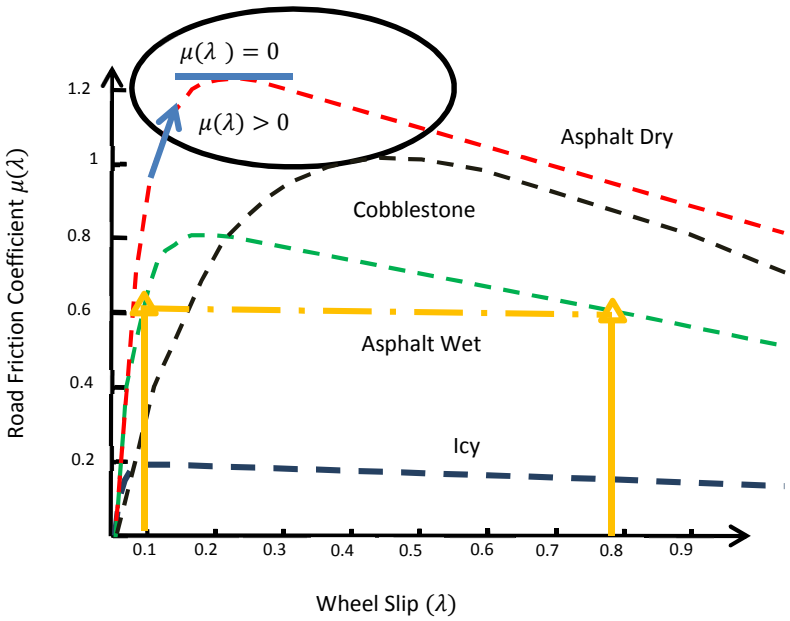

Figure 5-1 Tire Force VS longitudinal slip

5.2 Automatic Gain Scheduling

All of these effects leads one to think about gain scheduling methods for tuning the system for the best possible performance. In some of the problems, the time varying parameter is measurable (or can be estimated adequately). In this case, valuable extra information is available for the controller and the performance could be vastly improved. The well-known gain scheduling technique is of the most important tools for this problem. The issue here is to obtain the optimal and robust gains for the controller to maintain system robust stability and a good performance.

The traditional approach to solving this problem is to run the simulation or perform the experiments for different system operating points and produce either a multi-dimensional look up table or an analytic expression as a function of the parameter. This way, one selects a finite number of operating points and calculates the controller gains for each point while switching between the results. Although this method is often used in industry, in many cases, there is no guarantee for the overall system stability for all possibilities. In some cases, there might be abrupt changes in gains and there should also be a mechanism to prevent the controller parameters from changing suddenly.

The more elegant approach to dealing with this problem is designing the controller based on the information given on the boundary of the varying parameters and the rate of change of the parameters. This way, one can guarantee the stability of the system for the given range and avoid non-smooth behavior in the overall system. For linear systems, this procedure can be easily casted in a convex optimization problem and solving a series of LMIs for different operating points.

LPV analysis is clearly one of the most important control techniques to have significantly affected control engineering. Analysis of the LPV systems have been comprehensively reported in many papers (see [21, 127] and the reference therein). Among different methods of dealing with LPV systems, in this thesis, the Lyapunov-base method is considered since it can be directly used in a relatively simple and well-established controller design.

Intuitively and referring to (3.12), the driver model behavior is a function of the vehicle states and vehicle operating point parameters such as longitudinal velocity. Note that, in general, there will be some other parameters in real driving that are not captured in the simple formula used. Consider the model used in chapter 3. Given that, the vehicle model changes based on the longitudinal velocity and the friction coefficients, and the driver gains will be changed respectively.

There are a few approaches to analyzing time varying gains. One of these approaches could be to design a controller which is not only robust to the delay of a driver but is also robust to changes of the driver model parameters. Based on the formulation in (3.12), the gains K_1 and K_2 will be time varying and the controller must be robust with respect to the changes in these gains as well. Note that the other gains ($K_3 \quad K_N$) will also be time varying; however, they affect the uncertainty term which is dynamic and not important for the controller design procedure. It is easy to find a reasonable range for the parameters offline by solving the LQR problem for different cases where the longitudinal velocity and road friction coefficients are variable. Obviously, this procedure will relax the assumption dramatically and lead to a better controller design. There are many mature and well-developed robust controller designs for solving a control problem with parametric bounded uncertainty (see [15] and the reference thein). The main idea behind most of these methods is to consider a nominal value for the uncertain parameter and an uncertainty region (usually a convex polytope) in the vicinity of the parameter (or uncertain term). Taking advantage of robust control tools, one may find an optimal solution for the problem. If the uncertainty region is convex, the design procedure would be much easier and would require less computational effort.

Remark: Similar to the LTI controller design, the LMI conditions are not linear with respect to the controller parameters but bilinear. To deal with this issue, there are two main approaches, and both are described in [9]. One method is to add an extra optimization parameter and eliminate the bilinear term and the other one is a change of variable or congruent transformation. ■

Remark: Most of the methods in LPV analysis lead to a set of parameter-dependent matrix inequalities. Even in linear cases, the problem requires solving an infinite number of LMIs, which needs infinite time. This issue has been one of the main obstacles in LPV analysis during past decades. There are effective relaxation methods to convert the infinite dimensional LMIs to a finite number of LMIs by imposing some restrictions in the problem ([11]), but using the relaxation methods usually leads to an upper bound estimation for the robust control problem. Affine parameter dependency ([150]), sum of square ([152]), and polytypic domain for the parameters ([10]) are two of the most important methods. ■

5.3 LPV Modeling of the Driver-in-the-Loop System

There are many parameters in the vehicle model that are varying based on different conditions of time. From a vehicle handling perspective, the most important time varying parameter is longitudinal velocity. Most of the time, the other parameters can be ignored or modeled as the system states. Consider again the bicycle model of the vehicle with front steering given in (3.5):

$$\begin{aligned} ma_y = m\left(V_y + V_x r\right) &= F_{yr} + F_{yf}\cos\delta + F_{xf}\sin\delta \\ Ir = l_f F_{yf}\cos\delta \quad & l_r F_{yr} + l_f F_{xf}\sin\delta + M_z \end{aligned} \tag{5.1}$$

F_x and F_y are the nonlinear tire forces that the presented model cannot capture. The non-linearity of a tire is similar to a saturation model that prevents the tire force from growing linearly with respect to tire slip angle. There are several techniques proposed for modelling this behavior, however, most of them are too complex to directly use in control design. Moreover, all these techniques require information about the road friction coefficient, which is not easy to obtain. There are some papers presenting the results of controller design robust to road coefficient changes, however, they mostly yield a conservative design that is unacceptable for real application (see [77]). Another approach is to assume that an estimation of the road friction information is available. Then, a nonlinear or LPV controller can be casted respectively. For the sake of simplicity, in this chapter, by assuming that the road friction is constant and known. The extension of the model to LPV is possible by assuming the tire cornering stiffness is measurable or can be estimated.

Based on current technology, it is reasonable to assume that there exists a reliable estimation technique (using the stock IMU and the wheel speed sensor) or an accurate sensor such as GPS, to obtain the longitudinal velocity. It is assumed that the longitudinal velocity is measurable at each sampling time; therefore, the model in (3.5) can be represented in standard LPV form with known parameters. Similar to the method in Chapter 4, the effect of the driver can be captured in the model by considering that the steering wheel angle is a function of the desired future path (one or multiple preview point(s) in future) and the current vehicle states. This approach enables the controller to extract some information from the driver model rather than considering the driver input as a bounded uncertainty.

Remark: The main focus of this chapter is to solve the problem for a general case without any restriction on the driver modeling method. ■

Here, it is assumed that the driver input can be represented as a follows:

$$\delta(t) = k_1 V_y\big(t \quad \tau(t)\big) + k_2 r(t \quad \tau(t)) + \Omega \tag{5.2}$$

where $\tau(t)$ is the driver delay and similar to (4.5), Ω is the uncertainty. The LPV model of the system then can be presented as follows:

$$x(t) = A(\rho)x(t) + A_d(\rho)x\big(t \quad \tau(t)\big) + B_2 M_z(t) + E\Omega(t) \tag{5.3}$$

Where

$$A = \begin{matrix} \rho_1 \dfrac{\big(C_f + C_r\big)}{m} & \rho_1 \dfrac{\big(aC_f \quad bC_r\big)}{m} & \rho_2 \\ \rho_1 \dfrac{\big(aC_f \quad bC_r\big)}{I} & \rho_1 \dfrac{\big(a^2 C_f + b^2 C_r\big)}{I} & \end{matrix}$$

$$A_d = \begin{matrix} \rho_3 \dfrac{C_f}{mG_s} & \rho_4 \dfrac{C_f}{mG_s} \\ \rho_3 \dfrac{C_f}{IG_s} & \rho_4 \dfrac{C_f}{IG_s} \end{matrix}, B_2 = \begin{bmatrix} 0 \\ 1 \end{bmatrix}, E = \begin{matrix} \dfrac{C_f}{mG_s} \\ \dfrac{l_f C_f}{IG_s} \end{matrix}$$

where $\rho = \left[\frac{1}{V_x} \quad V_x \quad k_1 \quad k_2\right] = [\rho_1 \quad \rho_2 \quad \rho_3 \quad \rho_4]$ is the time varying measurable, bounded, and rate-bounded vector of parameters and $\tau_{min} \leq \tau(t) \leq \tau_{max}$ is the time varying bounded delay.

Remark: The driver has a bounded delay and a bounded delay derivative. i.e. $|\tau(t)| <$. It is easy to find an upper-bound for all human delay rate. ■

Referring to (5.3), there are three independent parameters in the modeling, noting that V_x and $\frac{1}{V_x}$ are dependent. Since the range of parameters are known and bounded, one can start by assuming that there is a convex polytope such as the box

$\Xi \quad [V_{x1} \quad , \quad V_{x2}] \times \left[\frac{1}{V_{x1}} \quad , \quad \frac{1}{V_{x2}}\right] \times [k_{1min} \quad , \quad k_{1max}] \times [k_{2min} \quad , \quad k_{2max}]$.

This representation induces conservation in analysis by assuming that V_x and $\frac{1}{V_x}$ vary arbitrarily in a box. This representation forces the LMIs to be true in the regions that exists outside the parameter domain. One way to analyze these two parameters is by considering a rectangle to obtain a convex set. Reducing the conservation, one may consider a triangle as a convex set containing the all possible combinations of V_x and $\frac{1}{V_x}$.

However, there will be a large space behind the curve that cannot occur in reality. Similar to the relaxation reported in [160], the conservation is reduced by confining the parameter ranges with a parallelogram. The line that connects two bounds of the V_x $\frac{1}{V_x}$ curve is $\ell_1 : y = \frac{x}{V_{x1}V_{x2}} + \frac{V_{x1}+V_{x2}}{V_{x1}V_{x2}}$ (see Figure 5-2).

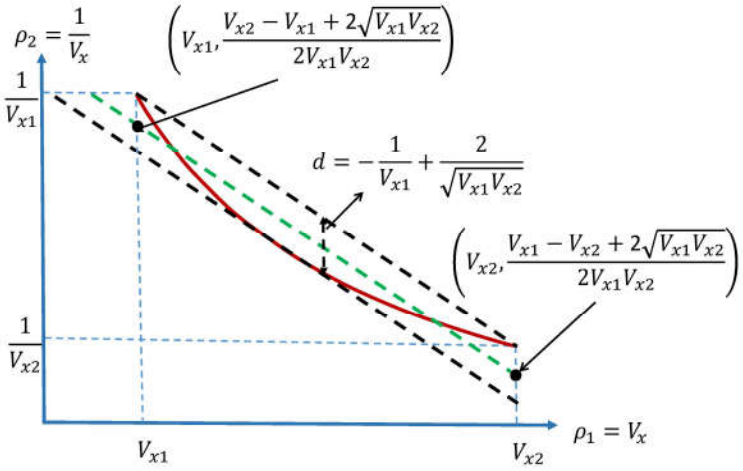

Figure 5-2 Uncertainty boundaries

The lower bound for the region can be defined by the line $\ell_2 : y = \frac{x}{V_{x1}V_{x2}} + \frac{2}{\sqrt{V_{x1}V_{x2}}}$, which has the same slope as $\ell_1$and is tangential to the curve $y = \frac{1}{x}$. Given that the distance between ℓ_1 and ℓ_2 is:

$$d = \frac{\left(\sqrt{V_{x2}} \quad \sqrt{V_{x1}}\right)^2}{V_{x1}V_{x2}} \tag{5.4}$$

the midpoints between two lines at the boundaries of the curve V_x $\frac{1}{V_x}$ are:

$$\zeta_1 = \left[V_{x1} \quad , \quad \frac{V_{x2} \quad V_{x1} + 2\sqrt{V_{x1}V_{x2}}}{2V_{x1}V_{x2}}\right]$$

$$\zeta_2 = \left[V_{x2} \quad , \quad \frac{V_{x1} \quad V_{x2} + 2\sqrt{V_{x1}V_{x2}}}{2V_{x1}V_{x2}}\right]$$

The line connecting the following points can cover all of the region in the parallelogram using the linear combination $\alpha_1\Phi_1 + \alpha_2\Phi_2$ where $\alpha_1 + \alpha_2 = 1$ and

$$\alpha_1 = \frac{|V \quad V_{x1}|}{|V_{x2} \quad V_{x1}|}, \alpha_2 = \frac{|V \quad V_{x2}|}{|V_{x2} \quad V_{x1}|}$$

$$\Phi_1 = \left[V_{x1} \quad , \quad \frac{V_{x2} \quad V_{x1} + 2\sqrt{V_{x1}V_{x2}}}{2V_{x1}V_{x2}} + \frac{\left(\sqrt{V_{x2}} \quad \sqrt{V_{x1}}\right)^2}{2V_{x1}V_{x2}}\mu(t)\right]$$

$$\Phi_2 = \left[V_{x2} \quad , \quad \frac{V_{x1} \quad V_{x2} + 2\sqrt{V_{x1}V_{x2}}}{2V_{x1}V_{x2}} + \frac{\left(\sqrt{V_{x2}} \quad \sqrt{V_{x1}}\right)^2}{2V_{x1}V_{x2}}\mu(t)\right]$$

where $|\mu(t)| \leq 1$. Also, one can write the equation for the middle line ℓ_3 as:

$$y = \quad \frac{x}{V_{x1}V_{x2}} + \frac{\left(\sqrt{V_{x2}} \quad \sqrt{V_{x1}}\right)^2}{2V_{x1}V_{x2}} + \mu(t)\frac{\left(\sqrt{V_{x2}} \quad \sqrt{V_{x1}}\right)^2}{2V_{x1}V_{x2}} \tag{5.5}$$

Using this approximation, the equation ((5.3)) can be rewritten as follows:

$$x(t) = \left(\tilde{A}(\rho) + \Delta\tilde{A}\right)x(t) + A_d(\rho)x\left(t \quad \tau(t)\right) + B_2M_z(t) + E\Omega(t) \tag{5.6}$$

$$A = \begin{bmatrix} A_{11} & \tilde{A}_{12} \\ A_{22} & \tilde{A}_{22} \end{bmatrix}, \Delta\tilde{A} = \begin{bmatrix} 0 & \mu(t)\frac{\left(\sqrt{V_{x2}} \quad \sqrt{V_{x1}}\right)^2}{2V_{x1}V_{x2}} \\ 0 & 0 \end{bmatrix}$$

$$\tilde{A}_{12} = \quad \rho_1\frac{\left(l_fC_f \quad l_rC_r\right)}{m} + V_{x1}V_{x2}\rho_1 \quad 0.5\left(\sqrt{V_{x2}} + \sqrt{V_{x1}}\right)^2$$

where $\rho = \left[\frac{1}{V_x} \quad k_1 \quad k_2\right]^T = [\rho_1 \quad \rho_2 \quad \rho_3]^T$. This transformation enables us to eliminate the parameter varying elements without imposing large deviations from the original model around the operating point.

5.4 Control Objective

The desired yaw rate value can be defined as a function of the driver's steering angle. Without loss of accuracy, the desired vehicle lateral velocity is considered to be zero. Thus, the tracking error can be written as follows:

$$e(t) = x(t) \quad x_d(t) \tag{5.7}$$

where the desired value for lateral velocity is zero and the desired yaw-rate is given in (4.2).

$$x_d(t) = [0 \quad r_d]^T = [0 \quad f(\delta, V_x)]^T \tag{5.8}$$

Therefore, the corresponding error dynamics is:

$$e(t) = \left(\tilde{A}(\rho) + \Delta\tilde{A}\right)e(t) + A_d(\rho)e\left(t \quad \tau(t)\right) + B_2\bar{M}_z(t) + E\bar{\Omega}(t) \tag{5.9}$$

$$\bar{M}_z(t) = M_z(t) \quad r_d(t) + \tilde{A}_{22}r_d$$

$$\bar{\Omega}(t) = \Omega(t) + \left[\frac{\tilde{A} + \Delta\tilde{A}_{12}}{E_1} \quad , \quad \frac{\Delta\tilde{A}_{22}}{E_2}\right]x_d(t) + \left[\frac{A_{d12}}{E_1} \quad , \quad \frac{A_{d22}}{E_2}\right]x_d(t \quad \tau(t))$$

5.5 Torque Distribution Technique

Considering the bicycle model for the controller design process, the controller calculates the required control action to adjust the vehicle performance. The distributor considers the vehicle actuator and road traction capability constraints and optimally distributes a certain amount of torque to each wheel in a way such that the required torque is produced at CG. Based on the predefined configuration, the effect can be adjusting by changing the steering angle, braking, or adding more torque at each individual wheel or vehicle track.

An optimal torque distribution is used in this paper for transferring the torque (force) to the vehicle's tires. Note that in the torque vectoring technique for electric vehicles, the actuators can only produce longitudinal forces for each independent wheel.

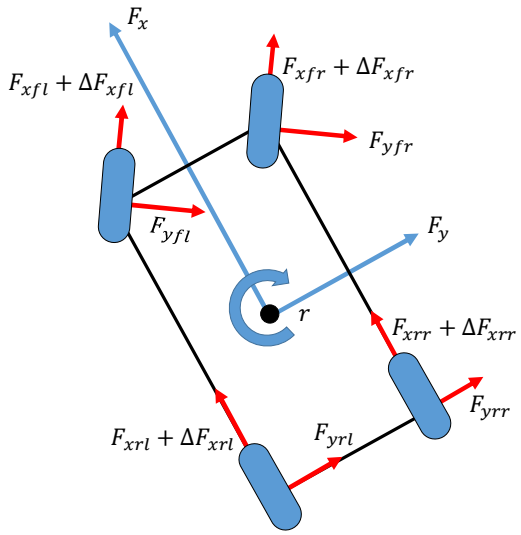

Figure 5-3 Torque Distribution technique

Applying the control action, the second order approximation of the vehicle yaw moment is:

$$r(F + \Delta F) \approx r(F) + \nabla r(F)\Delta F + \frac{1}{2}\nabla^2 r(F)\Delta F^2 \tag{5.10}$$

where $\nabla r(F)$ is the gradient of the vehicle yaw moment with respect to the tire forces. Then:

$$r(F + \Delta F) \quad r_d \approx \bar{M}_z \quad \nabla r(F)\Delta F \quad \frac{1}{2}\nabla^2 r(F)\Delta F^2 \tag{5.11}$$

For the distribution part, a more accurate model for the vehicle yaw moment is considered as follows:

$$\begin{aligned} r = l_f \sum_{i=1,2} \left(F_{xi}\sin\delta_i + F_{yi}\cos\delta_i\right) \quad l_r \sum_{i=3,4} \left(F_{xi}\sin\delta_i + F_{yi}\cos\delta_i\right) \\ +W \sum_{i=1,2} \left(F_{xi}\cos\delta_i \quad F_{yi}\sin\delta_i\right) \quad W \sum_{i=3,4} \left(F_{xi}\cos\delta_i \quad F_{yi}\sin\delta_i\right) \end{aligned} \tag{5.12}$$

where i indicates the vehicle's front left, front right, rear left, rear right corners, and W is the wheel base. Taking the derivative of the yaw moment with respect to longitudinal force (the only actuator) results in:

$$\begin{aligned} \nabla r = [l_f \sin\delta \quad W\cos\delta \quad l_f \sin\delta + W\cos\delta \quad W \quad W] \\ \nabla^2 r(F) = 0 \end{aligned} \tag{5.13}$$

The problem is now formulated as a standard optimization problem. Consider the following cost function for the torque distribution:

$$J = \frac{1}{2}\left(\Delta F^T R \Delta F + (\bar{M}_z \quad \nabla r(F)\Delta F)^T Q (\bar{M}_z \quad \nabla r(F)\Delta F)\right) \tag{5.14}$$

where Q and R, respectively, are a positive scalar and a positive definite matrix to adjust the importance of error tracking and control action. The optimal control action that minimizes J is:

$$\Delta F = (R + \nabla r^T Q \nabla r)^{-1} \nabla r^T Q \bar{M}_z = [\eta_1 \quad \eta_2 \quad \eta_3 \quad \eta_4]^T \bar{M}_z \tag{5.15}$$

Remark: The control allocation problem can also be cast as a standard linear programming or quadratic programming problem corresponding to ℓ_1- norm, ℓ_∞- norm or ℓ_2 -norm objective. Depending on the control objective, the method, including its physical limitations, can also be handled using an interior-point method. A thoroughly explanation about the methods of solving mixed optimization programming is presented in [3]. ■

Assume that ℓ_2 norm is chosen for solving the allocation problem. Based on (5.14), the distribution gain is a function of geometric characteristics of the vehicle, tuning parameters of R and Q, and the steering angle. Using the optimal torque distributor, the actuator gain can also be modeled in vehicle modeling.

Remark: One can use sequential problem solving to find the exact answer of the problem in two steps. First, one can find all of the solutions that minimize the difference between the requested moment and the control action moment (error). In the next step, among all of these solutions, a set of forces that minimizes control action can be chosen (in a desirable norm space). The process of solving this problem is easy to implement, but it does require solving a quadratic programing (or linear programing for ℓ_∞- norm) problem twice; whereas, the method used in this chapter provides an analytical solution that is easier to implement. ■

Program 1:

$$e \qquad \min_{\Delta F \in R^4} \| \bar{M}_z \quad \nabla r(F)\Delta F \| \tag{5.16}$$

Program 2:

$$\min_{\Delta F \in R^4} \| \Delta F \| \qquad st. \qquad \bar{M}_z \quad \nabla r(F)\Delta F \| = e \tag{5.17}$$

Now, one can write the following equations for the yaw rate dynamics which also includes the characteristics of the torque vectoring actuator:

$$Ir = aF_{yf} \quad bF_{yr} + \rho_5 \bar{M}_z \tag{5.18}$$

$$\rho_5 = W(\eta_2 \quad 2\eta_3 \quad \eta_1)$$

The parameter-varying effect of the actuator is now captured in the formulation. Note that the value can be calculated using the steering wheel angle signal.

5.6 Controller Design

In this section, it is assumed that the parameter varying terms are all accessible to the controller, and the synthesis problem of a memory-less control law is investigated. Considering the effect of the driver and the torque vectoring actuator, the goal is to design a memory-less state feedback parameter varying controller that is robust to time varying delay for the following system:

$$\sum_1 : \begin{array}{c} e(t) = \big(\tilde{A} + \Delta\tilde{A}\big)\big(\rho(t)\big)x(t) + A_d\big(\rho(t)\big)e\big(t \quad \tau(t)\big) + B_2\big(\rho(t)\big)\bar{M}_z(t) + E(\rho(t))\Omega(t), \\ z(k) = Ce(t), \\ y(k) = Ce(t) \\ e(k) = 0, \quad \tau_{max} \le t \le 0, \end{array} \tag{5.19}$$

where $e \in R^n$ is the state, $\bar{M}_z \in R^m$ is the control input, $\bar{\Omega} \in R^q$ is the exogenous disturbance signal assumed to belong to $\ell_{2\epsilon}$, $z(t) \in R^p$ is the control output to be attenuated, and $\rho(t) = \left[\frac{1}{V_x} \quad k_1 \quad k_2\right]$ is the parameter varying vector. Assuming that the longitudinal velocity is positive, the parameters are continuously differentiable functionx of time and all of the trajectories lie in a known compact set.

Controller design for the LPV systems is usually based on the worst-case scenario analysis in robust control literature. Most of the physical parameters have a certain range of variation with a bounded rate of variation. In worst-case analyses, the controller is designed to work under the extreme bounds of the range of the parameter and its corresponding derivative. This makes the LPV analysis conservative compared to the cases where some extra information about the parameters or derivatives are available. For instance, in Markov chain modeling, the probability of switching between the parameters is also used in the design (see [51]). For the case where there is no information about the rate of change in parameters, a quadratic stability method is normally used, which results in a conservative design for the case where the rates of change of

parameters are bounded. To refine the results, the literature suggests to use the parameter dependent Lyapunov function for analysis. This way, the analysis directly includes the parameters' rate of change values, which decrease design conservation (see [150]).

5.6.1 Delay analysis in LPV systems

Similar to chapter 4, the Lyapunov-Krasovskii method is used here to deal with the delayed system. Using this method, the time-delay derivative $\left(\tau(t)\right)$ must be less than 1. The assumption here is that the human delay derivative at each sampling time does not grow more than one unit, which makes sense based on human characteristics and action limitations in a short period of time. This assumption ensures that the controller collecting the information in order.

Assume that a phenomenon happens at time t, and there is a function of time varying delay of $\tau(t)$ in the transmission line, we want to receive the first set of data before the second pack of information which will be sent at $t = t + \Delta t$. Then:

$$t + \tau(t) < t + \Delta t + \tau(t + \Delta t) \;\Rightarrow\quad \Delta t < \tau(t + \Delta t) \quad \tau(t) \Rightarrow \quad 1 < \tau(t)$$

On the other hand, we always want to have new information coming from the delay channel. This means that $t \quad \tau(t)$ should always be increasing. If for some cases, it is decreasing, one may have the same data at the different time, i.e., $t_1 \quad \tau(t_1) = t_2 \quad \tau(t_2)$. To prevent this, the following condition must be satisfied:

$$t_1 \quad \tau(t_1) < t_2 \quad \tau(t_2)$$

$$t_1 \quad \tau(t_1) < t_1 + \Delta t \quad \tau(t_1 + \Delta t) \Rightarrow \tau(t_1 + \Delta t) \quad \tau(t_1) < \Delta t \Rightarrow \tau(t) < 1$$

Note that for the other cases, one can use a model transformation to deal with a delay derivative larger than one, however, it makes the design more complicated (see [134]).

For an unforced system with no delay, quadratic stability guarantees the system stability for unbounded parameter variation rate, and the necessary condition is:

$$A(\rho)^T P + PA(\rho) < 0, \qquad P > 0 \tag{5.20}$$

The robust stability, on the other hand, can take care of the system with an upper bounded parameter variation rate. This extra information decreases conservativeness of the system and makes the design process efficient. The necessary and sufficient condition using this method is:

$$\sum_i \frac{dP(\rho)}{d\rho_i}\rho_i + A(\rho)^T P(\rho) + P(\rho)A(\rho) < 0, \qquad P(\rho) > 0 \tag{5.21}$$

Lemma (Jensen's inequality):

Let ϕ be a be a convex integrable function and $z: [a,b] \rightarrow R, a < b$, be integrable over its domain of definition. Then, the following inequality holds:

$$\phi\left(\int_a^b z(s)ds\right) \leq (b \quad a)\int_a^b \phi\big(z(s)\big)ds$$

Now, let ϕ be quadratic function of $\phi = z^T Rz$, then:

Let $Z \in S_{>0}^n$ and $z: [a,b] \rightarrow R^n$ be an integrable function on its domain. Then,

$$\left(\int_a^b z(s)ds\right)^T R\left(\int_a^b z(s)ds\right) \leq (b \quad a)\int_a^b z(s)^T Rz(s)ds.$$

Theorem 5.1:

Given a lower and upper delay range of $0 \leq \tau(t) \leq \tau_{max}$ and an attenuation factor of $\gamma > 0$, the system (5.19) is asymptotically stable (for $\Delta\tilde{A} = 0, \mu(t) = 0$), using $\overline{M}_z(t) = Y(\rho)X^{-1}e(t)$, and $\overline{\Omega}(t) \in \ell_{2\epsilon}$, if there exists a continuously differentiable positive definite matrix function $P(\rho)$, positive definite matrices Q and R, and matrices $X, Y(\rho)$ such that the following LMI holds for $(\rho, \nu) \in \Delta_{\rho \times V_\nu}$.

$$\begin{matrix} \phi_{11} & \phi_{12} & A_d(\rho)X & E(\rho) & 0 & X & \tau_{max}R \\ & \phi_{22} & R & 0 & X^T C^T & 0 & 0 \\ & & \phi_{33} & 0 & 0 & 0 & 0 \\ & & & \gamma I & 0 & 0 & 0 \\ & & & & \gamma I & 0 & 0 \\ & & & & & P(\rho) & \tau_{max}R \\ & & & & & & R \end{matrix} < 0 \qquad (5.22)$$

$$\phi_{11} = \quad X \quad X^T$$

$$\phi_{12} = P(\rho) + \tilde{A}(\rho)X + B_2(\rho)Y(\rho)$$

$$\phi_{33} = \quad (1 \quad \bar{\gamma})Q \quad R$$

$$\phi_{22} = \pm\sum_i \frac{\partial P(\rho)}{\partial \rho_i}\nu_i \quad P(\rho) + Q \quad R$$

$$|\tau(t)| \leq \bar{\gamma} < 1$$

$$|\rho(t)| \leq \nu$$

Proof:

The proof is inspired by theorem 8.1.2 in [21]. Consider the following Lyapunov-Krasovskii function:

$$V(e_t, e_t) = e(t)^T P e(t) + \int_{t-\tau(t)}^{t} e(\theta)^T Q e(\theta) d\theta + \tau_{max} \int_{-\tau_{max}}^{0} \int_{t+\theta}^{t} e(\eta)^T R e(\eta) d\eta \, d\theta$$

Taking the derivative along the system trajectory and using Leibniz rule:

$$\begin{aligned}
\frac{dV}{dt} = {} & e(t)^T P e(t) + e(t)^T P e(t) + e^T(t) \sum_i \pm \frac{\partial P(\rho)}{\partial \rho_i} \frac{\partial \rho_i}{\partial t} e(t) + e(t)^T Q e(t) \\
& \begin{pmatrix} 1 & \tau(t) \end{pmatrix} \left(e\begin{pmatrix} t & \tau(t) \end{pmatrix}^T Q e\begin{pmatrix} t & \tau(t) \end{pmatrix} \right) + \tau_{max} \int_{-\tau_{max}}^{0} e(t)^T R e(t) d\theta \\
& \tau_{max} \int_{-h_{max}}^{0} e(t+\theta)^T R e(t+\theta) d\theta \\
= {} & e(t)^T P e(t) + e(t)^T P e(t) + e^T(t) \sum_i \pm \frac{\partial P(\rho)}{\partial \rho_i} \frac{\partial \rho_i}{\partial t} e(t) + e(t)^T Q e(t) \\
& \begin{pmatrix} 1 & \tau(t) \end{pmatrix} \left(e\begin{pmatrix} t & & (t) \end{pmatrix}^T Q e\begin{pmatrix} t & & (t) \end{pmatrix} \right) + \tau_{max}^2 \left(e(t)^T R e(t) \right) \\
& \tau_{max} \int_{t-\tau_{max}}^{t} e(\theta)^T R e(\theta) d\theta
\end{aligned}$$

Note that $|\tau(t)| = \bar{\mu} < 1$ and $\tau(t) \leq \tau_{max}$

$$\tau_{max} \int_{t-\tau_{max}}^{t} e(\theta)^T R e(\theta) d\theta \leq \tau_{max} \int_{t-\tau(t)}^{t} e(\theta)^T R e(\theta) d\theta$$

From Jensen's inequality:

$$\begin{aligned}
\tau_{max} \int_{t-\tau(t)}^{t} e(\theta)^T R e(\theta) d\theta \leq {} & \frac{\tau_{max}}{\tau(t)} \left(\int_{t-\tau(t)}^{t} e(\theta) d\theta \right)^T R \left(\int_{t-\tau(t)}^{t} e(\theta) d\theta \right) \\
= {} & \frac{\tau_{max}}{\tau(t)} [(e(t) \quad e(t \quad \tau(t)))^T R (e(t) \quad e(t \quad \tau(t)))]
\end{aligned}$$

$$\frac{dV}{dt} \leq e(t)^T P e(t) + e(t)^T P e(t) + e^T(t) \sum_i \pm \frac{\partial P(\rho)}{\partial \rho_i} \frac{\partial \rho_i}{\partial t} e(t) + e(t)^T Q e(t)$$
$$(1 \quad \tau(t)) \left(e(t \quad (t))^T Q e(t \quad (t)) \right) + \tau_{max}^2 \left(e(\theta)^T R e(\theta) \right)$$
$$\frac{\tau_{max}}{\tau(t)} [(e(t) \quad e(t \quad \tau(t)))^T R (e(t) \quad e(t \quad \tau(t)))]$$

$\frac{1}{\tau(t)}(e(t) \quad e(t \quad \tau(t)))$ always exists ($e(t)$ exist, and $\frac{\tau_{max}}{\tau(t)} \leq 1$)

$$\frac{dV}{dt} \leq e(t)^T P e(t) + e(t)^T P e(t) + e^T(t) \sum_i \pm \frac{\partial P(\rho)}{\partial \rho_i} \nu_i \, e(t) + e(t)^T Q e(t)$$
$$(1 \quad \bar{\mu}(t)) \left(e(t \quad (t))^T Q e(t \quad (t)) \right) + \tau_{max}^2 \left(e(\theta)^T R e(\theta) \right)$$
$$[(e(t) \quad e(t \quad \tau(t)))^T R (e(t) \quad e(t \quad \tau(t)))]$$

Now replace the values from the equation (5.19):

$$= \left(A e(t) + A_d e(t \quad \tau(t)) + E\Omega(t) \right)^T P e(t) + e(t)^T P \left(A e(t) + A_d e(t \quad \tau(t)) + E\Omega(t) \right)$$
$$+ e^T(t) \sum_i \pm \frac{\partial P(\rho)}{\partial \rho_i} \nu_i \, e(t) + e(t)^T Q e(t)$$
$$(1 \quad \bar{\mu}) \left(e(t \quad \tau(t))^T Q e(t \quad \tau(t)) \right)$$
$$+ \tau_{max}^2 \left(\left(A\tau(t) + A_d e(t \quad \tau(t)) + E\Omega(t) \right)^T R \left(A\tau(t) + A_d e(t \quad \tau(t)) \right. \right.$$
$$\left. \left. + E\Omega(t) \right) \right) \quad [(e(t) \quad e(t \quad \tau(t)))^T R (e(t) \quad e(t \quad \tau(t)))]$$

$$\Psi = [e(t) \quad e(t \quad \tau(t)) \quad \Omega(t)]$$

$$A^T P + PA + \sum_i \frac{\partial P(\rho)}{\partial \rho_i} \nu_i + Q \quad R \qquad PA_h + R \qquad PE$$
$$(1 \quad \mu)Q \quad R \quad 0$$
$$0$$
$$+ \tau_{max}^2 \begin{bmatrix} A^T \\ A_h^T \\ E^T \end{bmatrix} R [A \quad A_h \quad E]$$
$$< 0$$

Introducing the ℓ_2 performance test, one can show that the H_∞ norm of system (5.19) does not exceed a certain level of γ. Now it is possible to define the following Hamiltonian and show that its derivative is always negative for all non-zero Ψ:

$$H(t) = V(t) \quad \int_0^T (\gamma\omega(\theta)^T\omega(\theta) \quad \gamma^{-1}z(\theta)^T z(\theta)d\theta$$

If $H < 0$ then integration leads to:

$$z(t)^T z(t) < \gamma^2\omega(t)^T\omega(t)$$

Hence:

$$H(t) = V(t) \quad \gamma\omega(\theta)^T\omega(\theta) + \gamma^{-1}z(\theta)^T z(\theta) < 0$$

$$A^TP + PA + \sum_i \frac{\partial P(\rho)}{\partial \rho_i}\nu_i + Q \quad R \qquad PA_d + R \qquad PE \qquad + \tau_{max}^2 \begin{bmatrix} A^T \\ A_d^T \\ E^T \end{bmatrix} R[A \quad A_d \quad E]$$

$$(1 \quad \mu)Q \quad R \quad 0$$

$$\gamma I$$

$$+ \gamma^{-1}\begin{bmatrix} C^T \\ 0 \\ 0 \end{bmatrix}[C \quad 0 \quad 0] < 0$$

Given that:

$$\tau_{max}^2 \begin{bmatrix} A^T \\ A_d^T \\ E^T \end{bmatrix} R[A \quad A_d \quad E] + \gamma^{-1}\begin{bmatrix} C^T \\ 0 \\ 0 \end{bmatrix}[C \quad 0 \quad 0]$$

$$= \begin{bmatrix} C^T & \tau_{max}RA^T \\ 0 & \tau_{max}A_h^T \\ 0 & \tau_{max}E^T \end{bmatrix}\begin{bmatrix} \gamma^{-1} & 0 \\ 0 & R^{-1} \end{bmatrix}\begin{bmatrix} C & 0 & 0 \\ \tau_{max}RA & \tau_{max}RA_d & \tau_{max}RE \end{bmatrix}$$

$$A^TP + PA + \sum_i \pm\frac{\partial P(\rho)}{\partial \rho_i}\nu_i + Q \quad R \qquad PA_d + R \qquad PE \qquad C^T \qquad \tau_{max}A^TR$$

$$(1 \quad \mu)Q \quad R \quad 0 \quad 0 \quad \tau_{max}A_d^TR < 0 \ (\ )$$

$$\gamma I \quad 0 \quad \tau_{max}E^TR$$

$$\gamma I \quad 0$$

$$R$$

The problem is that this formulation involves cross terms of decision variables that cause difficulties in the control design procedure. In the design section, one needs to change the system matrix A to $A + BK$, and this term results in a bilinear matrix inequality that needs more complex algorithm to solve (usually based on bisection method). Note that by having these terms, a congruence transformation can-not linearize the problem.

One approach is to decouple the crossed terms using the projection-lemma ([47]) based methods (see [162] and [21]). Then, one can rewrite ($\varkappa = \Upsilon|_{X=Y=0}$) as:

$$\varkappa + \quad ^{T} \quad ^{T} \quad + \quad ^{T} \quad ^{T} \quad < 0$$

$$^{T} = [\ \ I \quad A \quad A_d \quad E \quad 0 \quad I \quad 0], \quad = [I \quad 0 \quad 0 \quad 0 \quad 0 \quad 0 \quad 0], \quad ^{T} = X^T$$

Now using projection lemma, one only need to show that:

$$\begin{matrix} ^{T}_{1}\varkappa \ \ _{1} < 0 \\ ^{T}_{2}\varkappa \ \ _{2} < 0 \end{matrix}$$

Where $_{1}$ and $_{2}$ are null space of and . Following the lemma, it is easy but lengthy process to show that the feasibility of (5.22) shows feasibility of $\widehat{\Omega}$:

$$\widehat{\Omega} = \begin{matrix} \phi_{11} & \phi_{12} & A_d(\rho)X & E(\rho) & 0 & X & \tau_{max}R \\ & P(\rho) + \tilde{A}(\rho)X & R & 0 & X^T C^T & 0 & 0 \\ & & \phi_{33} & 0 & 0 & 0 & 0 \\ & & & \gamma I & 0 & 0 & 0 \\ & & & & \gamma I & 0 & 0 \\ & & & & & P(\rho) & \tau_{max}R \\ & & & & & & R \end{matrix}$$

Substituting $A(\rho)$ with $A(\rho) + B_2(\rho)K(\rho)$and performing congruence transformation with

$$\begin{matrix} X^{-1} & 0 & 0 & 0 & 0 & 0 \\ & X^{-1} & 0 & 0 & 0 & 0 \\ & & X^{-1} & 0 & 0 & 0 \\ & & & I & 0 & 0 \\ & & & & X^{-1} & 0 \\ & & & & & X^{-1} \end{matrix}$$

And letting $Y(\rho) = K(\rho)X^{-1}$ completes the proof.

Note that since $|\omega| \leq v$ and it enters linearly in the matrix inequalities, one only needs to check the LMI feasibilities at the vertices of this convex hull.

Given that the uncertainty term can be written as $\Delta\tilde{A} = \Pi\, \mu(t)\, \Gamma$ where Π and Γ are constant matrices and $\mu(t)^T\mu(t) \leq 1$, one can easily extend the result of theorem 5.1 to consider the effect of structured uncertainty $\Delta\tilde{A}\ (\rho)$.

Theorem 5.2:

Given the lower and upper delay range of $0 \leq \tau(t) \leq \tau_{max}$ and an attenuation factor of $\gamma > 0$, the system (5.19) is asymptotically stable, using $\bar{M}_z(t) = Y(\rho)X^{-1}e(t)$, and $\Omega(t) \in \ell_{2\epsilon}$, if there exists a continuously differentiable positive definite matrix function $P(\rho)$, positive definite matrices Q and R, and matrices $X, Y(\rho)$ such that the following LMI holds for $(\rho, \nu) \in \Delta_{\rho \times V_\nu}$.

$$\widehat{\Upsilon} = \begin{bmatrix} \Upsilon & \rho\overline{\Pi} & \overline{\Gamma}^T \\ & \sigma I & 0 \\ & & \sigma I \end{bmatrix} < 0 \tag{5.23}$$

where Υ is defined in (5.23), $\overline{\Pi} = [0 \quad \Pi^T \quad 0]^T$, and $\overline{\Gamma} = [0 \quad \Gamma X \quad 0]^T$.

Proof:

Recalling that $\Delta\tilde{A} = \Pi\mu(t)\Gamma$, one can write:

$$\begin{aligned} &\Upsilon + [0 \quad \Pi \quad 0 \qquad 0]^T\mu[0 \quad 0 \quad \Gamma X \quad 0 \qquad 0] + \\ &[0 \quad 0 \quad X^T\Gamma^T \quad 0 \qquad 0]^T\mu^T[0 \quad \Pi^T \quad 0 \qquad 0] < 0 \end{aligned} \tag{5.24}$$

By Lemma 1 in chapter 4, there exists some $\sigma > 0$ for the inequality (5.24), such that:

$$\begin{aligned} &\Upsilon + \sigma[0 \quad \Pi \quad 0 \qquad 0]^T[0 \quad \Pi^T \quad 0 \qquad 0] + \\ &\sigma^{-1}[0 \quad 0 \quad X^T\Gamma^T \quad 0 \qquad 0]^T\mu^T[0 \quad 0 \quad \Gamma X \quad 0 \qquad 0] < 0 \end{aligned}$$

Using the Schur complement, the inequality (5.23) can be obtained.

5.7 Simulation Results

In this section, the Robust LPV controller is evaluated in different scenarios. The CarSim software is integrated with Matlab Simulink to provide an accurate vehicle model (see Figure 5-4). It is also assumed that the driver model is a multi-point preview path follower where the corresponding parameters can be calculated by solving an LQR problem at each sampling time. Since this paper addresses only the control part, the parameters are assumed to be accessible directly by the controller. Note that the parameters need to be estimated without using the future path of the vehicle. One way is to consider a moving average window on the past few seconds of the road information and applying an appropriate identification method assuming that the desired path is tracked with an acceptable error. Another option is offline calculation of the gains using the known preview-point driver models and scheduling them based on longitudinal velocity.

The vehicle parameters for a slippery road condition in the simulation are reported in Table 2. In the simulation, the requested torque transfers to the wheels and is used by an independently controllable electric motor. Also, to obtain good results on a slippery road, it is assumed that a traction controller prevents a large longitudinal tire slip-ratio. In cases where there is a conflict between the traction controller and lateral controller, the priority is given to the traction controller to maintain the tire angular velocity in a certain range.

During the simulation, it is assumed that the delay $\tau(t) \leq 215ms, \tau(t) \leq 0.1$, the longitudinal speed $(50kp \leq V_x \leq 90\,kp)$, $|V_x| \leq 5\frac{m^2}{s}$, $2 \leq k_1 \leq 4$, $2 \leq k_2 \leq 6, |k_1| = |k_2| \leq 1.5$ and $\bar{\tau}(t) = 215ms$. Usually, for lower longitudinal speeds, the controller is off and the traction control takes care of the vehicle stability. An acceleration-in-turn maneuver is an example of an exceptional case where accurate longitudinal speed estimation is required. This estimation starts from zero and is assumed to be handled by another control patch.

Solving the semi-infinite LMIs, the gridding-method is employed to convert it to a tractable finite-dimensional problem where each parameter space is divided into 10 intervals (see [21] for details of convergence conditions). It is also assumed that the parameter varying matrices have polynomial basis as: $Y(\rho) = Y_0 + Y_1\rho + Y_2\rho^2$. Note that optimization is over an open set of matrices, so, achieving the minimum in not possible as it is looking for an infimum. The readers are referred to [155] for a thorough discussion on solving LMIs numerical problems.

Table 2 : Vehicle parameters

Variable	Value	Units	Description
C_f	38000 62000	$\frac{N}{rad}$	Front-axle cornering stiffness
C_r	33000 63000	$\frac{N}{rad}$	Rear-axle cornering stiffness
a	1.42033	m	Front axle to center of mass distance
b	1.43767	m	Rear axle to center of mass distance
m	2270	kg	Vehicle mass
I	4600	$kg.m^2$	Vehicle yaw moment of inertia
G	20		Hand wheel to road wheel angle ratio

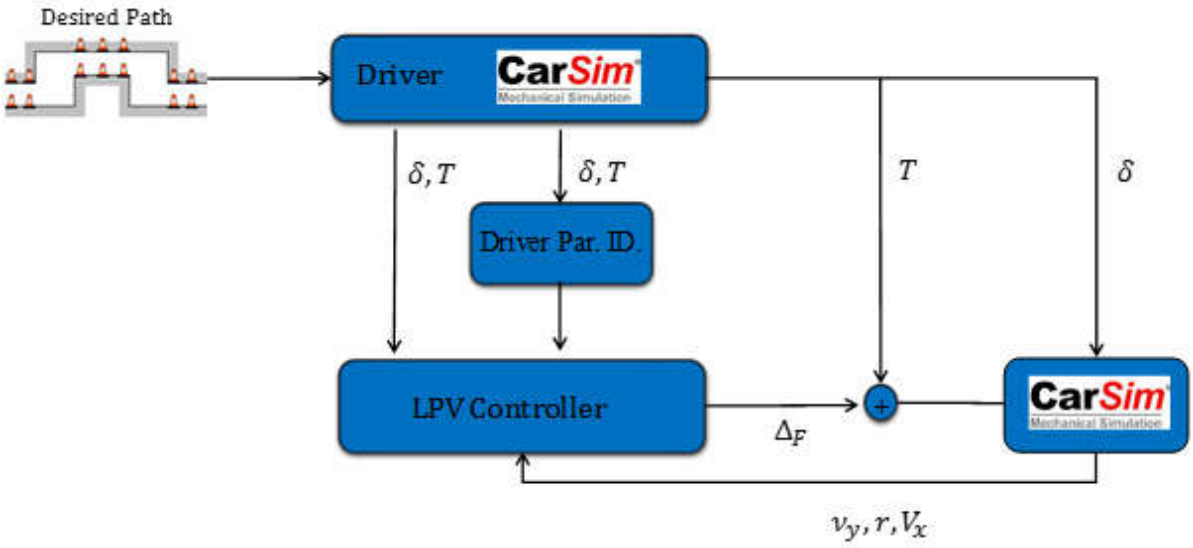

Figure 5-4: Simulation structure

The LMIs are solved using YALMIP interface integrated with MOSEK and the following controller's gains are:

$$K(dry) = \begin{bmatrix} 6.24\rho_1 + 4.74\rho_2 + 32.8\rho_4 + 256 \\ 29.8\rho_1 \quad 22.7\rho_2 + 68.2\rho_4 \quad 1244 \end{bmatrix}, \gamma = 7.3 \tag{5.25}$$

Now considering the tire cornering stiffness of wet road, another set of gains can be obtained as follows:

$$K(wet) = \begin{bmatrix} 32.8\rho_1 + 23.9\rho_2 \quad 12.5\rho_4 + 1177 \\ 180\rho_1 \quad 131\rho_2 + 147\rho_4 \quad 6466 \end{bmatrix}, \gamma = 7.3 \tag{5.26}$$

Note that the trend of changing parameters in controllers makes sense since on dry road conditions, the yaw-tracking gain is much higher than the lateral velocity gains while the lateral velocity gain is higher for wet road conditions. Also, one can solve the optimization to minimize the attenuation factor which results in $\gamma_{dry} = 4.48$ and $\gamma_{wet} = 6.47$. Note that these are present in high gain controllers that are not favorable for real applications.

To show the effectiveness of the controller, it is compared to the LTI controller designed in chapter 4. Note that the simulated driver (preview time = $1.3s, 200ms \leq \tau \leq 350ms$) can not track the wet road path ($\mu = 0.5$) at ($V_x = 80\ kp$,) when the controller is off. The vehicle side slip angle is shown in Figure 5-5, where the proposed controller keeps the vehicle side slip angle smaller than the robust LTI controller. The desired path (the blue line in Figure 5-6) is generated by the driver model in CarSim when the preview time is long ($1.5\ sec$), reaction time delay is small ($0 \leq \tau(t) \leq 50ms$), and the road surface is dry. The fixed controller is tuned by assuming that the vehicle velocity and driver model parameters are constant. A simple least square algorithm is also used to identify the CarSim driver model parameters in real-time. Then, the identified parameters and the required vehicle states are fed to the proposed controller. As it is shown in Figure 5-5 and Figure 5-6, the LPV version outperforms the LTI controller.

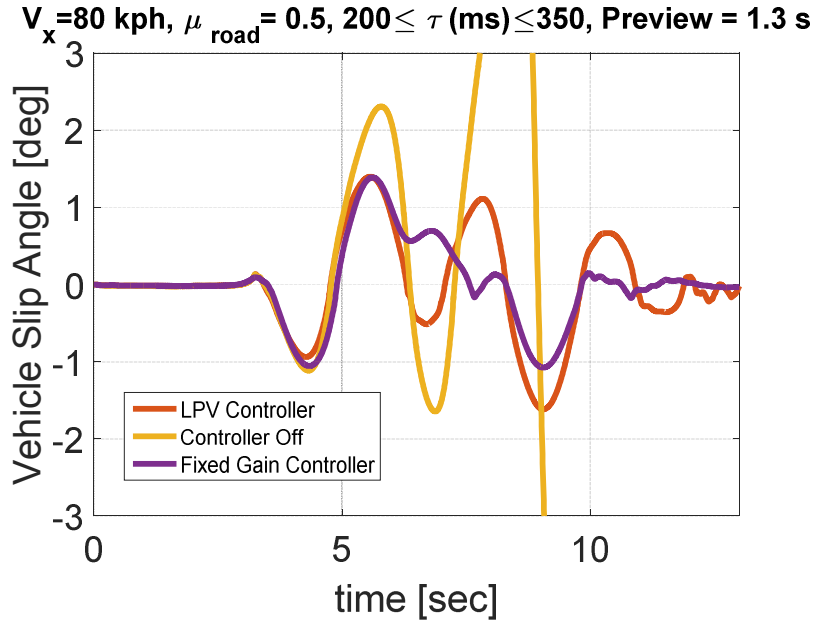

Figure 5-5 Vehicle Slip angle - Wet surface

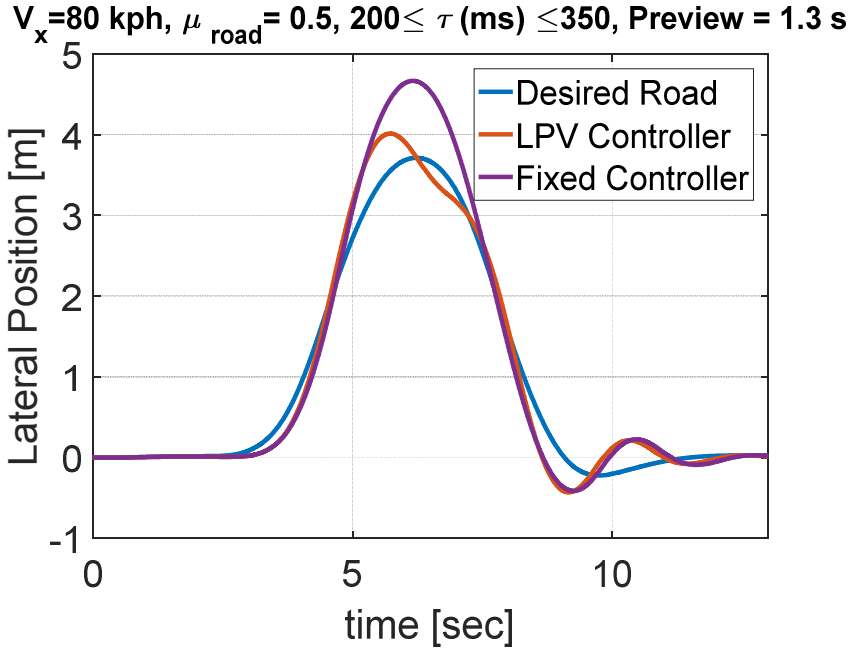

Figure 5-6 Path Following performance comparison

As expected, the performance of the controllers is directly related to the amount of information that is available to them. The LPV control method uses extra information about the changes in driving style and the longitudinal speed and adapts its action correspondingly, however, the fixed robust controller cannot catch up to the large deviation from the nominal design point. Also, the fixed controller makes the vehicle performance more conservative and the vehicle tends to show more understeer behavior.

5.8 Summary

A new formulation for the vehicle lateral control problem integrated with driver model was presented. The modeling allows the controller to lessen its conservatory behavior by extracting useful information from the driver's steering wheel input. As the driver model's parameters are generally time varying, the closed loop model is presented using an LPV framework. Considering the delay in a driver's action, a robust LPV controller is then designed for the delayed uncertain LPV problem. The same idea can be extended to the case where the parameter varying torque distributor is also included in the controller design process.

First, one or more scheduling variables need to be defined in order to parameterize the operating space. Following that, a family of parametric systems can be modeled, and finally, a parametric controller, guaranteeing the desired control objectives in every operating point, needs to be designed. The transient behavior between operating points should also be ensured and deemed acceptable. The LPV systems are finite-dimensional time-varying with fixed state-space structure of some vector of varying, but measurable at any instant, parameters. If the nonlinear tire model vehicle can be estimated accurately with an LPV model, then the $H_\infty \quad LPV$ method can be adapted to address the nonlinear controller design problem. It is also expected that using the $H_\infty \quad LPV$ method can be a good alternative for the proposed delayed uncertain robust controller.

System Dynamics: Things today are the things of yesterday plus any changes. The changes are the result of the things of yesterday. Now extend this to tomorrow.

"William S. Bonnell"

Chapter 6
Performance Analysis using Stochastic Driver Model

6.1 Introduction

In the previous chapter, it is shown that, if the controller could recognize a driving-style, it could adjust itself to serve the driver's request better. To accomplish this, the policy maker algorithm would need to be able to determine which of the human driver's states is currently active and to predict transitions between driving style states.

There are many different types of systems that might show sudden changes in their dynamic behavior. The economy system, an aerospace plant, a fault in the system, and human behavior may change their operating points abruptly. More generally, the parameter-dependent dynamic system analysis inherently has the potential to cover more real world applications. Remember that, the deterministic approach to dealing with the mode-dependent system was studied in Chapter 5 where an LPV controller was designed to take care of all of parameter variations in the system. One approach to modeling this type of behavior is using Markov Jump Linear System (MJLS). Many of the linear system analysis tools have been developed and extended for different practical notions in this class of stochastic hybrid systems (see [16, 30, 35] for more details).

The main aim in this chapter is to further analyze the designed parameter dependence introduced in the previous chapter. The LPV robust controller designed in Chapter 5 guarantees system stability and the disturbance rejection level of γ. It is shown that taking the driver model gains as measurable time-varying parameters will facilitate the design process. However, it is known that there is a level of conservation coming from the inequalities in the controller design. It is also worth mentioning that since in an LPV design, there is no information about the switching between different modes of the system (driving style and longitudinal speed), the controller should be designed to perform robustly with respect to any changes in the parameters. In real situations, extreme abrupt changes are very rare when compared to normal driving conditions.

By adding extra information (probability of switching) about the system, the aim is to obtain a better (lower) estimation on the disturbance attenuation level of the closed loop LPV system.

Adding another piece of information about the way that the parameters are changing should improve the estimation of the uncertainty attenuation level that is obtained using the robust LPV method. The goal is to consider the driver as a system with several interconnected subsystems with their own particular responses. Assuming that the transition probability of switching between this bank of standard simple controllers is available – which can be identified offline or based on an on-line learning rule –, one can reformulate the control problem to one of the standard forms of robust controller design for jump linear systems. One approach to modeling the transition probability is to consider a Markov network between the different model states. As the vehicle states involved in the modeling are measurable or can be adequately estimated, the driver's current state can be determined. Based on the transition probability relation, the next step can be predicted. The controller can then configure itself to achieve the best possible performance. Intuitively, this method suggests to break a driver's behavior into finite sets and a probability will be assigned for transmission from each set. It is worth mentioning that there has recently been an increasing interest in modeling driving styles using stochastic and Markov chain modeling (see [22, 23, 85] and the references therein).

The main advantage of using this method over the LPV method is that the transition between the sets are more realistic in this model. Although one can argue about the definition of the transition rate in an LPV analysis – the rate of changes of parameters i.e. ρ -, in an LPV approach, only the bounds of this change of rate will be considered in analysis. Here, a nominal value for the rate of changes in parameters is accessible, and that will help us improve the disturbance rejection capability of the controller.

Observing this capability, the closed loop model of the system using the designed LPV controller (5.19), the whole system is reformulated given that extra information on driving style is available.

Remark: Although this technique for modeling, analysis, and control brings a certain set of versatility by extracting more information about the system uncertainties, finding the probability transition matrix is not an easy task in practical application. To make the abstract notion more practical, many researchers extended the analysis to cases where the transition probability matrix is not known or partially known with incomplete information (see [36, 161]). A natural direct approach for stability analysis will be considering a fixed mode independent Lyapunov function for each operating point to guarantee stability by imposing some conservation to the analysis. The alternative approach is using a mode-dependent Lyapunov function to take advantage of the extra information embedded in the transition probability matrix of the system.

Recently, both H_2 and H_∞ control of MJLS are addressed using a mode-dependent Lyapunov function (see [51, 106, 107]).

6.2 Driver Identification

Usually, abrupt changes are undesirable in a control process. It is well-known that a smooth analysis in control theory is always easier to solve and implement compared to a non-smooth analysis. Abrupt changes could be a result of changes in environment, a failure, or any changes in system that forces the system to work in another operating point. A human driver is inherently a very complex stochastic model who may change their driving style at any instance resulting in changes of the model operation point. For over 50 years, there have been a number of attempts carve out a logical framework for modeling this type of systems.

The identification process should ideally be able to send a message to a semi-autonomous controller when it needs to kick-in and take over vehicle control. It may provide the driver with a hint signal or activate an alarm to signal that a hazardous situation has been detected. In this approach, the control system tries to predict the car's trajectory based on estimations of the driver behavior and actively take control of the car if the probability of threat is higher than a given threshold. A better driver model and a more accurate parameter identification technique can reduce the rate of intervention of the autonomous controller and improve the overall driving experience.

6.2.1 Current Approach for Driver Identification

There are many different driver identification methods in the literature. The main idea behind most of them is to use the desired path and vehicle states of the vehicle as a reference, and then, by calculating the difference between the driver action, the driver model parameters can be estimated or identified.

Therefore, the most important assumption in all available methods is the availability of the desired path of the vehicle. Note that there is a clear difference between a driver's desired path and the desired path provided by the path planning block. One of the main questions using the conventional method is to really distinguish between two desired paths.

6.2.2 Proposed Method for Driver Parameter Identification

The bedrock of this thesis is to avoid using the desired path information for control purposes. Hence, here a slightly less accurate method is proposed that does not use preview (future) information. We propose to use a moving average window in the past and monitor the driver and vehicle behavior constantly (see Figure 6-1). This way, one can always have a lot of extremely important information to identify the driver. The focus is to use only available and commercialized sensors on a regular vehicle and prevent using unconventional sensors to determine the desired path.

The main assumption here is that the identification is always running on a normal condition. A normal condition is defined to be the situation where the driver tracks his/her desired path carefully. As the desired path tracking error is not available, it is assumed that this error is small. Instead the vehicle states that are measurable and indirectly indicate the effect of the desired path are used. Thus, for the rest of this chapter a general model for identifying driver behavior is considered.

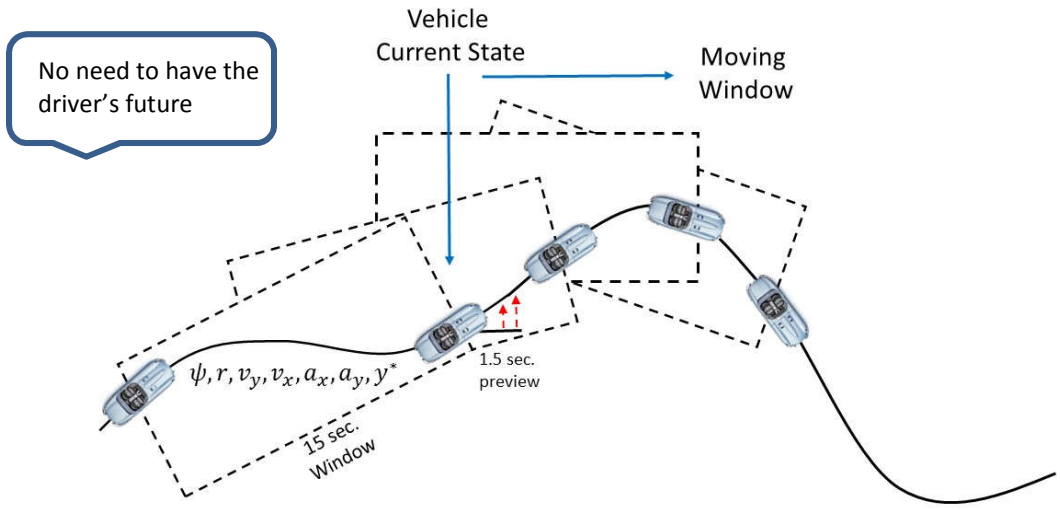

Figure 6-1: Driver identification moving window

The identification is always running in each sampling time until the algorithm detects that the driving is abnormal. Defining the index for this condition will be related to a threshold for the vehicle yaw-rate and the lateral velocity. Clearly, large values for lateral velocity (or side slip angle)

are indices for situations that are not normal. By passing this treshhold, the identification algorithm will be stopped and held until the driving condition returns to normal.

6.3 Identification Model

The focus in the identification method here is only to show the potential of the proposed idea, so a simple but general model is used to mimic the driver behavior. The regressor vector for the identification purpose must be chosen such that all of the signals are available based on current commercialized technology. On the other hand, the identification process should imitate real situations. To address these requirements, the following model is assumed for the identification process.

$$\delta = k_1 v_y + k_2 r + k_3 \psi + k_4 a_y + k_5 v_x + k_6 a_x + \sum_{i=7}^{N} k_i \Delta y_i \tag{6.1}$$

The proposed model includes the most important element of steering in a normal condition. A driver always considers the vehicle states and the desired road to steer the vehicle. It is known that a human has perfect feeling about acceleration (a_x, a_y) in both directions. The longitudinal and lateral velocity (v_x, v_y) are clearly part of any driver decision for turning the steering wheel. Steering a vehicle is always a function of vehicle heading (ψ) and the corresponding rate (r). It is also generally accepted that each driver uses a certain number of future preview points. As the identification is running in a normal condition, it is assumed that the vehicle position is the same as the driver's desired path. Using a GPS, all of the information on the lateral position can be recorded. Thus the last term in the identification model is the preview information Δy_i that has already been recorded because the identification is running in a window of preview points in the past.

Assume that the sampling rate is Δt, the moving window time is T_w, and the driver preview time is T_p second. The identification is then performing on the last $N_p := \frac{T_w}{\Delta t}$ samples. At each sampling time, the following problem needs to be solved:

$$\min \|A\theta \quad \delta\| \tag{6.2}$$

where $A \in R^{(N_w - N_p) \times N_p + 7}$, the steering wheel angle is $\delta \in R^{N_w}$, $\|.\|$ is any appropriate norm, and the regressor vector is $\theta = \begin{bmatrix} k_1 & k_2 & k_3 & k_4 & k_5 & k_6 & k_7 & k_{N_p+7} \end{bmatrix}$.

By logging all of this information, there are many handy approaches to identifying the parameters. We used a simple least-square method to minimize the ℓ_2 norm of error over the moving window.

Remark: Note that for the sake of simplicity, dynamic driver behavior is considered here. One can improve the current method by adding dynamic constraints to the identification methods.■

6.4 Driver Parameter Identification Using Experimental Data

In order to use the proposed method to identify the driver, a series of test experimental data that are produced at the University of Waterloo (UW) is used. The Mechatronics Vehicle Systems Laboratory at UW contains hundreds of vehicle handling test data in different situations. The tests are mostly double lane changes while the vehicle has different speeds and the surface friction error is also varying from 0.25 to 0.95. The data which is used in the rest of this chapter was collected from the Autobox and GPS module mounted on a Chevrolet Equinox (see Figure 6-2). The mounted stock IMU sensor provides the required measurements for the yaw-rate, longitudinal and lateral acceleration. Longitudinal and lateral velocity are estimated with acceptable accuracy. The GPS module provides information on vehicle position. The vehicle heading angle (ψ) can also be calculated directly from the GPS data. The steering wheel angle is also accessible using the stock steering sensor.

Figure 6-2 Experimental data for driver identification

The information from 120 tests have been collected and a log of about 40 minutes of driving is collected. Two male drivers drove the car during these tests. Most of the tests have been for stability controller tuning, and they cover a wide range of situations from a normal double lane change driving on dry asphalt to a harsh double lane changes on icy road. There are some cases of double lane changes on wet surfaces.

Note that there are a few cases where the vehicle became unstable and the driver lost control on an icy road while performing a harsh maneuver. We will see that these tests usually result in

a different range of parameters and should be removed from the analysis. The main reason is that the normal driving assumption (small path tracking error) is not valid anymore.

6.4.1 Experimental Data

Figure 6-3 shows the lateral position versus the longitudinal displacement of the vehicle for all of the experimental tests. Clearly, there are many different cases that produce enough excitation for testing the algorithm.

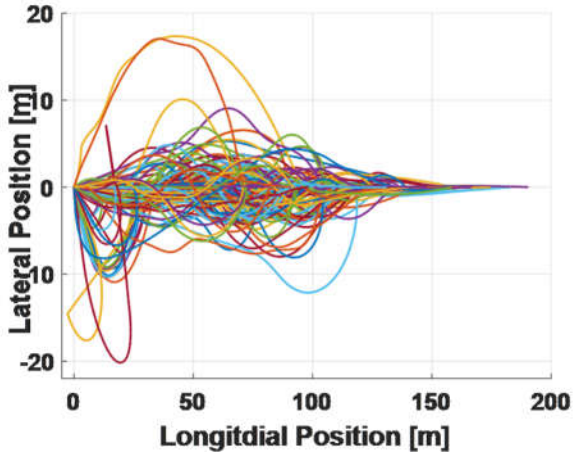

Figure 6-3 Vehicle Position (from GPS)

Following that, the driver steering wheel angle is shown in Figure 6-4.

Vehicle longitudinal velocity, yaw- rate, and lateral velocity are depicted in Figure 6-5, Figure 6-6, and Figure 6-7.

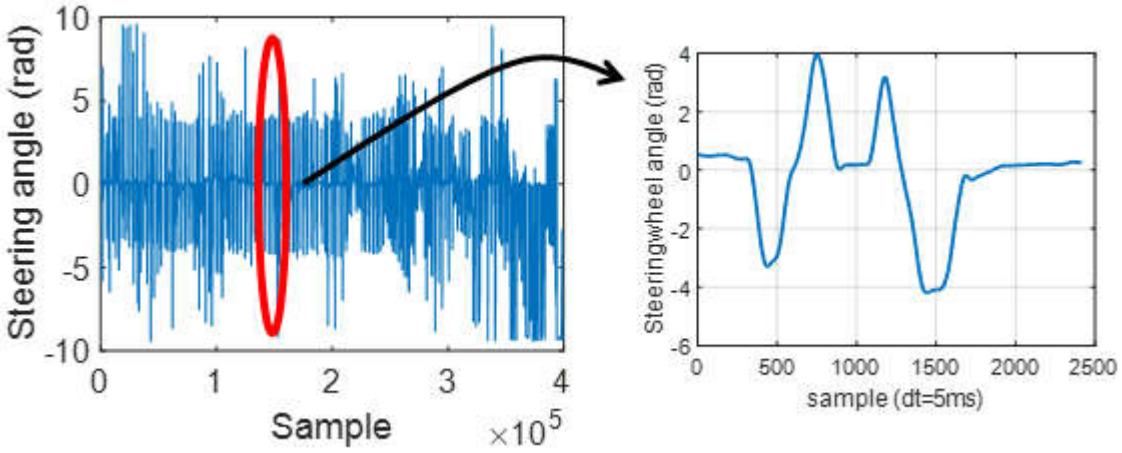

Figure 6-4 Driver Steering wheel angle

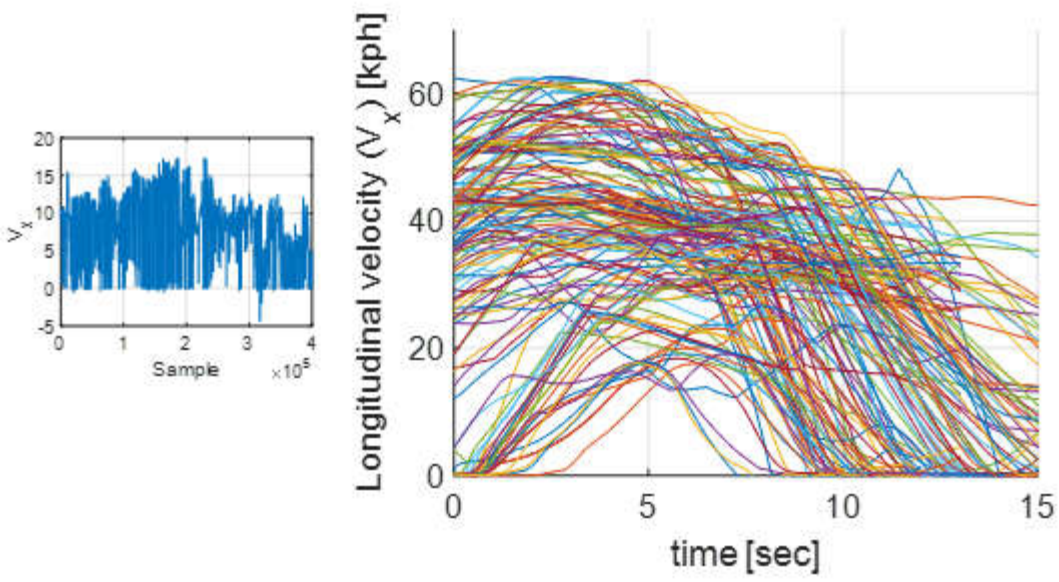

Figure 6-5 Vehicle Longitudinal Velocity

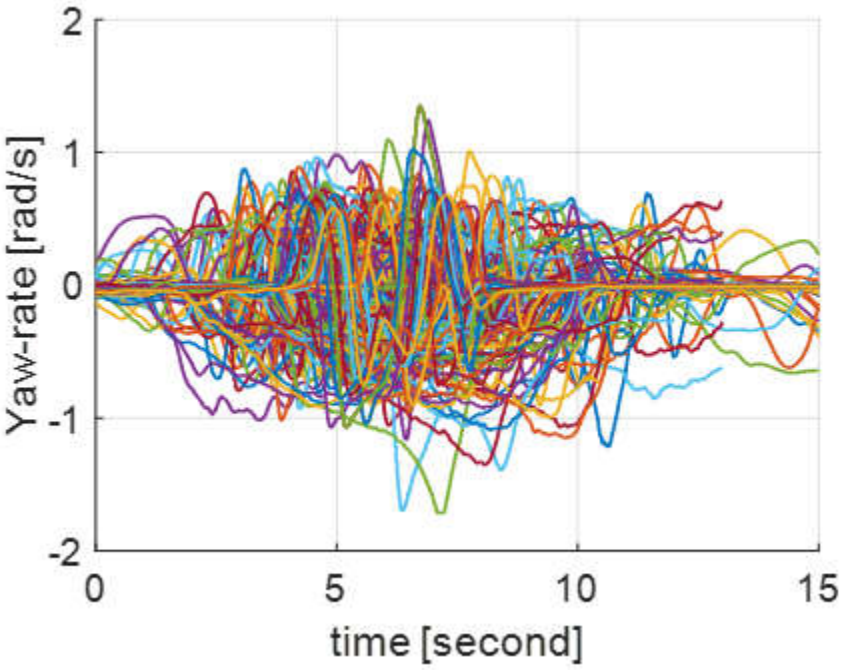

Figure 6-6 Vehicle Yaw-rate

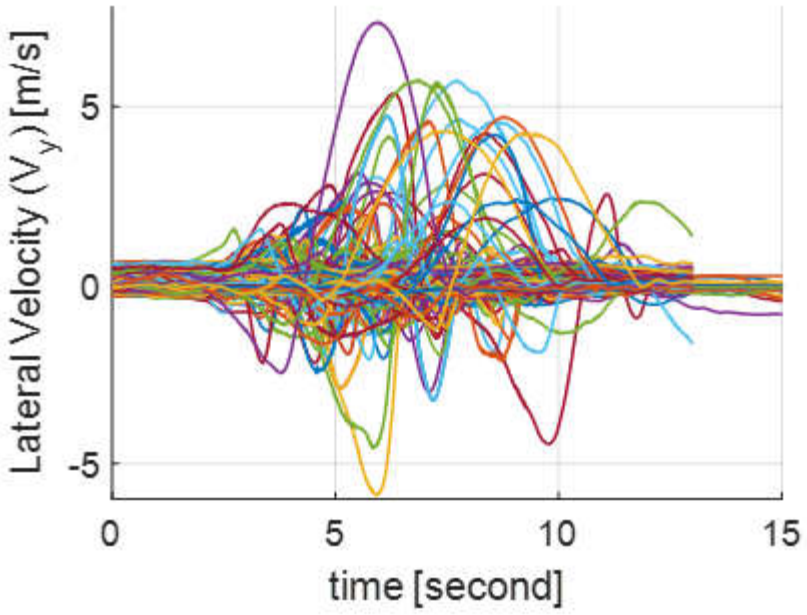

Figure 6-7 Vehicle Lateral Velocity

Form the above figures, one can conclude that there is enough excitation for the algorithm to identify the parameters for a wide range of driving conditions. More specifically, the lateral velocity shows that the dataset is rich and includes the complete spectrum mild to very harsh maneuvers.

6.4.2 Parameter Clustering

Given that the focus is in finding different modes of a driving style; a clustering method is needed to classify the results. Based on the experimental results, the data is clustered when the driver preview point times were assumed to be 1.5 second. Also, it is assumed that the moving window is on the past 15 seconds. The proposed algorithm is run using the data gathered from driving of two different drivers in different situations. For the sake of simplicity, the identification is performed with both 1 Hz and 0.2 Hz of identification frequency.

First, the driver model parameters are identified every 5 seconds. The idea is to look at a 15 seconds of logged data and run the identification method to obtain an appropriate set of gain. The result for k_1 (the lateral velocity gain) is shown in Figure 6-8. The right side shows the normalized frequency of occurance of k_1.

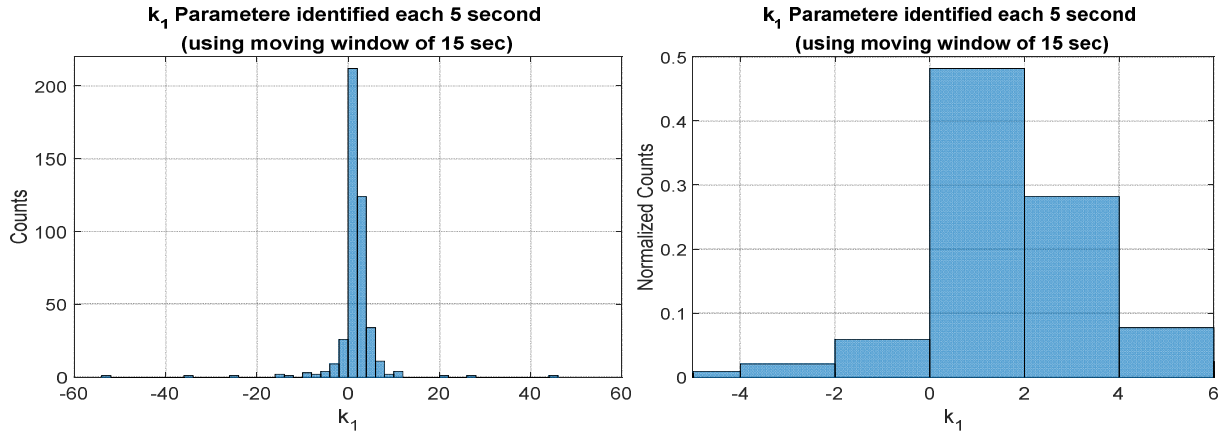

Figure 6-8 The frequency of K_1 gain

Based on the given experimental data set, there are some extreme cases where the identification process should be stopped. If the process is offline, these values should be treated as outliers. The threshold can be defined based on each application, and here, a bound for the lateral velocity (side slip angle) is considered and the the outliers are removed based on this simple rule. In one process, an outlier is detected. The lateral velocity in this test is very high and the logitudinal velocity shows negative values which means that the car was spinning (see Figure 6-9 Figure 6-10)

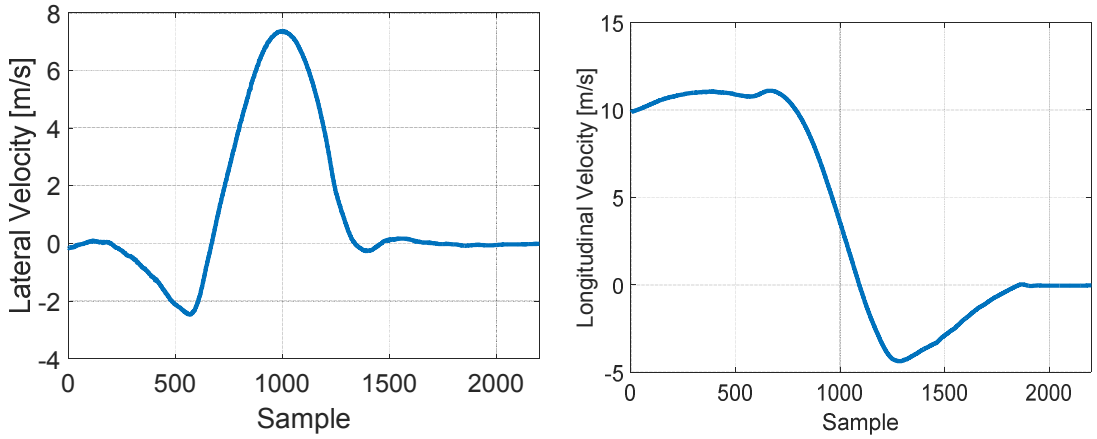

Figure 6-9 V_y and V_x for a very harsh test

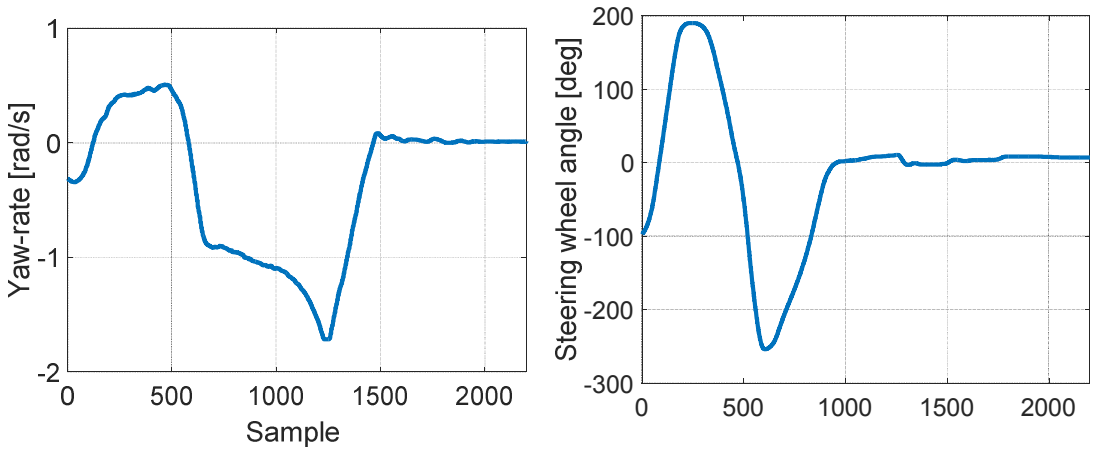

Figure 6-10 yaw-rate and steering wheel of a very harsh test

After removing the detected unnormal driving condition, the following histogram k_1 is obtained (see Figure 6-11).

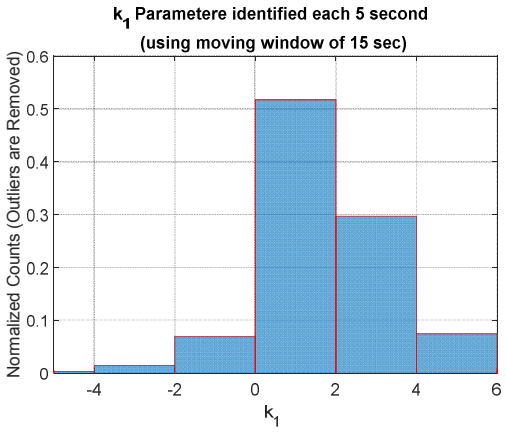

Figure 6-11 Driver parameter identification k_1

Following the same method, the other driver parameters for the driver model are estimated as it is shown in Figure 6-12.

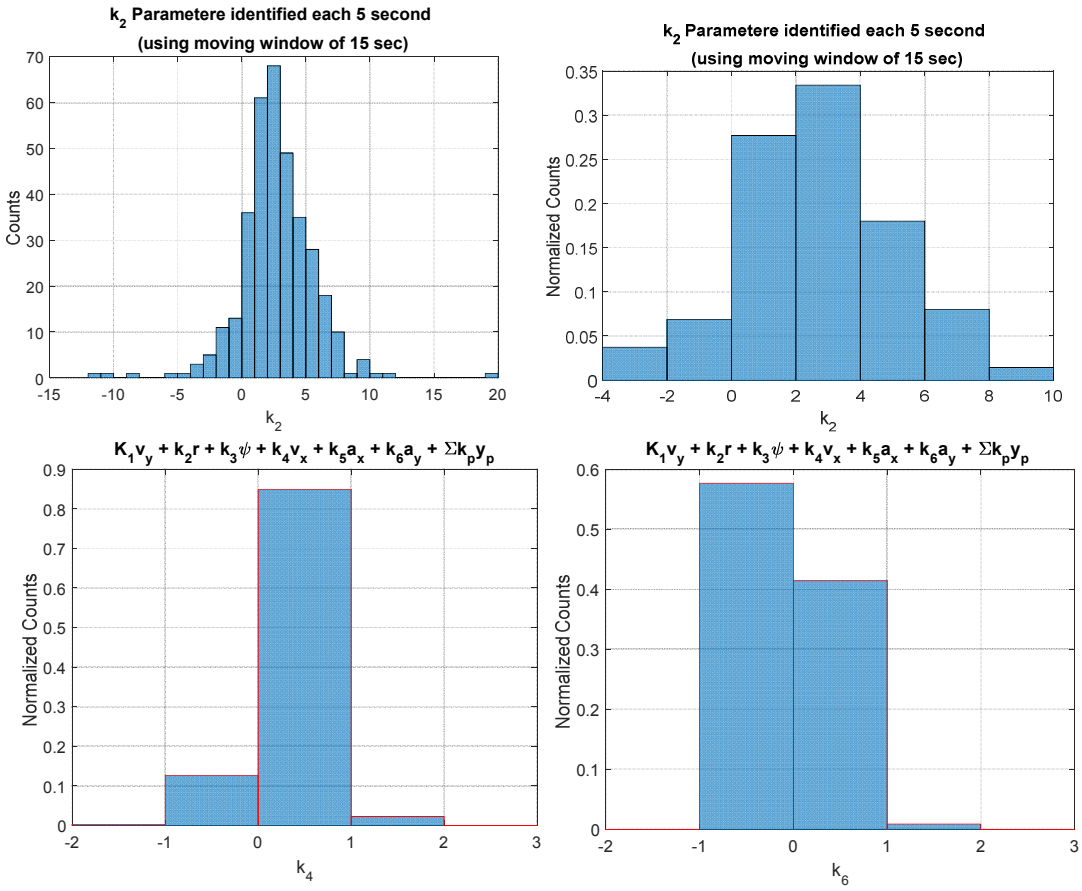

Figure 6-12 Driver identification parameters

In order to validate the identified parameters, a part of the data is randomly selected and the steering wheel that is based on the identified model is compared to the actual recorded steering wheel. Figure 6-13 shows the data fit and how it corresponds to the mean square error for four randomly selected data. As shown, the algorithm closely tracks the human driver's steering wheel.

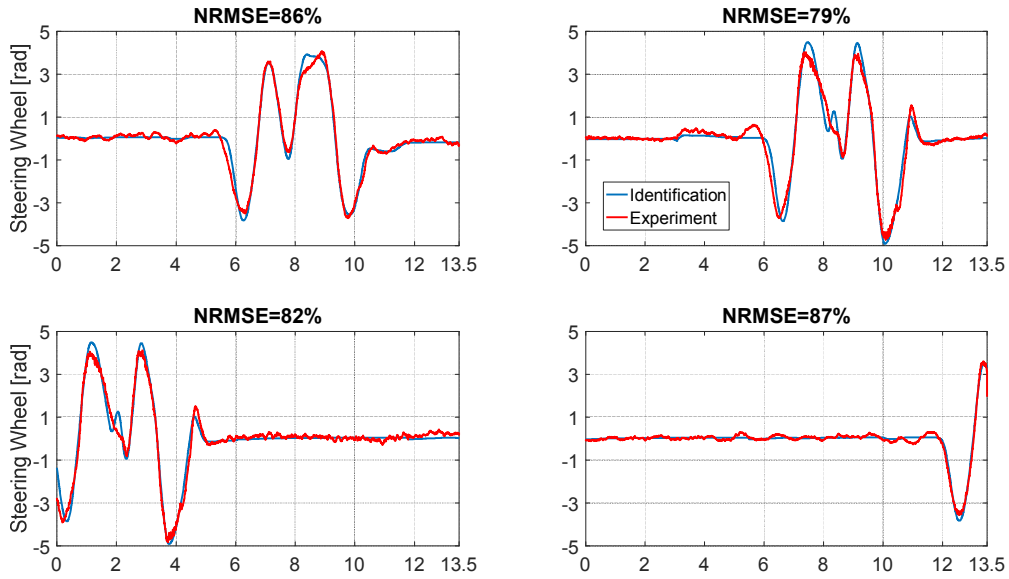

Figure 6-13 Data fitting of experimental results with identified model (each 5 second)

In order to investigate the effect of identification frequency, the identification is ran every second and compared with the previous results. This way, the data set that is used for each parameter will be 5 times bigger that the previous one. Then, the clustering is performed on the new set of data The normalized root mean square of fitting at each section is also calculated and shown in Figure 6-13.

$$\text{Normalized root mean square error (NRMSE)} = 1 \quad \frac{\|\mathrm{X}_{\mathrm{ref}} \quad \hat{X}\|}{\|X_{ref} \quad mean(X_{ref})\|} \tag{6.3}$$

where X_{ref} is the reference data and $\hat{X}$ is the identified vector. The results show a negligible difference which supports the idea that the proposed algorithm is promising. Note that using this method, the 2200 sets of gains ($k_1 \quad k_N$) is identified. Some of the most important gains are shown in Figure 6-14. It can be observed that compared to the previous case – where the identification frequency was five time lower – the results are almost identical. The other observation is that the distribution of the parameters is very close to a normal distribution.

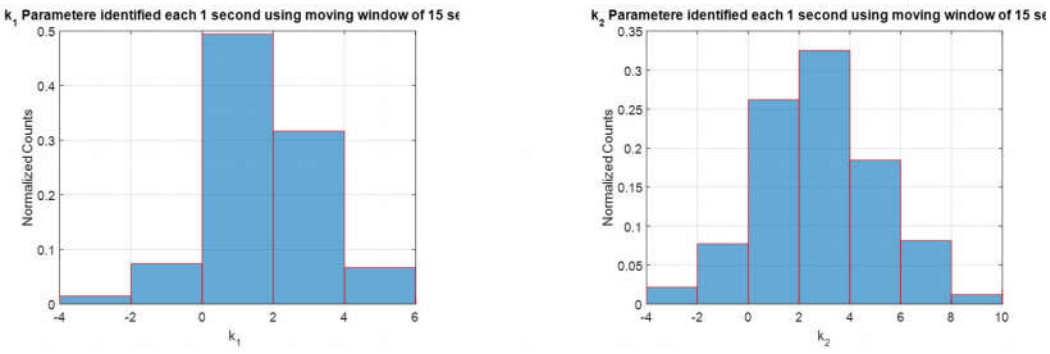

Figure 6-14 Parameter Identification at each 1 second

Figure 6-15 compares the experimental results with four randomly selected parts of the data. The figure depicted good results in terms of estimating the steering wheel angle of a driver.

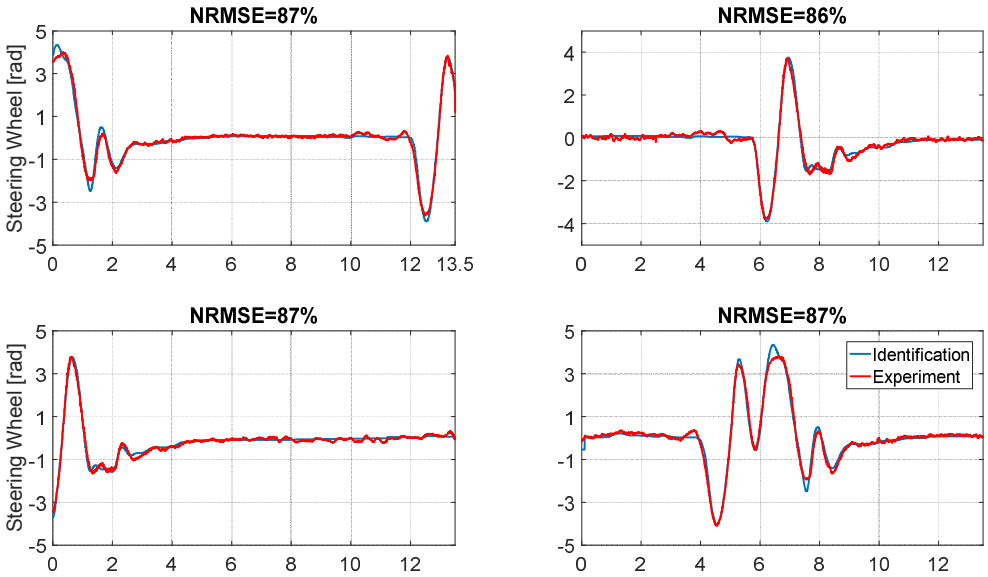

Figure 6-15 Data fitting of experimental results with identified model (each 1 second)

In order to analyze the effectiveness of the algorithm, the mean square error of the steering wheel estimation (for both cases of 1 second and 5 second identification) is presented in Figure 6-16. It can be seen that the distribution is similar to a one sided normal distribution. Based on this approximation, the mean of identification error is under 30 degrees on the steering wheel (Maximum 11% error) with a deviation of about 25 degree. These values are completely negligible compared to actual steering wheel.

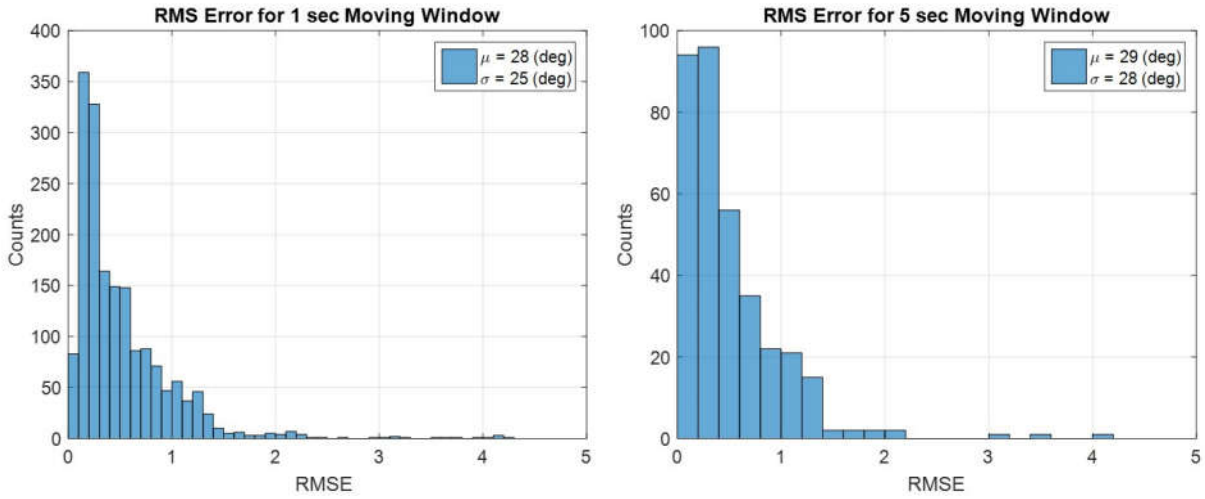

Figure 6-16 Mean Square Error of the identification process

Remark: The identification method proposed does not require any additional sensor or future information. This makes it immediately applicable even on most conventional vehicles. Besides providing important parameters to tune the controller better, one can use this extra information to recognize if the driving condition is normal. Another application is to personalize an autonomous driving vehicle to revise the control actions such that the driver does not feel the switching between him/her self and the automobile decision maker. There is still lots of room for improving the basic version. The state of ego vehicles, the relative distance and velocity from other moving objects and many more can be of a driver's interest when making the decision.■

6.5 Finding Markov Probability Transition Matrix

There are several gains for the described driver model in (6.1). Based on the offline test on the experimental results, several number of gain sets are obtained (see (6.4)). For example, in the 1 sec identification case, 2200 sets of gain are obtained. The focus here is to import the driver characteristics into the system modeling and improve the controller design and the worst-case estimation of disturbance rejection. Sticking to the idea presented in Chapter 4, the only gains that can be easily augmented with the vehicle handling dynamics, are k_1 and k_2. Clearly, there is a pool of gain-sets (2200 based on the experimental data set) for each of these gains. According to the clustering in the previous section, one can define a finite number of modes for each gain. The probability of switching between different modes can then be calculated according to the

frequency of jumping from mode i to mode j. For k_1 and k_2 the following bins (6.4) for clustering the gains are defined:

$$\begin{matrix} \infty < k_1 < 0 \\ 0 < k_1 < 2 \\ 2 < k_1 < 4 \\ 4 < k_1 < 6 \\ 6 < k_1 < \infty \end{matrix} \quad , \quad \begin{matrix} \infty < k_2 < 0 \\ 0 < k_2 < 2 \\ 2 < k_2 < 4 \\ 4 < k_2 < 6 \\ 6 < k_2 < \infty \end{matrix} \tag{6.4}$$

The transition probability matrix for the gains can be calculated as follows:

$$\Pi_1 = \begin{matrix} 0.52 & 0.28 & 0.12 & 0.04 & 0.04 \\ 0.07 & 0.73 & 0.17 & 0.02 & 0.01 \\ 0.04 & 0.27 & 0.6 & 0.08 & 0.008 \\ 0.03 & 0.21 & 0.18 & 0.41 & 0.18 \\ 0.15 & 0.15 & 0.1 & 0.15 & 0.45 \end{matrix} \tag{6.5}$$

$$\Pi_2 = \begin{matrix} 0.43 & 0.35 & 0.13 & 0.07 & 0.03 \\ 0.085 & 0.53 & 0.31 & 0.05 & 0.026 \\ 0.072 & 0.22 & 0.54 & 0.15 & 0.028 \\ 0.03 & 0.15 & 0.24 & 0.35 & 0.24 \\ 0.14 & 0.015 & 0.11 & 0.21 & 0.65 \end{matrix} \tag{6.6}$$

The transition probability matrices in (6.5) and (6.6) defines the probability of jump between different modes in each set of gain. It is assumed that there are five modes for each sets of gains. Note that the probability matrix for $k_1$is consistent with the results from the histogram. It can be seen that the highest probability of k_1 is remaining at mode 2. Referring to the histogram in Figure 6-11, the highest frequency lies in the section, $0 \leq k_1 \leq 2$.

However, in order to make the transition Markov jump system ready for analysis, one needs to have the transition probability matrix of switching between each pair of (k_{1i}, k_{2j}) to $(k_{1i'}, k_{1j'})$ where $(\{i, i'\}, \{j, j'\}) \in R^{5\times5}$. The same approach can be used to find the probability matrix as:

$$\Pi_t = \Pi_1 \quad \Pi_2 \in R^{25\times25} \tag{6.7}$$

where is the kronecker product.

This shows that there are 50 elements in two transition probability matrices of Π_1 and Π_2 that should be identified to obtain Π_t. The elements of Π_1 and Π_2 in (6.5) and (6.6) are identified using 2200 pairs of gains for k_1 and k_2; however, the result can be different if the identification process is performed over smaller sets of gains. The variations of each element of the total transition matrix Π_t is studied using 100 different sets of data with a random number of gains (between 150 to 2200) in each set of k_1 and k_2. The relative standard deviation (coefficient of variation (c.v)) is calculated for each of the elements, which shows relatively small deviation among all of elements. Figure 6-17 shows the standard deviation (σ), median, and $c.v = \frac{\sigma}{\mu}$ of the results of four different elements of Π_t where μ is the mean value. This shows that the number of gains does not have significant effect on the value of the identified elements.

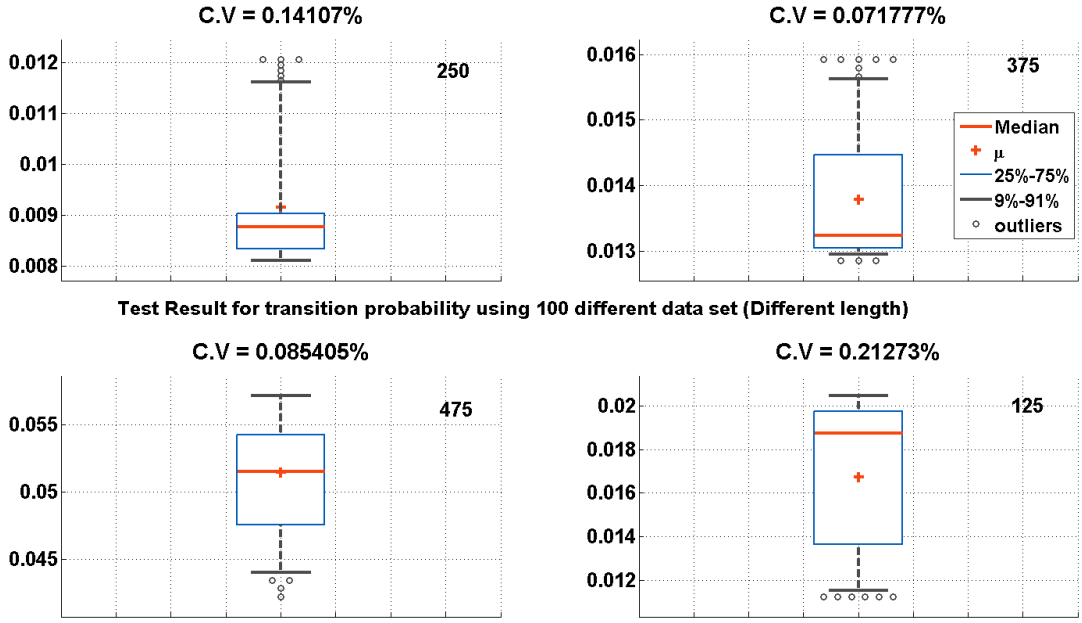

Figure 6-17: Coefficient of variation for four elements of transition probability matrix of Π_t

Remark: The transition probability that is obtained in (6.5) and (6.6) is for discrete jump systems. In order to make it applicable in continuous time framework, it is assumed that each mode can spend a continuous amount of time in any state. This way a driver moves from each state to the another in accordance with a (discrete-time) Markov chain. However, the amount of time that he/she spends in each state is exponentially distributed (such as Poisson process). For more information on discrete to continuous time transformation see example 5.6.3 in [73].

6.6 Stochastic Analysis of Linear Parameter Varying Closed Loop System

The main aim here is to further analyze the LPV controller designed in Chapter 5 (see (5.23)). The LPV controller is designed to schedule the controller based on the driver parameters (driving style) and the longitudinal speed. In this section, the aim is to add extra information about the probability of the transition between different modes of the driver gains and improve the disturbance rejection level estimation of the controller.

To address this problem, the Markov Jump Linear System provides versatile tools in the realm of both analysis and control.

Definition:

Let (Ω, F, P) be a probability space and $\{r_t, t \geq 0\}$ be a stochastic process taking values in $S = \{1,2, \quad , N\}$. Then, $\{r_t, t \geq 0\}$ is said to be a Markov process with state space S if:

$$P(r(t) = i | r(w): w \leq s) = P\big(r(t) = i | r(s)\big)$$

holds for all $0 \leq s \leq t$ and $i \in S$.

The stability of linear switching control is an interesting field in control theory. Abrupt changes and switching in real world applications are the most important motivators of many scientists who are working on MJLS. There are at least two major approaches to dealing with this branch of systems. One is to consider a family of Lyapunov functions for analyzing the minimum dwell time. This way there is no need to have uniformly decreasing Lyapunov functions in all of switching times. The other method is analyzing state-dependent switching rules. In most of the versions of this method, the Lyapunov function at each mode needs to be increasing at all times. The famous Lyapunov-Metzler inequality is the most important stability analysis of this type of switching systems. It can be shown that the mean-square stability of MJLS is a special case of the general stability proof of mode-dependent switching systems that use the Metzler inequality, which can also be presented via LMIs.

Remark: Although, linear Markov jump systems might be similar to a natural extension of ordinary linear systems, this class of system can show very different behavior. As an example, just by looking at the stability (or instability) of the modes or operating points of a MJLS, one cannot guarantee stability of the whole system. There are many interesting examples of unstable systems that have stable linear modes or even systems with unstable modes that are MSS (see [35, 70]). The stability of a MJLS depends on a balance between stability of each system mode and the transition matrix. In other words, the stability of each operation mode is neither a necessary nor a sufficient condition for the mean-square stability of the system. Mean-square stability depends

on a balance between the transition probability of the Markov chain and the operation modes. This illustrate peculiar properties of MJLS systems. ■

Now, consider the unforced continuous-time Markov Jump Linear System (MJLS) of

$$\dot{x}(t) = A\big(r(t)\big)x(t), \qquad r(t), t \geq 0 \tag{6.8}$$

where $r(t)$ taking values in the space S with infinitesimal generator of:

$$\Pr\{r(t+\ \ ) = j | r(t) = i\} = \begin{cases} \lambda_{ij}(\ \ ) + o(\ \ ) & i \neq j \\ 1 + \lambda_{ii}(\ \ ) + o(\ \ ) & i = j \end{cases}, \lambda_{ii}(\ \ ) = \sum_{j=1, j\neq i}^{N} \lambda_{ij}(\ \ ) \tag{6.9}$$

where $\lambda_{ij} > 0$, $\quad > 0$, and $\lim_{h\to 0}\left(\frac{o(h)}{h}\right) = 0.$

Note that the jump rate λ_{ij} that is considered here is constant. There are cases where the jump could be dependent on the system states or even on the control action input.

Definition:

For system (6.8), the equilibrium point 0 is:

(i) Asymptotically mean square stable, if for any initial condition and initial distribution for $r(t)$, $\lim_{t\to\infty} E\left\{\left\|x\big(t, x_0, r(t)\big)\right\|^2\right\} = 0$

(ii) Exponentially mean square stable, if for any initial condition and initial distribution for $r(t)$, there exist constants $\alpha, \beta > 0$ such that $E\left\{\left\|x\big(t, x_0, r(t)\big)\right\|^2\right\} \leq \alpha\|x_0\|^2 e^{-\beta t}$

(iii) Stochastically stable, if for any initial condition and initial distribution $r(t)$, $\int_0^\infty E\left\{\left\|x\big(t, x_0, r(t)\big)\right\|^2\right\} dt \leq +\infty$

(iv) Almost surely (asymptotically) stable, if for any initial condition and initial distribution $r(t)$, $P\left\{\lim_{t\to\infty} E\left\{\left\|x\big(t, x_0, r(t)\big)\right\|^2\right\} = 0\right\} = 1.$

Referring to ([40]) it is known that (i), (ii), and (iii) are equivalent and imply (iv).

For more analysis on the markov jump linear system see appendix.

6.7 Extension to Retarded Delay Systems

Consider the following MJLS with time-varying bounded delay:

$$\begin{gathered} x(t) = A\big(r(t)\big)x(t) + A_d\big(r(t)\big)x\big(t \quad \tau(t)\big) + E\big(r(t)\big)\omega(t) \\ z(t) = C\big(r(t)\big)x(t) \\ y(t) = Cx\big(r(t)\big) \\ x(t) = 0, \forall t \in [\quad 2\tau_m, 0] \end{gathered} \tag{6.10}$$

where $x(t)$ is the state, $\omega(t) \in R^m \in \ell_{2\epsilon}$ is the bounded disturbance input, and $y(t) \in R^q$ and $z(t) \in R^p$ are measured and controlled outputs, respectively. The delay has an upper bound of τ_m and an upper rate bound of μ. It is assumed that the process $\{r(t)\}$ is a Markov process with probability matrix of $\Pi \quad [\lambda_{ij}]$ defined in (6.9).

6.7.1 Stability of Stochastic Retarded System

Lemma 1 ([62]): improvement on Jensen inequality

Assume that $R \in R^{n\times n}$, scalars $a < b$, and a function $\phi \in PC([a, b, R^n])$ are given. The following inequality always holds:

$$\begin{gathered} \frac{1}{b \quad a}\left(\begin{bmatrix}\zeta_1\\ \zeta_2\end{bmatrix}^T \begin{bmatrix}3R & 0\\ 0 & 5R\end{bmatrix}\begin{bmatrix}\zeta_1\\ \zeta_2\end{bmatrix} + \left(\int_a^b \phi(s)ds\right)^T R\left(\int_a^b \phi(s)ds\right)\right) \\ \leq \int_a^b \phi^T(s)R\phi(s)ds \end{gathered} \tag{6.11}$$

$$\zeta_1 = \int_a^b \phi(s)ds \quad \frac{2}{b \quad a}\int_a^b \int_a^s \phi(u)du\, ds$$

$$\zeta_2 = \int_a^b \phi(s)ds \quad \frac{6}{b \quad a}\int_a^b \int_a^s \phi(u)du\, ds + \frac{12}{(b \quad a)^2}\int_a^b \int_a^s \int_a^u \phi(v)dv\, duds$$

Theorem 6.1:

For given delay bounds of $\tau(t) \in [\ _1 \quad _2]$, the system in (6.10) is stochastically stable, if there exists matrix $X \in R^{3n\times 3n}$, and symmetric positive definite matrices $S_1, S_2, R_2 \in R^{n\times n}, P_i \in R^{4n\times 4n}$ and mode dependent matrices of $Q_{1i}, Q_{2i}, R_{1i} \in R^{n\times n}$ such that the following set of LMIs hold for all $i \in S$:

$$\mathrm{H_i(h)} \quad \mathrm{H_1} \quad \mathrm{H_2^T \Phi H_2} < 0 \tag{6.12}$$

$$\sum_{j=1}^{N} \pi_{ij} Q_{1j} \le R_3, \sum_{j=1}^{N} \pi_{ij} Q_{2j} \le R_4, \sum_{j=1}^{N} \pi_{ij} R_{1j} \le \frac{1}{\ _1} S_2 \tag{6.13}$$

$$\Phi = \begin{bmatrix} \tilde{R}_2 & X \\ & \tilde{R}_2 \end{bmatrix} \ge 0 \tag{6.14}$$

where

$$\begin{aligned} \mathrm{H_i} = {} & G(\ )^T P_i G_0 + G_0^T P_i G(\ ) + G(\ )^T \left(\sum_{j=1}^{N} \pi_{ij} P_j \right) G(\ ) \\ & + [e_1^T \quad e_2^T] \begin{bmatrix} Q_{1i} + \ _1R_3 + \ _{12}R_4 & 0 \\ 0 & Q_{2i} \end{bmatrix} [e_1^T \quad e_2^T]^T \\ & [e_2^T \quad e_4^T] \begin{bmatrix} Q_{1i} & 0 \\ 0 & Q_{2i} \end{bmatrix} [e_2^T \quad e_4^T]^T \\ & + (Ae_1 + A_d e_3)^T \left[\ _1R_{1i} + \ _{12}R_2 + \frac{1}{2} \ _{12}^2 S_1 + \frac{1}{2} \ _1^2 S_2 \right] (Ae_1 \\ & + A_d e_3) \end{aligned} \tag{6.15}$$

$$\mathrm{H_1} = G_1^T F^T \tilde{R}_1 F G_1 + 2G_4^T \hat{S}_1 G_4 + 4G_5^T \hat{S}_1 G_5 + G_6^T \hat{S}_2 G_6$$

$$\mathrm{H_2} = \begin{bmatrix} FG_2 \\ FG_3 \end{bmatrix}, \hat{S}_i = \begin{bmatrix} S_i & 0 \\ 0 & S_i \end{bmatrix} (i \in \{1 \quad 2\}), \tilde{R}_{1i} = diag\{R_{i1}, \quad 3R_{1i}, \quad 5R_{1i}\}, \tilde{R}_2 = diag\{R_2, \quad 3R_2, \quad 5R_2\}$$

$$F = \begin{bmatrix} 1 & 1 & 0 & 0 \\ 1 & 1 & 2 & 0 \\ 1 & 1 & 6 & 6 \end{bmatrix} I$$

$$G(\ ) = \begin{matrix} e_1 \\ \ _1e_5 \\ (\quad \ _1)e_6 + (\ _2 \quad)e_7 \\ \frac{1}{2} \ _1^2 e_8 \end{matrix}, G_0 = \begin{bmatrix} Ae_1 + A_d e_3 \\ e_1 \quad e_2 \\ e_2 \quad e_4 \\ \ _1(e_1 \quad e_5) \end{bmatrix}$$

$$\zeta_0(t) = \Big[x(t), \quad x(t \quad _1), \quad x\big(t \quad (t)\big), \quad x(t \quad _2), \quad \frac{1}{_1}\int_{t_{h_1}}^{t} x(s)ds,$$

$$\frac{1}{(t) \quad _1}\int_{t_{h(t)}}^{t_{h_1}} x(s)ds\,, \quad \frac{1}{_2 \quad (t)}\int_{t_{h_2}}^{t_{h(t)}} x(s)ds\,, \quad \frac{2}{\frac{2}{1}}\int_{-h_1}^{0}\int_{t+s}^{t} x(u)du\,ds,$$

$$\frac{2}{(\ (t) \quad _1)^2}\int_{-h(t)}^{-h_1}\int_{t+s}^{t} x(u)du\,ds\,, \quad \frac{2}{\big(_2 \quad (t)\big)^2}\int_{-h_2}^{-h(t)}\int_{t+s}^{t} x(u)du\,ds, \quad \omega^T(t)\Big]^T$$

$$G_1 = col\{e_1, e_2, e_5, e_8\}, G_2 = col\{e_2, e_3, e_6, e_9\}, G_3 = col\{e_3, e_4, e_7, e_{10}\},$$

$$G_4 = col\{e_2 \quad e_6, e_3 \quad e_7\}$$

$$G_5 = col\{e_2 + 2e_6 \quad 3e_9, e_3 + 2e_7 \quad 3e_{10}\}, G_6 = col\{e_1 \quad e_5, \quad e_1 \quad 2e_5 + 3e_8\}$$

Proof:

As shown in ([19]), one can show that the $\{(x_t, r_t), t > \bar{\tau}\}$ is a Markov process starting from$(\phi(.), r_0)$. Let's define a set of Lyapunov function candidates as follows:

$$V(x_t, r_t, t) = \sum_{i=1}^{9} V_i(x_t, r_t, t)$$

$$V_1(x_t, r_t, t) = \tilde{x}^T P(r_t)\tilde{x}, V_2(x_t, r_t, t), V_2(x_t, r_t, t) = \int_{t-h_1}^{t} x^T(s)Q_1(r_t)x(s)ds,$$

$$V_3(x_t, r_t, t) = \int_{t-h_2}^{t-h_1} x^T(s)Q_2(r_t)x(s)\,ds$$

$$V_4(x_t, r_t, t) = \ _1\int_{-h_1}^{0}\int_{t+s}^{t} x^T(u)R_1(r_t)x(u)\,duds,$$

$$V_5(x_t, r_t, t) = \ _{12}\int_{-h_2}^{-h_1}\int_{t+s}^{t} x^T(u)R_2x(u)\,duds$$

$$V_6(x_t, r_t, t) = \int_{-h_2}^{-h_1}\int_{s}^{-h_1}\int_{t+u}^{t} x^T(\theta)S_1x(\theta)\,d\theta duds,$$

$$V_7(x_t, r_t, t) = \int_{-h_1}^{0}\int_{t+\beta}^{t} x(u)^T R_3x(u)du\,d\beta$$

$$V_8(x_t, r_t, t) = \int_{-h_2}^{-h_1}\int_{t+\beta}^{t} x(u)^T R_4x(u)du\,d\beta,$$

$$V_9(x_t, r_t, t) = \int_{-h_1}^{0}\int_{\theta}^{0}\int_{t+\beta}^{t} x(u)^T S_2x(u)du\,d\beta d\theta$$

$$\tilde{x}(t) = \left[x^T(t) \quad \int_{t_{h_1}}^{t} x^T(s)ds \quad \int_{t_{h_1}}^{t_{h_2}} x^T(s)ds \quad \int_{-h_1}^{0}\int_{t+s}^{t} x^T(u)du\,ds \right]^T = G(\ )\zeta_0$$

Assuming that is the weak infinitesimal generator of the defined Markov chain, then one has the following for $\forall r_t = i, i \in S$:

$$\begin{aligned} V_1(x_t, r_t, t) = {} & \big(G_0\zeta_0(t)\big)^T P_i(r_t)\big(G(\ )\zeta_0(t)\big) + \big(G(\ )\zeta_0(t)\big)^T P_i(r_t)(G_0\zeta_0(t)) \\ & + \big(G(\ )\zeta_0(t)\big)^T \left(\sum_{j=1}^{N} \pi_{ij} P_j\right)\big(G(\ )\zeta_0(t)\big) \end{aligned} \tag{6.16}$$

$$\begin{aligned} V_2(x_t, r_t, t) = {} & x^T(t)Q_{1i}(r_t)x(t) \quad x^T(t \quad _1)Q_{1i}(r_t)x(t \quad _1) \\ & + \int_{t-h_1}^{t} x^T(u)\left(\sum_{j=1}^{N} \pi_{ij} Q_{1j}\right)x(u)du \end{aligned}$$

$$\begin{aligned} V_3(x_t, r_t, t) = {} & x^T(t \quad _1)Q_{2i}(r_t)x(t \quad _1) \quad x^T(t \quad _2)Q_{2i}(r_t)x(t \quad _2) \\ & + \int_{t-h_2}^{t-h_1} x^T(u)\left(\sum_{j=1}^{N} \pi_{ij} Q_{2j}\right)x(u)du \end{aligned}$$

$$\begin{aligned} V_4(x_t, r_t, t) = {} & _1\Bigg(\int_{t-h_1}^{t} x^T(u)R_{1i}(r_t)x(u)\,du + \ _1\big(x^T(t)R_{1i}(r_t)x(t)\big) \\ & + \int_{-h_1}^{0}\int_{t+s}^{t} x^T(u)\left(\sum_{j=1}^{N} \pi_{ij} R_{1j}\right)(r_t)x(u)\,duds \Bigg) \end{aligned}$$

$$V_5(x_t, r_t, t) = \ _{12}\Bigg(\int_{t-h_2}^{t-h_1} x^T(u)R_{2i}x(u)\,du + \ _{12}\big(x^T(t)R_2x(t)\big) \Bigg)$$

$$V_6(x_t, r_t, t) = \frac{1}{2} \ {}^{2}_{12}x^T(t)Sx(t) \quad \int_{-h_2}^{-h_1}\int_{t+s}^{t-h_1} x^T(u)S_1x(u)du\,ds$$

$$V_7(x_t, r_t, t) = \ _1x(t)^T R_3 x(t) \quad \int_{t-h_1}^{t} x(u)^T R_3 x(u)du$$

$$V_8(x_t, r_t, t) = \ _{12}x(t)^T R_4 x(t) \quad \int_{t-h_1}^{t-h_2} x(u)^T R_4 x(u)du$$

$$V_9(x_t, r_t, t) = \frac{1}{2}\ {}_1^2x(t)^T S_2 x(t) \quad \left(\int_{-h_1}^{0}\int_{t+s}^{t} x(u)^T S_2 x(u)\, duds\right)$$

using (6.15) and (6.16), one can write:

$$V(x_t, r_t, t) \le \zeta_0^T(t)\mathrm{H}\zeta_0(t) \qquad {}_1\int_{t_{h_1}}^{t} x(u)^T R_{1i} x(u) du \qquad {}_{12}\int_{t-h_2}^{t-h_1} x^T(u) R_2 x(u)\, du$$
$$\int_{-h_2}^{-h_1}\int_{t+s}^{t-h_1} x^T(u) S_1 x(u) du\, ds \quad \int_{-h_1}^{0}\int_{t+s}^{t} x(u)^T S_2 x(u)\, duds$$

using lemma 1, for $\int_{t_{h_1}}^{t} x(u)^T R_{1i} x(u) du$, one can write:

$${}_1\int_{t-h_1}^{t} x^T(s) R x(s) ds$$
$$\le \quad \left(\begin{pmatrix} x(t) & x(t \quad {}_1) \end{pmatrix}^T R \begin{pmatrix} x(t) & x(t \quad {}_1) \end{pmatrix} + \begin{bmatrix}\zeta_1 \\ \zeta_2\end{bmatrix}^T \begin{bmatrix} 3R & 0 \\ 0 & 5R \end{bmatrix} \begin{bmatrix}\zeta_1 \\ \zeta_2\end{bmatrix}\right)$$

where:

$$\zeta_1 = x(t) + x(t \quad {}_1) \quad \frac{2}{{}_1}\int_{t-h_1}^{t} x(s)\, ds$$

$$\zeta_2 = (t) \quad x(t \quad {}_1) \quad \frac{6}{{}_1}\int_{t-h_1}^{t} x(s)\, ds \quad \frac{12}{{}_1^2}\int_{t-h_1}^{t}\int_{s}^{t-h_1} x(u)\, duds$$

then,

$${}_1\int_{t-h_1}^{t} x^T(s) R_{1i} x(s) ds \le \quad \zeta_1^T(t) F^T \tilde{R}_{1i} F \zeta_1$$
$$\zeta_1(t) = G_1 \zeta_0(t)$$

This procedure can be applied to the other term as well.

$${}_{12}\int_{t-h_2}^{t-h_1} x^T(s) R_2 x(s) ds \le \quad \zeta_0\ (t) G_2^T F^T \tilde{R}_1 F G_2 \zeta_0$$

On the other hand, it can be shown that:

$$\int_{-h_1}^{0}\int_{t+s}^{t} x(u)^T S_2 x(u)\,duds \leq \frac{2}{\frac{2}{1}}\left({}_1x(t) \quad \int_{t-h_1}^{t} x(s)ds\right)^T S_2 \left({}_1x(t) \quad \int_{t-h_1}^{t} x(s)ds\right) \quad \frac{4}{\frac{2}{12}}\eta^T S_2 \eta$$

where

$$\eta = 2\left({}_1x(t) \quad \int_{t-h_1}^{t} x(s)ds\right) \quad \frac{6}{12}\left(\frac{1}{2} \quad {}^2_1x(t) \quad \int_{-h_1}^{0}\int_{t+s}^{t} x(u)\,duds\right)$$

And the same procedure for the other term taking into account that:

$$\int_{-h_2}^{-h_1}\int_{t+s}^{t-h_1} \phi(u)^T S_1 \phi(u)\,duds \geq \int_{-h(t)}^{-h_1}\int_{t+s}^{t-h_1} \phi(u)^T S_1 \phi(u)\,duds + \int_{-h_2}^{-h(t)}\int_{t+s}^{t-h(t)} \phi(u)^T S_1 \phi(u)\,duds$$

Therefore,

$$\int_{-h_2}^{-h_1}\int_{t+s}^{t-h_1} x^T(u) S_1 x(u) du\,ds \leq \zeta_0^T(t)\Xi_4\zeta_0$$
$$\int_{-h_1}^{0}\int_{t+s}^{t} x(u)^T S_2 x(u)\,duds \leq \zeta_0^T(t)\Xi_5\zeta_0$$

These conditions directly result in:

$$V(x_t, x_t, r_t, t) \leq \zeta_0^T(t)\Omega(\ )\zeta_0(t) \leq \min_{i\in S}\{\lambda_{min}(\Omega(\ )(i))\}\zeta_0^T(t)\zeta_0(t)$$

The negative definiteness of $\Omega(\ )$ can be easily relaxed by $\Omega(\ _1) < 0$ and $\Omega(\ _2) < 0$. Using the Schur complement, one can now show that $V(x_t, x_t, r_t, t) \leq cx\tilde{}^T(t)\tilde{x}(t) \leq cx^T(t)x(t)$. Observe that the Dynkin's formula results in:

$$E(V(x_t, x_t, r_t, t)) \quad E\left(V(x_{h_2}, x_{h_2}, r_{h_2}, \ _2)\right) \leq cE\left(\int_{h_2}^{t} x(s)^T x(s)ds\right) for\ t \geq \ _2$$

$$E\left(\int_{h_2}^{t} x(s)^T x(s)ds\right) \leq \frac{1}{c}E\left(V\left(x_{h_2}, x_{h_2}, r_{h_2}, \ _2\right)\right) \quad \frac{1}{c}E\left(V(x_t, x_t, r_t, t)\right)$$
$$\leq \frac{1}{c}E\left(V\left(x_{h_2}, x_{h_2}, r_{h_2}, \ _2\right)\right)$$

Similar to the proof of theorem 1 in ([158]), it can be shown that $E\left(\int_{h_2}^{t} x(s)^T x(s)ds\right)$ Is bounded by the initial value function which guarantees stochastically stability of system (6.10) for any time-varying delay satisfying the bounded rate condition. This completes the proof.

6.7.2 Robust Analysis of Retarded Markov Jump Linear System

Referring to system (6.10), the following definition and theorem leads us to find an upper bound estimation for H_∞ performance of retarded MJLS.

Definition:

Given a scalar $\gamma > 0$, system (6.10) is said to be stochastically stable with an H_∞ performance level γ if the following two requirements are met:

System (6.10) with $\omega = 0$ is said to be stochastically stable.

Under zero initial conditions and for all nonzero $\omega \in L_2[0, \infty)$, the following inequality holds:

$$E\left[\int_0^\infty z^T(s)z(s)ds\right] \leq \gamma^2 \int_0^\infty \omega^T(s)\omega(s)ds$$

Theorem 6.2:

For given scalars $\gamma > 0$, delay bounds of $\tau(t) \in [\ _1 \quad _2]$, the system in (6.10) is stochastically stable with an H_∞ performance level γ, if there exists a matrix $X \in R^{3n\times 3n}$, and symmetric positive definite matrices $S_1, S_2, R_2 \in R^{n\times n}, P_i \in R^{4n\times 4n}$ and mode dependent matrices of $Q_{1i}, Q_{2i}, R_{1i} \in R^{n\times n}$ such that the following set of LMIs hold for all $i \in S$:

$$\widehat{\Omega}(\ ) = \begin{bmatrix} \Omega(\ ) & P_i E_i & e_1^T C^T \\ & \gamma I & 0 \\ & & \gamma I \end{bmatrix} < 0, G_0 = \begin{bmatrix} A_i e_1 + A_{di} e_3 + E_i e_{11} \\ e_1 \quad e_2 \\ e_2 \quad e_4 \\ {}_1(e_1 \quad e_5) \end{bmatrix} \tag{6.17}$$

Proof:

Let's define the performance function $J_T = E\left[\int_0^T [z^T(t)z(t) \quad \gamma^2\omega^T(t)\omega(t)]dt\right]$

$$\hat{\zeta}_0 = [\zeta_0^T \quad \omega(t)^T]^T$$

$$V(x_t, x_t, r_t, t) + \frac{1}{\gamma} z^T(t) z(t) \quad \gamma\omega^T(t)\omega(t) \leq \zeta_0^T(t)\widehat{\Omega}(\ )\zeta_0(t) \leq \quad c|x(t)|^2$$

Thus $\gamma\omega^T(t)\omega(t) \geq \quad V(x_t, x_t, r_t, t) + \frac{1}{\gamma} z^T(t) z(t)$ holds for any $t \geq 0$. Using Dynkin's formula:

$$E\left[\int_0^T \gamma\omega^T(t)\omega(t)dt\right] \geq E[V(x_t, x_t, r_t, t)] \quad V(x_0, x_0, r_0, 0) + \frac{1}{\gamma} E\left[\int_0^T z^T(t) z(t) dt\right]$$

$$E\left[\int_0^T \gamma\omega^T(t)\omega(t)dt\right] \geq \frac{1}{\gamma} E\left[\int_0^T z^T(t) z(t) dt\right], \int_0^T \gamma\omega^T(t)\omega(t)dt \geq \frac{1}{\gamma} E\left[\int_0^T z^T(t) z(t) dt\right]$$

The results show improvement in the estimation of disturbance rejection of the system. It is worth mentioning that designing a controller using the Markov chain method is another alternative for solving this problem. However, as the standard version of the Markov jump linear controller is based on a stochastic process, implementation of the controller in a real situation will be problematic.

6.8 Linear Parameter Varying Controller Performance Analysis

In the previous chapter, an LPV controller was designed for the parameter varying driver-in-the-loop system of (5.3). To investigate the system performance, Theorem 5.2 is used to find the robust LPV controller with the corresponding disturbance rejection factor. Using the boundaries given for the varying parameters $\left(\frac{1}{V_x}, k_1, k_2\right)$, the controller (5.25) is designed and the attenuation level of $\gamma = 7.3$ is achieved for damping the uncertainties in the closed loop system. The main goal here is to extend the analysis using extra information that is available from the Markov modeling of the behavior of the driver. It is shown that having the transition probability of the model, one can incorporate this information to better analyze system performance.

By integrating the system (5.3) and the controller designed in Theorem 5.2, a closed loop system of the form (6.10) is obtained. Here, it is assumed that the extra information about the driver mode switching probability is also known. Using the same method in 6.7, one can revise Theorem 5.1 to find the best estimation of the upper bound of disturbance rejection for the MJLS (see Appendix).

Applying Theorem 6.2, the lower disturbance rejection of $\gamma = 4.98$ is obtained. Note that, the controller and the system representation remain fixed. In this estimation, it is only assumed that

the switching between the system modes is based on a given transition probability rather than bounded rate arbitrary jumps.

Remark: Using an appropriate MJLS analysis technique, one can continue the derivation and find the policy to guarantee "almost-sure" stability of the system. The extension of current theorem to the controller design, however, is straight forward and similar to the methods in chapter 4 and 5. ■

Remark: A tighter lower bound disturbance rejection is obtained using Theorem 6.2 by adding another constraint to the system. The availability of the probability transition matrix for driver mode switching is the cost of improving this estimation.■

The same problem also can be solved using the proposed theorem for robust stability of MJLS in 6.1. Compared to theorem 5.2, an improved version of the well-known Jensen inequality is used in this theorem to reduce the level of conservation. By applying theorem 6.1 on the closed loop system, the attenuation factor of $\gamma = 4.62$ is obtained.

An academic license of MOSEK ([108]) is used in all of the calculation and the simulation condition remains the same for fair comparison.

6.9 Summary

Given that identifying current driving style is very important for implementation of LPV controller, a method for identifying the driver parameter (style) was proposed in this chapter. The most important difference between the proposed method and current approaches is to use only the current and previous driving information to model the driver. All of the other methods need some future road data to identify the driver. We proposed to look at a previous moving window on the driving information to identify the current state of the driver. The algorithm was applied to a set of experimental data collected at the University of Waterloo. Then, based on the range of parameter variation, several modes were defined for the driver and using Markov modeling, a transition probability was obtained for each mode. Using the proposed method for augmenting the driver model with the vehicle model, a retarded Markov jump linear system with uncertainty was obtained. A new theorem was proposed for analyzing system stability and finding the disturbance rejection level of the system.

To show the effectiveness of the method, the closed loop LPV system in Chapter 5 was revisited and it was assumed that the driver switches between different modes with a known probability transition rule. The results show that using this extra information, a better disturbance rejection estimation is obtained when compared to the results of chapter 5. Similar comparison between the Markov jump linear system and LPV is reported in [31] where it is shown that adding extra information about the switching probability of different modes of a system improve the performance analysis.

"Finally, we make some remarks on why linear systems are so important. The answer is simple: because we can solve them!"

Richard Feynman

Chapter 7
Redesign Considering Nonlinearities

7.1 Introduction

A main cause of unstable behavior of both longitudinal and lateral velocities is that the tires are saturated in response to harsh/emergency maneuvers, aggressive/performance driving, low friction contact, and slick road conditions. Behavior of a vehicle at the limits of adhesion is quite different from its nominal one; for example, in cases where front tires lose their grip, the vehicle may go into oscillatory response (understeer behavior); on the other hand, if the rear tires enter a saturated region, it is more likely to spin and shoe into oversteer behavior. A vehicle working to its limits makes a novice driver unable to control the vehicle.

The following are the three main assumptions in previous chapters that are relaxed in this chapter:

1. Small steering wheel angle (Figure 7-1 (a)): To obtain a linear vehicle model, one need to assume that $(\sin\delta \approx \delta\,, \cos\delta \approx 1)$. Hwever for harsh maneuvers this assumption induces calculation error.
2. Linear tire model (infinite tire capacity) (Figure 7-1 (b)): Tire force saturation is a known disadvantage of dealing with a linear vehicle model.
3. Negligible longitudinal tire force: There are scenarios that the assumption is not valid anymore. For example, an acceleration in turn or an on-throttle double lane change maneuvers are the cases that this assumption can be violated.

The main focus of this chapter is on nonlinear analysis and controller design for improving the handling behavior of a vehicle considering the effect of the human driver. Similar to the previous chapters, to make an implementable approach, it is assumed that the desired road information

is not available. An important assumption here is not to use the exact values of longitudinal and lateral forces in the control process.

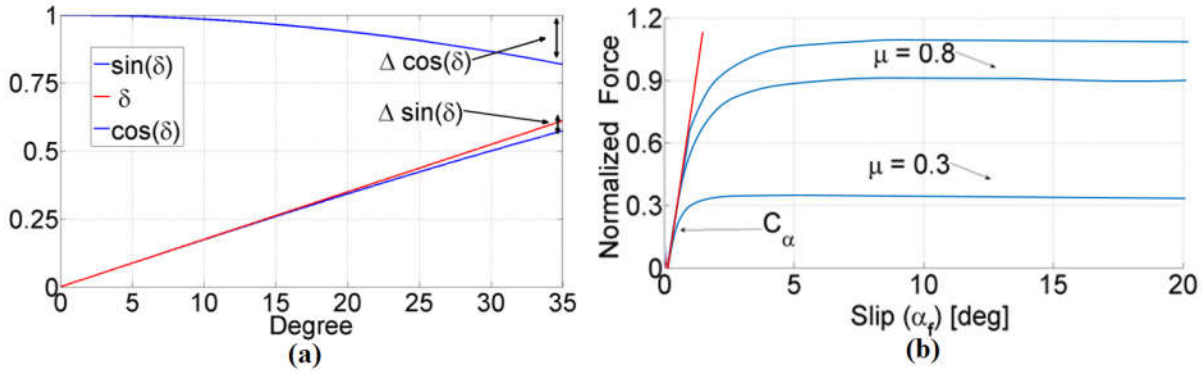

Figure 7-1: Vehicle model nonlinearities

The nonlinear equations of motion are formulated such that the nonlinear damping technique can be adopted to stabilize the yaw rate error. For two different robust designs, it is also shown that the yaw rate error will be confined inside a certain neighborhood even in the presence of uncertainty. The size of this neighborhood is directly proportional to the gain of the robust control terms and the driver characteristics.

Although a plethora of techniques exist for the control of nonlinear systems without delays, control design for nonlinear delayed systems introduce significant feedback design challenges that may cause very loose stability bounds. Incorporating the driver delay in the analysis is postponed until future work. However, the effect of driver delay is investigated in simulation results.

7.2 Nonlinear Vehicle Model

The vehicle model used in this chapter is a nonlinear bicycle model that describes the most important vehicle states for vehicle handling control (see Figure 3-1). The two-dimensional model is described by (3.2). The LuGre tire model ([32]) is used to generate the cornering front and rear forces as a function of the vehicle's tire velocity and the road condition. Compared to other conventional approaches such as Pacejka ([72]), this model utilizes relative velocities rather than slip ratios and slip angles. The change of the input (relative velocity instead of slip ratio/angle) provides a precise notion of the tire states. The main reason is that the normalization action (during slip ratio/angle calculation) is not needed, and only the effect of velocity is considered without any cancellation. The model captures the dynamic behavior of the tire specifically near

the regular load regions. The cornering forces can be presented by the following nonlinear expression:

$$F_{ij} = \left(\sigma_{0ij} z_{ij} + \sigma_{1ij} z_{ij} + \sigma_{2i} v_{rij}\right) F_{nj} \tag{7.1}$$

$$z_{ij} = v_{rij} \quad \left(\frac{\sigma_{0ij}|v_{rij}|}{\theta g(v_{rij})} + \kappa_i R_{eff} \omega'\right) z_{ij} \tag{7.2}$$

where for $i \in \{x, y\}$ and $j \in \{f, r\}$, z_{ij} is the tire deflection, $F_{nf(r)}$ is the front (rear) normal tire force, θ is the road classification factor, ω' is the wheel rotational speed, and R_{eff} is the effective tire radius. The function $g(v_{rij})$ is related to the normalized Coulomb friction μ_c, the normalized state friction μ_s, the transition between these two friction states by Stribeck relative velocity v_s, and the relative velocity v_{rij} as follows:

$$\begin{aligned} g(v_{r,i,j}) &= \mu_{c,i} + \left(\mu_{s,i} \quad \mu_{c,i}\right) e^{\left(\frac{v_{r,i,j}}{v_s}\right)^{\alpha}} \\ v_{r,y,f} &= \sin(\alpha_f) \sqrt{v_f} \\ v_{r,y,r} &= \sin(\alpha_r) \sqrt{v_r} \\ v_{r,x,f} &= R_{eff}\omega \quad \cos(\alpha_f) \sqrt{v_f} \\ v_{r,x,r} &= R_{eff}\omega \quad \cos(\alpha_r) \sqrt{v_r} \end{aligned} \tag{7.3}$$

where σ_0 (σ_1, σ_2) is the rubber (relative damping, relative viscous) damping parameter, α is the tire parameter to show the steady state friction and slip interaction, and $\alpha_{f(r)}$ is vehicle corner slip angles.

$$\begin{aligned} v_f &= \left(v_y + ar\right)^2 + v_x^2 \\ v_r &= \left(v_y \quad br\right)^2 + v_x^2 \end{aligned} \tag{7.4}$$

Figure 7-2 illustrates how the longitudinal tire force saturates as the slip angle increases. The driver model used here is a general model based on the vehicle states and human desired road

path. Note that the linear predictive driver model of (3.12) cannot predict the tire saturation and assumes that the tire capacity is not physically bounded.

Remark: In this chapter, the problem is solved for a generic driver model, however, one can use the discrete model of (3.9) and convert the DLQR problem to the corresponding continuous time using different approaches such as δ domain method ([53]). The gains can then be computed by solving the continuous linear quadratic Riccati (CLQR) equation. ■

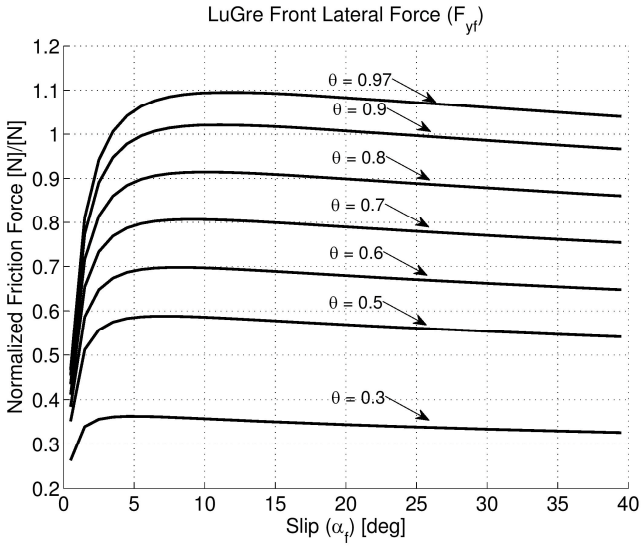

Figure 7-2 Lateral force LuGre tire saturation corresponding to different road condition [Normalized]

The model in (3.9) only captures the linear behavior which mimics most drivers' understanding of vehicle dynamics. In this regard, when the tire enters the saturation zone (see Figure 7-2), many drivers still steer the vehicle based on the linear tire model assumption. In this case, the driver usually continually demands more lateral or longitudinal tire forces when the tire is no longer capable of providing more capacity. This is one source of poor performance of a driver-vehicle system which happens with most novice drivers, especially when driving on roads with a low friction coefficient. Figure 7-3 shows how the nonlinear tire saturation phenomenon prevents the driver from properly steering the car. The simulation is done for a standard double-lane-change with 90 kph on a wet road condition $(\mu = 0.5)$ while the driver has small amount of reaction delay (between 160ms to 210 ms) and 1.5 seconds of preview time.

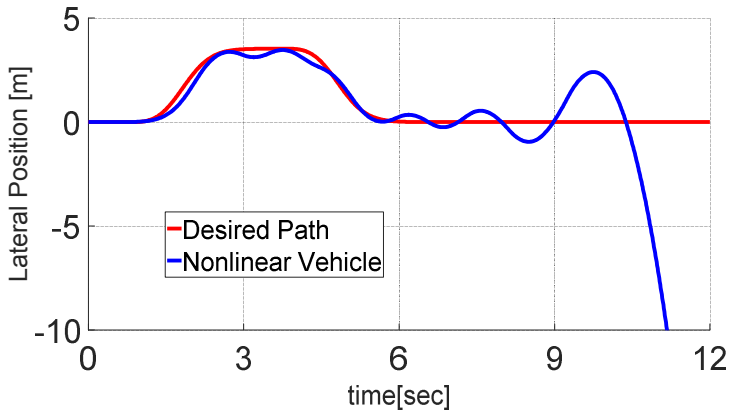

Figure 7-3 Longitudinal Velocity =90 KpH, 160 ms ≤τ≤ 210ms

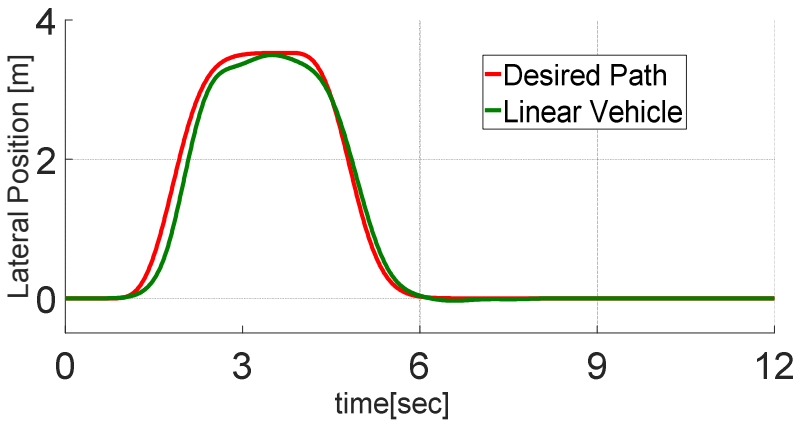

Figure 7-4 Longitudinal Velocity =90 KpH, 160 ms ≤τ≤ 210ms

In Figure 7-4, an infinite tire capacity is assumed for the vehicle. Note that using a linear bicycle model to describe the handling characteristics of a vehicle, the forces linearly proportional to the tire slip angle ($F = C\alpha$). This approach lets the tire forces increase in proportion to the tire slip angle. This is exactly what a novice driver expects from the vehicle. Thus, the driver can steer the vehicle smoothly. Figure 7-4 demonstrates that even a novice driver can steer the vehicle on a low friction surface if the tires are not saturated.

Remark: In most of vehicle controller design papers, the authors assume a linear model for the vehicle. There are two main reasons for this assumption. The first one is to prevent nonlinear design challenges. Secondly, engineers are always interested in keeping the vehicle in the linear region or in the extreme cases, at the edge of its tire capacities. Then, one can argue that if a controller works properly, the vehicle must almost always be maintained in the linear working region. Thus, for controller design, one can expect more of linear vehicle behavior rather than nonlinear responses. ■

Noting Figure 7-3 one can immediately conclude that the driver could not safely complete the maneuver if a nonlinear vehicle model were to be used in the simulation. For this simulation, the nonlinear LuGre tire model is used. The model saturates as the slip angles reach higher values (see Figure 7-2). Conversely, consider the case where the maneuver is mild, at a lower speed, and the tire forces are not saturated yet. In this region, both linear and nonlinear tire models produce the same values for the forces. The driver is also expecting a linear tire behavior, so he/she can control the vehicle properly and there is almost no difference between the linear and nonlinear model. Figure 7-5 represents a novice driver's performance in steering the car into a double lane change maneuver when the road is dry and the speed is low enough such that the vehicle remains in the linear operating point condition.

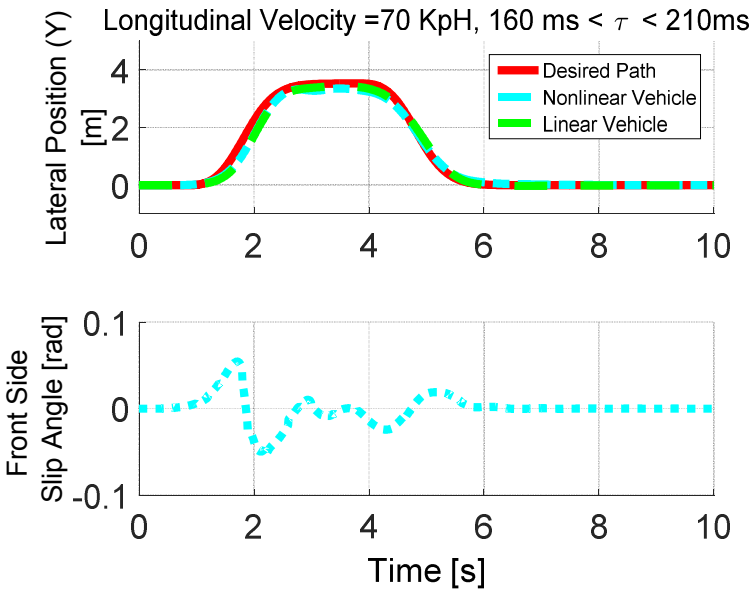

Figure 7-5: Novice driver steering linear and nonlinear vehicle, $\mu = 0.9$

The discussion and simulation results show that the nonlinear characteristics of the tires are very important in vehicle control analysis. Thus, designing a controller with consideration to the driver's limitations and the tire saturation behavior is very important and needs to be properly addressed.

7.3 Defining Control Problem

The main aim of the controller design is to track the desired vehicle yaw rate while keeping the vehicle lateral velocity bounded. By considering (3.2), the robust control methodology is used to produce the required yaw moment at the vehicle C.G. that reduces the vehicle yaw rate error. The desired value for the yaw rate is directly proportional to the current steering angle. It is also known that the desired lateral velocity value can also be defined; although, the lateral velocity state is coupled with the yaw rate state through the zero dynamics. Thus, using yaw moment control technique, there is no possibility of simultaneously steering the vehicle's lateral velocity and the yaw rate to the desired values.

7.3.1 Yaw Rate Tracking Controller Design

By considering the force estimation uncertainties, one can extend equations (3.2) to the following uncertain model for the lateral dynamic of vehicle:

$$v_y = \frac{1}{m}\left(\left(\hat{F}_{yf} + \Delta F_{yf}\right)\cos\delta + \left(\hat{F}_{xf} + \Delta F_{xf}\right)\sin\delta\right) \quad ue_r \quad ur_d + \frac{\hat{F}_r + \Delta F_{yr}}{m} \tag{7.5}$$

$$e_r = \frac{1}{I_z}\left(a\left(\hat{F}_{yf} + \Delta F_{yf}\right)\cos\delta + b\left(\hat{F}_{xf} + \Delta F_{xf}\right)\sin\delta\right) + \frac{M}{I_z} \quad r_d \quad \frac{b\left(\hat{F}_{yr} + \Delta F_{yr}\right)}{I_z} \tag{7.6}$$

where $e_r = r \quad r_d$ is the difference between actual and desired value of the yaw rate and the vehicle driver model is: $\delta = k_1 v_y + k_2 e_r + k_2 r_d + \omega \quad \psi + \omega$.

Note that, based on the LuGre tire model, the norms of the lateral and longitudinal forces are bounded. These forces are highly dependent on the road friction condition, which is hard to estimate; therefore, it is assumed that the estimated forces have bounded uncertainties ΔF. To make the control design implementable in real time, this uncertain estimation is used in the control structure. The disturbance and estimation error terms as well as their coefficients in (7.5) and (7.6) are stacked in the following vectors:

$$\phi = \begin{matrix} aF_{yf}\cos\psi + aF_{xf}\sin\psi \\ aF_{yf}\sin\psi + aF_{xf}\cos\psi \\ a\cos\psi \\ a\sin\psi \\ b \end{matrix}, \Delta = \begin{matrix} \cos\omega \\ \sin\omega \\ \Delta F_{yf}\cos\omega + \Delta F_{xf}\sin\omega \\ \Delta F_{yf}\sin\omega + \Delta F_{xf}\cos\omega \\ \Delta F_{yr} \end{matrix}, \tag{7.7}$$

$$\phi^T \frac{\partial \phi}{\partial \psi} = 0 \tag{7.8}$$

From the boundedness of $\Delta F_{xf}, \Delta F_{yf}, \Delta F_{yr}$, one can conclude that:

$$\|\Delta\|_\infty \leq \left(1 + \Delta F_{xf}^2 + \Delta F_{yf}^2 + \Delta F_{yr}^2\right)^{\frac{1}{2}} \tag{7.9}$$

Using the vectors defined (7.7), the yaw error dynamics (7.6) can be rewritten as:

$$e_r = \frac{\phi^T \Delta}{I_z} \quad \frac{bF_{yr}}{I_z} + \frac{M}{I_z} \quad r_d \tag{7.10}$$

The main objective is to devise a method to attenuate the effects of Δ in (7.5) and (7.6). In this research, first the nonlinear *damping* method in [79] is adopted to fulfill such a control task. Consider the following control law:

$$M = bF_{yr} + I_z r_d \quad I_z \bar{k} e_r \quad I_z \kappa e_r \|\phi\|^2 \tag{7.11}$$

Where $\bar{k}$ and κ are design parameters, (7.11) acts as a nonlinear damper for (7.5) and (7.6) to drain the artificial energy of the system. Considering $V = \frac{1}{2} e_r^2$ as a measure of deviation from the desired state. We have:

$$V = e_r\left(\frac{\phi^T\Delta}{I_z} \quad \frac{bF_{yr}}{I_z}+\frac{M}{I_z} \quad r_d\right) = \frac{\phi^T\Delta e_r}{I_z} \quad \bar{k}e_r^2 \quad \kappa e_r^2\|\phi\|^2$$

$$\leq \quad \bar{k}e_r^2 \quad \kappa e_r^2\|\phi\|^2+\frac{1}{I_z}\|\phi\|\|\Delta\|_\infty|e_r| = \quad \bar{k}e_r^2 \quad \kappa\left(e_r\|\phi\| \quad \frac{\|\Delta\|_\infty}{2I_z\kappa}\right)^2+\frac{\|\Delta\|_\infty^2}{4I_z^2\kappa} \tag{7.12}$$

$$\leq \quad 2\bar{k}V+\frac{\|\Delta\|_\infty^2}{4I_z^2\kappa}$$

Then one can conclude that $|e_r(t)|$ is bounded by:

$$\|e_r(t)\|_\infty \leq \max\left\{|e_r(0)|, \frac{\|\Delta\|_\infty}{2I_z\sqrt{\kappa\bar{k}}}\right\} \tag{7.13}$$

Using Gronwall Lemma [79], we obtain:

$$V(t) \leq V(0)e^{-2\bar{k}t}+\frac{1}{8I_z^2\bar{k}\kappa}\max(\|\Delta\|_\infty^2)\left(1 \quad e^{-2\bar{k}t}\right) \tag{7.14}$$

hence,

$$\|e_r(t)\| \leq \sqrt{2}\|e(0)\|e^{-\bar{k}t}+\frac{1}{I_z}\sqrt{\frac{\left(1 \quad e^{-2\bar{k}t}\right)}{2\bar{k}\kappa}}\|\Delta\|_\infty^2 \tag{7.15}$$

From (7.15), it is clear that the trajectory of the system will be trapped inside a neighborhood of the desired yaw rate. The size of this neighborhood decreases as the value of κ increases. Hence, the performance of the robust control law (7.11) directly depends on κ. However, it should be noted that with higher values of κ, the controller in (7.11) becomes a high-gain feedback controller that increases the control effort.

One can study the boundedness of the lateral velocity v_y by analyzing the subsystem (7.5). The $\frac{F_{yr}}{m}$ term in (7.5) can be expressed as:

$$F_{yr} = \left(\sigma_0 z_{yr} + \sigma_1 z_{yr} + \sigma_{2r}\sin(\alpha_r)\sqrt{\left(v_y \quad br\right)^2 + v_x^2}\right)F_{nr} \tag{7.16}$$

Considering the cases where the vehicle longitudinal velocity (v_x) is high, the term $\left(v_y \quad br\right)^2$ is negligible compared to v_x^2.

Using this approximation and the change of variable $d = \frac{v_y - br}{v_x}$, (7.5) becomes:

$$d = \quad \frac{v_x F_{nr}\sigma_{2r}}{m}\sin(d) + \Lambda, \tag{7.17}$$

$$\Lambda = \frac{1}{m}(\sigma_{0yr} z_{yr} F_{nr} + \sigma_{1r} z_{yr} F_{nr} + \Delta F_{yr} + \left(F_{yf} + \Delta F_{yf}\right)cos\,\chi$$
$$+\left(F_{xf} + \Delta F_{xf}\right)sin\,\chi) \quad ue_r \quad ur_d \quad br$$

The norm of e_r is bounded according to (7.15). It is also known that the tire deflection (z_{yr}) and its time derivative (z_{yr}) are bounded, which results in the boundedness of the norm of Λ.

Now, consider $V_d = \frac{1}{2}d^2$ as a Lyapunov function candidate for analyzing (7.17), one can write:

$$V_d = \quad \frac{v_x F_{nr}\sigma_{2r}}{m} d\sin(d) \; + \Lambda d \leq \quad \frac{2F_{nr}\sigma_{2r}}{\pi m} d^2 + \|\Lambda d\| \tag{7.18}$$

Using the fact that $d\left(\frac{2d}{\pi} \quad \sin d\right) \leq 0$ (see Figure 7-6) for $\left|\frac{v-br}{v_x}\right| \ll 1$ and choosing $0 < \theta < 1$:

$$V_d \leq \quad \frac{2(1 \quad \theta)F_{nr}\sigma_{2r}}{\pi m} d^2 \quad \left(|d|\sqrt{\frac{2\theta F_{nr}\sigma_{2r}}{\pi m}} \quad \frac{\|\Lambda\|}{2}\sqrt{\frac{\pi m}{2\theta F_{nr}\sigma_{2r}}}\right)^2 + \frac{\|\Lambda\|^2 \pi m}{8\theta F_{nr}\sigma_{2r}} \tag{7.19}$$
$$\leq \quad \frac{4(1 \quad \theta)F_{nr}\sigma_{2r}}{\pi m} V_d + \frac{\|\Lambda\|^2 \pi m}{8\theta F_{nr}\sigma_{2r}}$$

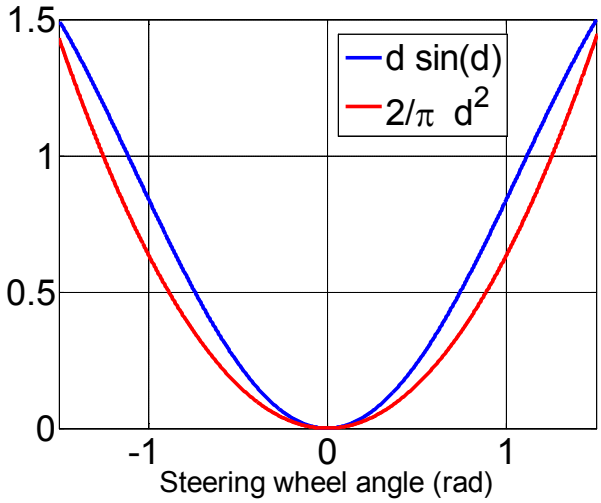

Figure 7-6 : Comparing $\frac{2}{\pi}d^2$ and $d\ sin(d)$

Boundedness of the norm of lateral velocity (v) can be established using the Gronwall lemma. Equation (7.19) shows that $V_d(t)$ will converge to a neighborhood of the origin. The size of this set is upper-bounded by:

$$\frac{\|\Lambda\|^2\pi^2m^2}{32(1 \quad \theta)\theta F_{nr}^2\sigma_{2r}^2} \tag{7.20}$$

Note that there is no control parameter to adjust this bound. One may use physical parameters of the original system to reach the desired performance.

The control law (7.11) steers the trajectory of the system into a small neighborhood around the desired point. We are also interested in comparing the nonlinear approach with methods that are eliminating the effects of disturbances. To fulfill such a design, the following input is proposed as an alternative to (7.11) :

$$M' = bF_{yr} \quad r_d \quad I_z\bar{k}'e_r \quad \left(\sum_{i=1}^{5}|\phi_i|\|\Delta_i\|_\infty\right)sign\,(e_r) \tag{7.21}$$

The last term in (7.21) is added to ensure that the time derivative of the artificial energy of the system ($V = \frac{1}{2}e_r^2$) remains negative definite for all ($t > 0$). Using (7.21), (7.12) changes to:

$$V = e_r \left(\frac{\phi^T \Delta}{I_z} \quad \frac{bF_{yr}}{I_z} + \frac{M'}{I_z} \quad r_d \right)$$
$$= \frac{\phi^T \Delta e_r}{I_z} \quad \bar{k}' e_r^2 \quad \frac{1}{I_z} e_r \left(\sum_{i=1}^{5} |\phi_i| \|\Delta_i\|_\infty \right) sign\,(e_r) \tag{7.22}$$

since

$$\frac{\phi^T \Delta e_r}{I_z} \quad \frac{1}{I_z} e_r \left(\sum_{i=1}^{5} |\phi_i| \|\Delta_i\|_\infty \right) sign\,(e_r) \leq 0, \tag{7.23}$$

It is easy to conclude that $V \leq \quad 2\bar{k}' V$ and the exponential convergence of e_r to zero follows. It is worth noting that, instead of using the upper bound on the stack vector Δ in (7.11), the term in (7.21) depends on the upper bounds of each component of Δ. This suggests that one can attenuate each term of uncertainty separately at the expense of using discontinuous feedback control law. More precisely, one can use adjustable gains to attenuate the effect of road disturbance on the steering angle and at the same time to reflect the importance of eliminating the effect of uncertainties in force estimation. An implication of this is the possibility of adaptively tuning the authority between the driver and the controller by varying the aforementioned gains.

7.3.2 Back-Stepping Method

In this section, the possibility of using a backstepping control method is discussed to suppress the effects of uncertainties in both subsystems (3.2) through a recursive design based on the nonlinear damping technique. The latter requires that for each step of the backstepping method, the controller stabilizes the respective subsystem by attenuating the effects of disturbances. Since in (3.2), the steering angle (δ) depends on both v_y and r, the first step of control design involves solving a nonlinear parametric equation. To circumvent this issue, the following variable is defined:

$$s = k_1 v_y + k_2 r \tag{7.24}$$

where k_1 and k_2 are the driver gains that obtain from the human modeling identification. The new variable s can be interpreted as the effect of the vehicle yaw-rate and the lateral velocity on the driver's decision. Using $[s \quad r]^T$ as the new state vector for system (3.2), the dynamics of the system can be written as:

$$\begin{aligned} s &= f_1 + f_2\cos(s+\omega) + f_3\sin(s+\omega) \quad k_1 v_x r + k'M \\ r &= f_4 + f_5\cos(s+\omega) + f_6\sin(s+\omega) + k"M \end{aligned} \tag{7.25}$$

where

$$f_1 = \left(\frac{k_1}{m} \quad \frac{bk_2}{I_z}\right)F_{yr},\ f_2 = \left(\frac{k_1}{m} + \frac{ak_2}{I_z}\right)F_{yf}$$

$$f_3 = \left(\frac{k_1}{m} + \frac{ak_2}{I_z}\right)F_{xf}$$

$$f_4 = \quad \frac{b}{I_z}F_{yr}, f_5 = \frac{a}{I_z}F_{yf}, f_6 = \frac{a}{I_z}F_{xf}$$

$$k' = \frac{k_2}{I_z}, k" = \frac{1}{I_z}$$

In this regard, one can use the transformation:

$$\gamma = r \quad \frac{k"}{k'}s \tag{7.26}$$

which eliminates the input term at the second subsystem (7.25). The reason that one cannot perform such a method for the first subsystem again stems from the difficulties which arise in the design process of the nonlinear robust control technique.

Given that the desired states are:

$$s = k_2 r_d, \quad r = r_d \tag{7.27}$$

in terms of new variables,

$$\begin{aligned} e_s &= s \quad k_2 r_d \\ e_\gamma &= \gamma + \left(\frac{k"}{k'}k_2 \quad 1\right)r_d = \gamma \end{aligned} \tag{7.28}$$

the system (7.25) can be expressed as:

$$e_s = f_1 + f_2\cos(e_s + k_2 r_d + \omega) + f_3\sin(e_s + k_2 r_d + \omega) \tag{7.29}$$

$$
\begin{aligned}
& k_1 v_x \left(e_\gamma + r_d + \frac{1}{k_2} e_s\right) + k' M \quad k_2 r_d \\
e_\gamma = {} & f_1' + f_2' \cos(e_s + k_2 r_d + \omega) + f_3' \sin(e_s + k_2 r_d + \omega) \\
& + \frac{k_1}{k_2} v_x \left(e_\gamma + r_d + \frac{1}{k_2} e_s\right)
\end{aligned}
\tag{7.30}
$$

where f_i' are defined by:

$$
f_1' = \frac{k''}{k'} f_1 + f_4, \qquad f_2' = \frac{k''}{k'} f_2 + f_5, \qquad f_3' = \frac{k''}{k'} f_3 + f_6 \tag{7.31}
$$

To apply the backstepping procedure, consider the subsystem (7.30). Using the following vectors:

$$
\phi_\gamma = \begin{bmatrix} f_2' \cos(k_2 r_d) + f_3' \sin(k_2 r_d) \\ f_2' \sin(k_2 r_d) + f_3' \cos(k_2 r_d) \end{bmatrix}, \Delta_\gamma = \begin{bmatrix} \cos(e_s + \omega) \\ \sin(e_s + \omega) \end{bmatrix} \tag{7.32}
$$

the dynamic of e_γ in (7.30) turns into:

$$
e_\gamma = f_1' + \phi_\gamma^T \Delta_\gamma + \frac{k_1}{k_1} v_x \left(e_\gamma + r_d + \frac{1}{k_2} e_s\right) \tag{7.33}
$$

In the first step of the control design, e_s must be regarded as a fictitious input for (7.30) to steer γ to its respective reference signal. In other words, we seek for $e_s = \alpha(e_\gamma, r_d, t)$ that stabilizes the subsystem (7.30). The following choice:

$$
e_s' = \frac{k_2^2}{k_1 v_x} \left(\frac{k_1}{k_2} v_x e_\gamma + \frac{k_1}{k_2} v_x r_d + f_1' + \bar{k} e_\gamma + \kappa e_\gamma \|\phi_\gamma\|^2\right) \tag{7.34}
$$

achieves this goal. This can be seen by considering $V = \frac{1}{2} e_\gamma^2$ as a Lyapunov function candidate. Using (7.30), the time derivative of V along the solution of (7.29) and (7.30) becomes:

$$
\begin{aligned}
V &= e_\gamma \left(\phi_\gamma^T \Delta_\gamma \quad \bar{k} e_\gamma \quad \kappa e_\gamma \|\phi_\gamma\|^2\right) \\
&\leq \bar{k} e_\gamma^2 \quad \kappa e_\gamma^2 \|\phi_\gamma\|^2 + \|\phi_\gamma\| \|\Delta_\gamma\|_\infty |e_\gamma|
\end{aligned}
\tag{7.35}
$$

$$\leq \quad \bar{k}e_\gamma^2 + \frac{\|\Delta\|_\infty^2}{4\kappa}$$

which clearly demonstrates the ISS stability of the subsystem (7.30). By tuning κ , one can achieve the desired robust control performance for (7.30). In the next step of control design, e_s' acts as a reference signal for e_s and the actual controller must be designed in a way that ensures the convergence of e_s to e_s'.

This task can be simplified by defining the transformation $z = e_s \quad e_s'$. Employing the Lyapunov function:

$$V = \frac{1}{2}e_\gamma^2 + \frac{1}{2} \quad ^2 \tag{7.36}$$

for the complete system (7.29), (7.30) and computing its time derivative along the system trajectories results in:

$$V = e_\gamma \left(f_1' + \phi_\gamma^T \Delta_\gamma + \frac{k_1}{k_2} v_x \left(e_\gamma + r_d + \frac{1}{k_2} e_s' \right) \right) + z(e_s \quad e_s') \tag{7.37}$$

Using the definition of e_s:

$$V = \quad \bar{k}e_\gamma^2 + \frac{\|\Delta\|_\infty^2}{4\kappa} + z(e_s \quad e_s') + \frac{k_1}{k_2} v_x e_\gamma (e_s \quad e_s') \tag{7.38}$$

Next, by defining the following vectors:

$$\begin{gathered} \xi = e_s + k_2 r_d \\ \phi_s = \begin{bmatrix} f_2 \cos(\xi) + f_3 \sin(\xi) \\ f_2 \sin(\xi) + f_3 \cos(\xi) \end{bmatrix}, \Delta_s = \begin{bmatrix} \cos(\omega) \\ \sin(\omega) \end{bmatrix} \end{gathered} \tag{7.39}$$

and inserting the dynamic of e_s from (7.29) into (7.38):

$$\begin{gathered} V \leq \quad \bar{k}e_\gamma^2 + \frac{\|\Delta\|_\infty^2}{4\kappa} + \frac{k_1}{k_2} v_x e_\gamma z \\ + z \left(f_1 + \phi_s^T \Delta_s + k_1 v_x \left(e_\gamma + r_d + \frac{1}{k_2} e_s \right) + k' M \quad k_2 r_d \quad e_s' \right) \end{gathered} \tag{7.40}$$

The control action M might be designed to compensate for the effects of Δ_γ in (7.30) and assures the convergence of e_s to the virtual input of (7.29). To attain such objectives simultaneously, consider the following choice of control:

$$\begin{aligned} M = \quad & \frac{1}{k'}(f_1 \quad k_1 v_x \left(r_d + \frac{1}{k_2} e_s\right) \quad k_2 r_d \quad e_s' \\ & \kappa' z \|\phi_s\|^2 + \bar{\bar{k}} z \quad \left(\frac{k_1}{k_2} \quad k_1\right) v_x e_\gamma \,) \end{aligned} \tag{7.41}$$

Substituting (7.41) in (7.40), results in:

$$\begin{aligned} V \leq \quad & \bar{k} e_\gamma^2 + \frac{\|\Delta\|_\infty^2}{4\kappa} + z\left(\phi_s^T \Delta_s \quad \kappa' z \|\phi_s\|^2 \quad \bar{\bar{k}} z\right) \\ \leq \quad & \bar{k} e_\gamma^2 \quad \bar{\bar{k}} e_s^2 + \frac{\|\Delta\|_\infty^2}{4\kappa} + \frac{\|\Delta\|_\infty^2}{4\kappa'} \\ \leq \quad & 2\min\left(\bar{k}, \bar{\bar{k}}\right) V + \frac{\kappa + \kappa'}{4\kappa\kappa'} \|\Delta\|_\infty^2 \end{aligned} \tag{7.42}$$

Applying Gronwall lemma, ($X = [e_\gamma \quad z]^T$):

$$\|X\| \leq \sqrt{2}\|X(0)\| e^{-\min(\bar{k}, \bar{\bar{k}})t} + \sqrt{\frac{\kappa + \kappa'}{2\kappa\kappa' \min\left(\bar{k}, \bar{\bar{k}}\right)}} \|\Delta\|_\infty^2 \tag{7.43}$$

which proves the ISS stability of X. Although, the effects of Δ_γ and Δ_s are suppressed in different steps of the control scheme, the norm of the second term in (7.43) relies on both κ and κ' , and to reach the desired performance for e_s and e_γ , their minimum must be increased. However, the former does not imply the convergence of v and r to the neighborhood of the desired values.

On the other hand, one can find the $z \Rightarrow 0$ or $e_s \Rightarrow e_s'$ as κ and κ' tend to infinity. In order to calculate the upper-bound on e_s , one can use (7.43) to write:

$$|z| \leq \|X\|$$

$$|e_s| \leq \sqrt{2}\|X(0)\|e^{\min(\bar{k},\bar{\bar{k}})t} + \sqrt{\frac{\kappa+\kappa'}{2\kappa\kappa'\min(\bar{k},\bar{\bar{k}})}}\|\Delta\|_\infty^2$$

$$+\left|\frac{k_2^2}{k_1 v_x}\left(\frac{k_1}{k_2}v_x e_\gamma + \frac{k_1}{k_2}v_x r_d + f_1' + \bar{k}e_\gamma + \kappa e_\gamma\|\phi_\gamma\|^2\right)\right|$$

$$\leq (1+\alpha)\left(\sqrt{2}\|X(0)\|e^{\min(\bar{k},\bar{\bar{k}})t}\right) + \left|k_2 r_d + \frac{k_2^2}{k_1 v_x}f_1'\right|$$

$$+(1+\alpha)\left(\sqrt{\frac{\kappa+\kappa'}{2\kappa\kappa'\min(\bar{k},\bar{\bar{k}})}}\|\Delta\|_\infty^2\right) \tag{7.44}$$

$$\alpha = k_s + \frac{k_2^2\bar{k}}{k_1 v_x} + \frac{\kappa k_2^2\|\phi_\gamma\|^2}{k_1 v_x}$$

The first term in (7.44) vanishes in time and the last term can become small by choosing high values for κ and κ', however, the second term in (7.44) does not contain any control parameters and cannot be attenuated by the control law (7.41).

If one wishes to eliminate the effects of uncertainties on the final bound of the states i.e. e_γ and e_s, it is possible to start with the following fictitious non-smooth control law for the subsystem (7.29) in place of (7.34):

$$e_s' = \frac{k_2^2}{k_1 v_x}\left(\frac{k_1}{k_2}v_x(r_d + e_\gamma) + f_1' + \bar{k}e_\gamma + \Xi\right) \tag{7.45}$$

$$\Xi = \sum_{i=1}^{2}|\phi_{i\gamma}|\|\Delta_{i\gamma}\|sign(e_\gamma)$$

It can be shown that the effects of Δ_γ would be removed by (7.45). In the next step of the control design, M must be chosen in a way such that the time derivative of the Lyapunov function:

$$V = \frac{1}{2}\left(e_\gamma^2 + (e_s + e_s')^2\right) \tag{7.46}$$

becomes negative definite for $[e_\gamma \quad z]^T$.

Since e_s' contains a non-smooth term, the regular derivative of V can not be computed at $e_\gamma = 0$. However, if the input M can be chosen such that the $generalized\ derivative$ ([131]) of V becomes negative, which is sufficient for the stability of the $[e_\gamma \quad z]^T$ system. However, using a non-smooth Lyapunov function for the control design can result in unwanted chattering. This problem can also be addressed by using a *Flattened Robust Control Lyapunov function*. (see [44]).

7.4 Simulation

The proposed control techniques are evaluated using the vehicle model along with the LuGre model tire. The simulation condition is a standard ISO 3888-1 harsh double-lane-change maneuver ([116]). The vehicle and tire model parameters are given in Table 3-1 and

Table 7-1.

Table 7-1 Tire Specification

Variable	Value	Variable	Value	Variable	Value
κ_x	8.9031	κ_y	5.5645	$\sigma_{0,x,f}$	660
$\sigma_{0,x,r}$	640	$\sigma_{0,y,f}$	150	$\sigma_{0,y,r}$	160
$\sigma_{1,x}$	0.75	$\sigma_{1,y}$	0.75	$\sigma_{2,y}$	0.001
$\sigma_{2,x}$	0.006	v_s	7	$\mu_{c,x}$	0.975
$\mu_{c,y}$	0.975	$\mu_{s,y}$	1.9	$\mu_{s,x}$	1.454

Note that the LuGre tire parameters should be tuned according to the real vehicle tire data to capture both lateral and longitudinal tire characteristics. The lateral and longitudinal forces are calculated in the tire model and are used in the nonlinear vehicle model. To simulate the estimation errors, a random uncertainty is added to the tire model output and then this signal is used as the input for the controller. In other words, ($F_U = F + \Delta F$) where $0.5F \leq \Delta F \leq 0.5F$ (see Figure 7-7 and Figure 7-8). The driver is also modeled with a time varying delay to mimic human behavior. The sampling time is chosen to be $T = 10$ ms such that is appropriate for real-time implementation. The desired yaw-rate is calculated by (4.2).

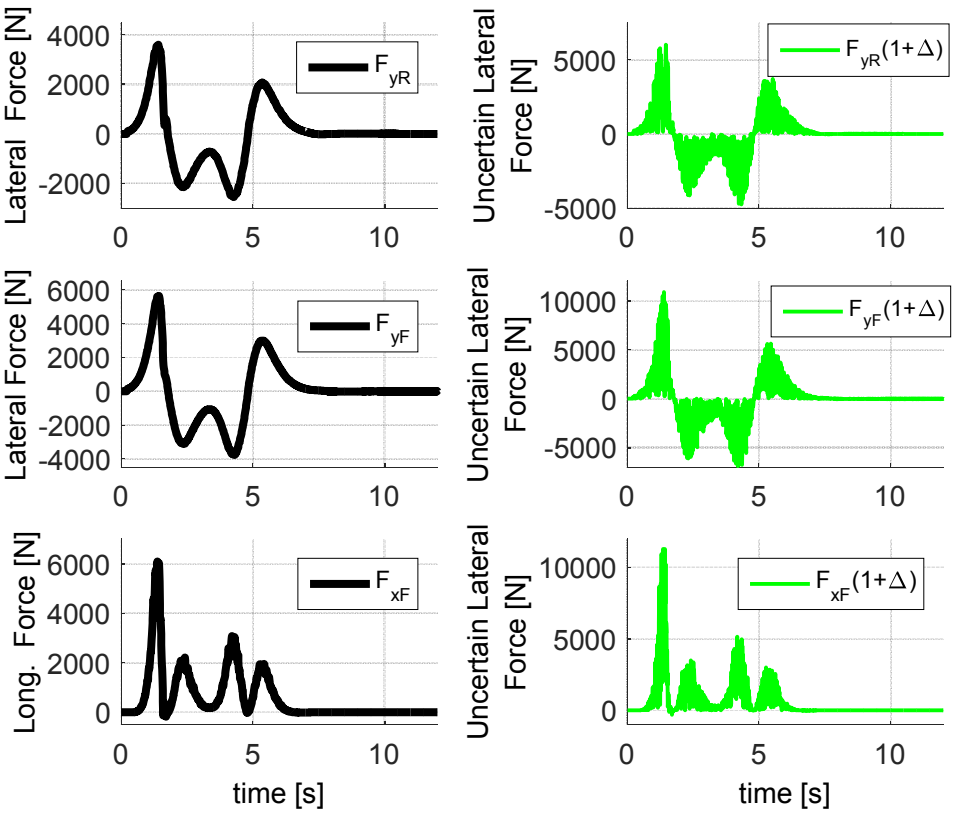

Figure 7-7: Tire forces and corresponding estimated forces (Normal Driving)

Note that in the simulation, an extreme level of uncertainty is assumed to show the effectiveness of the controller. In the left column of Figure 7-7 and Figure 7-8, the tire forces are shown for two maneuvers. It is assumed that there is no braking in the maneuver and the traction only produces positive longitudinal forces. In the right column, the uncertain signal based on $(1+\Delta)F, |\Delta| \leq 0.5$ is shown.

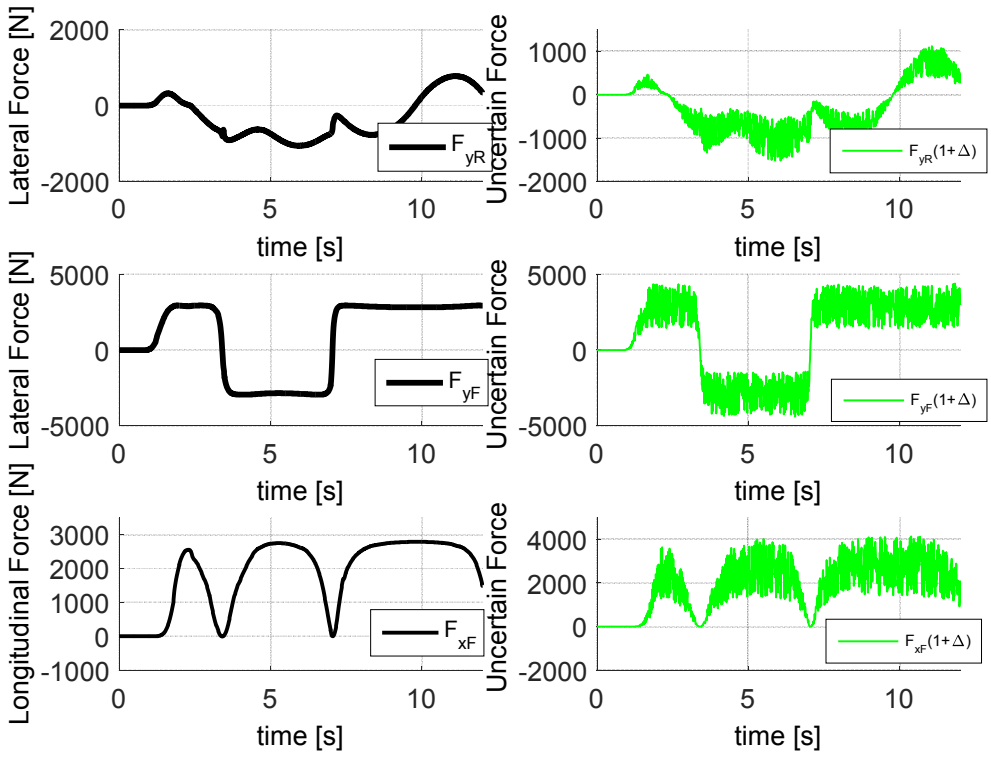

Figure 7-8: Tire forces and corresponding estimated forces. ($\boldsymbol{Saturated\ tire}\quad \boldsymbol{v_x = 120\ KpH, 400\ ms \leq \tau \leq 450ms, \mu = 0.2}$)

While the controller is off, the driver cannot pass the route at a high speed, on a slippery road and with a large driver delay (more than 300 ms) (see Figure 7-3). Turning on the controller enables the driver to do the double lane change in this condition. Figure 7-9 presents the lateral position of vehicle as well as the yaw rate tracking errors. The performance of both controller 1 (7.11) and controller 2 (7.21) are demonstrated and the lateral position of the vehicle is compared to the desired path of the driver in both cases. It is also shown that a very good yaw rate tracking is obtained in the both cases.

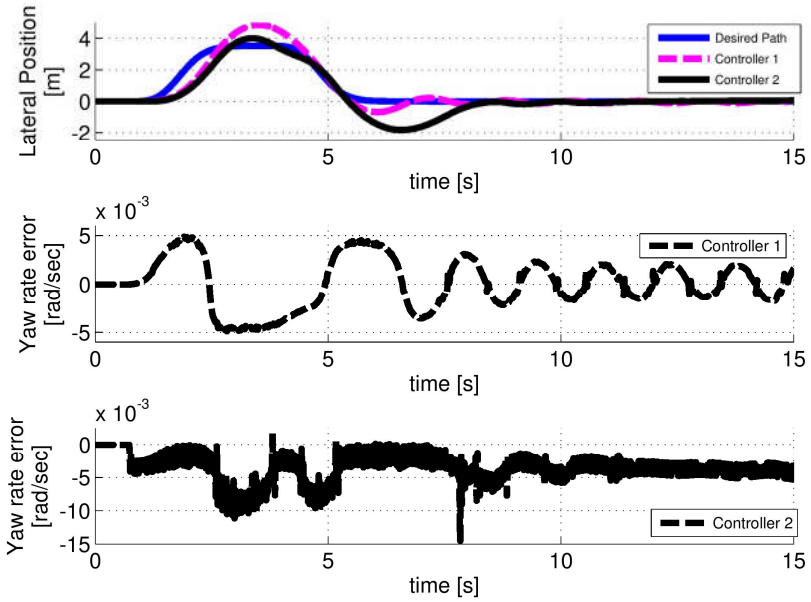

Figure 7-9: Controller Performance, $\boldsymbol{v_x = 120\ KpH, 300\ ms \leq \tau \leq 350ms, \mu = 0.7}$

Figure 7-10 also shows the control action of each of the proposed controllers. As mentioned in the control design section, the output of the controller 2 suffers from chattering and discontinuity.

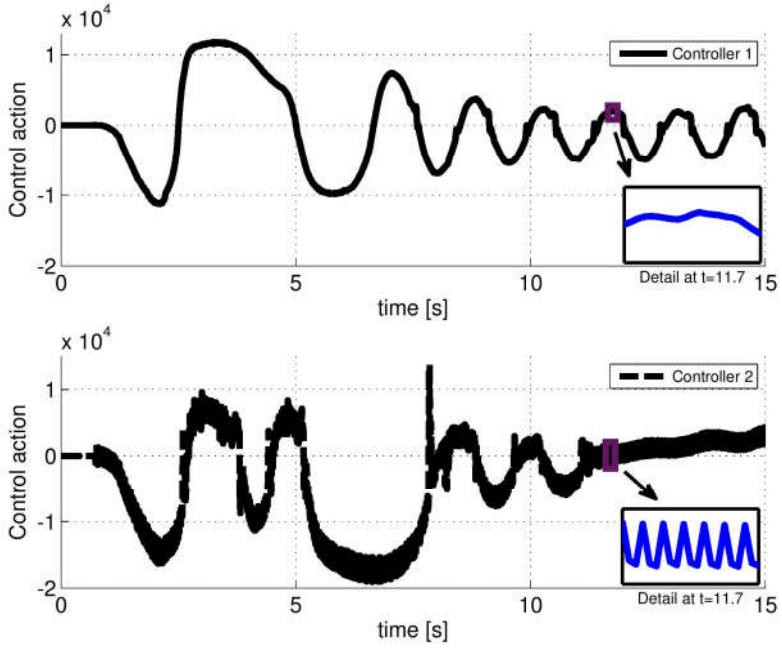

Figure 7-10 Control Action, $\boldsymbol{v_x = 120\ KpH, 300\ ms \leq \tau \leq 350ms, \mu = 0.7}$

It is assumed that the velocity is increased to $120\ Kp$ and the driver is a novice driver with a relatively large delay of $400\ ms \leq \tau \leq 450ms$, and the vehicle runs on an icy road ($\mu = 0.2$). In this scenario, the system without the controller loses stability and results in very poor performance. The yaw rate error and lateral velocity state of the vehicle in this situation are shown in Figure 7-11. With the controller, the vehicle still preserves stability to demonstrate the effectiveness of the proposed method.

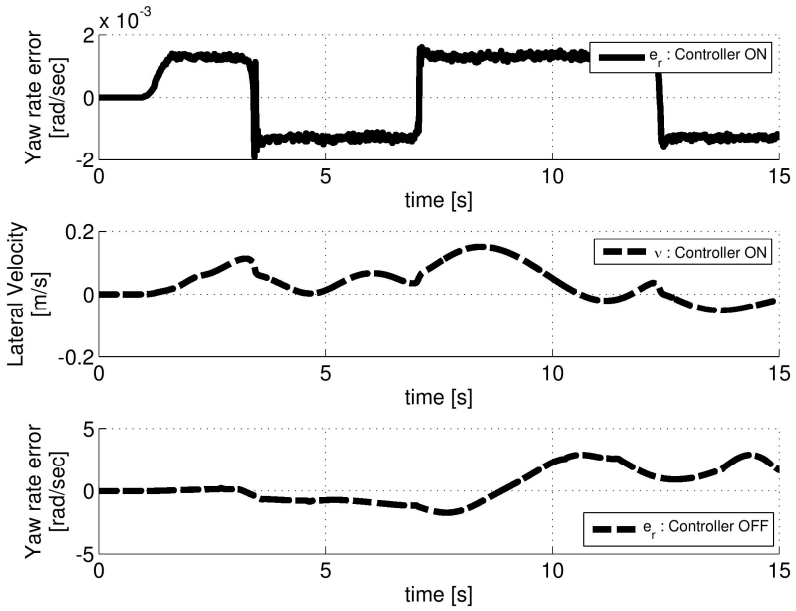

Figure 7-11: $\boldsymbol{v_x = 120\ KpH, 400\ ms \leq \tau \leq 450ms, \mu = 0.2}$

7.5 Summary

In this chapter, using a general form for the driver model, a robust control approach was adopted to design a vehicle controller considering nonlinear characteristics of a vehicle. It was shown that such nonlinearities could be potential sources of poor performance for a driver who would expect linear behavior from the system. Simulation results support the idea that designing a controller while considering the driver model improves overall performance of the system. The obtained stability criteria for different cases enhances the understanding of the effect of the human-in-the-loop in vehicle stability and performance. Future work needs to be done to specifically deal with the driver delay terms in real-time implementation.

Chapter 8
Conclusion and Future work

8.1 Conclusion

Human-in-the-loop analysis is a central issue in many engineering subfields. The main difficulty lies in modeling human behavior that is not trivial even for specific task related behaviors. The problem will be more difficult in driver-vehicle interaction since knowing the intention of a driver introduces another level of complexity to the problem. This fact makes the driver-in-the-loop analysis more complicated than many other human-machine interaction situations. In other words, even having the perfect model of a human driver (if possible) is not enough since it seems impossible (or extremely difficult) to predict the intention of a driver for control purposes.

Due to these difficulties, in the majority of research and studies on vehicle dynamics, the effect of the driver as a dynamic system is ignored. On the other hand, there are concrete results showing the existence of driver reaction delay and different driving skills and styles.

Roughly speaking, all driver models are functions of vehicle states and a future path planning of the driver. The main goal in this study was to avoid any assumptions on the accessibility to a driver's desires.

In the first step, it was shown that the driver's lag and driving style were extremely important in the vehicle stability analysis. The simulation results that used a general driver model expectedly show that the driver delay and level of skill has a direct effect on vehicle performance. Next, the driver model was augmented with the vehicle handling motion equations and a closed loop presentation of the system was obtained. Given that the controller can only use the current information about the road and vehicle state, the segment of the driver steering signal that is a function of future data, was modeled as a bounded uncertainty. This way, without adding extra sensors, some parts of the steering wheel angle signal (driver model), which is a function of the vehicle state, can be used in the decision making process to improve overall vehicle performance. The extracted information can be of help in casting new decision-making processes that partially consider the driver model in their analyses.

Observing that the state space representation is a retarded system with uncertainty, the Lyapunov Krasowski method is used to analyze the system and design an appropriate controller. The designed LTI H_∞ controller in Chapter 4 guarantees system stability in the presence of the unknown time-varying delay as well as modeling and process uncertainties. It is also emphasized that the method can be easily implemented with both torque-vectoring (differential-braking) and

an active steering actuator structure. The next stage was to relax the assumptions by considering a parameter-varying model for the driver. Combining a parameter varying vehicle and driver model, an LPV uncertain retarded delay was obtained. Knowing that the driver parameter varies in a certain range, an LPV controller was designed to guarantee vehicle stability while gain-scheduling based on driver model parameter variations and longitudinal vehicle speed was performed.

Knowing that to run an LPV controller, one needs to update the driver model parameter, the next step was to propose a technique to identify the driver parameter. To resolve inaccessibility of future road preview information, it was proposed using a moving window over the past data of the vehicle and driver. This method is only applicable in a normal driving condition and would fail when the lateral path following of the vehicle is not accurate; however, it does not require any future information.

The identification method was applied to a set of experimental data that was gathered at Mechatronics Vehicle Systems Lab at the University of Waterloo. The identified parameters were then clustered into a finite number of sets and the transition probability of switching between the sets was calculated. Having the transition probability, a Markov jump based model was developed for the regarded uncertain linear system and a theorem was proposed for stability analysis of the system.

Further analysis showed that having the switching probability between different modes of a driver, one can go one step farther and improve the behavior analysis of a LPV system. The proposed Markov jump analysis was applied to the closed loop system of an LPV controller and the driver-in-the-loop LPV model. The results demonstrated that having extra information about the switching probability of the driver mode would improve the estimation of disturbance attenuation level.

Finally, the effect of non-linear vehicle characteristics in driver performance was studied in the last chapter. Most of the novice drivers expect a linear (proportional) response from the vehicle in all conditions. More specifically, a novice driver does not have proper judgment about the longitudinal and the lateral tire force saturation phenomenon. It is shown in simulation that this is a reason for poor performance of the vehicle. Studying this effect needs nonlinear analysis tools and the last chapter is the extension of the driver-in-the-loop methodology to the case where the vehicle is in the nonlinear operation area. A thorough nonlinear analysis was performed and different nonlinear approaches were proposed to counteract the effect of nonlinearity and measurement uncertainty while the controller consider the effect of human

driver. All of the nonlinear analysis results show that the driver has a direct effect in the closed loop performance of the vehicle.

8.2 Driver Condition Monitoring

The driver identification method proposed in Chapter 6 can be employed as a driving condition monitoring system. Consider that the identification block has enough rich data-set to classify the gains in a finite number of modes for normal driving conditions. Assume that the driver's states change radically while the vehicle is still in a normal condition, i.e., the side slip angle and yaw rate are still in an acceptable range. These abrupt changes can be detected using the identification method which is detailed in Chapter 6.

8.3 Personalization of Driving Style

Another important application for the classification is personalization of driving styles of semi-autonomous vehicle.

There are many applications for using this classification. Currently, a few insurance companies started new plans called "usage-based" or "pay-as-you-drive", that includes the driving style in the insurance rate as well. Based on the proposed model, a small data collector can be mounted on the vehicles to collect data and evaluate the driving style of each individual driver.

The driving identification technique can also be revised for use in a "smart transmission shifter (gearbox)". This way, the gearbox controller can decide better based on identified driving style and the current status of the driver.

Imagine the case where there is more than one driver for a semi-autonomous vehicle or the driver's driving-style changes slightly from time to time. Using the identification method, the controller can cluster the driver parameter constantly and find the most often used driving style. Using this information, the semi-autonomous vehicle can take over the steering of the vehicle with minimum changes in vehicle traveling trend. The proposed technique can improve passenger comfort by making the drive feel as if the same driver still controls the vehicle. Also, the controller can detect that the driver has now changed, and based on the new driving style, it can change the gains such that the maximum likelihood is obtained.

More testing needs to be performed for different drivers and driving styles to validate the proposed model. The road geometry, the state of the ego vehicle, the relative distance, and the velocity of other vehicles and obstacles are important variables to consider when increasing model accuracy.

8.4 Actuator Limitations and Proposed Control System

The proposed controller design process assumes that the control actuators are ideal without any constraints. However, every actuator has its own capacity (amplitude saturation) which needs to be included in the control design. Unexpectedly large commands from the controller may force the system to operate in a mode that it is not designed for and this may cause irreparable harm. Thus, an analysis on the controller design with considerations to the actuator constraints seem to be vital. Besides that, all of the actuators have a delay in their response. Working on electric vehicles, all of the actuators are electric motors with a pretty small time constant; however, for conventional vehicles, performing torque vectoring or even differential braking will impose significant amount of delay, which affects the overall system performance. More precisely, the actuator dynamic should be considered in the design process to capture both time delay and the dynamic behavior of the actuators.

The new problem formulation of the LPV system could be revised to the following discrete-time retarded constrained uncertain system with a time-varying delay:

$$\sum_0 : \begin{array}{c} x(k+1) = A(\rho)x(k) + (A_d(\rho) + \Delta A_d)x\big(k \quad d(k)\big) + B_1(\rho)\omega(k) + B_2(\rho)u(k) \\ z(k) = C(\rho)x(k) \\ x(k) = 0, \quad d_2 \le k \le 0 \\ \|u(k)\| \le u_{max} \\ \|u(k+1) \quad u(k)\| \le u_{max} \end{array} \tag{8.1}$$

where $x(k) \in R^n$ is the state, $u(k) \in R^m$ is the control input vector, $\omega(k) \in R^q$ is the exogenous disturbance signal assumed to belong to $\ell_2[0,\infty)$. Furthermore, $z(k) \in R^p$ is the control output to be attenuated, and u_{max} denotes the maximum tolerable input control action. Matrices A, A_d, B_1, B_2, and C are assumed to be constant and with appropriate dimensions; $d(k)$ is a time-varying delay satisfying $0 < d_1 \le d(k) \le d_2$.

8.5 Control Authority Problem

The driver's steering angle depends on future road information (desired path), the vehicle states, and the driver's characteristics. In other words:

$$\delta = f(\text{desired path}, \text{curret vehicle states}, \text{driver charactristics}) \tag{8.2}$$

The future intention of the driver is not available to the control task. However, the current states are accessible. The driver's characteristics are also considered to be known with a bounded modeling uncertainty. It is common sense that a higher vehicle speed requires more attention from a driver. Reducing the vehicle speed, the car will be more stable and the effect of the driver's delay reduces. The problem arises when a vehicle is running at a high speed, and the driver has large amount of delay. In this case, the driver's steering angle makes the system unstable. An important reason for this inappropriate input command is the driver's delay. Consequently, the driver's panic makes everything worse. Figure 8-1 shows four different cases that happen in real driving conditions. The first case is a driver with small delay in observation and reaction driving at low speeds. In this case, a perfect driving condition is expected. Driving with low risk can result from either an expert driver (small delay) at low to high speeds, or a driver with large delay running a vehicle at low speeds. The last case is when a driver with a large delay drives a vehicle at high speeds. In this case, the vehicle stability is critical such that it cannot be addressed using only driver input.

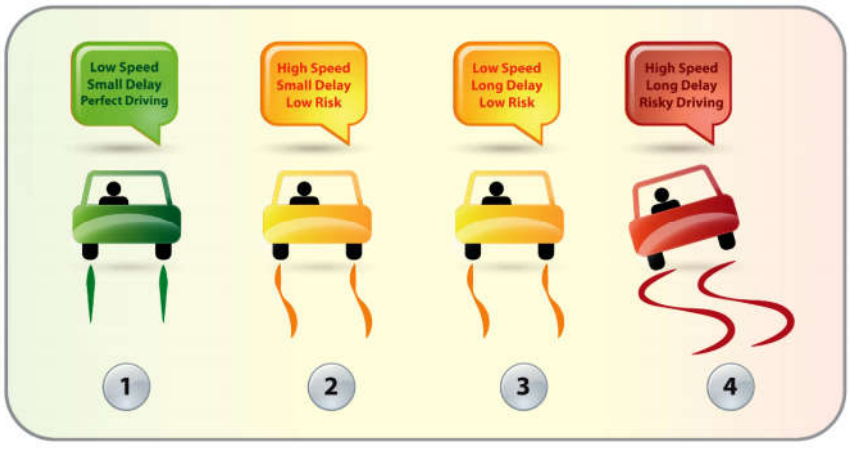

Figure 8-1 different driving conditions

Using the proposed controller, the effect of an unknown desired path on the vehicle steering can be attenuated with a certain coefficient or weight of γ. This coefficient represents the importance of the driver's decision. From this point of view, the coefficient of γ can be defined as a level of authority between the driver and the controller in the vehicle dynamic system. A bigger γ means a bigger the role for driver in vehicle control. Conversely, as γ decreases, the effect of the driver's decision will be reduced and the controller will have a bigger role in vehicle control.

Now, reconsider case 4 in Figure 8-1, where the vehicle is unstable because of the driver's oscillatory steering angle. In this case, lower values for coefficient of γ is more appropriate. Using lower γ, the vehicle is more robust in relation to the unknown information input. On the other hand, for the first case, higher values of γ are suitable for the vehicle control. The reason for this is the low vehicle speed and small driver delay. The following diagram could be used for the variation of γ versus vehicle speed.

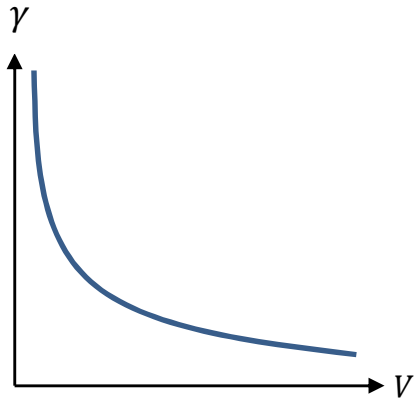

Figure 8-2: variation of γ versus velocity

Figure 8-2 shows that as the longitudinal velocity of vehicle decreases, the more authority needs to be given to the driver. For higher speeds, the vehicle controller should have a higher effect on vehicle control. It is obvious that using a small γ for a vehicle running at a low speed dramatically degrades vehicle performance. This is just a guideline for scheduling the controller gains based on the vehicle situation. The effect of the road friction coefficient is also another factor that can be studied.

Using the proposed controller, the effect of an unknown desired path on the vehicle steering can be attenuated with a certain coefficient or weight of γ. This coefficient represents the importance of the driver's decision. From this point of view, the coefficient of γ can be defined as a level of authority between the driver and the controller in the vehicle dynamic system. A bigger γ means a bigger the role for driver in vehicle control. Conversely, as γ decreases, the effect of the driver's decision will be reduced and the controller will have a bigger role in vehicle control.

Now, reconsider case 4 in Figure 8-1, where the vehicle is unstable because of the driver's oscillatory steering angle. In this case, lower values for coefficient of γ is more appropriate. Using lower γ, the vehicle is more robust in relation to the unknown information input. On the other hand, for the first case, higher values of γ are suitable for the vehicle control. The reason for this is the low vehicle speed and small driver delay. The following diagram could be used for the variation of γ versus vehicle speed.

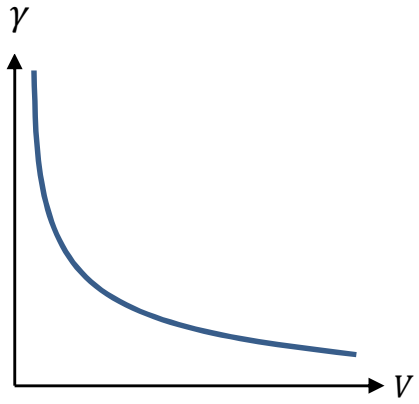

Figure 8-2: variation of γ versus velocity

Figure 8-2 shows that as the longitudinal velocity of vehicle decreases, the more authority needs to be given to the driver. For higher speeds, the vehicle controller should have a higher effect on vehicle control. It is obvious that using a small γ for a vehicle running at a low speed dramatically degrades vehicle performance. This is just a guideline for scheduling the controller gains based on the vehicle situation. The effect of the road friction coefficient is also another factor that can be studied.

Bibliography

[1] *Modelling driver behaviour in automotive environments critical issues in driver interactions with intelligent transport systems*: London : Springer, c2007, 2007.

[2] M. Abe, *Vehicle handling dynamics: theory and application*: Butterworth-Heinemann, 2009.

[3] B. Açıkmese, "Application of Lexicographic Goal Programming with Convex Optimization in Control Systems," in *AIAA Guidance, Navigation and Control Conference*, 2013.

[4] J. Ackermann, "Robust control prevents car skidding," *Control Systems, IEEE,* vol. 17, pp. 23-31, 1997.

[5] J. Ackermann, T. Bünte, and D. Odenthal, *Advantages Of Active Steering For Vehicle Dynamics Control*, 1999.

[6] M. Alirezaei, M. Corno, D. Katzourakis, A. Ghaffari, and R. Kazemi, "A Robust Steering Assistance System for Road Departure Avoidance," *Vehicular Technology, IEEE Transactions on,* vol. 61, pp. 1953-1960, 2012.

[7] S. J. Anderson, S. C. Peters, T. E. Pilutti, and K. Iagnemma, "An optimal-control-based framework for trajectory planning, threat assessment, and semi-autonomous control of passenger vehicles in hazard avoidance scenarios," *International Journal of Vehicle Autonomous Systems,* vol. 8, pp. 190-216, 2010.

[8] A. Apel and M. Mitschke, "Adjusting vehicle characteristics by means of driver models," *International journal of vehicle design,* 1997.

[9] P. Apkarian and R. J. Adams, "Advanced gain-scheduling techniques for uncertain systems," *Control Systems Technology, IEEE Transactions on,* vol. 6, pp. 21-32, 1998.

[10] P. Apkarian, J.-M. Biannic, and P. Gahinet, "Self-scheduled H-infinity control of missile via linear matrix inequalities," *Journal of Guidance, Control, and Dynamics,* vol. 18, pp. 532-538, 1995.

[11] P. Apkarian and H. D. Tuan, "Parameterized LMIs in control theory," *SIAM Journal on Control and Optimization,* vol. 38, pp. 1241-1264, 2000.

[12] N. Bekiaris-Liberis and M. Krstic, *Nonlinear control under nonconstant delays* vol. 25: SIAM, 2013.

[13] L. Besnard, Y. B. Shtessel, and B. Landrum, "Quadrotor vehicle control via sliding mode controller driven by sliding mode disturbance observer," *Journal of the Franklin Institute,* vol. 349, pp. 658-684, 2012.

[14] T. Besselmann, J. Lofberg, and M. Morari, "Explicit MPC for LPV Systems: Stability and Optimality," *Automatic Control, IEEE Transactions on,* vol. 57, pp. 2322-2332, 2012.

[15] S. Bhattacharyya, H. Chapellat, and L. Keel, "Robust control: the parametric approach," *Upper Saddle River*, 1995.
[16] W. Blair Jr and D. Sworder, "Feedback control of a class of linear discrete systems with jump parameters and quadratic cost criteria†," *International Journal of Control,* vol. 21, pp. 833-841, 1975.
[17] C. G. Bobier, "A Phase Portrait Approach to Vehicle Stabilization and Envelope Control," Stanford University, 2012.
[18] C. G. Bobier and J. C. Gerdes, "Sliding surface vehicle envelope control: A cooperative design between controller and envelope," in *American Control Conference (ACC), 2012*, 2012, pp. 6521-6526.
[19] E. Boukas, Z. Liu, and G. Liu, "Delay-dependent robust stability and H8 control of jump linear systems," *International Journal of Control,* vol. 74, pp. 329-340, 2001.
[20] S. P. Boyd and L. Vandenberghe, *Convex optimization*: Cambridge university press, 2004.
[21] C. Briat, *Linear parameter-varying and time-delay systems*: Springer, 2014.
[22] A. Carvalho, Y. Gao, S. Lefevre, and F. Borrelli, "Stochastic predictive control of autonomous vehicles in uncertain environments," in *12th International Symposium on Advanced Vehicle Control*, 2014.
[23] A. Carvalho, S. Lefévre, G. Schildbach, J. Kong, and F. Borrelli, "Automated driving: The role of forecasts and uncertainty—A control perspective," *European Journal of Control,* vol. 24, pp. 14-32, 7// 2015.
[24] L.-K. Chen and B.-J. Shieh, "Coordination of the authority between the vehicle driver and a steering assist controller," *WSEAS Transactions on Systems and Control,* vol. 3, pp. 353-364, 2008.
[25] L.-K. Chen and A. G. Ulsoy, "Design of a vehicle steering assist controller using driver model uncertainty," *International journal of vehicle autonomous systems,* vol. 1, pp. 111-132, 2002.
[26] L. K. Chen and A. G. Ulsoy, "Identification of a driver steering model, and model uncertainty, from driving simulator data," 2002, pp. 589-596.
[27] L. K. a. H. Chen, D.J., "Adaptive control with respect to driver model uncertainty," in *Proceedings of the International Symposium on Advanced Vehicle Control (AVEC)*. 2006.
[28] Y. Chen, W. Chen, X. Wei, and F. Zhao, "Linear quadratic Gaussian optimal control strategy for four-wheel steering vehicle," in *Proceedings of the FISITA 2012 World Automotive Congress*, 2013, pp. 641-650.
[29] E. Coelingh, L. Jakobsson, H. Lind, and M. Lindman, "Collision warning with auto brake: a real-life safety perspective," *Innovations for Safety: Opportunities and Challenges,* 2007.
[30] O. L. V. Costa, M. D. Fragoso, and R. P. Marques, *Discrete-time Markov jump linear systems*: Springer Science & Business Media, 2006.

[31] D. P. de Farias, J. C. Geromel, J. B. do Val, and O. L. V. Costa, "Output feedback control of Markov jump linear systems in continuous-time," *IEEE Transactions on Automatic Control,* vol. 45, pp. 944-949, 2000.

[32] C. C. De Wit, H. Olsson, K. J. Astrom, and P. Lischinsky, "A new model for control of systems with friction," *Automatic Control, IEEE Transactions on,* vol. 40, pp. 419-425, 1995.

[33] S. Di Cairano, D. Bernardini, A. Bemporad, and I. V. Kolmanovsky, "Stochastic MPC with learning for driver-predictive vehicle control and its application to HEV energy management," *Control Systems Technology, IEEE Transactions on,* vol. 22, pp. 1018-1031, 2014.

[34] M. T. Do, Z. Man, C. Zhang, H. Wang, and F. S. Tay, "Robust sliding mode-based learning control for steer-by-wire systems in modern vehicles," *Vehicular Technology, IEEE Transactions on,* vol. 63, pp. 580-590, 2014.

[35] O. L. do Valle Costa, M. D. Fragoso, and M. G. Todorov, *Continuous-time Markov jump linear systems*: Springer Science & Business Media, 2012.

[36] L. El Ghaoui and M. Ait Rami, "Robust state-feedback stabilization of jump linear systems via LMIs," *International Journal of Robust and Nonlinear Control,* vol. 6, pp. 1015-1022, 1996.

[37] L. El Ghaoui, F. Oustry, and M. AitRami, "A cone complementarity linearization algorithm for static output-feedback and related problems," *Automatic Control, IEEE Transactions on,* vol. 42, pp. 1171-1176, 1997.

[38] D. K. Faddeev and V. N. Faddeeva, "Computational methods of linear algebra," *Zapiski Nauchnykh Seminarov POMI,* vol. 54, pp. 3-228, 1975.

[39] P. Falcone, H. Eric Tseng, F. Borrelli, J. Asgari, and D. Hrovat, "MPC-based yaw and lateral stabilisation via active front steering and braking," *Vehicle System Dynamics,* vol. 46, pp. 611-628, 2008/09/01 2008.

[40] X. Feng, K. Loparo, Y. Ji, and H. J. Chizeck, "Stochastic stability properties of jump linear systems," *Automatic Control, IEEE Transactions on,* vol. 37, pp. 38-53, 1992.

[41] S. A. Ferguson, "The effectiveness of electronic stability control in reducing real-world crashes: a literature review," *Traffic Inj Prev,* vol. 8, pp. 329-38, Dec 2007.

[42] D. Filev, J. Lu, K. Prakah-Asante, and F. Tseng, "Real-time driving behavior identification based on driver-in-the-loop vehicle dynamics and control," in *Systems, Man and Cybernetics, 2009. SMC 2009. IEEE International Conference on*, 2009, pp. 2020-2025.

[43] B. A. Francis and J. C. Doyle, "Linear Control Theory with an \bfH_∞ Optimality Criterion," *SIAM Journal on Control and Optimization,* vol. 25, pp. 815-844, 1987.

[44] R. A. Freeman and P. V. Kokotovic, *Robust nonlinear control design: state-space and Lyapunov techniques*: Springer Science & Business Media, 2008.

[45] R. Frezza, A. Saccon, and D. Bacchet, "SmartDriver: a sensor based model of a car driver for virtual product development," in *Advanced Intelligent Mechatronics, 2003. AIM 2003. Proceedings. 2003 IEEE/ASME International Conference on*, 2003, pp. 366-370 vol.1.

[46] T. Fujioka, Y. Shirano, and A. Matsushita, "Driver's behavior under steering assist control system," in *Intelligent Transportation Systems, 1999. Proceedings. 1999 IEEE/IEEJ/JSAI International Conference on*, 1999, pp. 246-251.

[47] P. Gahinet and P. Apkarian, "A linear matrix inequality approach to H∞ control," *International journal of robust and nonlinear control,* vol. 4, pp. 421-448, 1994.

[48] P. Gaspar and J. Bokor, "Design of an LPV-Based Integrated Control for Driver Assistance Systems," in *Robust Control Design*, 2012, pp. 511-516.

[49] P. Gaspar, I. Szaszi, and J. Bokor, "Design of robust controllers for active vehicle suspension using the mixed μ synthesis," *Vehicle System Dynamics,* vol. 40, pp. 193-228, 2003.

[50] J. C. Geromel and P. Colaneri, "Stability and stabilization of continuous-time switched linear systems," *SIAM Journal on Control and Optimization,* vol. 45, pp. 1915-1930, 2006.

[51] J. C. Geromel, A. P. Gonçalves, and A. R. Fioravanti, "Dynamic output feedback control of discrete-time Markov jump linear systems through linear matrix inequalities," *SIAM Journal on Control and Optimization,* vol. 48, pp. 573-593, 2009.

[52] S. Glaser, B. Vanholme, S. Mammar, D. Gruyer, and L. Nouveliere, "Maneuver-Based Trajectory Planning for Highly Autonomous Vehicles on Real Road With Traffic and Driver Interaction," *Intelligent Transportation Systems, IEEE Transactions on,* vol. 11, pp. 589-606, 2010.

[53] G. C. Goodwin, S. F. Graebe, and M. E. Salgado, *Control system design* vol. 240: Prentice Hall New Jersey, 2001.

[54] B. A. Guvenc, T. Bunte, D. Odenthal, and L. Guvenc, "Robust two degree-of-freedom vehicle steering controller design," *Control Systems Technology, IEEE Transactions on,* vol. 12, pp. 627-636, 2004.

[55] B. A. Guvenc, B. A. Güvenç, and S. Karaman, "Robust yaw stability controller design and hardware-in-the-loop testing for a road vehicle," *Vehicular Technology, IEEE Transactions on,* vol. 58, pp. 555-571, 2009.

[56] J. K. Hale and S. M. Verduyn Lunel, *Introduction to Functional Differential Equations* vol. 99. New York: Springer- Verlage 1993.

[57] C. Hatipoglu, H. Ozbay, U. Ozguner, and T. B. Sahin, "H∞ controller design for automatic steering of vehicles with modeled time delays," 1997, pp. 260-265.

[58] A. Hazell, "Discrete-time optimal preview control," 2008.

[59] Y. He, M. Wu, Q.-L. Han, and J.-H. She, "Delay-dependent H ∞ control of linear discrete-time systems with an interval-like time-varying delay," *International Journal of Systems Science,* vol. 39, pp. 427-436, 2008/04/01 2008.

[60] R. G. Hebden, C. Edwards, and S. K. Spurgeon, "Automotive Steering Control in a Split-μ Manoeuvre Using an Observer-Based Sliding Mode Controller," *Vehicle System Dynamics,* vol. 41, pp. 181-202, 2004/01/01 2004.

[61] D. Hendricks, M. Freedman, P. Zador, and J. Fell, "The relative frequency of unsafe driving acts in serious traffic crashes. Report for Contract No," DTNH22-94-C-05020, National Highway Traffic Safety Administration, US Department of Transportation2001.

[62] L. V. Hien and H. Trinh, "Refined Jensen-based inequality approach to stability analysis of time-delay systems," *IET Control Theory & Applications,* vol. 9, pp. 2188-2194, 2015.
[63] R. Hindiyeh, "Dynamics and control of drifting in automobiles," Ph. D. thesis), Stanford University, 2013.
[64] J.-M. Hoc, "From human–machine interaction to human–machine cooperation," *Ergonomics,* vol. 43, pp. 833-843, 2000.
[65] H. Imine and T. Madani, "Sliding-mode control for automated lane guidance of heavy vehicle," *International Journal of Robust and Nonlinear Control,* vol. 23, pp. 67-76, 2013.
[66] T. Inagaki, "Smart collaboration between humans and machines based on mutual understanding," *Annual reviews in control,* vol. 32, pp. 253-261, 2008.
[67] T. Inagaki, H. Furukawa, and M. Itoh, "Human interaction with adaptive automation: Strategies for trading of control under possibility of over-trust and complacency," *Proc. HCI-AugCog International, CD-ROM,* vol. 10, 2005.
[68] M. Irmscher, T. Jürgensohn, and Willumeit, "Driver models in vehicle development," *Vehicle System Dynamics Supplement,* vol. 33, pp. 83-93, 1999.
[69] V. Ivanov, D. Savitski, and B. Shyrokau, "A Survey of Traction Control and Anti-lock Braking Systems of Full Electric Vehicles with Individually-Controlled Electric Motors," 2014.
[70] Y. Ji and H. J. Chizeck, "Jump linear quadratic Gaussian control in continuous time," *Automatic Control, IEEE Transactions on,* vol. 37, pp. 1884-1892, 1992.
[71] P. Jong Hyeon and A. Woo Sung, "H_∞ yaw-moment control with brakes for improving driving performance and stability," in *Advanced Intelligent Mechatronics, 1999. Proceedings. 1999 IEEE/ASME International Conference on*, 1999, pp. 747-752.
[72] I. Kageyama and H. B. Pacejka, "ON A NEW DRIVER MODEL WITH FUZZY CONTROL," *Vehicle System Dynamics,* vol. 20, pp. 314-324, 1992/01/01 1992.
[73] E. P. Kao, *An introduction to stochastic processes*: Cengage Learning, 1997.
[74] J. Kasselmann and T. Keranen, "Adaptive steering," *Bendix Technical Journal,* vol. 2, 1969.
[75] S. D. Keen and D. J. Cole, "Application of time-variant predictive control to modelling driver steering skill," *Vehicle System Dynamics,* vol. 49, pp. 527-559, 2011/04/01 2010.
[76] A. Khajepour, M. S. Fallah, and A. Goodarzi, *Electric and Hybrid Vehicles: Technologies, Modeling and Control-A Mechatronic Approach*: John Wiley & Sons, 2014.
[77] S. Khosravani, I. Fadakar, A. Khajepour, B. Fidan, B. Litkouhi, and S. K. Chen, "Nonlinear Robust Control of Vehicle Lateral Dynamics Considering Driver's Dynamics," in *ASME 2014 International Mechanical Engineering Congress and Exposition*, 2014, pp. V012T15A019-V012T15A019.
[78] S. Khosravani, A. Kasaiezadeh, A. Khajepour, B. Fidan, S.-K. Chen, and B. Litkouhi, "Torque-Vectoring-Based Vehicle Control Robust to Driver Uncertainties," *Vehicular Technology, IEEE Transactions on,* vol. 64, pp. 3359-3367, 2015.

[79] M. Kristic, I. Kanellakopoulis, P. V. Kokotovic, and D. Mayne, "Nonlinear and Adaptive Control Design," *IEEE transactions on automatic control,* vol. 41, pp. 1849-1852, 1996.
[80] K. Kritayakirana and J. C. Gerdes, "Autonomous Cornering at the Limits: Maximizing a" gG" Diagram by Using Feedforward Trail-Braking and Throttle-On-Exit," in *Advances in Automotive Control*, 2010, pp. 548-553.
[81] K. Kritayakirana and J. C. Gerdes, "Autonomous vehicle control at the limits of handling," *International Journal of Vehicle Autonomous Systems,* vol. 10, pp. 271-296, 2012.
[82] H. Kuzuya and S. Shin, "Development of robust motor servo control for rear steering actuator based on two-degree-of-freedom control system," *Mechatronics,* vol. 10, pp. 53-66, 2000.
[83] M. Land and J. Horwood, "Which parts of the road guide steering?," *Nature,* vol. 377, pp. 339-340, 09/28/print 1995.
[84] S. Lefèvre, A. Carvalho, and F. Borrelli, "A Learning-Based Framework for Velocity Control in Autonomous Driving."
[85] S. Lefèvre, A. Carvalho, Y. Gao, H. E. Tseng, and F. Borrelli, "Driver models for personalised driving assistance," *Vehicle System Dynamics,* vol. 53, pp. 1705-1720, 2015.
[86] L. Li, W. Ding, Z. Nan-Ning, and S. Lin-Cheng, "Cognitive Cars: A New Frontier for ADAS Research," *Intelligent Transportation Systems, IEEE Transactions on,* vol. 13, pp. 395-407, 2012.
[87] A. Lie, C. Tingvall, M. Krafft, and A. Kullgren, "The effectiveness of ESP (Electronic Stability Program) in reducing real life accidents," *Traffic Inj Prev,* vol. 5, pp. 37-41, Mar 2004.
[88] L. Lifu and W. Zhan, "Study on torque vectoring differential for vehicle stability control via hardware-in-loop simulation," in *Communication Software and Networks (ICCSN), 2011 IEEE 3rd International Conference on*, 2011, pp. 289-293.
[89] C.-F. Lin, A. G. Ulsoy, and D. J. LeBlanc, "Vehicle dynamics and external disturbance estimation for vehicle path prediction," *Control Systems Technology, IEEE Transactions on,* vol. 8, pp. 508-518, 2000.
[90] T. Lin, E. Tseng, and F. Borrelli, "Modeling driver behavior during complex maneuvers," in *American Control Conference (ACC), 2013*, 2013, pp. 6448-6453.
[91] A. Liu and A. Pentland, "Towards real-time recognition of driver intentions," in *Intelligent Transportation System, 1997. ITSC'97., IEEE Conference on*, 1997, pp. 236-241.
[92] A. M. Liu, "Modeling Differences in Behavior Within and Between Drivers," in *Human Modelling in Assisted Transportation*, ed: Springer, 2011, pp. 15-22.
[93] Z. Liu, G. Payre, and P. Bourassa, "Stability and oscillations in a time-delayed vehicle system with driver control," *Nonlinear Dynamics,* vol. 35, pp. 159-173, 2004.
[94] J. Lofberg, "YALMIP : a toolbox for modeling and optimization in MATLAB," in *Computer Aided Control Systems Design, 2004 IEEE International Symposium on*, 2004, pp. 284-289.
[95] C. C. MacAdam, "Application of an optimal preview control for simulation of closed-loop automobile driving," 1981.

[96] C. C. MacAdam, "Application of an optimal preview control for simulation of closed-loop automobile driving," *Systems, Man and Cybernetics, IEEE Transactions on,* vol. 11, pp. 393-399, 1981.
[97] C. C. Macadam, "Understanding and Modeling the Human Driver," *Vehicle System Dynamics,* vol. 40, pp. 101-134, 2003/08/01 2003.
[98] S. Mammar, "Two-Degree-of-Freedom H8 Optimization and Scheduling for Robust Vehicle Lateral Control," *Vehicle System Dynamics,* vol. 34, pp. 401-422, 2000/12/01 2000.
[99] S. Mammar and D. Koenig, "Vehicle handling improvement by active steering," *Vehicle system dynamics,* vol. 38, pp. 211-242, 2002.
[100] D. T. McRuer and E. S. Krendel, "The human operator as a servo system element," *Journal of the Franklin Institute,* vol. 267, pp. 381-403, 5// 1959.
[101] D. T. McRuer and E. S. Krendel, *Mathematical models of human pilot behavior*. Neuilly sur Seine: North Atlantic Treaty Organization, Advisory Group for Aerospace Research and Development, 1974.
[102] N. Mehrabi, R. Sharif Razavian, and J. McPhee, "Steering disturbance rejection using a physics-based neuromusculoskeletal driver model," *Vehicle System Dynamics,* vol. 53, pp. 1393-1415, 2015.
[103] W. Michiels and S.-I. Niculescu, *Stability, Control, and Computation for Time-Delay Systems: An Eigenvalue-Based Approach* vol. 27: Siam, 2014.
[104] A. Mihaly and P. Gaspar, "Identification of a linear driver model based on simulator experiments," in *Applied Computational Intelligence and Informatics (SACI), 2014 IEEE 9th International Symposium on*, 2014, pp. 13-18.
[105] R. Montanari, G. Wenzel, S. Mattes, F. Kuhn, F. BELLOTTI, and D. Morreale, "COMUNICAR: Integrated on-vehicle human machine interface designed to avoid driver information overload," in *9th World Congress on Intelligent Transport Systems*, 2002.
[106] C. F. Morais, M. F. Braga, R. C. Oliveira, and P. L. Peres, " 2 control of discrete-time Markov jump linear systems with uncertain transition probability matrix: improved linear matrix inequality relaxations and multi-simplex modelling," *IET Control Theory & Applications,* vol. 7, pp. 1665-1674, 2013.
[107] C. F. Morais, M. F. Braga, R. C. Oliveira, and P. L. Peres, " ∞ state feedback control for MJLS with uncertain probabilities," *Automatica,* vol. 52, pp. 317-321, 2015.
[108] MOSEK, "Modeling Manual, MOSEK ApS,," *Available online from: http://www.mosek.com/resources/doc,* 2013.
[109] M. Mulder, M. Mulder, M. Van Paassen, and D. Abbink, "Haptic gas pedal feedback," *Ergonomics,* vol. 51, pp. 1710-1720, 2008.
[110] X. Na and D. J. Cole, "Linear quadratic game and non-cooperative predictive methods for potential application to modelling driver–AFS interactive steering control," *Vehicle System Dynamics,* vol. 51, pp. 165-198, 2013/02/01 2012.

[111] X. Na and D. J. Cole, "Modelling and Identification of a Driver Controlling a Vehicle Equipped with Active Steering, where the Driver and Vehicle Have Different Target Paths."
[112] D. S. Naidu, *Optimal control systems*: CRC Press, 2003.
[113] B. NÉMETH, "Integrated Control Design of Vehicle Stability Systems based on LPV Methods."
[114] H. Okuda, N. Ikami, T. Suzuki, Y. Tazaki, and K. Takeda, "Modeling and analysis of driving behavior based on a probability-weighted ARX model," *Intelligent Transportation Systems, IEEE Transactions on,* vol. 14, pp. 98-112, 2013.
[115] R. Parasuraman, T. B. Sheridan, and C. D. Wickens, "A model for types and levels of human interaction with automation," *Systems, Man and Cybernetics, Part A: Systems and Humans, IEEE Transactions on,* vol. 30, pp. 286-297, 2000.
[116] Y. Peng and X. Yang, "Comparison of various double-lane change manoeuvre specifications," *Vehicle System Dynamics,* vol. 50, pp. 1157-1171, 2012.
[117] A. Pentland and A. Liu, "Toward augmented control systems," in *IEEE Intelligent Vehicles*, 1995, pp. 350-355.
[118] A. J. Pick and D. J. Cole, "A mathematical model of driver steering control including neuromuscular dynamics," *Journal of Dynamic Systems, Measurement and Control, Transactions of the ASME,* vol. 130, // 2008.
[119] A. J. Pick and D. J. Cole, "A Mathematical Model of Driver Steering Control Including Neuromuscular Dynamics," *Journal of Dynamic Systems, Measurement, and Control,* vol. 130, pp. 031004-1-9, May 2008.
[120] M. Plöchl and J. Edelmann, "Driver models in automobile dynamics application," *Vehicle System Dynamics,* vol. 45, pp. 699-741, 2007.
[121] A. Puggelli, "Formal Techniques for the Verification and Optimal Control of Probabilistic Systems in the Presence of Modeling Uncertainties," 2014.
[122] T. Qu, H. Chen, D. Cao, H. Guo, and B. Gao, "Switching-Based Stochastic Model Predictive Control Approach for Modeling Driver Steering Skill," *Intelligent Transportation Systems, IEEE Transactions on,* vol. 16, pp. 365-375, 2015.
[123] P. Raksincharoensak, T. Mizushima, and M. Nagai, "Direct yaw moment control system based on driver behaviour recognition," *Vehicle System Dynamics,* vol. 46, pp. 911-921, 2008/09/01 2008.
[124] R. Roy, P. Micheau, and P. Bourassa, "Intermittent predictive steering control as an automobile driver model," *Journal of Dynamic Systems, Measurement and Control, Transactions of the ASME,* vol. 131, pp. 1-6, 2009.
[125] L. Saleh, P. Chevrel, and J.-F. Lafay, "Optimal Control with Preview for Lateral Steering of a Passenger Car: Design and Test on a Driving Simulator," in *Time Delay Systems: Methods, Applications and New Trends*. vol. 423, R. Sipahi, T. Vyhlídal, S.-I. Niculescu, and P. Pepe, Eds., ed: Springer Berlin Heidelberg, 2012, pp. 173-185.

[126] L. Saleh, P. Chevrel, F. Mars, J.-F. Lafay, and F. Claveau, "Human-like cybernetic driver model for lane keeping," in *Proceedings of the 18th World Congress of the International Federation of Automatic Control*, 2011, pp. 4368-4373.

[127] J. S. Shamma, "An overview of LPV systems," in *Control of linear parameter varying systems with applications*, ed: Springer, 2012, pp. 3-26.

[128] R. S. Sharp, "Driver steering control and a new perspective on car handling qualities," *Proceedings of the Institution of Mechanical Engineers, Part C: Journal of Mechanical Engineering Science,* vol. 219, pp. 1041-1051, 2005.

[129] R. S. a. V. Sharp, V., "Optimal preview car steering control," *Supplements to Vehicle System Dynamics,* vol. 35, pp. 101-117, 2001.

[130] T. B. Sheridan, *Humans and automation: System design and research issues*: John Wiley & Sons, Inc., 2002.

[131] D. Shevitz and B. Paden, "Lyapunov stability theory of nonsmooth systems," *IEEE Transactions on automatic control,* vol. 39, pp. 1910-1914, 1994.

[132] V. Shia, Y. Gao, R. Vasudevan, K. D. Campbell, T. Lin, F. Borrelli*, et al.*, "Semiautonomous vehicular control using driver modeling," *Intelligent Transportation Systems, IEEE Transactions on,* vol. 15, pp. 2696-2709, 2014.

[133] V. A. Shia, Y. Gao, R. Vasudevan, K. D. Campbell, T. Lin, F. Borrelli*, et al.*, "Semiautonomous vehicular control using driver modeling," *Intelligent Transportation Systems, IEEE Transactions on,* vol. 15, pp. 2696-2709, 2014.

[134] E. Shustin and E. Fridman, "On delay-derivative-dependent stability of systems with fast-varying delays," *Automatica,* vol. 43, pp. 1649-1655, 2007.

[135] R. Sipahi and S. I. Niculescu, "Chain stability in traffic flow with driver reaction delays," in *American Control Conference, 2008*, 2008, pp. 4922-4927.

[136] I. O. f. Standardization, *Passenger Cars-- Test Track for a Severe Lane-change Manoeuvre: Part 1 : Double Lane-change*: International Organization for Standardization, 1999.

[137] J. Stoev, E. Hostens, and S. Vandenplas, "Driver Modeling for Heavy Hybrid Vehicle Energy Management," in *Vehicle Power and Propulsion Conference (VPPC), 2014 IEEE*, 2014, pp. 1-6.

[138] M. Sundbom, P. Falcone, and J. Sjoberg, "Online driver behavior classification using probabilistic ARX models," in *16th International IEEE Conference on Intelligent Transportation Systems (ITSC)*, 2013.

[139] F. Tahami, S. Farhangi, and R. Kazemi, "A Fuzzy Logic Direct Yaw-Moment Control System for All-Wheel-Drive Electric Vehicles," *Vehicle System Dynamics,* vol. 41, pp. 203-221, 2004/01/01 2004.

[140] K. L. Talvala, K. Kritayakirana, and J. C. Gerdes, "Pushing the limits: From lanekeeping to autonomous racing," *Annual Reviews in Control,* vol. 35, pp. 137-148, 2011.

[141] S. H. Tamaddoni, S. Taheri, and M. Ahmadian, "Optimal preview game theory approach to vehicle stability controller design," *Vehicle System Dynamics,* vol. 49, pp. 1967-1979, 2011/12/01 2011.

[142] J. P. Timings and D. J. Cole, "Vehicle trajectory linearisation to enable efficient optimisation of the constant speed racing line," *Vehicle System Dynamics,* vol. 50, pp. 883-901, 2012/06/01 2012.
[143] J. Treat, N. Tumbas, S. McDonald, D. Shinar, R. Hume, R. Mayer*, et al.*, "Tri-level study of the causes of traffic accidents: final report. Executive summary," 1979.
[144] A. Tustin, "The nature of the operator's response in manual control, and its implications for controller design," *Electrical Engineers - Part IIA: Automatic Regulators and Servo Mechanisms, Journal of the Institution of,* vol. 94, pp. 190-206, 1947.
[145] R. H. Tütüncü, K. C. Toh, and M. J. Todd, "Solving semidefinite-quadratic-linear programs using SDPT3," *Mathematical programming,* vol. 95, pp. 189-217, 2003.
[146] A. Y. Ungoren and H. Peng, "An adaptive lateral preview driver model," *Vehicle System Dynamics,* vol. 43, pp. 245-259, 2005.
[147] J.-Y. Wang and M. Tomizuka, "Robust H< sub>∞</sub> lateral control of heavy-duty vehicles in automated highway system," in *American Control Conference, 1999. Proceedings of the 1999*, 1999, pp. 3671-3675.
[148] T. A. Wenzel, K. J. Burnham, R. A. Williams, and M. V. Blundell, "Closed-loop driver/vehicle model for automotive control," in *Systems Engineering, 2005. ICSEng 2005. 18th International Conference on*, 2005, pp. 46-51.
[149] D. Woods, "The effects of automation on human's role: Experience from non-aviation industries," *Flight deck automation: Promises and realities,* pp. 61-85, 1989.
[150] F. Wu, X. H. Yang, A. Packard, and G. Becker, "Induced L 2-norm control for LPV system with bounded parameter variation rates," in *American Control Conference, Proceedings of the 1995*, 1995, pp. 2379-2383.
[151] J. Wu, Q. Wang, X. Wei, and H. Tang, "Studies on improving vehicle handling and lane keeping performance of closed-loop driver–vehicle system with integrated chassis control," *Mathematics and Computers in Simulation,* vol. 80, pp. 2297-2308, 2010.
[152] F. Wu* and S. Prajna, "SOS-based solution approach to polynomial LPV system analysis and synthesis problems," *International Journal of Control,* vol. 78, pp. 600-611, 2005.
[153] L. Xian-sheng, Z. Jian-guo, and W. Meng-yao, "Driving Stability of Closed Loop Tractor-Semitrailer Vehicle System with Optimal Driver Model," in *Measuring Technology and Mechatronics Automation, 2009. ICMTMA'09. International Conference on*, 2009, pp. 514-517.
[154] L. Xie, "Output feedback H∞ control of systems with parameter uncertainty," *International Journal of Control,* vol. 63, pp. 741-750, 1996.
[155] L. Zaccarian and A. R. Teel, *Modern anti-windup synthesis: control augmentation for actuator saturation*: Princeton University Press, 2011.
[156] G. Zames, "Feedback and optimal sensitivity: Model reference transformations, multiplicative seminorms, and approximate inverses," *Automatic Control, IEEE Transactions on,* vol. 26, pp. 301-320, 1981.

[157] B. Zhang, S. Xu, and Y. Zou, "Improved stability criterion and its applications in delayed controller design for discrete-time systems," *Automatica,* vol. 44, pp. 2963-2967, // 2008.
[158] B. Zhang, W. X. Zheng, and S. Xu, "Filtering of Markovian jump delay systems based on a new performance index," *Circuits and Systems I: Regular Papers, IEEE Transactions on,* vol. 60, pp. 1250-1263, 2013.
[159] H. Zhang and J. Wang, "Vehicle lateral dynamics control through AFS/DYC and robust gain-scheduling approach," 2015.
[160] H. Zhang, X. Zhang, and J. Wang, "Robust gain-scheduling energy-to-peak control of vehicle lateral dynamics stabilisation," *Vehicle System Dynamics,* vol. 52, pp. 309-340, 2014.
[161] L. Zhang and J. Lam, "Necessary and sufficient conditions for analysis and synthesis of Markov jump linear systems with incomplete transition descriptions," *Automatic Control, IEEE Transactions on,* vol. 55, pp. 1695-1701, 2010.
[162] R. Zope, J. Mohammadpour, K. Grigoriadis, and M. Franchek, "Delay-dependent output feedback control of time-delay LPV systems," in *Control of Linear Parameter Varying Systems with Applications*, ed: Springer, 2012, pp. 279-299.

Appendix

Schur Complement

Lemma [20]: Let X be a symmetric matrix given by $X = \begin{bmatrix} A & B \\ B^T & C \end{bmatrix}$ then:

$$X > (\geq)0 \quad A > (\geq)0, \; C \quad B^T A^{-1} B > (\geq)0.$$

$$X > (\geq)0 \quad C > (\geq)0, \; A \quad BC^{-1}B^T > (\geq)0.$$

$$S^T = \begin{bmatrix} S_{11} & S_{12} \\ & S_{22} \end{bmatrix}$$

$$S < 0$$

$$S_{11} < 0, S_{22} \quad S_{12}^T S_{11}^{-1} S_{12} < 0$$

$$S_{22} < 0, S_{11} \quad S_{12} S_{22}^{-1} S_{12}^T < 0$$

Example:

$$\begin{bmatrix} A^TP + PA & PB & C^T \\ & \gamma I & D^T \\ & & \gamma I \end{bmatrix} < 0 \;\rightarrow\; \gamma I < 0, \begin{bmatrix} A^TP + PA & PB \\ & \gamma I \end{bmatrix} + \gamma^{-1} \begin{bmatrix} C^T \\ D^T \end{bmatrix} [C \quad D] < 0$$

$$\begin{bmatrix} A^TP + PA + \gamma^{-1}C^TC & PB + \gamma^{-1}C^TD \\ & \gamma I + \gamma^{-1}D^TD \end{bmatrix} < 0 \rightarrow \begin{bmatrix} A^TP\gamma + P\gamma A + C^TC & \gamma PB + C^TD \\ & \gamma^2 I + D^TD \end{bmatrix} < 0$$

$$\begin{bmatrix} A^TP + PA + C^TC & PB + C^TD \\ & \gamma^2 I + D^TD \end{bmatrix} < 0$$

The S-procedure (Quadratic Form)

Lemma [20]: Let $T_0, \quad , T_p \in \quad^{n \times n}$ be symmetric matrices. If there exists $\tau_1 \geq 0$, $\quad , \tau_p \geq 0$ such that $T_0 \quad \sum_{i=1}^{p} \tau_i T_i > 0$, then the following condition on $T_0, \quad , T_p$ holds:

$\zeta^T T_0 \zeta > 0$ for all $\zeta \neq 0$ such that $\zeta^T T_i \zeta \geq 0, i = 1, \quad , p.$

Example:

Consider the following constraint on the variable P:

For all $\zeta \neq 0$ and π satisfying $\pi^T \pi \leq \zeta^T C^T C \zeta$,

$$\begin{bmatrix} \zeta \\ \pi \end{bmatrix}^T \begin{bmatrix} A^T P + PA & PB \\ B^T P & 0 \end{bmatrix} \begin{bmatrix} \zeta \\ \pi \end{bmatrix} < 0.$$

This constraint is equivalent to the existence of $\tau \geq 0$ such that:

$$\begin{bmatrix} A^T P + PA + \tau C^T C & PB \\ B^T P & \tau I \end{bmatrix} < 0.$$

Bounded Real Lemma:

The matrix inequality

$$A^T P + PA + \gamma^{-2} PBB^T P + C^T C < 0$$

Can be converted to the following LMI:

$$\begin{bmatrix} A & P + PA + C^T C & PB \\ & B^T P & \gamma^2 I \end{bmatrix} < 0$$

Using the Schur lemma and defining a new variable $Q = \gamma^{-1} P$, one can further simplifies it as:

$$A^T Q + AQ + \gamma^{-1} QPBB^T Q + \gamma^{-1} C^T C < 0$$

$$\begin{bmatrix} A^T Q + QA + \gamma^{-1} C^T C & QB \\ B^T Q & \gamma I \end{bmatrix} = \begin{bmatrix} A^T Q + QA & QB \\ B^T Q & \gamma I \end{bmatrix} + \begin{bmatrix} C^T \\ 0 \end{bmatrix} \gamma^{-1} I [C \quad 0] < 0$$

$$\begin{bmatrix} A^T Q + QA & QB & C^T \\ & \gamma I & 0 \\ & & \gamma I \end{bmatrix} < 0$$

Bounded Real Lemma for MJLS ([35])

Consider the space of all random processes $\Omega = \{\Omega(t); t \in R^+\} \in R^r$ such that

$$\|\Omega\|_{2\epsilon} \quad \sqrt{\int_0^T E(\|\Omega\|^2)dt}$$

Is finite. Assume that this space is represented by $L_2^r(\Gamma, F, P, [0, T])$.
Consider the following H_∞ problem:

$$G_\Omega = \begin{cases} x(t) = A_{\theta(t)}x(t) + J_{\theta(t)}\Omega(t) \\ z(t) = C_{\theta(t)}x(t) + L_{\theta(t)}\Omega(t) \\ v_0 = (x_0, \theta_0), P(\theta_0 = i) = v_i, i \in S \end{cases} \qquad (i)$$

Where $A = (A_1, \quad, A_N) \in H^n$, $J = (J_1, \quad, J_N) \in H^{r,n}, C = (C_1, \quad, C_N) \in H^{n,p}$, and $L = (L_1, \quad, L_N) \in H^{r,p}$. Mean-Square stability implies Stochastic stability; the system is stochastically stable if for any arbitrary initial condition and $\Omega = 0$:

$$\mathrm{E}\left\{\int_0^\infty \|x(t)\|^2 dt | (x_0, t_0)\right\} \leq \infty$$

The system is mean-square stable if for all zero-input responses:

$$\lim_{t\to\infty} E\big(\|x(t)\|^2 | (x_0, t_0)\big) = 0$$

Bounded Real Lemma:
Given $\gamma > 0$, the following statements are equivalent:

(i) The system given in (i) is internally MSS with $\|G_\Omega\| < \gamma$

(ii) There is a set if positive definite matrices of $P = (P_1, \quad, P_N) > 0 \in H^{n+}$ that $W = (W_1(P), \quad, W_N(P)) < 0 \in H^m$, where $m \quad n + r$,

$$W_i = \begin{bmatrix} \phi_{11,i} + C_i^T C_i & \phi_{12,i} \\ & \phi_{22,i} \end{bmatrix}$$

$$\phi_{11,i} = A_i^T P_i + P_i A_i + \sum_{j=1}^N \lambda_{ij} P(j)$$

$$\phi_{12,i} = P_i J_i + C_i^T L_i$$

$$\phi_{22,i} = L_i^T L_i \quad \gamma^2 I_r$$

(iii) There is $R = (R_1, \quad , R_N) > 0 \in H^{n+}$ such that

$$\begin{matrix} A_i^T R_i + R_i A_i + \sum_{j=1}^{N} \lambda_{ij} R(j) & R_i J_i & C_i^T \\ & & \\ & \gamma I_r & L_i^T \\ & & \gamma I_p \end{matrix} < 0$$

Linear Quadratic Tracking (LQT) Optimal Controller Design [112]

Consider the linear system:

$$\begin{cases} x(t) = Ax(t) + Bu(t) & x(t_0) = x_0 \\ y(t) = Cx(t) \end{cases}$$

where $x \in \ ^n$, $u \in \ ^m$, and $y \in \ ^r$, the state, control, and output vectors. The quadratic performance index is:

$$J = \frac{1}{2}\left[(x(T) \quad x_r(T))^T Q_f (x(T) \quad x_r(T))\right] + \frac{1}{2}\int_{t_0}^{T} [(x(T) \quad x_r(T))^T Q (x(T) \quad x_r(T)) + u^T(t) R u(t)] dt$$

As such, t_0 is initial time, and the finial time is T. The symmetric control and state weighting symmetric matrices, $R > 0, Q_f \geq 0$ and $Q \geq 0$, are chosen by the designer to ensure appropriate penalties for the control and tracking error costs. The pair $\{A, B\}$ is assumed to be controllable, and $\{A, C\}$ is observable. The state trajectory $x_r(t)$ is related to the desired state trajectory satisfying the plant dynamic constraint. For the case in this report, the infinite horizon LQT ($T \rightarrow \infty$) with $t_0 = 0$, and $Q_f = 0$ is considered; thus, the optimal control law consists of the sum of the two components given by:

$$u(t) = K_{ss} x(t) + R^{-1} B^T v_{ss}$$

where $K_{ss} = R^{-1} B^T P_{ss}$ and P_{ss} is the solution of $A^T P_{ss} + P_{ss} A \quad P_{ss} B R^{-1} B^T P_{ss} + Q = 0$, and

$$v(t) = [A \quad BK_{ss}]^T v(t) \quad Q x_r(t), v_{ss} = v(t)|_{t \rightarrow \infty}$$

Lyapunov – Krasowski Method[56]

Consider the following system:

$$\begin{cases} x(t) = f(t, x_t) & t > t_0 \\ x_{t_0} = \phi(\theta) & \forall \theta \in [\ \ \tau, 0] \end{cases}$$

Definition:

If V: × $_{n,r}$ → ^{n} is continuous and $x(t_0, \phi)$ is the solution of (4.24), the Dini's derivative is defined by:

$$V(t, \phi) = \lim_{h \to 0^+} \sup \frac{1}{-} \left[V\left(t + \ \ , x_{t+h}(t_0, \phi)\right) \quad V(t, \phi) \right]$$

Theorem:

Suppose that the function f: × $_{n,\tau}$ → ^{n} takes bounded set of $_{n,\tau}$ in bounded sets of ^{n} and u, v, ω: $^{+}$ → $^{+}$ are continuous nondecreasing functions, $u(s)$ and $v(s)$ are positive for $s > 0$, and $u(0) = v(0) = 0$.

If there is a continuous function V: × $_{n,r}$ → such that:

$$u(\|\phi(0)\|) \leq V(t, \phi) \leq v(\|\phi\| \ \ )$$
$$V(t, \phi) \leq \ \ \omega(\|\phi(0)\|)$$

Then, the trivial solution $x = 0$ of the system (4.7) is uniformly stable.

Where $x_t(.)$ for a given $t \geq t_0$, denotes the restriction of $x\ (.)$ to the interval $[t \quad \tau, t]$ translated to $[\ \ \tau, 0]$, i.e.

$$x_t(\theta) = x(t + \theta), \ \forall \theta \in [\ \ \tau, 0].$$

If $u(s) \to \infty$ as $s \to \infty$ the solution is uniformly stable.

If $\omega(s) > 0$ for $s > 0$, then the solution $x = 0$ is uniformly asymptotically stable.

The condition (i) means that the candidate V is positive-definite and has an infinitesimal upper bound, and the negativity of the derivative of V in (ii) means that the candidate is not increasing along system's trajectory.

Infinitesimal Generator ([35])

In a Banach space X a one parameter family $\phi(s) \in B(X), s \in R^+$, is called a semigroup of bounded linear operators on X if $\phi(0) = I$ and the semigroup property $\phi(t+s) = \phi(t)\phi(s)$ for every $t, s \in R^+$ is satisfied. The infinitesimal generator of the semigroup $\phi(t)$ is defined as:

$$x \quad \lim_{h \to 0} \frac{\phi(\ )x \quad x}{}$$

Markov Jump Linear System Analysis:

In order to analyze the system given in (6.8), one can consider the following quadratic Lyapunov function:

$$V\big(x(t), r(t)\big) = x^T(t) P\big(r(t)\big) x(t), P\big(r(t)\big) > 0$$

Let $\mathcal{A}$ be the infinitesimal generator of x, defined by its action on compactly-supported twice differentiable continuous second derivative functions $V(x(t), r(t))$:

$$\mathcal{A}V\big(x(t), r(t)\big) = \lim_{\Delta \to 0} \frac{\mathrm{E}^{\mathrm{x}}[V(x(t+\Delta), r(t+\Delta) | x(t), r(t)] \quad V\big(x(t), r(t)\big)}{\Delta}$$

Let Δ be a stopping time with $\mathrm{E}^{\mathrm{x}}[\Delta] < +\infty$, and let $V(x(t), r(t))$ be C2 with compact support. Then Dynkin's formula holds:

$$\mathrm{E}^{\mathrm{x}}[V(x(t+\Delta), r(t+\Delta) | x(t), r(t)] = V\big(x(t), r(t)\big) + \mathrm{E}^{\mathrm{x}}\left[\int_0^{\Delta} \mathcal{A}V\big(x(s), r(s)\big)\, ds\right]$$

It may be seen as a stochastic generalization of the (second) fundamental theorem of calculus.

$$A(x + \ ) \quad A(x) \approx f(x) \quad + HOT, \qquad f(x) = \lim_{h \to 0} \frac{A(x + \ ) \quad A(x)}{}$$

Conditioning on $r(t) = i$ and applying the law of total probability and conditional expectation yields ($x(t+\Delta) = (I + A_i \Delta) x(t)$):

$$\mathcal{A}V\big(x(t), r(t)\big) = \lim_{\Delta \to 0} \frac{1}{\Delta} \left[\sum_{j=1}^{N} \Pr\{r(t+\Delta = j | r(t) = i\} x^T(t+\Delta) P(j) x(t+\Delta) \right.$$
$$\left. x^T(t) P(i) x(t) \right]$$

$$= \lim_{\Delta\to 0}\frac{1}{\Delta}\left[\sum_{j=1}^{N}\Pr\{r(t+\Delta=j|r(t)=i\}x^T(t)\big(I+A_i^T\Delta\big)P(j)(I+A_i\Delta)x(t) \quad x^T(t)P(i)x(t)\right]$$

$$= x^T(t)Q(i,t)x(t)$$

$$Q(i,t) = \lim_{\Delta\to 0}\frac{1}{\Delta}\left[\sum_{j=1,i\neq j}^{N}\Pr\{r(t+\Delta=j|r(t)=i\}\left(I+A_i^T\Delta\right)P(j)(I+A_i\Delta)\right.$$

$$\left.+\Pr\{r(t+\Delta=i|r(t)=i\}\left(I+A_i^T\Delta\right)P(i)(I+A_i\Delta) \quad P(i)\right] =$$

$$= \lim_{\Delta\to 0}\frac{1}{\Delta}\left[\sum_{j=1,i\neq j}^{N}\frac{\Pr\{r(\Delta=j,r(0)=i\}}{\Pr\{r(0)=i\}}\big(I+A_i^T\Delta\big)P(j)\big(I+A_j\Delta\big)\right.$$

$$\left.+\frac{\Pr\{r(\Delta=i,r(0)=i\}}{\Pr\{r(0)=i\}}P(i) \quad P(i)\right] + A_i^TP(i)+P(i)A_i$$

$$\lim_{\Delta\to 0}\left[\frac{\Pr\{r(\Delta=i,r(0)=i\}}{\Pr\{r(0)=i\}}\right]=1, \lim_{\Delta\to 0}\frac{1}{\Delta}\left[\frac{\Pr\{r(\Delta=i,r(0)=i\}}{\Pr\{r(0)=i\}} \quad 1\right]=\lambda_{ii}$$

$$\lim_{\Delta\to 0}\frac{1}{\Delta}\left[\frac{\Pr\{r(\Delta=j,r(0)=i\}}{\Pr\{r(0)=i\}}\right]=\lambda_{ij}$$

$$= \lim_{\Delta\to 0}\frac{1}{\Delta}\left[\sum_{j=1,i\neq j}^{N}\frac{\Pr\{r(\Delta=j,r(0)=i\}}{\Pr\{r(0)=i\}}\big(A_i^T\Delta P(j)+P(j)A_j\Delta+A_i^T\Delta P(j)A_j\Delta\big)\right]+\sum_{j=1}^{N}\lambda_{ij}P(j)$$

$$+A_i^TP(i)+P(i)A_i =$$

$$= \sum_{j=1,i\neq j}^{N}\lambda_{ij}\lim_{\Delta\to 0}\big(A_i^T\Delta P(j)+P(j)A_j\Delta+A_i^T\Delta P(j)A_j\Delta\big)+\sum_{j=1}^{N}\lambda_{ij}P(j)+A_i^TP(i)+P(i)A_i$$

$$= A_i^TP(i)+P(i)A_i+\sum_{j=1,j\neq i}^{N}\lambda_{ij}P(j)$$

Note that this condition is similar to the famous Lyapunov-Metzler inequality for guaranteeing state-dependent switching system stability (see [50]).